

**ELUCIDATION OF DNA DAMAGE RESPONSE PATHWAYS AND
FUNCTIONAL EFFICIENCY OF DNA REPAIR GENES
ASSOCIATED WITH REPROGRAMMED
OSTEOSARCOMA CELL LINES**

By

CHOONG PEI FENG

A thesis submitted to the Department of Pre-Clinical Science,
Faculty of Medicine and Health Sciences,
Universiti Tunku Abdul Rahman,
in partial fulfillment of the requirements for the degree of
Doctor of Philosophy of Medical Sciences

May 2018

ABSTRACT

ELUCIDATION OF DNA DAMAGE RESPONSE PATHWAYS AND FUNCTIONAL EFFICIENCY OF DNA REPAIR GENES ASSOCIATED WITH REPROGRAMMED OSTEOSARCOMA CELL LINES

Choong Pei Feng

Osteosarcoma (OS) is a prevalent cancer of the bone happening mostly in children and adolescence. Alterations and mutations to genes associated with proliferation and differentiation increased the risk of OS tumourigenicity. Reprogramming of OS cell lines to a primitive phase could be used to understand the pathogenesis of OS. Furthermore, the DNA damage response (DDR) of reprogrammed cancer cells has not been well established.

By using retroviral OSKM, OS cell lines were reprogrammed to pluripotency. Colonies from iG-292 and iSaos-2 showed ESC-like morphology, expressing pluripotency markers, formed embryoid body-like spheres and expressed markers from three germ layers as well as showing ability to differentiate into adipocytes and osteocytes. However, *in vivo* study showed teratoma formation only in reprogrammed G-292, iG-292.

In the second part of this study, hierarchical clustering analysis from global gene expression profile of parental and reprogrammed OS demonstrated distinctive separation of two population. Differentially expressed genes (DEGs)

were grouped into DNA repair, cell cycle and apoptosis pathways. Our data showed that iG-292 displayed more DEGs than iSaos-2 in all pathways. Subsequently, quantification of cyclobutane pyrimidine dimers (CPDs) showed lower level of CPDs in iG-292 than parental G-292 suggested that iG-292 may have more effective CPDs removal mechanism. Further analysis of nucleotide excision repair (NER) genes demonstrated up-regulation of GADD45G, XPA, RPA, MNAT1, ERCC1, PCNA and POLL, in iG-292. This indicated that the up-regulation of GADD45G together with up-regulation of other NER genes synergistically repaired UV damage by rapid removal of CPDs.

In conclusion, based on the criteria of iPSC, a fully reprogrammed iG-292 was successfully generated. Down-regulation of DDR genes in reprogrammed OS suggested better genome integrity in reprogrammed OS. Thus, this study demonstrated DDR profile of reprogrammed OS cells and in particular the involvement of GADD45G in DNA repair mechanism of reprogrammed OS cells.

ACKNOWLEDGEMENTS

First and foremost, I would like to express my greatest appreciation and gratefulness to my supervisor, Prof. Dr. Alan Ong Han Kiat for his continuous guidance, patience, encouragement and advice that have assisted me throughout my PhD project. I would also like to thank to my co-supervisor, Emeritus Prof. Dr. Cheong Soon Keng for his excellent comments and suggestions. Both of them have given me tremendous guidance and support as well as broadened my horizon in stem cells and reprogramming perspective.

I would also like to thank Dr. Shigeki Sugii from Singapore BioImaging Consortium, A*Star, Singapore for providing the Yamanaka factor vectors used in this study and Prof. Dr. Swaminathan in helping to analyse the histology in the animal study. This work was supported by HIR-MoE Grant (UM.C/625/1/HIR/MOHE/CHAN/3) and MAKNA research funding (MSC and GT-grant).

A grateful appreciation to my parents and my sibling, who are always there to provide me moral and emotional support in my life. To my ever interested, encouraging and enthusiastic husband, Choo Chee Wei, for believing in me. To my two superb princesses, thank you for your presence in my life. You are the most beautiful gift I ever receive.

Last, but not the least, I would like to express my gratitude to all my laboratory members, Ms. Teh Hui Xin, Dr. Teoh Hoon Koon, Dr. Lim Kian Lam, Ms. Nalini Devi, Ms. Tai Lihui, Mr. Vimalan, Mr. Lim Sheng Jye and everyone in UTAR FMHS Postgraduate Laboratories and Faculty General Office. It was my great pleasure to be working with you all throughout the project.

APPROVAL SHEET

This thesis entitled “**ELUCIDATION OF DNA DAMAGE RESPONSE PATHWAYS AND FUNCTIONAL EFFICIENCY OF DNA REPAIR GENES ASSOCIATED WITH REPROGRAMMED OSTEOSARCOMA CELL LINES**” was prepared by CHOONG PEI FENG and submitted as partial fulfillment of the requirements for the degree of Doctor of Philosophy of Medical Sciences at Universiti Tunku Abdul Rahman.

Approved by:

(Prof. Dr. Alan Ong Han Kiat)

Date:

Professor/Supervisor

Department of Pre-clinical Sciences

Faculty of Medicine and Health Sciences

Universiti Tunku Abdul Rahman

(Emeritus Prof. Dr. Cheong Soon Keng)

Date:

Senior Professor/Co-supervisor

Department of Medicine

Faculty of Medicine and Health Sciences

Universiti Tunku Abdul Rahman

FACULTY OF MEDICINE AND HEALTH SCIENCES
UNIVERSITI TUNKU ABDUL RAHMAN

Date: _____

SUBMISSION OF THESIS

It is hereby certified that **Choong Pei Feng** (ID no: **14UMD07970**) has completed this thesis entitled “ELUCIDATION OF DNA DAMAGE RESPONSE PATHWAYS AND FUNCTIONAL EFFICIENCY OF DNA REPAIR GENES ASSOCIATED WITH REPROGRAMMED OSTEOSARCOMA CELL LINES” under the supervision of Prof. Dr. Alan Ong Han Kiat (Supervisor) from the Department of Pre-clinical Sciences, Faculty of Medicine and Health Sciences, and Emeritus Prof. Dr. Cheong Soon Keng (Co-supervisor) from Department of Medicine, Faculty of Medicine and Health Sciences, Universiti Tunku Abdul Rahman.

I understand that University will upload softcopy of my thesis in pdf format into UTAR Institutional Repository, which may be made accessible to UTAR community and public.

Yours truly,

(Choong Pei Feng)

DECLARATION

I CHOONG PEI FENG hereby declare that the thesis is based on my original work except for quotations and citations which have been duly acknowledged. I also declare that it has not been previously or concurrently submitted for any other degree at UTAR or any other institutions.

CHOONG PEI FENG

Date: _____

TABLE OF CONTENTS

	PAGE
ABSTRACT	ii
ACKNOWLEDGEMENT	iv
APPROVAL SHEET	vi
SUBMISSION SHEET	vii
DECLARATION	viii
TABLE OF CONTENTS	ix
LIST OF TABLES	xvi
LIST OF FIGURES	xvii
LIST OF ABBREVIATIONS	xx
CHAPTER	
1.0 INTRODUCTION	1
2.0 LITERATURE REVIEW	5
2.1 Osteosarcoma	5
2.1.1 OS tumourigenesis	6
2.2 Induced pluripotent stem cells	8
2.2.1 Application of iPSC	9
2.3 Reprogramming of cancer cells	11
2.3.1 Application of cancer reprogramming	11
2.4 DNA damage response (DDR)	16
2.4.1 DNA damage response in pluripotent cells	16
2.4.2 DNA damage response in OS	18
2.4.3 Nucleotide excision repair (NER)	19

3.0	MATERIALS AND METHODS	22
3.1	Overview of Methods	22
3.2	Generation of iPSC from OS cell lines	25
3.2.1	Osteosarcoma (OS) Cell Lines	25
3.2.2	Culture of OS Cell Lines	25
3.2.3	Culture of 293FT Cell Line	27
3.2.4	Culture and Inactivation of Mouse Embryonic Fibroblast (MEF) Feeder Layer	28
3.2.5	Culture of Human Embryonic Stem Cells (hESC), BG01V, Cell Line	30
3.3	Bacteria Culture Media	32
3.3.1	Lysogeny Broth (LB) Agar Plate	32
3.3.2	Lysogeny Broth (LB) Media	32
3.3.2.1	Antibiotic Selective Marker	33
3.3.3	Preparation of Plasmid pMX-Retroviral Vector	33
3.3.3.1	Retrieval of Plasmids	33
3.3.3.2	Storage of Transformed Plasmids	34
3.3.3.3	Plasmid Extraction	34
3.3.4	Verification of Plasmids	37
3.3.4.1	Restriction Enzyme (RE)	37
3.3.4.2	Gel Electrophoresis	38
3.3.5	Retroviral packaging	38
3.3.5.1	Transfection for Retrovirus: Green Fluorescent Protein (GFP)	39
3.3.5.2	Transfection Efficiency of pMX-GFP in OS cell line	40

	3.3.5.3	Transfection of 293FT cells with Retrovirus Vectors: OCT4, SOX2, KLF4, c-MYC	41
	3.3.6	Retrovirus Transduction	43
	3.3.7	Maintenance and Passaging of Reprogrammed OS Cell Lines	44
3.4		Characterisation of OS-Induced Pluripotent Stem Cells (OS-iPSC)	44
	3.4.1	Morphology Evaluation under Microscope Observation	44
	3.4.2	Alkaline Phosphatase (AP) Live Staining	45
	3.4.3	Expression of Pluripotent Markers via Immunofluorescence (IF) Staining	45
	3.4.4	Expression of Pluripotent Markers via Gene Expression	48
	3.4.4.1	Total Ribonucleic Acid (RNA) Extraction	48
	3.4.4.2	cDNA Conversion	49
	3.4.4.3	Quantitative Real-Time Polymerase Chain Reaction (qPCR)	51
	3.4.4.4	Calculation and Analysis	53
	3.4.5	Embryoid Body Formation and Spontaneous Differentiation	53
	3.4.6	Differentiation into adipocytes	54
	3.4.7	Differentiation into Osteoblasts	55
	3.4.8	Teratoma/ Xenograft Formation	56
3.5		Global gene expression of the reprogrammed OS cells using microarray technology	57
	3.5.1	Total Ribonucleic Acid Extraction (RNA)	58

3.5.2	Global Gene Expression via Affymetrix GeneChip PrimeView Human Gene Expression Array	59
3.6	Evaluation of DNA repair, cell cycle and apoptosis processes	61
3.6.1	Validation of genes via Taqman Gene Expression Assay	61
3.6.2	Calculation and Analysis	63
3.7	Functional assay to examine the functionality of DNA repair mechanism.	64
3.7.1	Ultraviolet (UV) irradiation	64
3.7.2	Deoxyribonucleic Acid (DNA) extraction	65
3.7.3	Cyclobutane pyrimidine dimers (CPD) quantitation	66
4.0	RESULTS AND DISCUSSION (PART 1)	68
	<u>Reprogramming & Characterisation of reprogrammed OS cells</u>	
4.1	Microscopic Observation of Human Osteosarcoma Cell Lines	68
4.2	Transduction Efficiency via Green Fluorescence Protein (pMX-GFP)	70
4.2.1	Transduction in G-292 and Saos-2 Cell Lines with pMX-GFP	70
4.3	Transduction with Plasmid OSKM	73
4.3.1	Transduction of G-292 and Saos-2 cell lines with Plasmid OSKM at 72 hours and 5 days Post-Transduction	73
4.3.2	OSKM Transduction Results in G-292 and Saos-2	75
4.4	Characterisation of Established Osteosarcoma Derived Induced Pluripotent Stem Cells (OS-iPSC)	78

4.4.1	Morphological observation from G-292-Derived Induced Pluripotent Stem Cells (iG-292) and Saos-2-Derived Induced Pluripotent Stem Cells (iSaos-2)	78
4.4.2	Alkaline Phosphatase (AP) Live Staining on OS-iPSC	82
4.4.3	Expression of Pluripotent Markers via Immunofluorescence (IF) Staining	84
4.4.4	mRNA Expression of Pluripotent Markers in Reprogrammed OS cells	87
4.4.5	Embryoid body (EB) formation and spontaneous differentiation	89
4.4.6	Differentiation into adipocytes and osteoblasts (Mesoderm lineage differentiation)	91
4.4.7	Teratoma/ Xenograft Formation	93
4.5	Discussion	96
4.5.1	Reprogramming of osteosarcoma cell lines, G-292 and Saos-2	96
4.5.2	Characterisation of Established Osteosarcoma Derived Induced Pluripotent Stem Cells (OS-iPSC)	99
4.6	Conclusion	106
5.0	RESULTS AND DISCUSSION (PART 2)	107
	<u>Evaluation of DNA repair, cell cycle and apoptosis processes from global gene expression of the reprogrammed OS cells using microarray technology</u>	
5.1	Introduction	107
5.2	RNA preparation and integrity	108
5.3	Global gene expression profile in parental and reprogrammed OS	110

5.4	Gene ontology enrichment analysis of the highly differentially expressed genes	115
5.5	Elucidation of DNA Damage Response (DDR) pathways upon OS reprogramming via global gene expression profiling	122
5.6	Validation of differentially expressed genes associate in DNA repair, cell cycle and apoptosis processes	127
5.7	Discussion	131
5.7.1	Reprogrammed OS are genotypically different from parental via global gene expression profiling	131
5.7.2	Diverse Gene Ontology enrichment analysis on reprogrammed OS	132
5.7.3	Elucidation of DNA damage response (DDR) pathways of reprogrammed OS, iG-292 and iSaos-2	134
5.8	Conclusions	138
6.0	RESULTS AND DISCUSSION (PART 3)	139
	<u>Functional assay to explicate genes related to DNA repair mechanism in reprogrammed OS</u>	
6.1	Introduction	139
6.2	Morphological observation on reprogrammed and parental OS after UV irradiation	141
6.3	Detection of cyclobutane pyrimidine dimers (CPDs) in reprogrammed and parental OS upon UV irradiation	146
6.4	Analyses of Nucleotide Excision Repair (NER) genes expression in reprogrammed and parental OS upon UV irradiation	148
6.5	Discussion	152

6.5.1	Reprogrammed OS, iG-292, demonstrated more effective DNA repair response in rapid removal of CPDs and up-regulation of NER genes	153
6.5.2	GADD45G roles in tumour suppression and enhancing NER	155
6.6	Conclusions	159
7.0	CONCLUSIONS AND FUTURE STUDIES	160
7.1	Conclusions	160
7.2	Future studies	162
	REFERENCES	163
	APPENDICES	179

LIST OF TABLES

Table	Title	Page
3.1	Medium composition of OS medium for G-292 in 500 ml	26
3.2	Medium composition of OS medium for Saos-2 in 500 ml	27
3.3	Medium composition of 293FT medium in 500 ml	28
3.4	Medium composition of MEF medium in 500 ml	30
3.5	Medium composition of hESC medium in 500 ml	31
3.6	Reaction mixtures of restriction enzyme	37
3.7	Amount of plasmid DNA for retroviral transfection in ratio of 3:2:1	42
3.8	Component A and B (Lipofectamine 2000 protocol)	42
3.9	Pluripotent and secondary antibodies and dilution factors	47
3.10	Reverse Transcription Reaction Mixture	50
3.11	Thermal Cycler protocol for cDNA synthesis	51
3.12	qPCR reaction components	52
3.13	Thermal Cycler protocol for qPCR	52
3.14	Taqman® qPCR reaction components	62
3.15	Thermal Cycler protocol for Taqman® qPCR	63
5.1	Purity, integrity and concentration of RNA samples extracted from parental OS and reprogrammed OS cells	109
5.2	Differentially expressed entities and genes between parental and reprogrammed OS with fold change ≥ 2 and significance level, $p < 0.05$.	114
5.3	Differentially expressed genes (DEGs) from each DNA repair, cell cycle and apoptosis processes were selected for validation with the microarray results reported in fold change (FC).	128

LIST OF FIGURES

Figure		Page
2.1	Application of iPSC technology	15
2.2	Nucleotide excision repair (NER) mechanism	21
3.1	Flow chart of research methodology of the study	24
4.1	Morphology of adherent human osteosarcoma (OS) cell lines in tissue culture plates	69
4.2	Determination of transfection efficiency using pMX-GFP in parental cells after 48 hours	71
4.3	Transduction efficiency of pMX-GFP in G-292 and Saos-2	72
4.4	Post-transduction of G-292	74
4.5	Post-transduction of Saos-2	74
4.6	Emergence of ESC-like colonies on Day 21 post-transduction	76
4.7	Reprogramming efficiency in G-292 and Saos-2	77
4.8	Various iG-292 clones at different passages	80
4.9	Various iSaos-2 clones at different passages	81
4.10	Alkaline phosphatase staining	83
4.11	Immunofluorescence (IF) staining of parental G-292 and Saos-2 cells	85
4.12	Immunofluorescence (IF) staining of iG-292 and iSaos-2 cells at Passage 5 and Passage 15	86
4.13	Expression of pluripotent genes in reprogrammed OS	88
4.14	Embryoid bodies (EB) formation	90
4.15	Multilineage genes expression during EB formation in iG-292 and iSaos-2	90

4.16	Adipogenesis and osteogenesis in G-292 and iG-292	92
4.17	Adipogenesis and osteogenesis in Saos-2 and iSaos-2	92
4.18	Tumour from parental G-292 and Saos-2	94
4.19	Formation of iG-292 teratoma and three germ layers	95
5.1	Hierarchical clustering analysis of parental and reprogrammed OS	112
5.2	Distribution of gene ontology enriched categories for reprogrammed OS, iG-292	117
5.3	Distribution of gene ontology enriched categories for reprogrammed OS, iSaos-2	118
5.4	Distribution of gene ontology enrichment categories based on up-regulated DEGs in both iG-292 and iSaos-2 respectively	120
5.5	Distribution of gene ontology enrichment categories based on down-regulated DEGs in both iG-292 and iSaos-2 respectively	121
5.6	Analysis of DNA repair gene expression in both reprogrammed OS	124
5.7	Analysis of cell cycle gene expression in both reprogrammed OS	125
5.8	Analysis of apoptosis gene expression in both reprogrammed OS	126
5.9	Comparison between microarray data and qPCR validation data for DNA repair genes	129
5.10	Comparison between microarray data and qPCR validation data for cell cycle genes.	129
5.11	Comparison between microarray data and qPCR validation data for apoptosis genes	130
6.1	Representative images on parental G-292 after 40 J/m ² UV irradiation	142
6.2	Representative images on parental Saos-2 after 40 J/m ² UV irradiation	143

6.3	Representative images on reprogrammed iG-292 after 40 J/m ² UV irradiation	144
6.4	Representative images on reprogramed iSaos-2 after 40 J/m ² UV irradiation	145
6.5	Cyclobutane pyrimidine dimers (CPDs) concentration in parental and reprogrammed OS after UV irradiation	147
6.6	Nucleotide excision repair (NER) genes expression after UV irradiation on G-292 and iG-292	150
6.7	Nucleotide excision repair (NER) genes expression after UV irradiation on Saos-2 and iSaos-2	151
6.8	A schematic diagram showing potential effect of GADD45G on NER upon reprogramming	158

LIST OF ABBREVIATIONS

5-FU	5-fluorodeoxyuridine
6-4 PP	6-4 photoproduct
AP	Alkaline phosphatase
APE1	Human apurinic endonuclease 1
ATCC	American Type Culture Collection
BCL2L11	B cell lymphoma-2-like 11
BER	Base excision repair
bFGF	Basic fibroblast growth factor
BNIP3L	BCL2/adenovirus E1B 19 kDa interacting protein 3-like
BSA	Bovine serum albumin
CASP4	Caspase 4
CASP8	Caspase 8
CCNA1	Cyclin A1
CCNE1	Cyclin E1
CDK	Cyclin dependent kinase
CDKN2A	Cyclin dependent kinase inhibitor 2A
CHK2	Check point kinase 2
CML	Chronic myeloid leukaemia
c-MYC	c-Myc avian myelocytomatosis viral oncogene homolog
CPD	Cyclobutane pyrimidine dimer
DAPK1	Death-associated protein kinase-1
DDR	DNA damage response
DEG	Differentially expressed gene

DMEM	Dulbecco's Modified Eagle Medium
DNA	Deoxyribonucleic acid
dNTP	Deoxyribonucleotide triphosphate
DSB	Double-strand break
dsDNA	Double-stranded DNA
EB	Embryoid body
EDTA	Ethylenediaminetetraacetic acid
ELISA	Enzyme-linked immunosorbent assay
ERCC1	Excision-repair cross-complementing 1
ERCC2	Excision-repair cross-complementing 2
ESC	Embryonic stem cell
FC	Fold change
GADD45G	Growth arrest and DNA damage-inducible 45- γ
GAPDH	Glyceraldehyde 3-phosphate dehydrogenase
gDNA	Genomic DNA
GEO	Gene Expression Omnibus
GFP	Green fluorescent protein
GGR	Global genomic repair
GiPSC	Glioblastoma induced pluripotent stem cell
GO	Gene ontology
H&E	Hematoxylin and eosin
HRR	Homologous recombination repair
HSC	Haematopoietic stem cell
iG-292	G-292-derived induced pluripotent stem cell
IGF2	Insulin-like growth factor 2

iMEF	Inactivated mouse embryonic fibroblast
iPC	Induced pluripotent cancer cell
iPSC	Induced pluripotent stem cell
iSaos-2	Saos-2-derived induced pluripotent stem cell
KLF4	Kruppel-like factor 4
LB	Lysogeny broth
LFS	Li–Fraumeni syndrome
MCM9	Minichromosome maintenance protein 9
MDM2	Murine double minute 2
MEF	Mouse embryonic fibroblast
MLH1	MutL Homologue 1
MMEJ	Microhomology-mediated end joining
MMLV	Moloney murine leukaemia virus
MMR	Mismatch repair
MNAT1	MNAT, CDK activating kinase assembly factor 1
MRE11A	Meiotic recombination 11
mRNA	Messenger ribonucleic acid
MSC	Mesenchymal stem cell
NCBI	National Center for Biotechnology Information
NEAA	Non-essential amino acid
NER	Nucleotide excision repair
NHEJ	Non-homologous end joining
OB	Osteoblast
OCT3/4	Octamer-binding transcription factor 3/4
OS	Osteosarcoma

OSKM	OCT4, SOX2, KLF4, c-MYC
PanIN	Pancreatic intraepithelial neoplasia lesions
PARP1	Poly (ADP-ribose) polymerase-1
PARP3	Poly (ADP-ribose) polymerase-3
PCNA	Proliferating cell nuclear antigen
PCR	Polymerase chain reaction
PDAC	Pancreatic ductal adenocarcinoma
POLL	Polymerase (DNA) lambda
PSC	Pluripotent stem cell
qPCR	Quantitative real-time polymerase chain reaction
RB	Retinoblastoma
RE	Restriction enzyme
REX1	ZFP42 zinc finger protein
RIN	RNA integrity number
RNA	Ribonucleic acid
ROCK	Rho-associated, coiled-coil containing protein kinase
RPA	Replication protein A
RT	Room temperature
SD	Standard deviation
SDS	Sodium dodecyl sulfate
SEM	Standard error of mean
siRNA	Silencing RNA
SNP	Single nucleotide polymorphism
SOX2	Sex-determining region Y (SRY)-related box 2
ssDNA	Single stranded DNA

SSEA3	Stage specific embryonic antigens 3
SSEA4	Stage specific embryonic antigens 4
TAE	Tris-acetate-EDTA
TCR	Transcription coupled repair
TNFRSF1A	Tumour necrosis factor receptor superfamily 1A
TP53	Tumour protein 53
UV	Ultraviolet
UVC	Ultraviolet C
VA	Valproic Acid
XPA	Xeroderma pigmentosum complementation group A
XPC	Xeroderma pigmentosum complementation group C
XPB	Xeroderma pigmentosum complementation group D
XPD	Xeroderma pigmentosum complementation group D
XPF	Xeroderma pigmentosum complementation group F

CHAPTER 1

INTRODUCTION

Osteosarcoma (OS) or bone cancer can be considered as ancient disease. One of the earliest case of OS was just documented to be dated between 1.6-1.8 million years old in the South African Journal of Science (Odes et al., 2016). This new discovery implied that the aetiology for OS are already buried deep within our historical evolution and not related to our present lifestyle. OS is a common bone tumour diagnosed in children and adolescence, affecting the patients during their productive years. In 2007, OS was one of the five most frequent cancers diagnosed in children in Malaysia (Zainal and Nor, 2007). Conventional treatment for OS, by combining chemotherapy and surgery, increased 5-year patients' survival rate to 60%-70% (Mankin et al., 2004). OS pathogenesis has been linked to genetic changes during the osteoblast differentiation process (Gokgoz et al., 2001). Genetic modifications have been associated to proliferation and differentiation capacity impairment that eventually increased the potential of OS tumourigenicity (Kenyon and Gerson, 2007) . Understanding the genetic changes during the differentiation process, could provide valuable insight into the pathogenesis of OS, especially in recurrent and metastatic OS.

Development in the field of induced pluripotent stem cells (iPSC) provided the means to study OS pathogenesis. iPSCs are pluripotent cells reprogrammed from human somatic cells through ectopic expression of OSKM transcription factors (Takahashi et al., 2007). Reprogramming of OS cell lines to a more primitive stage could help to understand the pathogenesis of OS as well as to yield a larger population of pluripotent cancer cells for drug resistance study (Tafani, 2012).

Zhang et al. (Zhang et al., 2013) demonstrated that reprogrammed sarcoma cells lost their tumorigenicity and dedifferentiated to mesenchymal stem cells (MSC) stage. The study also showed differentiation of mature connective tissues and red blood cells from haematopoietic stem cell (HSC)-like cells, suggesting the ability of sarcoma cells to reverse back to a mutual stage of ancestor iPSC branching out for HSC and MSC. This study showed that cancer cells could be 'normalised' via reprogramming. However not much is known about the genomic stability underlying the reprogramming process in sarcoma cells. Reprogramming cancer cells into induced pluripotent cancer cells (iPC) have shown to be able to reset some of the characteristics of cancer, and the reprogrammed cancer cells behave distinctly from their parental cells upon reprogramming (Mahalingam et al., 2012; Allegrucci et al., 2011).

DNA repair network in human stem cells is highly efficient that becomes less efficient upon differentiation for better genomic governance (Rocha et al., 2013). DNA damage repair mechanism is an important process to protect genome integrity and suppress tumorigenesis. A study comparing embryonic

stem cells (ESC) and iPSC showed that their stress defence mechanisms are amazingly similar (Armstrong et al., 2010). Another study showed that repair mechanism was more efficient in human iPSC compared to ESC (Fan et al., 2011). These findings demonstrated that iPSC was extremely efficient in repair mechanisms to safeguard genetic stability.

To date, most of the reported DNA repair studies were conducted on normal cell lines and non-cancerous iPSC. However, there is lack of report till date on the profile of DNA damage response of reprogrammed cancer cells as well as functionality of DNA repair pathway genes post cancer cells reprogramming. Hence, this study was conducted to investigate global gene expression analysis in reprogrammed OS and parental cells. This study hypothesised that genes associated with DNA repair, apoptosis and cell cycle are differentially expressed in reprogrammed OS cells as compared to parental cells, which lead to more effective DNA repair mechanism, thus greater genetic stability in reprogrammed OS cells.

Main objectives and specific objectives of the present study

The study has two main objectives. Each main objectives has its own specific objectives as listed below:

1. The first main objective of the study was to generate and characterise reprogrammed OS cells. This objective was accomplished through the following specific objectives in the study:
 - (i) To reprogramme OS cell lines (G-292 and Saos-2) to pluripotency using retrovirus – OSKM method.
 - (ii) To characterise the reprogrammed OS cells, iG-292 and iSaos-2.

2. The second main objective of the study was to elucidate the DNA damage response pathways and functional efficiency of DNA repair genes associated with reprogrammed osteosarcoma cell lines. This objective was accomplished through the following specific objectives in the study:
 - (iii) To elucidate the DNA damage response of the reprogrammed OS cells based on global gene expression analysis via microarray technology.
 - (iv) To evaluate and validate highly differentially expressed genes associated with the DNA repair, apoptosis and cell cycle processes of reprogrammed OS cells in comparison with the non-reprogrammed parental OS cells.
 - (v) To explicate candidate genes associated with DNA repair mechanism in reprogrammed OS via functional study.

CHAPTER 2

LITERATURE REVIEWS

2.1 Osteosarcoma

Osteosarcoma (OS) is a disease caused by complex, multistep, and multifactorial process. According to Malaysia National Cancer Registry in 2007, OS is one of the top five cancers occurring in children, both male and female (Zainal and Nor, 2007). OS is bone tumour, occurring in young children and adolescents. OS contains almost 60% of the mutual histological subtypes of paediatric bone sarcoma (Lin et al., 2017). OS is mostly aggressive locally and has a propensity to generate early systemic metastases, especially to the lungs (Luetke et al., 2013). Overall childhood 5-year survival rate for OS still remain low, between 60-70%, despite introduction of chemotherapy in early 1970s (Gatta et al., 2014).

Nearly 60% of OS are positioned in the distal femur or proximal tibia. About 75% of the cases occur in the metaphysis of long bones. In children and adolescents, 80% of these outgrowth arise from the bones around the knee, whereas in patients above age 25 years 40% of lesions are located in flat bones (Merimsky et al., 2004) .

Since the introduction of chemotherapy together with gradually-improved surgical techniques, the 5-year survival for patients with localised OS has improved to almost 60% in the 1970s (Ando et al., 2013). However, this figure remains unchanged since then. This could be due to lack of understanding of the molecular mechanisms of osteosarcoma progression that prohibited significant enhancement in the survival of patients over the past 40 years. Novel and innovative therapeutic and diagnostic approaches are essential to improve the overall outcome of the patients (Sampson et al., 2013).

The causal reason for OS is still not known. The common cause for OS is often linked to overactive bone cells production that happens during adolescent (Meyers and Gorlick, 1997). Combination of genetic changes caused immature bone to become tumour cells instead of mature bone cells. However, one consistent finding in all these OS researches pointed to higher incidence of OS in individuals with mutation in genes that involved in stabilising the genome, such as *p53* and retinoblastoma (*RBI*). Impairment of these related genes cause defective maintenance of DNA (Fuchs and Pritchard, 2002; Martin et al., 2012).

2.1.1 OS tumourigenesis

OS tumourigenesis has been associated with modifications in several genes. In particular, OS is famous for *p53* and *RBI* genes mutation. OS is also associated with high level of genomic instability (Selvarajah et al., 2007). This could be due to mutation of *p53* as mutant forms of *p53* is significantly associated with

greater genomic instability in OS (Overholtzer et al., 2003). Deregulation of TP53, product of *p53* gene, is linked in OS advancement and occurs due to mutation of the gene locus at 17p13.1 (Martin et al., 2012). Thus, OS is often characterised as having extensive genomic instability, uncontrolled apoptosis, uncontrolled cell cycle, and lack of differentiation ability (Martin et al., 2012; Varshney et al., 2016).

p53 is a tumour suppressor that is responsible in cell cycle regulation by controlling DNA repair and has a crucial role in regulating apoptosis. Therefore, it is not a surprise that the expression of mutant *p53* could modify cellular resistance to DNA damage (Hansen, 2002). *p53* mutation occurs frequently in human cancers and mutation of *p53* increased the risk in cancer development. For example, individuals with Li-Fraumeni syndrome, a disease associated with germline *p53* mutations, have higher chance of OS incidence (Hansen et al., 1985; Malkin, 1993; Fuchs and Pritchard, 2002).

Many genomic rearrangements have been distinguished in OS using genomic and transcriptomic analysis, such as rearrangements of TP53, RB1, CDKN2A and MDM2, as well as PMP22–ELOVL5 gene fusions (Stephens et al., 2011; Kansara et al., 2014; Chen et al., 2014). Lorenz et al. reported that TP53 rearrangements are the major mechanism of *p53* inactivation in OS (Lorenz et al., 2016).

Two well established osteosarcoma cell lines, G-292 and Saos-2, were used in this project. G-292 clone A141B1 cell line was established from a

primary osteosarcoma of a 9-year-old Caucasian female (Chandar et al., 1992; Zhang et al., 1995). Saos-2 cell line was among the earliest generated OS cell lines and was frequently used for OS studies. Saos-2 cell line has been derived from the primary osteogenic sarcoma of an 11-year-old Caucasian female since 1973 (Niforou et al., 2006). These two cell lines showed deletion and rearrangement in *p53* expression, with G-292 consist of rearrangement in the first intron of the *p53* gene, while Saos-2 exhibited deletion in *p53* gene (Chandar et al., 1992; Zhang et al., 1995).

2.2 Induced pluripotent stem cells

In 2006, Takahashi and Yamanaka established a novel method of reprogramming adult terminally differentiated cells to pluripotency which is less controversial. This new breakthrough involved the use of retroviral OSKM transcription factors (Takahashi and Yamanaka, 2006) into the target cells. In their study, they narrowed down to these 4 transcription factors from 24 candidate genes. Different variants of the 4-factor combination have shown success in reprogramming other cell types (Maherali et al., 2007; Wernig et al., 2007; Okita et al., 2008; Stadtfeld et al., 2008). The reprogrammed cells have been termed “induced pluripotent stem cells or iPSC”.

2.2.1 Application of iPSC

Induced pluripotent stem cells (iPSC) have gained a lot of attention due to the enormous promising potential these cells hold. Personalised cellular therapy has been made possible with this novel approach. Adult somatic cells could be reprogrammed to an embryonic stem cell (ESC)-like status genetically by expressing genes and factors crucial for governing the characteristics of ESC. Hypothetically, iPSC can be reprogrammed and induced to differentiate into various clinically useful cell types for regenerative medicine including haematopoietic stem cells (HSC), blood cells, platelet, immune cells and other somatic cells. The use of iPSC-derived cell types may gain optimal clinical benefit as the likelihood of immune rejection should be greatly reduced because of the genetic similarity of the iPSC to the individual from whom they were derived.

The advantages of generation of iPSC are (i) tissues derived from iPSC could be used to avoid probable immune rejection as iPSC-derived cells or tissues are almost similar donor cell; (ii) customised transplantation therapy; (iii) valuable to be used for understanding of disease mechanisms, as well as to screen drugs; (iv) use of ESC faces ethical controversies and it is impractical to produce patient-specific or disease-specific ESC, which are essential for their successful application.

The iPSC technology also spearhead and provided a different kind of human *in vitro* drug screening platform by offering other methods to screen

agents and compounds for safety and efficacy. The increasing amount of human disease iPSC models produced using patient-specific cells has opened the opportunity to conduct studies on a wide range of ailments, including rare diseases. Drug toxicity and drug advance reaction assays conducted with cells derived from diseased-specific iPSC can deliver extra level of safety prior to advancing to clinical trials. The incorporation of iPSC technology into drug developmental studies holds great potential for personalised medicine (Ko and Gelb, 2014).

Apart from undergoing genome transcriptional changes, reprogrammed cells also reorganise their epigenetic patterns, including DNA methylation and histone modifications to ES cell-like status (Papp and Plath, 2011). However, the level and distribution of histone modifications and DNA methylation show some differences between ES and iPS cells, which may be contributed by epigenetic memory of reprogrammed cells (Hawkins et al., 2010). iPS cell line could demonstrate epigenetic memory of the initial cell types by efficiently differentiate into cell type of origin, but showed decreased competency to differentiate into other lineages (Kim et al., 2010). This epigenetic memory is essential for disease modelling in generating primitive cell type that harbour the intrinsic information of the disease.

Aggressive tumour cells are similar with multipotent progenitors as they share various stem cell-like characteristics, contributing to the concept of tumour cell plasticity. Studies involving transplantation of tumour cells into embryo models, have revealed the possibility to control and regress the

metastatic phenotype, further suggesting future potential effort in identifying innovative targets for medical intervention derived from integrative work of tumourigenic and embryonic signals. The application of developmental principles in the study of cancer biology has the potential to create new perspectives on tumour cell plasticity (Kasemeier-Kulesa et al., 2008).

2.3 Reprogramming of cancer cells

Since the introduction of iPSC from somatic cells, researchers in cancer field are interested to investigate this novel dedifferentiation method on cancer cells. Recent discoveries have shown that high grade tumour, which are usually poorly differentiated, also over-express human ESC genes, such as *OCT3/4*, *SOX2*, and *NANOG* transcription factors (Linn et al., 2010; Samardzija et al., 2012).

2.3.1 Application of cancer reprogramming

Disease-specific cells may be reprogrammed and re-differentiated to any specific cell types. This disease-specific iPSCs are capable of recapitulating the disease phenotype to generate the *in vitro* model of specific disease in the laboratory for disease modelling or gene therapy approaches. Successful examples include amyotrophic lateral sclerosis (ALS) (Dimos et al., 2008) and Huntington's disease (Zhang et al., 2010) for disease modelling as well as

sickle-cell anemia (Hanna et al., 2007) and α 1-anti-trypsin deficiency (Yusa et al., 2011) for gene correction.

Lin et al. reported in 2008 that by using miR-302 family, they could reprogrammed human skin cancer cells, melanoma, into a pluripotent condition (Lin et al., 2008). Lin et al. suggested that discovering the mode that stem cells replace transcriptional regulators involved in cancer-related mechanism may bring to innovative discovery in cellular and cancer treatment. Miyoshi and team also reprogrammed gastrointestinal cancer cells using defined factors (Miyoshi et al., 2010). Miyoshi et al. anticipate that previously undefined cancer treatments could be assessed with the introduction of induced pluripotent cancer (iPC).

Zhang et al. reprogrammed 5 sarcoma cell lines using lentiviruses expressing OSKM plus *LIN28* and *NANOG*. Their results suggested that the tumorigenicity of the parental sarcoma cells can be retracted by generation of terminally differentiated cells from reprogrammed sarcomas. Further genetic and epigenetic analysis revealed that the sarcoma cell lines were reprogrammed back to a pre-mesenchymal stem cell and partially reprogrammed fibroblast state. This partial or incomplete reprogramming status appears to be sufficient to restore the capacity to attain terminal differentiation in multiple lineages (Zhang et al., 2013).

Recent experiment on glioblastoma iPSC (GiPSC) to study malignancy after reprogramming showed that while the cells remained malignant post-

reprogramming, malignancy of GiPSC was successfully suppressed when differentiated into mesodermal lineages (Stricker et al., 2013).

In pancreatic ductal adenocarcinoma (PDAC) reprogramming to pancreatic intraepithelial neoplasia lesions (PanIN), the study showed progression to an aggressive form of PDAC when PDAC-iPSC was injected into immunodeficient mice (Kim et al., 2013). The PanIN-like cells secreted various proteins which were involved in the human pancreatic cancer progression. Furthermore, a number of these proteins were found to be linked to the HNF4 α transcription factor network. Since the expression of HNF4 α has never been reported previously in PDAC development or progression, reprogramming of PDAC enable the discovery of this HNF4 α network activation in early-to-intermediate stage of pancreatic cancer.

In a recent study, patient-derived iPSCs have been generated to model Li–Fraumeni syndrome (LFS)-associated bone cancer development, revealing the usefulness of iPSCs as an *in vitro* disease model to understand OS aetiology (Lee et al., 2015). They derived osteoblast (OB) from LFS iPSC and these LFS iPSC-derived OB displayed well-defined OS gene expression signature that strongly correlate with clinical prognosis. This study indicated the possibility of reprogramming somatic cells from LFS patients to a pluripotent state and used to study inherited human cancer syndromes with iPSCs.

A study conducted by Zeng et al. showed generation of iPSCs from a RB patient carrying a heterozygous RB1 (S888A) mutation (Zeng et al., 2016).

Even though RB-iPSCs expressed pluripotency markers by RT-PCR and immunofluorescence, as well as demonstrating capability of differentiation to all germ layers via EB formation, no investigations on pathological and/or mechanistic aspect were conducted in this study (Zeng et al., 2016).

Combining molecular information collected from these iPSC models with the present knowledge of OS biology will assist us in gaining deeper understanding of the pathological mechanisms triggering osteosarcomagenesis, which will eventually aid in the prospective development of future OS therapies. Therefore, elucidation of individuallised OS-associated gene functions to investigate the potential pathological mechanisms involved in stages of OS development: initiation and progression; is vital for future OS detection and treatment (Figure 2.1).

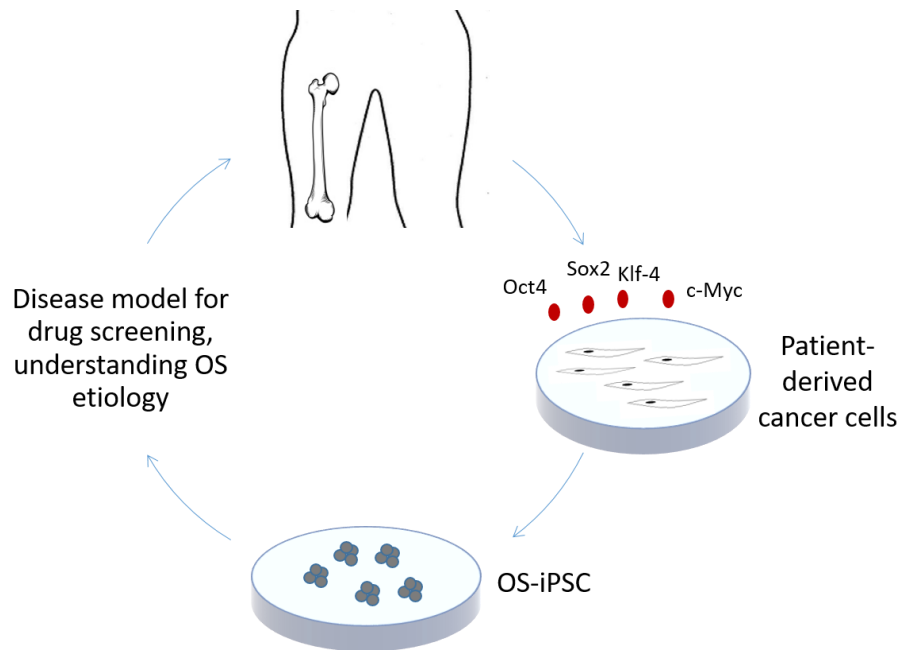


Figure 2.1. Application of iPSC technology. Reprogramming of patient-derived cancer cells could be utilised for disease modelling and drug screening.

2.4 DNA damage response (DDR)

Three main mechanisms cover DNA damage response, which are: DNA repair, cell-cycle checkpoint control, and DNA damage-induced apoptosis. Collectively these mechanisms work together to promote genomic integrity and suppress tumorigenesis. As DNA is the storehouse of genetic material in each cell, it is important to govern its integrity and stability. The ability to repair DNA damage in cells is regarded as an important process to protect genome integrity. Cells use different DNA repair mechanisms to repair the damage when it locates the damaged site. The well-known DNA repair mechanisms are single-strand damage and double-strand breaks. In single-strand damage, excision repair mechanisms help to remove the damaged or broken nucleotide and replace it with a new nucleotide complementary to the other undamaged DNA strand; such as base excision repair (BER), nucleotide excision repair (NER) and mismatch repair (MMR). Three mechanisms exist to repair double-strand breaks (DSBs): non-homologous end joining (NHEJ), microhomology-mediated end joining (MMEJ), and homologous recombination (Wood et al., 2001).

2.4.1 DNA damage response in pluripotent cells

Pluripotent cells, such as stem cells, have explicit DNA repair mechanism needs due to their extraordinary capacity of self-renewal and differentiation into different cell types. Owing to this, the DNA repair network in human stem cells

is highly efficient that slowly becomes less effective upon differentiation (Kenyon and Gerson, 2007; Rocha et al., 2013).

The ability to reprogram a somatic cell to pluripotency has also brought up the question on whether the induced pluripotent stem cells possess the same DNA repair mechanism as embryonic stem cells. Armstrong et al. demonstrated the oxidative stress resistance and mitochondrial biogenesis of human iPSC cell lines are similar to human ESC (Armstrong et al., 2010). Their study showed that human iPSC clones reduced their mitochondrial genome copy number to the levels typical of human ESC and were capable of mounting a similar oxidative stress defense to human ESC.

Luo et al. studied the DNA repair mechanism and genomic instability via microsatellite assay in human pluripotent stem cells in comparison with non-pluripotent human cells (Luo et al., 2012). The team found that pluripotent cells possess greater DNA repair abilities and this ability was more heterogeneous than the differentiated cell lines tested. Apart from that, the team also recommended the importance of assessing pluripotent cells for DNA repair defects when they found an iPSC line that showed a normal karyotype, but also demonstrated reduced DNA repair abilities and microsatellite instability. Thus, Luo et al. suggested the need to perform DNA repair assessment in pluripotent cells, with the aim of characterising their genomic stability status, before any usage in pre-clinical or clinical.

2.4.2 DNA damage response in OS

Cancer cells may employ different mechanisms to develop resistance to chemotherapeutic agents. Depending on the cellular setting, different mechanisms such as drug inactivation, decreased drug uptake, up- and down-regulation of the drug target, increased DNA damage repair and drug elimination have all been associated to contribute to both intrinsic and acquired resistance to chemotherapy (Gottesman, 2002).

In OS, several DNA repair pathways, for example the nucleotide excision repair (NER) pathway, can defend OS cells from the adverse effect of oxidative DNA damage. Variation in genes and proteins can cause enhanced DNA repair and result in failure of apoptotic pathways induced by the chemotherapy agents (Vos, 2016).

Expression of DNA damage genes were shown in a few studies to be elevated in OS. In one of the study on base excision repair (BER), showed one of the main enzymes within the BER pathway, which is the human apurinic endonuclease 1 (APE1), to be elevated in OS samples and by using APE1-silencing RNA (siRNA) targeting technology to decrease the expression of *APE1* in OS cell lines, it provided a window of opportunity to sensitise OS cells to alkylating and oxidative ionizing radiation and chemotherapeutic agents (Wang et al., 2004).

Murine double minute 2 homolog (MDM2) is an oncoprotein that attaches to p53 and negatively regulate p53, thus restraining DNA damaging agents to initiate p53 activation (Fuchs and Pritchard, 2002). Referring to OS, high expression of MDM2 gene was linked to OS progression and metastasis (Ladanyi et al., 1993; Sigal and Rotter, 2000). Furthermore, p53 and MDM2 pathways are often mutated in OS (Lonardo et al., 1997). Thus, this affected the DNA damage response mechanism and efficiency in OS.

2.4.3 Nucleotide Excision Repair (NER)

Nucleotide excision repair (NER) is a highly flexible and versatile DNA repair mechanism as it is responsible for an extensive range of DNA lesions. NER operates to eliminate of any lesions that deform the DNA double helix, or obstruct in base pairing and hinder DNA duplication and transcription. The most frequent examples of these lesions are the cyclobutane pyrimidine dimers (CPDs) and 6-4 photoproducts (6-4 PPs), the two foremost forms of injuries induced by ultraviolet (UV) light (Costa et al., 2003).

The NER pathway comprises at least four steps: (a) DNA damage identification by a protein complex which consist of xeroderma pigmentosum complementation group C (XPC); (b) loosening of the DNA double helix by the transcription factor IIIH (TFIIH) complex that involves xeroderma pigmentosum complementation group D (XPD); (c) elimination of the damaged site by an excision-repair cross-complementing 1 (ERCC1) and xeroderma pigmentosum

complementation group F (XPF) complex; and (d) synthesis of new complementary nucleotide by DNA polymerases (Costa et al., 2003) (Figure 2.2).

Association of NER genes polymorphisms which will eventually affect cisplatin efficacy, have been inspected by a large number of studies. A total of twelve studies have taken into account the variants of NER genes and the effect of these variants in the response to cisplatin (Caronia et al., 2009; Zhang et al., 2012; Teng et al., 2013; Zhang et al., 2015; Goričar et al., 2015; Wang et al., 2015).

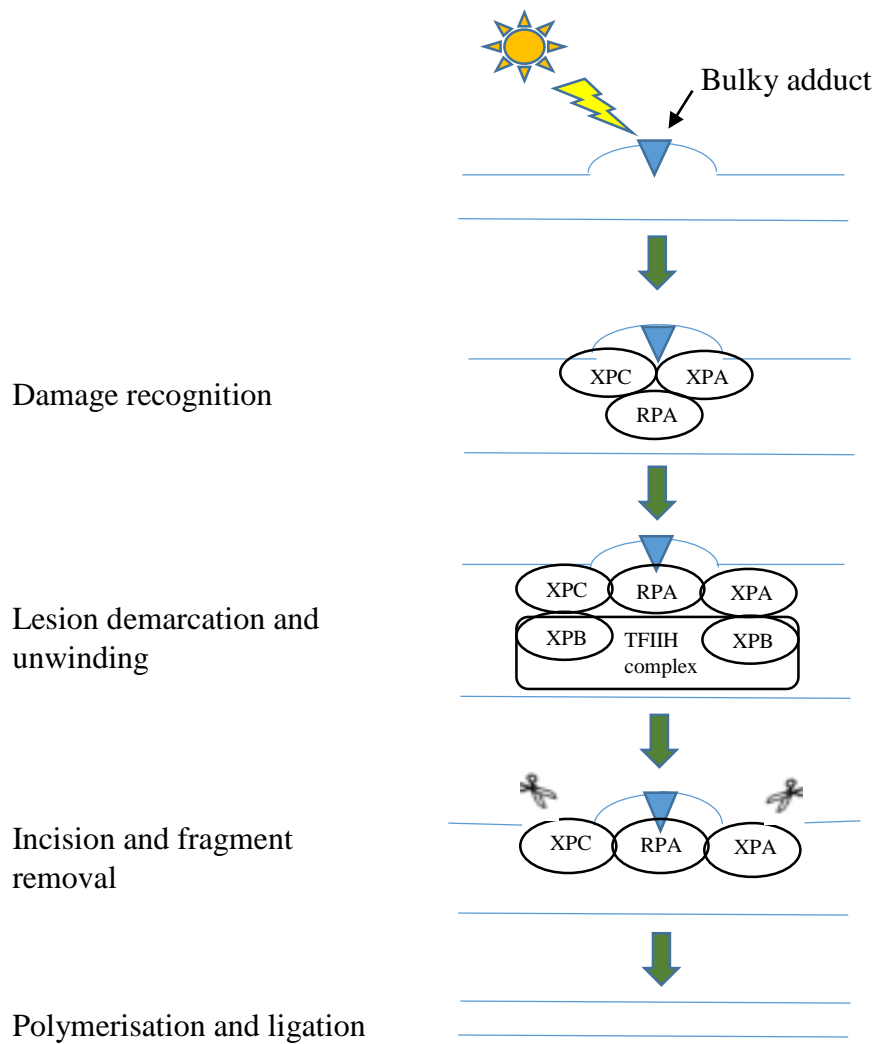


Figure 2.2. Nucleotide excision repair (NER) mechanism. NER acts on larger lesions or adducts and includes lesion identification, formation of the TFIIH complex, unwinding, incision and fragment removal of 25–30 nucleotide before polymerisation and ligation to repair damaged site.

CHAPTER 3

MATERIALS AND METHODS

3.1 Overview of Methods

Osteosarcoma reprogramming was conducted on two osteosarcoma (OS) cell lines, G-292 and Saos-2. Both G-292 and Saos-2 were purchased from American Type Culture Collection (ATCC) (Manassas, USA). Commercially available 293FT cell line (human embryonal kidney cells) (Thermo Fisher Scientific, USA) was used in retroviral transfection due to its highly transfectable characteristics. Embryonic stem cells (ESC), BG01V, was purchased from ATCC and used as positive control for immunofluorescence staining, Quantitative Real-Time PCR (qPCR) and teratoma study. Osteosarcoma reprogramming was generated through retroviral transduction of four transcription factors and co-cultured on mouse embryonic fibroblast (MEF) feeder layer (Merck Millipore, Darmstadt, Germany). Prior to reprogramming, 293FT cells were used to produce supernatant containing retroviral vectors of four transcription factors (OCT3/4, SOX2, KLF4 and cMYC, namely OSKM). The efficiency of transfection was monitored with green fluorescent protein (GFP) vector. 3 days after reprogramming, transduced OS cells were transferred to mitotically inactivated MEF (iMEF) and were observed for colonies formation. Reprogrammed OS cells were characterised by morphology, expression of pluripotent markers, ability to form embryoid body, ability to

differentiate into three germ layers *in vitro* and teratoma formation. Putative ESC-like colonies (iPSC) were cultured on feeder layers for more than 5 passages. Global gene expression were conducted using Affymetrix Human PrimeView Chip (Affymetrix, CA, USA) on both the parental and reprogrammed cells. GeneSpring GX 13.0 software (Agilent Technologies, CA, USA) was used to analyse the microarray data. Highly differentially expressed genes involved in DNA damage response (DDR) pathways were identified and validated with Taqman Gene Expression (Applied Biosystems, USA) qPCR system. Functional assay, which is UV irradiation assay, was applied to both parental and reprogrammed cells to check the status of DNA repair in respective cells. Expression of the genes related in DNA repair mechanism were further detected using qPCR. An overview of the research methodology is shown in Figure 3.1.

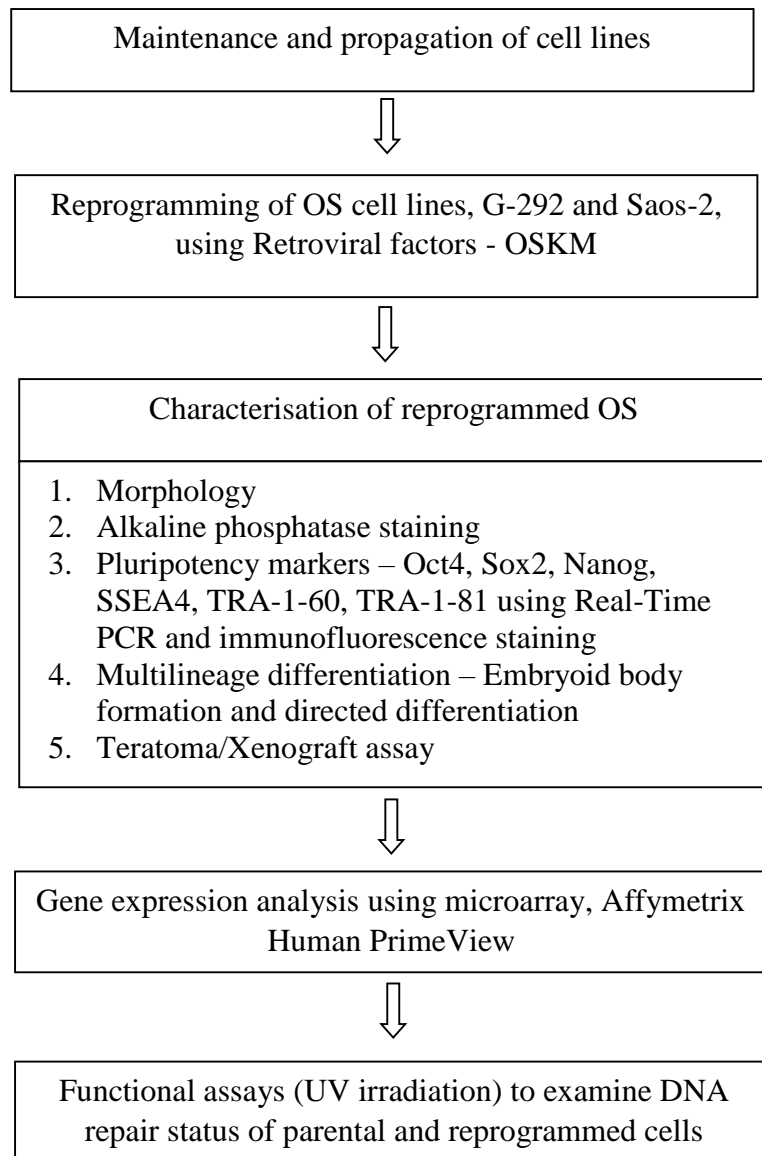


Figure 3.1. Flow chart of research methodology of the study.

3.2 Generation of iPSC from OS cell lines

3.2.1 Osteosarcoma (OS) Cell Lines

Two OS cell lines, G-292 and Saos-2 were purchased from American Type Culture Collection (ATCC, USA). G-292 cell line was derived from the bone of a 9 year old Caucasian female. G-292 cells exhibited fibroblastic morphology and was adherent in culture flask. Saos-2 cell line was derived from the bone of an 11 year old Caucasian female. Saos-2 cells exhibited osteoblast-like morphology and was adherent in culture flask. Both G-292 and Saos-2 cells are mutated in *p53* expression.

3.2.2 Culture of OS Cell Lines

Cryopreserved vials were removed from liquid nitrogen and thawed with gentle agitation in 37 °C water bath (Mettler, Germany). Both vials were handled in aseptic technique using 70% ethanol and all cell culture procedures were done in a Class II Biosafety cabinet (ESCO, Singapore). Approximately 1×10^6 thawed cells were transferred into 15 ml conical tubes with 9 ml of culture medium according to the cell type and were centrifuged at 300 x g for 5 minutes. Medium composition for both OS cells are summarised in Table 3.1 and Table 3.2. After centrifugation, medium was discarded without disturbing the cell pellet and the pellet was resuspended in 10 ml of fresh complete medium by gentle pipetting. OS cells were then

seeded evenly at a ratio of 1:3 in T75 culture treated flask and incubated in an incubator at 37 °C in a 5% CO₂. Cells were monitored daily using EVOS XL Cell Imaging System (Invitrogen, USA). The medium was changed every two days and subculturing was done once the cells reached 90% confluency. Subculturing procedure was conducted using 0.25% Trypsin-EDTA (Gibco, USA) at a ratio of 1:4. Briefly, medium was discarded and 3 ml of 0.25% Trypsin-EDTA was added to the flask. Cells were observed under microscope until cell layer is dispersed. 6 ml of complete medium was added to the flask, cells were aspirated with gentle pipetting and reseeded at 1:4 in new culture flasks. Cells were returned to incubator for further culture.

Table 3.1: Medium composition of OS medium for G-292 in 500 ml

Medium composition	Working Concentration	To prepare 500 ml medium
McCoy's 5a	89%	445 ml
Fetal Bovine Serum	10%	50 ml
Penicillin- Streptomycin	1%	5 ml

Table 3.2: Medium composition of OS medium for Saos-2 in 500 ml

Medium composition	Working Concentration	To prepare 500 ml medium
DMEM/F12	88%	440 ml
Fetal Bovine Serum	10%	50 ml
L-glutamine	1%	5 ml
Penicillin- Streptomycin	1%	5 ml

3.2.3 Culture of 293FT Cell Line

Approximately 1×10^6 thawed 293FT cells were transferred into 15 ml conical tubes with 9 ml of DMEM high glucose (Gibco, USA) supplemented with 10% FBS, 1% penicillin/streptomycin, 1 mM sodium pyruvate 100x, 6 mM L-glutamine 100x, 0.1 mM non-essential amino acid (NEAA 100x) and 50 ug/ml Geneticin 100x (Gibco, USA). Medium composition for 293FT cells is summarised in Table 3.3. Tubes containing 293FT cells were centrifuged at $300 \times g$ for 5 minutes to pellet down the cells. Medium was discarded without disturbing the cell pellet and the pellet was resuspended in 10 ml of fresh complete medium by gentle pipetting. 293FT cells were then split evenly at a ratio of 1:3 in T75 culture treated flask and incubated in an incubator at 37°C in a 5% CO_2 . Cells were monitored daily using EVOS XL Cell Imaging System (Invitrogen, USA). The medium was changed every two days and subculturing was done once the cells reached 90%

confluency. Subculturing procedure was conducted using 0.25% Trypsin-EDTA (Gibco, USA) at a ratio of 1:4.

Table 3.3: Medium composition of 293FT medium in 500 ml

Medium composition	Working Concentration	To prepare 500 ml medium
DMEM high glucose	85%	425 ml
Fetal Bovine Serum	10%	50 ml
L-glutamine	1%	5 ml
Penicillin- Streptomycin	1%	5 ml
Sodium Pyruvate 100x	1 mM	5 ml
NEAA 100x	0.1 mM	5 ml
Geneticin, 50 mg/ml	500 µg/ml	5 ml

3.2.4 Culture and Inactivation of Mouse Embryonic Fibroblast (MEF)

Feeder Layer

Approximately 5×10^6 MEF cells (Merck Millipore, Germany) were thawed and transferred into 15 ml conical tubes with 9 ml DMEM high glucose supplemented with 15% FBS and 1% penicillin/streptomycin (Gibco, USA). Medium composition for MEF cells is summarised in Table 3.4. Tubes containing MEF cells were centrifuged at $300 \times g$ for 5 minutes to pellet down the cells. After centrifugation, medium was discarded without disturbing the

cell pellet and the pellet was resuspended in 10 ml of fresh complete medium by gentle pipetting. MEF cells were then seeded evenly at a ratio of 1:6 in 100 mm culture treated dish and incubated in an incubator at 37 °C in a 5% CO₂. Cells were monitored daily using EVOS XL Cell Imaging System (Invitrogen, USA). The medium was changed every two days and subculturing was done once the cells reached 90% confluency. Subculturing procedure was conducted once using 0.25% Trypsin-EDTA (Gibco, USA) at a ratio of 1:2.

Mitotically inactivation of MEF cells was done using 10 µg/ml of Mitomycin-C (Calbiochem, Merck, Germany). MEF cells was cultured in 100 mm culture treated dish. When MEF reached 80-90% confluency, 100 µl of 1 mg/ml Mitomycin-C was added into the culture dish and incubated at 37 °C in 5% CO₂ for 2-3 hours. After 2-3 hours of incubation, MEF was washed at least 3 times to remove residues of Mitomycin-C. Inactivated MEF (iMEF) was harvested by trypsinisation and cell count was performed in a hemacytometer. iMEF was seeded at a density of 2×10^5 cells per well in a 6-well plate precoated with 0.1% gelatin. iMEF was incubated at 37 °C in a 5% CO₂ incubator at least one day before being used as feeder layer.

Table 3.4: Medium composition of MEF medium in 500 ml

Medium composition	Working Concentration	To prepare 500 ml medium
DMEM high glucose	84%	420 ml
Fetal Bovine Serum	15%	75 ml
Penicillin- Streptomycin	1%	5 ml

3.2.5 Culture of Human Embryonic Stem Cells (hESC), BG01V, Cell Line

Cryovial containing hESC (ATCC, USA) was thawed with gentle agitation in 37 °C water bath. Immediately after thawed, the cells were transferred into a 15 ml conical tube and 9 ml of hESC medium was added in a dropwise manner. Medium composition of hESC is summarised in Table 3.5. The tube was centrifuged at 300 x g for 5 minutes and supernatant was discarded. 2 ml of hESC medium was added gently into the tube and the bottom of the tube was gently flicked to dislodge the colonies from the pellet. hESC colonies were transferred into a fresh well coated with iMEF (feeder layer) and Rho-associated, coiled-coil containing protein kinase (ROCK) inhibitor (Sigma-Aldrich, USA) was added into the well of a 6-well plate. Final concentration of ROCK inhibitor in each well was 10 mM. hESC colonies were cultured at 37 °C in a 5% CO₂ incubator. Medium was changed every day and colonies were monitored using EVOS XL Cell Imaging System (Invitrogen, USA).

Passaging of hESC colonies were done manually under aseptic technique in a laminar flow hood (ESCO, Singapore). hESC colonies were identified and marked with a marking tool under Eclipse TS100 inverted microscope (Nikon, Japan). Identified colonies were manually cut under stereomicroscope (Olympus, Japan) into grids by using a sterile scalpel. By using a P200 pipette with tips, each grid was slowly and carefully picked and transferred to a fresh well of a 6-well plate coated with iMEF. hESC colonies were cultured at 37 °C in a 5% CO₂ incubator.

Table 3.5: Medium composition of hESC medium in 500 ml

Medium composition	Working Concentration	To prepare 500 ml medium
DMEM/F12	78%	390 ml
Knock-out Serum Replacement	20%	100 ml
Non-essential Amino Acid 100x	0.1 mM	5 ml
L-Glutamine 100x	4 mM	5 ml
B-Mercaptoethanol 14.3 M	0.1 mM	35 µl
Human Fibroblast Growth Factor, 50 µg/ml	10 ng/ml	100 µl
Penicillin-Streptomycin	0.1%	500 µl

3.3 Bacteria Culture Media

3.3.1 Lysogeny Broth (LB) Agar Plate

Lysogeny broth (LB) agar plate contained medium commonly used to grow *Escherichia coli* (*E.coli*), DH5-Alpha strain (Invitrogen, USA). 5 g of commercial LB powder supplemented with tryptone, yeast extract and sodium chloride (NaCl) (Sigma-Aldrich, USA) was weighed and put into a flask containing 250 ml of double distilled water. 3.75 g of agar (Sigma-Aldrich, USA) was added into the flask. The mixture was autoclaved at 121 °C for 20 minutes and cooled to 55 °C – 60 °C in a water bath. Ampicillin (Gibco, USA) was added into LB agar medium at a concentration of 50 µg/ml. Then, LB agar medium was decanted into sterile 100 mm petri dishes and allowed to polymerise. LB-Ampicillin agar plates were covered with aluminium foil before storage at 4 °C to prevent possible degradation of antibiotics. Preparation was performed in a laminar hood (ESCO, Singapore).

3.3.2 Lysogeny Broth (LB) Media

Lysogeny broth (LB) medium was commonly used in the culture of *E. coli*. For the medium preparation, 3.75 g of LB powder (Sigma-Aldrich, USA) was dissolved in 250 ml of double distilled water in a 500 ml flask. The medium was autoclaved at 121 °C for 20 minutes and cooled to 55 °C – 60 °C

in a water bath. Ampicillin was added into the LB medium at a concentration of 50 µg/ml and prepared medium was stored at room temperature (RT).

3.3.2.1 Antibiotic Selective Marker

Ampicillin was used as a selection marker in this experiment. The transformed *E. coli* expressed ampicillin resistance gene and were allowed to grow in the medium with the antibiotic. For the stock preparation of Ampicillin, 50 mg of Ampicillin was dissolved in 1 ml of double distilled water. The mixture was filtered and stored at -20 °C. The working concentration of Ampicillin used for culturing of plasmids was 50 µg/ml.

3.3.3 Preparation of Plasmid pMX-Retroviral Vector

3.3.3.1 Retrieval of Plasmids

pMX-based retroviral vectors, hOCT4 (Plasmid 17217) (Addgene), hSOX2 (Plasmid 17218) (Addgene), hKLF4 (Plasmid 17219) (Addgene), hc-MYC (Plasmid 17220) (Addgene), retroviral gag-pol packaging plasmid (Plasmid 8449) (Addgene), VSV-G expression plasmid (Plasmid 8454) (Addgene) and pMX-GFP (Plasmid) (Addgene) used in this experiment were generously provided by Dr. Shigeki Sugii, DUKE-NUS Graduate Medical School, Singapore. The plasmids were retrieved from glycerol stock from -80 °C freezer. Plasmid vectors from respective glycerol stock were streaked on

LB agar plate treated with ampicillin (Sigma-Aldrich, USA) using an inoculum loop. LB agar plates were pre-incubated overnight at 37 °C. Streaked plates were incubated not more than 16 hours due to the overgrowth stage of the bacteria after 16 hours. After 16 hours of incubation, colonies were picked for liquid culture in LB Broth. Plasmids map and other details are attached in Appendix A-G.

3.3.3.2 Storage of Transformed Plasmids

A single colony of *E. coli* from the streaked LB-Ampicillin plate was picked and cultured in 3-5 ml of LB-Ampicillin medium in a 15 ml conical tube at 37 °C, overnight (approximately 16 hours). Conical tubes containing transformed *E. coli* were placed in shaking incubator (IKA, China) at a speed of 300 rpm. Plasmids stocks were made with 200 µl of sterile glycerol and 800 µl of transformed *E. coli* into cryovials. To ensure homogeneous mixture, the cryovials were vortexed vigorously before freezing at -80 °C.

3.3.3.3 Plasmid Extraction

A single colony from the LB-Ampicillin agar plate of each plasmid was inoculated into 3 ml LB-Ampicillin medium in a 15 ml conical tube. At least 3 replicates were made to determine the growth ability of each colony. The *E. coli* cultured tubes were incubated at 37 °C in a shaking incubator (approximately 300 rpm) (IKA, China). Colony that grew well in the 15 ml tube was selected based on the cloudy haze LB-Ampicillin medium. 250 µl –

500 µl from 3 ml LB-Ampicillin medium containing well grown transformed *E. coli* was transferred into 250 ml LB-Ampicillin medium and incubated overnight at 37 °C in shaking incubator for culture expansion. Depending on the copy numbers of plasmid, about 250-500 ml of medium with well grown transformed *E. coli* was centrifuged to pellet the bacteria prior to plasmid extraction. Plasmid extraction was performed using PureLink® HiPure Plasmid Filter Maxiprep Kit (Invitrogen, USA) according to manufacturer's protocol. For high copy number plasmids, 100-200 ml of an overnight LB-Ampicillin culture per sample was sufficient while for low copy number plasmids, 250-500 ml of an overnight LB-Ampicillin culture per sample was needed. After centrifugation at 4000 x g for 10 minutes, excessive supernatant was discarded without disturbing the pellet. Each vector was extracted respectively according to PureLink ® protocol. Briefly, 10 ml of Resuspension Buffer (R3) with RNase A was added to the pellet and cells were resuspended till homogeneous. RNase A is included to degrade cellular RNA when the cells are lysed. Next, 10 ml of Lysis Buffer (L7) containing sodium dodecyl sulfate (SDS), to solubilise the cell membrane, and sodium hydroxide (NaOH) to break down the cell wall, was added into the mixture. NaOH helps to disrupt the hydrogen bond between the DNA bases, transforming the double-stranded DNA (dsDNA) in the cell, including the genomic DNA (gDNA) and plasmid, to single stranded DNA (ssDNA). This process is called denaturation. The mixture was gently inverted until the lysate mixture was thoroughly homogeneous before incubation at RT for 5 minutes. It is important to be gentle during the lysis step because vigorous mixing or vortexing will shear the genomic DNA producing shorter sections of DNA

that can re-anneal and contaminate the plasmid prep. Then, 10 ml Precipitation Buffer (N3) was added to neutralise and precipitate the lysate. At this step, the mixture was mixed by gentle inversion of the tubes but not vortexed until the mixture was thoroughly homogeneous. The mixture was centrifuged at 12,000 x g for 10 minutes at RT. Supernatant from the centrifugation was loaded onto the equilibrated column and allowed to drain by gravity flow. The column was washed with 60 ml Wash Buffer (W8) and the excess flow-through was discarded. For elution and precipitation of DNA, 15 ml Elution Buffer (E4) was added to the column to elute the plasmid DNA by gravity flow. The elution tube contains the purified plasmid DNA and the column was discarded. Following this, 10.5 ml isopropanol was added to the elution tube. Isopropanol was used to precipitate the plasmid DNA which was subsequently pelleted by centrifugation at 12,000 x g for 30 minutes at 4 °C. Upon centrifugation, supernatant was carefully discarded and DNA pellet was resuspended in 5 ml 70% ethanol to remove any salt content of the extraction. Elution was centrifuged again at 12,000 x g for 5 minutes at 4 °C and the supernatant was discarded leaving behind the DNA pellet. The DNA pellet was air-dried for 10 minutes prior to resuspension in 300 µl of TE Buffer (TE). Plasmid DNA of each vector was transferred into labelled 1.5 ml microcentrifuge tubes. Concentration and purity of the DNA plasmids were measured by NanoPhotometer UV/Vis spectrophotometer (Implen, Germany). The ratio of A260/A280 for pure plasmid DNA was achieved in the range of 1.8-2.0. Plasmid concentration and purity are summarised in Appendix H.

3.3.4 Verification of Plasmids

3.3.4.1 Restriction Enzyme (RE)

Restriction enzyme method was used to confirm the identity of the plasmids. Different lengths of DNA fragments generated by restriction digest produce an explicit pattern of bands upon gel electrophoresis, and can be used for plasmid fingerprinting. Two types of restriction enzymes (RE) were utilised as the plasmids varies in restriction enzyme recognition sequences. Restriction enzyme reaction mixtures were summarised in Table 3.6. Types of RE and plasmid DNA (OSKM) sizes are detailed in Appendix I. Approximately 0.2 µg of each plasmid was needed for restriction digestion. The master mixes were prepared according to manufacturer's protocol (Invitrogen, USA) before adding into each plasmid DNA. The solution was mixed thoroughly, spun down and incubated at 37 °C in a water bath for 5-15 minutes to digest the DNA.

Table 3.6. Reaction mixtures of restriction enzyme

Component	Volume (µl)
Water, nuclease-free	15
10x FastDigest Buffer	2
FastDigest enzyme	1
Plasmid DNA (~0.2 µg)	2
Total	20

3.3.4.2 Gel Electrophoresis

Agarose gel electrophoresis was performed to identify the restriction enzyme product size of each vector. 1% agarose gel was prepared by dissolving 1 g agarose powder (SeaKem® LE, Lonza, Switzerland) in 100 ml of 1x TAE buffer. Agarose solution was heated in microwave for 2 minutes until all agarose powder had completely dissolved and was let to cool to 70 °C in a water bath. Casting tray and comb were rinsed and dried prior to use. 25-30 ml agarose was poured into the clean casting tray with comb and let to solidify at RT. After the agarose gel solidified, the comb was removed slowly without breaking the gel. The entire tray with the gel was placed in an electrophoresis tank, filled with 1x TAE buffer (Tris-acetate-EDTA) (Invitrogen, USA). 10 µl of digested plasmid DNA was mixed with 2 µl of 6x loading dye (Amresco, USA) and loaded into the wells of the agarose gel. The digested DNA was run on 1% agarose gel electrophoresis at 80 V for 45 minutes with 1 kB DNA ladder as marker. The agarose gel was subjected to visualisation under ultraviolet light (UVPLLC, USA) and gel image was captured.

3.3.5 Retroviral packaging

Retrovirus belongs to the viral family of *Retroviridae*. *Retroviridae* is a family of enveloped viruses that reproduce in a host cell through reverse transcription. Retrovirus consists of a single strand RNA molecule with a

DNA intermediate. Once the virus gets inside the host cell cytoplasm, the virus uses its own reverse transcriptase enzyme to produce DNA from its RNA, thus this created the name *retro*. Retrovirus are able to bind to a host cell because its membrane contain glycoproteins, which bind to a receptor protein on a host cell. Retrovirus also consists of proteins such as gag proteins, pol proteins and env proteins. Group-specific antigen (gag) proteins are major constituents of the viral capsid, while the Pol proteins are accountable for synthesis of viral DNA and integration into host DNA after infection. Env proteins, such as VSV-G, play an important role in association and entry of virus into the host cell. GAG-POL and VSV-G genes were integrated into packaging cell line (293FT) to produce vectors that deliver all the viral proteins needed for capsid production and virion maturation of the vector (Johnson and Telesnitsky, 2010). The 293FT cell lines (human embryonic kidney cells) were used to package retroviruses containing GFP and four Yamanaka (O/S/K/M) vectors.

3.3.5.1 Transfection for Retrovirus: Green Fluorescent Protein (GFP)

All procedure involving active virus supernatants or concentrated virus particles was performed in a Biosafety Level 2 containment with appropriate biological safety cabinet and sufficient personal protection equipment.

Tissue culture grade 100 mm petri dishes were coated with 0.1% gelatin. For optimal transfection, approximately 3×10^6 293FT cells were seeded into 100 mm petri dishes and incubated at 37 °C in 5% CO₂ one day

earlier in order to achieve at least 70-80% confluency on the day of transfection. After 22 hours of seeding, medium was changed to serum-free 293FT medium for starvation for 2 hours before transfection. Transfection reagent, Lipofectamine 2000 (Invitrogen, USA) was prepared and incubated 30 minutes prior to use. The components for Lipofectamine 2000 and plasmids used are summarised in Tables 3.8 and 3.9 respectively. After 2 hours starvation, fresh complete 293FT growth medium was used to replace the serum-free medium. GFP, Lipofectamine mixture, VSV-G and GAG-POL were added to each 100 mm petri dishes and cells were cultured at 37 °C in 5% CO₂. Fresh 293FT growth medium was changed the next day. Transfected cells were monitored under Zeiss Imager A.1 Fluorescence Microscope (Carl Zeiss, Germany) at 24 and 48 hours post transfection to determine transfection efficiency.

3.3.5.2 Transfection Efficiency of pMX-GFP in OS cell line

Transfection efficiencies in G-292 and Saos-2 cells were assessed using manual calculation method of GFP expressing cells, regarded as positive cells, under Zeiss Imager A.1 Fluorescence Microscope (Carl Zeiss, Germany) at 24 and 48 hours post transfection. At least four separate fields were counted in each transfected cell line to determine the transfection efficiencies. Formula for calculation is as below:

Total GFP positive cells in 4 separate fields

Efficiency = $\frac{\text{Total number of cells in 4 separate fields}}{\text{Total number of cells in 4 separate fields}} \times 100 \%$

3.3.5.3 Transfection of 293FT cells with Retrovirus Vectors: OCT4, SOX2, KLF4, c-MYC

100 mm tissue culture grade petri dishes were coated with 0.1% gelatin and labelled accordingly to the vectors, OCT3/4, SOX2, KLF4 and c-MYC. Approximately 3×10^6 293FT cells were seeded into 100 mm petri dishes and incubated at 37 °C in 5% CO₂ one day earlier in order to achieve at least 70-80% confluency on the day of transfection. After 22 hours of seeding, medium was changed to serum-free 293FT medium for starvation for 2 hours before transfection. Transfection reagent, Lipofectamine 2000 (Invitrogen, USA) was prepared and incubated 30 minutes prior to use. The components for Lipofectamine 2000 and plasmids used are summarised in Tables 3.7 and 3.8 respectively. After 2 hours starvation, fresh complete 293FT growth medium was used to replace the serum-free medium. Respective Yamanaka vectors, (Retro-O/S/K/M), Lipofectamine mixture, VSV-G and GAG-POL were added to each 100 mm petri dishes and cells were cultured at 37 °C in 5% CO₂. Fresh 293FT growth medium was changed the next day. First viral supernatant collection was done 24 hours post-transfection and briefly centrifuged at 400 x g for 5 minutes to remove debris. Viral supernatant was filtered with 0.45 µm PVDF filter unit and 0.8 µl from 10 mg/ml stock of Polybrene (Merck Millipore, Germany) was added to the viral supernatant. Fresh viral supernatant was used to transduce OS cell immediately after collection.

Table 3.7. Amount of plasmid DNA for retroviral transfection in ratio of 3:2:1

Vectors	Amount (µg)
Plasmid (O/S/K/M) / GFP	16.5
GAG-POL	11.0
VSV-G	5.5

Table 3.8. Component A and B (Lipofectamine 2000 protocol)

Component A: Dilution of Lipofectamine 2000 in blank DMEM

Mixture	OCT4	SOX2	KLF4	c-MYC	GFP
Lipofectamine 2000	50 µl				
Blank DMEM	450 µl				
Total	500 µl				

Component B: Dilution of plasmid DNA in blank DMEM

Mixture	OCT4	SOX2	KLF4	c-MYC	GFP
Plasmid	5.2 µl	5.2 µl	5 µl	4.1 µl	15 µl
GAG-POL	18.3 µl				
VSV-G	7.9 µl				
Blank DMEM	468.6 µl	468.6 µl	468.8 µl	469.7 µl	458.8 µl
Total	500 µl				

3.3.6 Retrovirus Transduction

OS cell lines, G-292 and Saos-2, were cultured and passaged to ensure active proliferation in cells to achieve optimal reprogramming. Approximately 20×10^4 G-292 cells and 10×10^4 Saos-2 cells were each seeded in a six-well plate and incubated overnight at 37 °C in 5% CO₂ to attain 60-70% confluency on the day of transduction. Fresh retroviral supernatants was supplemented with 8 mg/ml Polybrene (Merck Millipore, Germany) prior to transduction. Equal amounts (500 µl each) of supernatants containing each of the four retroviruses carrying the *OCT3/4*, *SOX2*, *c-MYC* and *KLF4* genes were mixed (made up of 2 ml for each well) and added to the cells. The plates were centrifuged at 800 x g for 50 min and incubated overnight at 37 °C in 5% CO₂ and 2% O₂. The spinfection procedure was used to increase transduction efficiency. Fresh ESC medium (DMEM/F12 supplemented with 20% Knockout serum replacement, 4 mM L-glutamine, 0.1 mM beta-mercaptoethanol, 0.1 mM nonessential amino acid, 10 ng/ml bFGF and 0.1% Penicillin/Streptomycin) was changed on the next day and subsequently every day. Transduced G-292 and Saos-2 cells were transferred to iMEF on day 3 post transduction. ESC medium containing 2 mM Valproic Acid (VPA) (Stemgent, USA) was used in the initial 7 days after transduction. Cells were monitored every day for the formation of colonies.

3.3.7 Maintenance and Passaging of Reprogrammed OS Cell Lines

ESC-like colonies appeared at Day 16 onwards to an appropriate size for passaging. Colonies were picked manually based on ESC-like morphologies. Colonies picked for passing displayed defined border, packed with cells displaying large nucleus. Colonies were identified and marked with a marking tool under Eclipse TS100 inverted microscope (Nikon, Japan). Identified colonies were manually cut under stereomicroscope (Olympus, Japan) into grids by using a sterile scalpel. By using a P200 pipette with tips, each grid was slowly and carefully picked and transferred to a fresh well coated with iMEF. ESC-like colonies were cultured at 37 °C in a 5% CO₂ incubator. Derived colonies were passaged every 6-7 days.

3.4 Characterisation of OS-Induced Pluripotent Stem Cells (OS-iPSC)

3.4.1 Morphology Evaluation under Microscope Observation

Evaluation on the morphology of the colonies was the primary screening for reprogramming. Stable reprogrammed colonies appeared similar to ESC morphologies with well-defined borders and highly packed cells with large nucleus. The morphologies of the colonies were observed under Eclipse TS100 inverted microscope (Nikon, Japan) and all images were properly recorded.

3.4.2 Alkaline Phosphatase (AP) Live Staining

Alkaline phosphatase (AP) Live Stain was used to stain putative ESC-like colonies. AP is a hydrolase enzyme known for removing phosphates from many kinds of molecules in alkaline condition. It is known to have high expression in pluripotent stem cells such as embryonic germ cells, ESC and iPSC. AP Live staining was done according to manufacturer's protocol (Invitrogen, USA). Briefly, colonies were incubated with AP Live Stain for 20-30 minutes before washing the colonies twice with DMEM/F12. Fresh DMEM/F12 was added prior to visualization using Zeiss Imager A.1 Fluorescence Microscope (Carl Zeiss, Germany).

3.4.3 Expression of Pluripotent Markers via Immunofluorescence (IF) Staining

As iPSC are deemed as ESC-like, expression of ESC associated pluripotent cell markers is one of the vital characteristics. Pluripotency markers commonly used include OCT3/4, SSEA4, TRA-1-60 and TRA-1-81. Octamer-binding transcription factor 3/4 (OCT3/4) also known as POU domain, class 5, transcription factor 1 (POU5F1) is a protein implicated in the self-renewal of undifferentiated ESC ((Zaehres et al., 2005; Chambers and Tomlinson, 2009; Johansson and Simonsson, 2010). Stage Specific Embryonic Antigens 3 (SSEA3) and Stage Specific Embryonic Antigens 4 (SSEA4) are distinct carbohydrate surface markers associated with glycolipids. Both markers are

produced during oogenesis and showed expression in the membranes of oocytes, zygotes and early stage embryos (Henderson et al., 2002). TRA-1-60 and TRA-1-81 are keratin sulfate antigens that emerged on human embryonal carcinoma (EC) cells and human pluripotent stem cell surfaces (Schopperle and DeWolf, 2007). Often both nuclear and surface markers antibody combinations are used when determining the expression of the markers. For nuclear markers such as OCT3/4, cells need to be permeabilised before staining with primary antibodies.

Immunofluorescence staining was performed on parental cells (G-292 and Saos-2) and reprogrammed counterparts (reprogrammed G-292, termed as iG-292 and reprogrammed Saos-2, termed as iSaos-2) to evaluate the pluripotency status upon reprogramming. Immunofluorescence is a method that employ immunochemical technique that uses fluorescent dye attached to antibodies. Antibodies bind to antigens on the specimens and fluorescent dye illuminated at specific wavelength was recorded using fluorescence microscopy. Parental cells G-292 and Saos-2, as well as reprogrammed G-292 (iG-292) and reprogrammed Saos-2 (iSaos-2) were seeded in a 12-well plate for immunofluorescence staining. Cells were fixed with 4% v/v paraformaldehyde (Sigma-Aldrich, USA) at RT for 15 minutes and washed three times with PBS containing 1% bovine serum albumin (BSA). For intracellular (OCT4) staining, cells were permeabilised using 0.2% Triton-X (Sigma-Aldrich, USA) in PBS for 15 minutes at RT and washed three times with 1% BSA/PBS. For intercellular (SSEA4, TRA-1-60 and TRA-1-81) staining, no permeabilisation step was needed and may proceed to blocking step. After permeabilisation, cells were blocked with 10% rabbit serum for 1 hour at RT. Blocking solution was

removed and cells were washed three times with 1% BSA/PBS. Cells were then incubated with primary antibodies, diluted in 1% BSA/PBS overnight at 4 °C. Antibodies used in this study were summarised in Table 3.9. After overnight incubation, cells were washed again with 1% BSA/PBS and incubated with a secondary antibody containing fluorescein-conjugated rabbit anti-mouse IgG (Merck Millipore, Germany) for at least 1 hour at RT in the dark. Cells were washed three times with 1% BSA/PBS before stained with Prolong Gold Antifade containing DAPI (Invitrogen, USA) for 5 minutes. Stained cells were observed under Zeiss Imager A.1 Fluorescence Microscope (Carl Zeiss, Germany).

Table 3.9. Pluripotent and secondary antibodies and dilution factors

Antibodies	Company	Dilution
OCT4	Stem Cell Technologies, Canada	1:200
SSEA-4	Stem Cell Technologies, Canada	1:200
TRA-1-60	Stem Cell Technologies, Canada	1:200
TRA-1-81	Stem Cell Technologies, Canada	1:200
Fluorescein conjugated Rabbit anti-Mouse IgG	Merck Millipore, Germany	1:100

3.4.4 Expression of Pluripotent Markers via Gene Expression

3.4.4.1 Total Ribonucleic Acid (RNA) Extraction

The integrity and purity of the isolated RNA is crucial for a successful PCR reaction. RNA extraction was performed using Qiagen RNeasy® Mini Kit (Qiagen, Germany) according to manufacturer's protocol. Approximately 3×10^6 cells were harvested via trypsinisation and lysed in 600 μ l RLT Buffer. β -mercaptoethanol was added to RLT buffer prior to usage. Cells were disrupted and homogenised using QIAshredder (Qiagen, Germany) centrifuged at maximum speed for 2 minutes. The flow-through was collected and transferred to gDNA eliminator in a 2 ml collection tube and centrifuged at 8000 x g for 30 seconds. The flow-through was collected again and one part of 70% ethanol (~600 μ l) was added to the flow-through and resuspended. 700 μ l of flow-through was transferred to RNeasy spin column in a 2 ml collection tube, spinned for 8000 x g for 15 seconds and flow-through was discarded. This step was repeated for the remaining samples. Then, 700 μ l of RW1 buffer was added to the column and centrifuged at 8000 x g for 15 seconds. Flow-through was discarded after centrifugation. Next, 500 μ l of RPE buffer was added to wash the column and centrifuged at 8000 x g for 15 seconds. After the centrifugation, flow-through was discarded and another 500 μ l of RPE buffer was added to the column. Column was centrifuged at 8000 x g for 2 minutes and flow-through was discarded. The RNeasy column was transferred to a new 2 ml collection tube and centrifuged at full speed for 1 minute to remove any possible carry over. Column was then placed in a new 1.5 ml microcentrifuge tube and 30 μ l

of RNase-free water was added to the column. Column was incubated for 2 minutes at RT before centrifugation at 8000 x g for 1 minute to elute the RNA. This elution step was repeated using the eluent to maximise the recovery of RNA. Quality and quantity of the extracted RNA were determined by NanoPhotometer UV/Vis spectrophotometer. The A260/A280 ratio for pure RNA was accepted in the range of 1.8-2.0. The RNA integrity test was done on 1% agarose gel with 1 µl of RNA added to 1 µl of 6 x loading dye (Amresco, USA) ran on 80 V for 65 minutes. Agarose gel was later visualised using molecular imager, BioSpectrum Imaging System under ultraviolet light (UVP LLC, USA). Intact total RNA was observed with a clear 28s and 18s bands with intensity of 28S:18S rRNA band ratio at 2:1.

3.4.4.2 cDNA Conversion

Reverse transcription was performed to convert extracted RNA into cDNA prior to PCR experiments. cDNA synthesis was conducted according to manufacturer's protocol (RevertAid First Strand cDNA Synthesis Kit, Thermo Scientific, USA). RNA template, 5x Reaction Buffer, dNTPs and primers were thawed on ice. Each solution was mixed to ensure homogeneity and briefly centrifuged before pipetting. Reverse transcription mixture was prepared accordingly as in Table 3.10 and incubated at 65 °C for 5 minutes to denature the RNA and chilled immediately on ice. Next, the reaction tubes were placed on ice and added with 4 µl of 5x Reaction Buffer, 1 µl of RiboLock RNase Inhibitor, 2 µl of 10 mM dNTPs mix and 1 µl of RevertAid M-MuLV RT (summarised in Table 3.10). A thermal cycler (Eppendorf, Germany) was

programmed as outlined in Table 3.11. The reaction tubes were placed in the thermal cycler and program was started to synthesise cDNA from RNA template. All generated cDNA were kept at 4 °C until PCR was set up or stored at -20 °C for future use.

Table 3.10. Reverse Transcription Reaction Mixture

Reaction Mixture 1

Component	Volume/Reaction
Template RNA	x µl (up to 1 µg)
Oligo (dT) primers	1 µl
RNase-free water	Add to 12 µl
Sub-Total	12 µl

Addition to Reaction Mixture 1 after denaturing

Component	Volume/Reaction
Template RNA mixture from Reaction mix 1	12 µl
5x Reaction Buffer	4 µl
RiboLock RNase Inhibitor (20 U/µl)	1 µl
10 mM dNTP Mix	2 µl
RevertAid M-MuLV RT (200 U/µl)	1 µl
Total reaction	20 µl

Table 3.11 Thermal Cycler protocol for cDNA synthesis

Step	Temperature	Time
cDNA synthesis	42 °C	60 min
Reaction termination	70 °C	5 min
Cooling of the sample	4 °C	Hold

3.4.4.3 Quantitative Real-Time Polymerase Chain Reaction (qPCR)

Parental cell lines, G-292 and Saos-2, and reprogrammed counterparts, iG-292 and iSaos-2, were assessed for the expression levels of pluripotency genes via qPCR. Quantitative PCR (qPCR) is different from conventional PCR as qPCR enable determination of relative or absolute concentration of the amplified DNA in the sample. qPCR utilised fluorescent reporter dye (SYBR® Green) that binds to double-stranded DNA (dsDNA) to quantify the mRNA targets during PCR. The fluorescent signal from each samples were monitored whole PCR process and plotted against quantitation cycle (Cq). Lower Cq value means higher copy number of the target. PCR amplification efficiency was determined based on all the primers optimised against Embryonic Stem Cells (ESC) which is the gold standard pluripotency genes. Glyceraldehyde 3-phosphate dehydrogenase (GAPDH) was used as a control gene in this experiment. Briefly, appropriate number of reactions were prepared according to the volumes in Table 3.12 in 0.2 ml PCR grade, microcentrifuge tubes. The components were mixed thoroughly, then the 0.2 ml microcentrifuge tubes were centrifuged briefly to spin down the content and eliminate any bubbles. The tubes were then placed in the thermal cycler (Rotor-Gene Q, Qiagen, Germany).

The thermal cycler was programmed as outlined in Table 3.13 and once the tubes is in placement, the program was started. List of primers used are shown in Appendix J.

Table 3.12 qPCR reaction components

Component	Volume/ Reaction	Final Concentration
SYBR ® Select Master Mix (2x)	10 µl	1x
Forward primer (10 µM)	1 µl	0.5 µM
Reverse primer (10 µM)	1 µl	0.5 µM
RNase-free water	6 µl	-
cDNA (25 ng/µl)	2 µl	50 ng
Total	20 µl	

Table 3.13 Thermal Cycler protocol for qPCR

Step	Temperature	Duration	Cycle
UDG activation	50 °C	2 min	Hold
AmpliTaq ® Fast DNA Polymerase, UP Activation	95 °C	2 min	Hold
Denature	95 °C	15 second	40
Anneal/Extend	60 °C	1 min	

3.4.4.4 Calculation and Analysis

Expression of gene was assessed via Comparative C_T Method ($\Delta\Delta C_T$) normalised against Glyceraldehyde 3-phosphate dehydrogenase (GAPDH) as endogenous control or housekeeping gene. Experiments were conducted in triplicates to ensure reproducibility and accuracy of data obtained. The C_T mean value from each experiment was compared between parental and its reprogrammed counterpart and assessed to determine the differential expression of gene of interest. Comparative C_T was done by using threshold cycle values (C_T) generated during qPCR and were used in calculation to determine the fold change of the samples.

Statistical data analysis was carried out with Paired-t-Tests to compare the quantitative results of OS parental and its reprogrammed counterparts using SPSS Software version 22.0. All test were conducted at the 95% confidence level. Data were presented as Mean \pm Standard Deviation (SD) or Mean \pm Standard Error of Mean (SEM) and plotted into histograms. The significance level for the differences was set at $p < 0.05$.

3.4.5 Embryoid Body Formation and Spontaneous Differentiation

Colonies from iG-292 and iSaos-2 were manually cut into small pieces and transferred onto low-attachment dishes containing ESC medium and cultured in suspension for 8 days in 37 °C in 5% CO₂. Then, embryoid bodies

(EB) were cultured in ESC medium without FGF and in 0.1% gelatin coated-dishes for another 8 days to allow for spontaneous differentiation before harvesting the EB for RNA extraction. RNA was extracted from harvested EBs for molecular identification of three germ layers. RNA extraction was done using Qiagen RNeasy® Mini Kit (Qiagen, Germany) protocol as written in Sub-unit 3.3.4.1 and cDNA conversion was performed as previously discussed in Sub-unit 3.3.4.2. Gene expressions of three germ layers were assessed via qPCR as previously discussed in Sub-unit 3.3.4.3. Primers used for endoderm, ectoderm and mesoderm lineage identification were listed in Appendix K.

3.4.6 Differentiation into adipocytes

To induce adipogenesis, colonies were plated on 0.1% gelatin coated six-well plates and cultured in 2 ml adipogenic induction medium in a humidified atmosphere at 37 °C with 5% CO₂ for 2 to 3 weeks. Adipogenic induction medium was prepared from DMEM/F12 (Gibco, USA) supplemented with 10% FBS, 1% L-glutamine, 1% Penicillin/Streptomycin (Gibco, USA), 0.25 mM Methylisobutylxantine, 1 µM Dexamethasone and 100 µM Indomethacine (Sigma-Aldrich, USA). Induction medium was changed every alternate day and observed under microscope for lipid droplets formation. After 2-3 weeks of induction, cells were stained in Oil Red O as a histological stain to visualise the presence of lipid droplets. 5% Oil Red O stock solution was prepared by dissolving 0.1 g powder (Sigma-Aldrich, USA) in 20 ml 60% triethyl phosphate (Sigma-Aldrich, USA). Then, 1% Oil Red O working

solution was prepared by diluting 8 ml Oil Red O stock solution with 12 ml deionised water and filtered before use. Solution was stored in the dark in RT. Adipogenic medium was removed and washed thoroughly with 1 x PBS. PBS was aspirated out completely from the wells of the plate. Cells were fixed in 10% formalin (Sigma-Aldrich, USA) for 30 minutes. Fixation buffer was removed and cells were stained with 60% triethyl phosphate aqueous solution at RT for 5 minutes. Subsequently, 60% triethyl phosphate was removed and Oil Red O solution was added just enough to cover the cell monolayer. Staining was performed at RT for 15 minutes. Cells were washed with distilled water until the water became clear. Stained cells were observed under Eclipse TS100 inverted microscope and images were captured for analysis. Adipocytes consisting intracellular lipid vesicles displayed bright red staining.

3.4.7 Differentiation into Osteoblasts

To induce osteogenesis, colonies were incubated in osteogenic induction medium in a humidified atmosphere at 37 °C with 5% CO₂ for 2 to 3 weeks. Osteogenic induction medium consisted of DMEM/F12 supplemented with Alizarin Red S will be used to stain matrix mineralization associated with osteoblasts. 10% FBS, 1% L-glutamine, 1% Penicillin/Streptomycin (Gibco, USA), 50 µg/ml Ascorbate-2-phosphate, 10 mM β-glycerophosphate and 100 nM Dexamethasone (Sigma-Aldrich, USA). Induction medium was changed every alternate day. After 2-3 weeks of induction, cells were stained with Alizarin Red staining as a histological stain to visualise the presence of

mineralization or calcium deposition. Alizarin Red working solution was prepared from 25 ml of distilled water preheated to 45 °C before addition of 0.5 g Alizarin Red powder (Sigma-Aldrich, USA). Mixture was stirred and allowed to reach RT prior to adjusting the pH to pH 4.2 with 1 N sodium hydroxide (NaOH) (Sigma-Aldrich, USA). The solution was filtered and stored in dark at RT. Osteogenic medium was removed and cells were washed thoroughly with 1 x PBS. PBS was aspirated out from the wells of the plate before fixation in iced cold 70% ethanol for 1 hour at RT. Fixed cells were carefully rinsed twice with distilled water. Alizarin Red solution was added just enough to cover the cells and incubated for 30 minutes at RT. Alizarin Red was discarded and cells were washed several times with distilled water. Stained cells were observed under Eclipse TS100 inverted microscope and images were captured for analysis. Presence of calcium deposition was shown as bright orange-red precipitate.

3.4.8 Teratoma/ Xenograft Formation

Teratoma formation has been regarded as the ‘gold standard’ for determining pluripotency in iPSC work. Thus, it is an important tool for monitoring of pluripotency in pluripotent stem cells. All animal work performed has been subjected to approval from Universiti Tunku Abdul Rahman Research Ethics & Code of Conduct. For each graft, approximately 2×10^6 reprogrammed and parental cells were manually harvested, centrifuged for 5 minutes at 300 x g, washed and resuspended in a 1.5 ml tube containing

200 ml Matrigel (Corning, USA) and then injected subcutaneously with a 21 gauge syringe into nude mice (BioLASCO, Taiwan). Five nude mice were used for reprogrammed OS, iG-292 and iSaos-2, while three nude mice were used for parental cell lines, G-292 and Saos-2. Another three nude mice were injected with embryonic stem cells (ESC) as control. All nude mice were anaesthetised with anaesthetic drug (Ketamine 100mg/kg + Xylazine 10 mg/kg) and injected intra-peritoneally. Induced tumours were measured twice per week by using calliper. During the measurement, the greatest longitudinal diameter (length) and the greatest transverse diameter (width) were determined. Tumour volume based on calliper measurements were calculated by the modified ellipsoidal formula [*Tumour volume* = $1/2(\text{length} \times \text{width}^2)$]. When the tumour reached 1.2 cm in diameter, mice were sacrificed by anaesthesia followed by cervical dislocation. The tumours were dissected and fixed in 10% formalin. The tissues were processed in a tissue processor (Thermo Scientific, USA) before sectioned, stained with hematoxylin and eosin, and examined for the presence of tissue representatives of all three germ layers. Histopathology analysis was done by a pathologist.

3.5 Global gene expression of the reprogrammed OS cells using microarray technology

Once the reprogrammed colonies has been generated and characterised, determination of the global gene expression profiles in reprogrammed and the parental cells were done using whole genome Affymetrix Human PrimeView

GeneChip arrays (Affymetrix, USA). Total RNA was prepared from reprogrammed cell lines with 3 sub-clones each (total of 6 sub-clones were studied) and 2 parental cells, G-292 and Saos-2.

3.5.1 Total Ribonucleic Acid Extraction (RNA)

The integrity and purity of the isolated RNA is crucial for a successful global gene expression profiles. RNA extraction was performed using Qiagen miRNeasy® Mini Kit (Qiagen, Germany) according to manufacturer's protocol. Approximately 3×10^6 cells were harvested via trypsinisation and lysed in 700 μ l QIAzol Lysis Reagent. Cells were disrupted and homogenised using QIAshredder (Qiagen, Germany) centrifuged at maximum speed for 2 minutes. The homogenate was incubated at RT for 5 minutes. Then, 140 μ l chloroform was added to the homogenate and the tubes were shaken vigorously for 15 seconds. The mixture was incubated at RT for 2-3 minutes and centrifuged at 12,000 x *g* for 15 minutes at 4 °C. After the centrifugation, the upper aqueous phase was transferred carefully to a new collection tube. 1.5 volume (usually 525 μ l) of 100% ethanol into the aqueous phase and mixed thoroughly by pipetting up and down. Without any delay, 700 μ l of sample was transferred into RNeasy Mini spin column in a 2 ml collection tube, centrifuged at 8000 x *g* for 15 seconds at RT and flow-through was discarded. This step was repeated for the remaining samples. Then, 700 μ l of RWT buffer was added to the column and centrifuged at 8000 x *g* for 15 seconds to wash the column. Flow-through was discarded after centrifugation. Next, 500 μ l of RPE buffer was

added to wash the column and centrifuged at 8000 x g for 15 seconds. After the centrifugation, flow-through was discarded and another 500 µl of RPE buffer was added to the column. Column was centrifuged at 8000 x g for 2 minutes to dry the column and flow-through was discarded. The RNeasy column was transferred to a new 2 ml collection tube and centrifuged at full speed for 1 minute to remove any possible carry over. Column was then placed in a new 1.5 ml microcentrifuge tube and 30 µl of RNase-free water was added to the column. Column was incubated for 2 minutes at RT before centrifugation at 8000 x g for 1 minute to elute the RNA. This elution step was repeated using the eluent to maximise the recovery of RNA. Quality and quantity of the extracted RNA were determined by NanoPhotometer UV/Vis spectrophotometer. The A260/A280 ratio for pure RNA was accepted in the range of 1.8-2.0. The RNA integrity test was done using 2100 Bioanalyzer (Agilent, Germany). Bioanalyzer determined the RNA integrity number (RIN). RIN was utilised to estimate the integrity of total RNA samples based on the electrophoretic trace of RNA samples, including the presence or absence of degradation products. Samples with RIN more than seven were chosen for further microarray study.

3.5.2 Global Gene Expression via Affymetrix GeneChip PrimeView Human Gene Expression Array

For global gene expression, Affymetrix GeneChip PrimeView Human Gene Expression Array cartridge (Affymetrix, USA) was used. GeneChip PrimeView cartridge enables expression profiling using probe sets with an

emphasis on established, well annotated, content. Sequences used in the design of the array were selected from RefSeq version 36, UniGene database 219 and full-length human mRNAs from GenBank ®. This array enable measurement of gene expression of more than 36,000 transcripts and variants per sample.

Total RNA from reprogrammed cell lines, iG-292 and iSaos-2, with three sub-clones each (total of six sub-clones were studied) and two parental cells, G-292 and Saos-2 were subjected to RNA target preparation for microarray expression analysis using GeneChip ® 3' IVT Express Kit (Affymetrix, USA). The kit is based upon linear RNA amplification and employs T7 *in vitro* transcription technology. Total RNA was reverse transcribed to synthesise first-strand cDNA. The cDNA is then converted into a double-stranded DNA template for transcription. aRNA was synthesised and incorporated with biotin-conjugated nucleotide via *in vitro* transcription. aRNA is then purified to remove unincorporated NTPs, salts, enzymes and inorganic phosphate. Biotin-labelled aRNA was fragmented to prepare the samples for hybridisation onto GeneChip PrimeView expression arrays. Samples were loaded onto GeneChip PrimeView and placed into 45°C, 60 rpm hybridisation oven and incubated for 16 hours. After hybridisation for 16 hours, arrays were washed and stained on GeneChip® Fluidics Station. After complete washing and staining procedure, arrays were scanned using GeneChip® Scanner 3000 7G (Affymetrix, USA). After the array has been scanned, the image data was analysed using Affymetrix GeneChip® Command Console® Software (AGCC) (Affymetrix, USA). Microarray data was imported into GeneSpring GX 13.0 (Agilent, Germany) for analysis.

3.6 Evaluation of DNA repair, cell cycle and apoptosis processes

After the microarray analysis, high differentially expressed DNA repair, cell cycle and apoptosis genes between the parental and reprogrammed OS were validated using qPCR. Genes with fold change (FC) more than 2 (FC>2) and significance level, $p < 0.05$ were selected for validation. cDNA conversion was performed to convert extracted RNA into cDNA prior to PCR experiments as outlined in 3.4.4.2.

3.6.1 Validation of genes via Taqman Gene Expression Assay

TaqMan™ Gene Expression Assays (Applied Biosystems, USA) consist of a pair of unlabeled PCR primers and a TaqMan probe with a FAM™ dye label on the 5' end and minor groove binder (MGB) and nonfluorescent quencher (NFQ) on the 3' end in a single tube. During PCR, the TaqMan MGB probe anneals precisely to a complementary sequence between the forward and reverse primer sites. When the probe is still intact, the closeness of the reporter dye to the quencher dye results in suppression of the reporter fluorescence. The DNA polymerase cleaves probes that hybridised to the target. Cleavage separates the reporter dye from the quencher dye, and this separation results in increased fluorescence by the reporter. The increase in fluorescence is then amplified during PCR.

Briefly, Taqman® Gene Expression Assay (20x), cDNA samples and Taqman® Fast Advanced Master Mix (2x) were thawed on ice. Glyceraldehyde 3-phosphate dehydrogenase (GAPDH) was used as a control gene in this experiment. Appropriate number of reactions were prepared according to the volumes in Table 3.14 in 0.2 ml PCR grade, strip-tubes. The components were mixed thoroughly, then the 0.2 ml strip-tubes were centrifuged briefly to spin down the content and eliminate any bubbles. The tubes were then placed in the thermal cycler (StepOne Plus, Thermo Fisher Scientific, USA). The thermal cycler was programmed as outlined in Table 3.15 and once the tubes is in placement, the program was started. List of primers used are shown in Appendix L and M.

Table 3.14 TaqMan® qPCR reaction components

Component	Volume/ Reaction	Final Concentration
TaqMan® Fast Advanced Master Mix (2x)	10 µl	1x
TaqMan® Gene Expression Assay (20x)	1 µl	1x
cDNA template (10 ng/µl)	2 µl	20 – 50 ng
RNase-free water	7 µl	-
Total	20 µl	

Table 3.15 Thermal Cycler protocol for TaqMan® qPCR

Step	Temperature	Duration	Cycle
UNG incubation	50 °C	2 min	Hold
DNA Polymerase Activation	95 °C	20 sec	Hold
Denature	95 °C	1 sec	40
Anneal/Extend	60 °C	20 sec	

3.6.2 Calculation and Analysis

Expression of gene was assessed via Comparative C_T Method ($\Delta\Delta C_T$) normalised against Glyceraldehyde 3-phosphate dehydrogenase (GAPDH) as endogenous control or housekeeping gene. Experiments were conducted in triplicates to ensure reproducibility and accuracy of data obtained. The C_T mean value from each experiment was compared between parental and its reprogrammed counterpart and assessed to determine the differential expression of gene of interest. Comparative C_T was done by using threshold cycle values (C_T) generated during qPCR and were used in calculation to determine the fold change of the samples.

Statistical data analysis was carried out with ANOVA to compare the quantitative results of OS parental and its reprogrammed counterparts using SPSS Software version 22.0. All test were conducted at the 95% confidence

level. Data were presented as Mean \pm Standard Deviation (SD) or Mean \pm Standard Error of Mean (SEM) and plotted into histograms. The significance level for the differences was set at $p < 0.05$.

3.7 Functional assay to examine the functionality of DNA repair mechanism.

Functional assay was used to determine the functionality of DNA repair mechanism in reprogrammed OS in comparison with their parental counterparts. Functional test such as UV irradiation was used to generate damage to DNA in the cells and then the cells were harvested for DNA and RNA extraction.

3.7.1 Ultraviolet (UV) irradiation

After UV irradiation the cyclobutane pyrimidine dimers (CPD) are the most abundant and probably most cytotoxic lesions (Sinha and Häder, 2002). Detection of CPD would be done using Cell BioLabs' OxiSelect UV-Induced DNA damage ELISA Kit.

Prior to UV treatment, cells grown in 100 mm dish or 6-well plate till 80% confluency were washed and medium was replaced with 10 ml phosphate buffered saline (PBS) with Calcium and Magnesium. Irradiation of cells was performed at room temperature at UV dose of 40 J/m² UVC (254 nm) with

UVILite LF-206-LS (UVITEC, UK). UVC dose of 40J/m² was achieved with UV irradiation at 20 cm away from dish surface for 18 seconds. Cells were irradiated in 100 mm culture dish or 6-well plate without lids. Following treatments, cells were fed culture medium and incubated for 1 hour, 6 hours or 24 hours to allow DNA repair mechanism to take place. Cells at 1 hour, 6 hours and 24 hours were harvested for DNA extraction using Qiagen DNA extraction kit. UV-induced DNA damage was detected by OxiSelect UV-Induced DNA damage ELISA Combo Kit (CPD quantitation) (Cell Biolabs, USA).

3.7.2 Deoxyribonucleic Acid (DNA) extraction

DNA extraction was performed using Qiagen DNeasy Blood and Tissue Kit (Qiagen, Germany) according to manufacturer's protocol. Irradiated cells were harvested by trypsinisation and resuspended in 200 µl PBS (without Calcium and Magnesium). 20 µl of Proteinase K was added to the cells to digest any contaminating proteins. Then, 200 µl of Buffer AL was added and the mixture was mixed thoroughly by vortexing. 200 µl of 100% ethanol was added and mixed thoroughly by vortexing. The solution was then transferred to DNeasy Mini spin column, centrifuged for 1 minute at 6000 x g and flow-through was discarded. 500 µl of Buffer AW1 was added, centrifuged for 1 minute at 6000 x g and flow-through was discarded. Next, 500 µl of Buffer AW2 was added, centrifuged for 3 minute at 20,000 x g and flow-through was discarded. Spin column was transferred to a new 1.5 ml microcentrifuge tube. DNA was eluted by adding 50 µl of Buffer AE into the column and incubated

for 1 minute at RT before centrifugation for 1 minute at 6000 x g. DNA eluent was stored at -20°C.

3.7.3 Cyclobutane pyrimidine dimers (CPD) quantitation

Cell Biolabs' OxiSelect™ Oxidative UV-Induced DNA Damage ELISA Kit is an enzyme immunoassay developed for rapid detection and quantification of CPD in DNA samples. In the assay principle, CPD standards or unknown DNA samples were first heat denatured before adsorbed onto a 96-well DNA high-binding plate. The CPD present in the samples are probed with an anti-CPD antibody, followed by Horseradish Peroxidase (HRP) conjugated secondary antibody. The CPD content in an unknown sample is determined by comparing with a standard curve that is prepared from predetermined CPD-DNA standard.

Briefly, extracted DNA samples were converted into single-stranded DNA by incubating the sample at 95 °C for 10 minutes and rapidly chilled on ice for 10 minutes. Then, denatured DNA was diluted to 2 µg/mL in cold PBS. 100 µl of unknown denatured DNA sample or CPD-DNA standard were added to the wells of DNA High-Binding plate and incubated at 4 °C for overnight. After overnight incubation, DNA solutions were removed and washed twice with PBS. Plate was blotted on paper towels to remove excess fluid. The 150 µl of Assay Diluent was added to each well and blocked for 1 hour at RT. Next, Assay Diluent was aspirated and 100 µl of diluted anti-CPD antibody was

added to each well and incubated for 1 hour at RT on an orbital shaker (Fisher Scientific, USA). Plate was washed three times with 250 μ l 1X Wash Buffer with thorough aspiration between each wash. After the last wash, 150 μ l of prediluted 1X Blocking Reagent was added to each well and incubated for 1 hour at RT on an orbital shaker. Plate was washed and 100 μ l of diluted Secondary Antibody-Enzyme Conjugate was added to each well and incubated at RT for 1 hour on an orbital shaker. Plate was washed again and 100 μ l of Substrate Solution was added to each well, including the blank wells and incubated at RT for 10-15 minutes on an orbital shaker. The enzymatic reaction was stopped by adding 100 μ l of Stop Solution at the end of the incubation time. Absorbance of each well was read on a microplate reader, Tecan Infinite M200 (Tecan, Switzerland) using 450 nm as the primary wave length.

CHAPTER 4

RESULTS & DISCUSSION: PART 1

Reprogramming & Characterisation of reprogrammed OS cells

4.1 Microscopic Observation of Human Osteosarcoma Cell Lines

G-292 cell populations are adherent to tissue culture plates and are morphologically homogenous in culture. G-292 cell lines has a slow proliferate rate and only reached 80% confluency in five to six days (Figure 4.1).

Saos-2 exhibited deletion in *p53* gene, possessed osteoblastic features and proliferate rapidly, reaching 80% confluency in three-four days, making it possible to obtain large amounts of cells in short time. Saos-2 are adherent to tissue culture plates and morphologically homogenous with osteoblast-like appearance (Prideaux et al., 2014) (Figure 4.1).

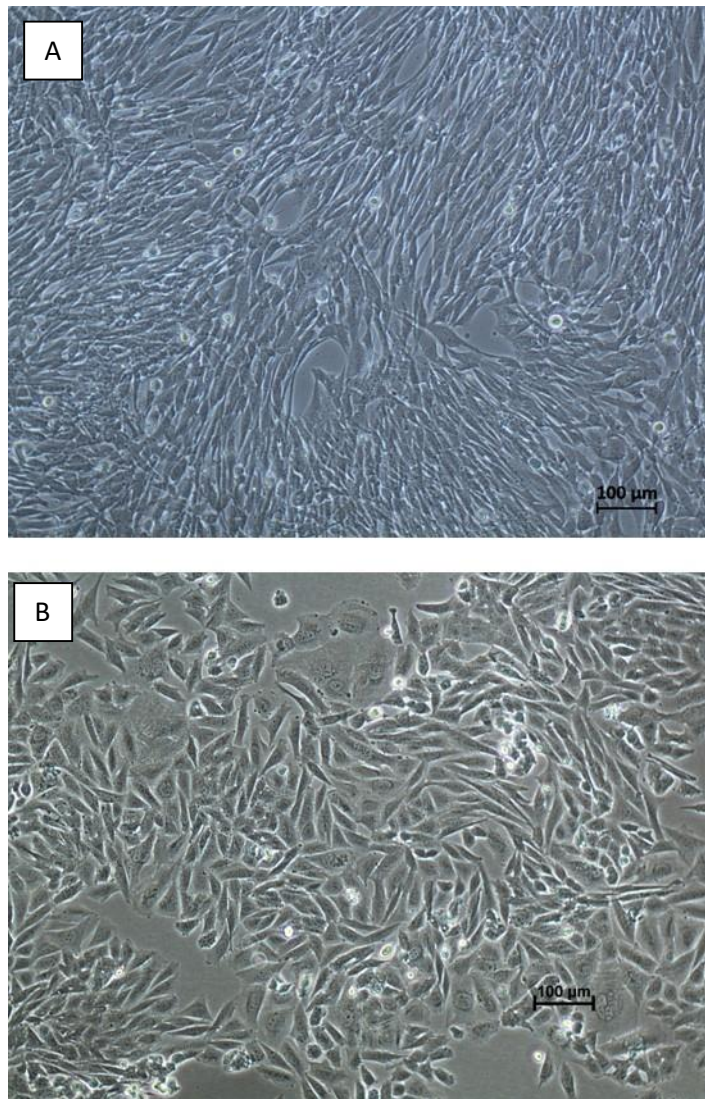


Figure 4.1. Morphology of adherent Human Osteosarcoma (OS) cell lines in tissue culture plates. (A) G-292 cell lines at 90% confluency displayed fibroblastic-like morphology. (B) Saos-2 cell lines at 80% confluency displayed osteoblast-like morphology. Nikon inverted microscope, original magnification: 10x.

4.2 Transduction Efficiency via Green Fluorescence Protein (pMX-GFP)

4.2.1 Transduction in G-292 and Saos-2 Cell Lines with pMX-GFP

To estimate transduction efficiency in target cells, *GFP* transduction was used as an internal control. Transductions were attained in both G-292 and Saos-2 cell lines with retroviral vector pMX, encoded with *GFP* (pMX-GFP, which encodes green fluorescent protein signal) at 48 hours confirming the uptake of *GFP* transgene. (Figure 4.2). Transduction efficiency was calculated based on total GFP positive cells in 4 separate fields/ Total number of cells in 4 separate fields x 100 %. The transduction efficiency results demonstrated higher efficiency in G-292 with $68.6 \pm 7.74\%$ as compared to Saos-2 with $50.97 \pm 7.20\%$. However, the difference in transduction efficiency was not statistically significant. GFP expressions were analysed using Zeiss Imager A.1 Fluorescence Microscope.

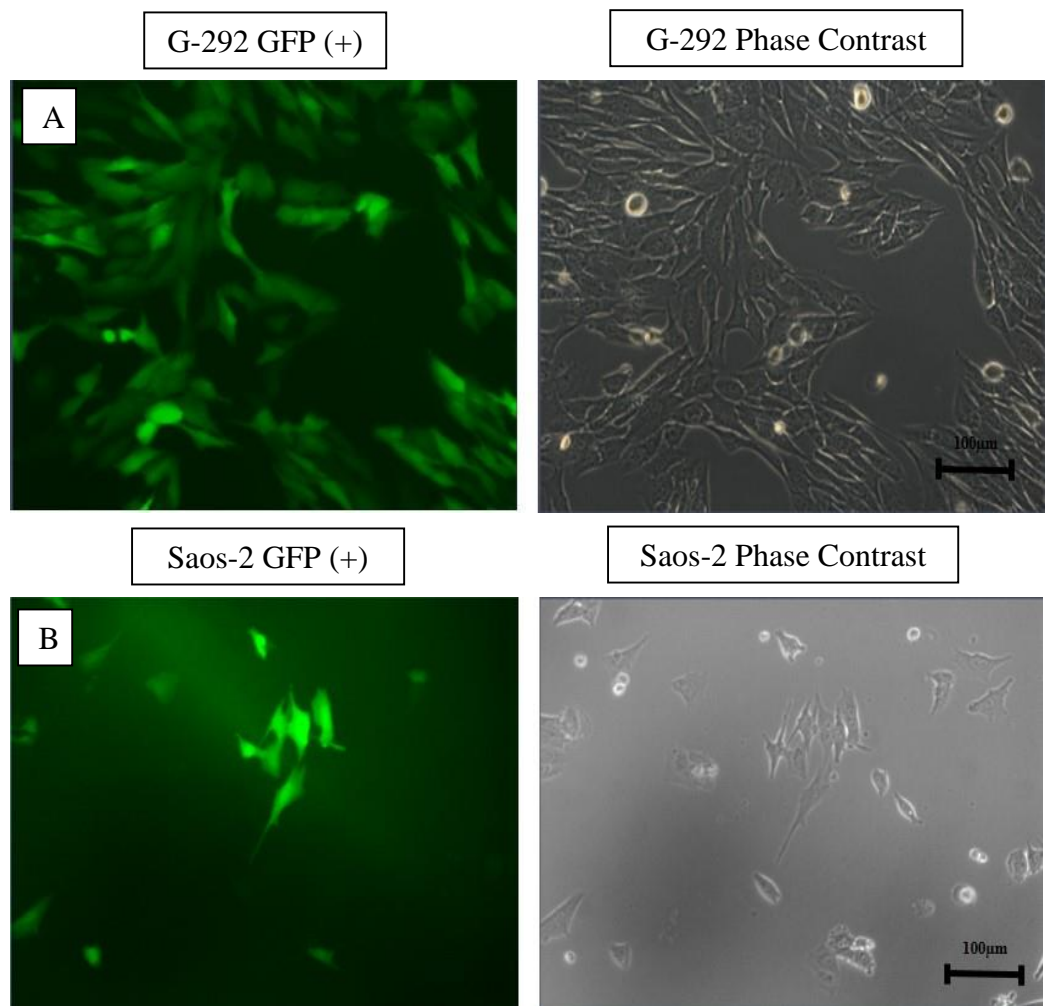


Figure 4.2. Determination of transfection efficiency using pMX-GFP in parental cells after 48 hours. (A) G-292 and (B) Saos-2. Zeiss Axiovert Inverted Microscope, original magnification: 10x

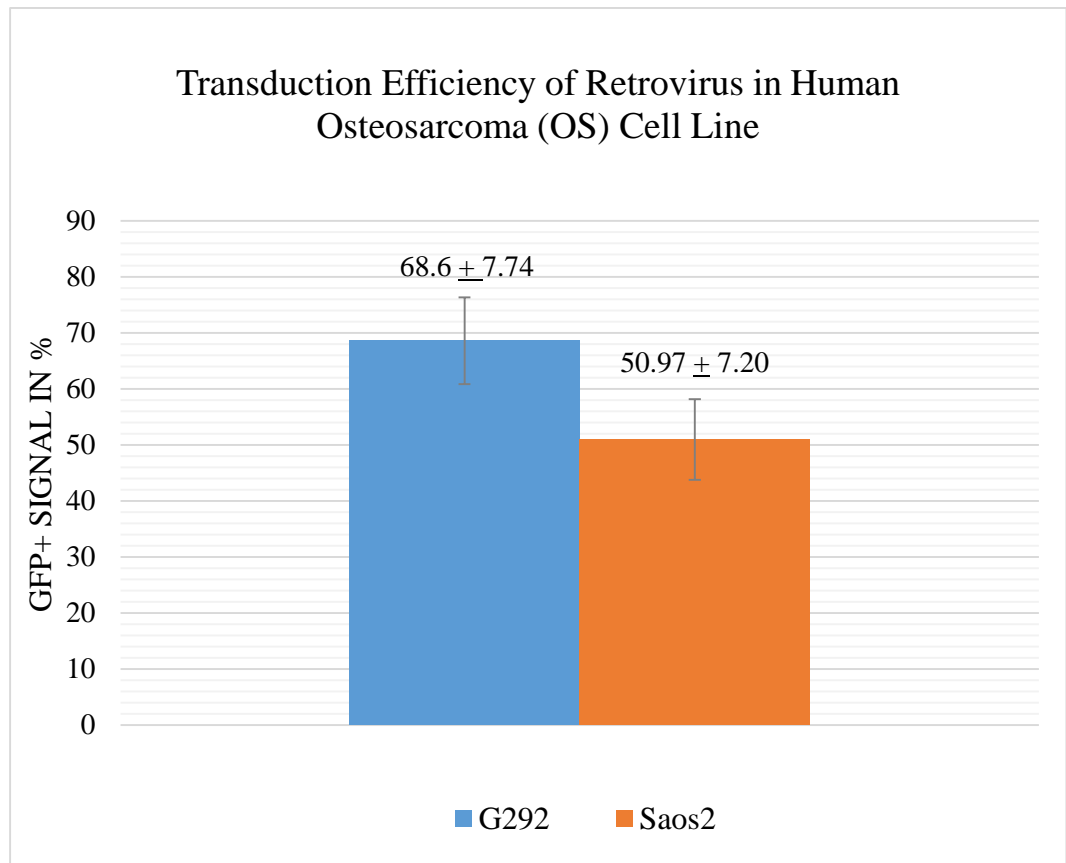


Figure 4.3. Transduction efficiency of pMX-GFP in G-292 and Saos-2.

Efficiency results are expressed as mean \pm standard deviation (SD). The difference transduction efficiency between G-292 and Saos-2 is not statistically significant ($p > 0.05$).

4.3 Transduction with Plasmid OSKM

4.3.1 Transduction of G-292 and Saos-2 cell lines with Plasmid OSKM at 72 hours and 5 days Post-Transduction

G-292 and Saos-2 cells were transduced with plasmids encoding transcriptional factors (OSKM). Seventy two hours after transduction, both transduced Saos-2 and G-292 cells were transferred to iMEF and observed again on Day 5 post-transduction (Figure 4.4 and Figure 4.5). There were no major morphological changes observed on both transduced cells at 72 hours post-transduction. ESC specific medium was changed daily and transduced cells on iMEF were monitored daily for colony formation. Valproic acid (VPA) was added in the reprogramming medium during the first 7 days of reprogramming to increase the reprogramming efficiency (Huangfu et al., 2008a).

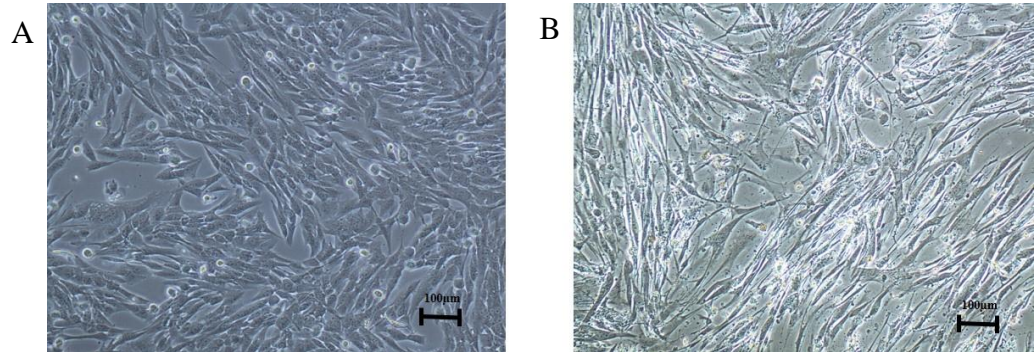


Figure 4.4. Post-transduction of G-292. (A) G-292 at 72 hours post-transduction before transfer to iMEF. (B) Transduced G-292 at 5 days post-transduction on iMEF. Nikon inverted microscope, original magnification: 10x.

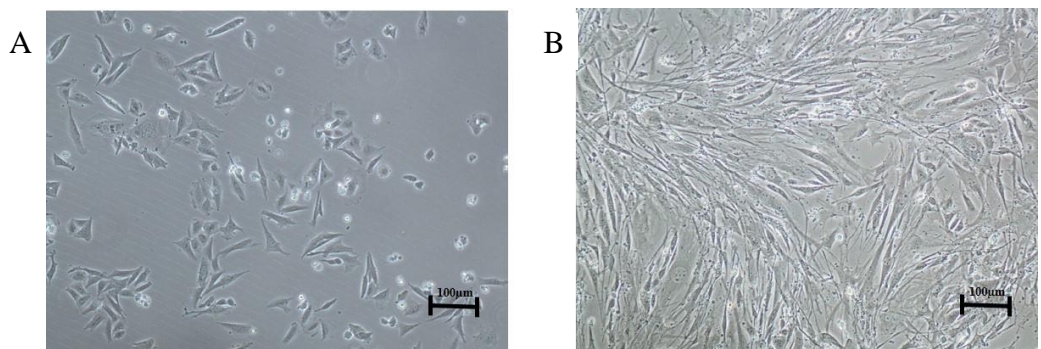


Figure 4.5. Post-transduction of Saos-2. (A) Saos-2 at 72 hours post-transduction before transfer to iMEF. (B) Transduced Saos-2 at 5 days post-transduction on iMEF. Nikon inverted microscope, original magnification: 10x.

4.3.2 OSKM Transduction Results in G-292 and Saos-2

Colony formation was observed to appear for both transduced cells started to appear around 15 days post-transduction. Colonies from both reprogrammed G-292 (iG-292) and reprogrammed Saos-2 (iSaos-2) showed ESC-like morphology with distinct border and cells tightly packed with each other. iG-292 and iSaos-2 have lost their parental morphology upon reprogramming (Figure 4.6). Saos-2 demonstrated the highest reprogramming efficiency (~0.30%) with the most ESC-like clusters, followed by G-292 (~0.17%) (Figure 4.7). The difference was not statistically significant. Multiple clones from both transduced G-292 and Saos-2 were picked manually and transferred onto fresh iMEF.

Reprogramming efficiency was calculated as below:

$$\text{Efficiency} = \frac{\text{Total colonies in a 100 mm dish}}{\text{Total number of cells seeded in a 100 mm dish}} \times 100 \%$$

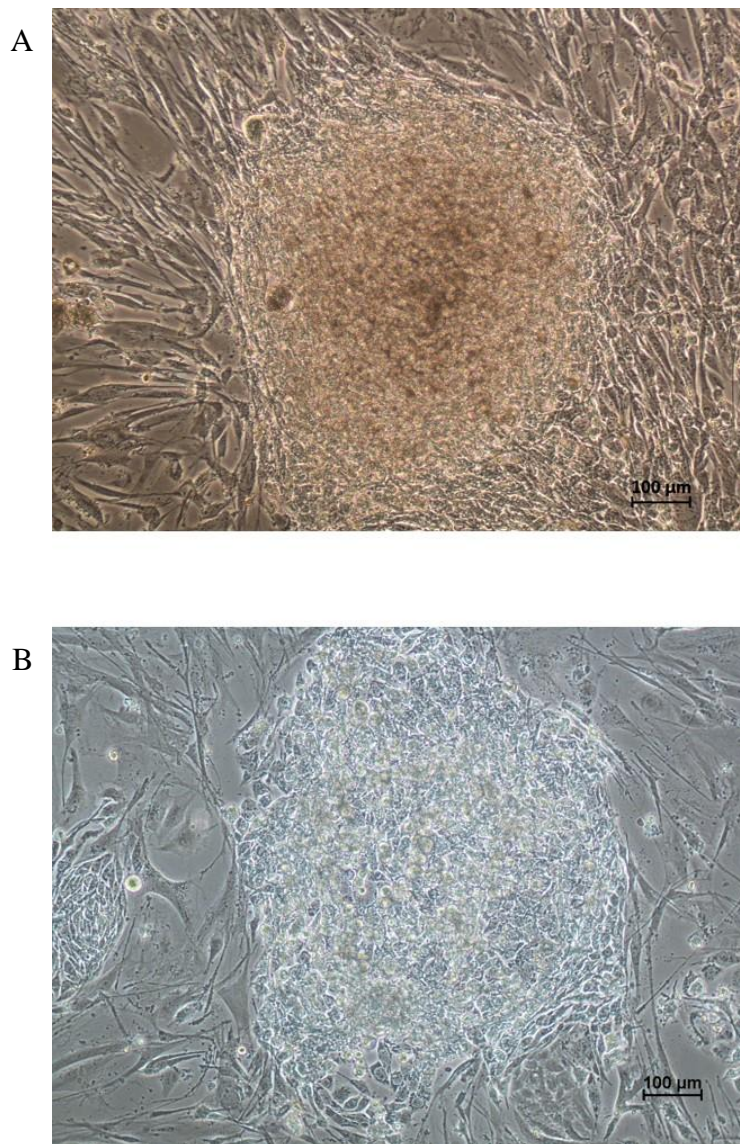


Figure 4.6. Emergence of ESC-like colonies on Day 21 post-transduction.
(A) One of the colonies of reprogrammed G-292 (iG-292). (B) One of the colonies of reprogrammed Saos-2 (iSaos-2). Nikon inverted microscope, original magnification: 10x.

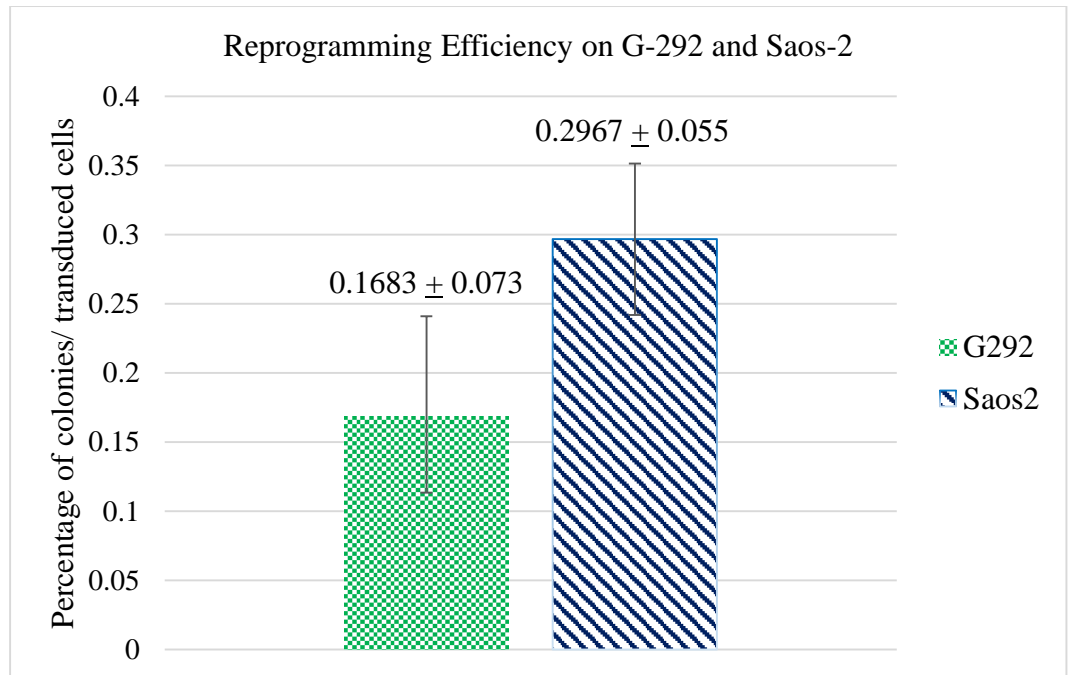


Figure 4.7. Reprogramming efficiency in G-292 and Saos-2. Efficiency results are expressed as mean \pm standard deviation (SD). The difference in transduction efficiency between G-292 and Saos-2 are not statistically significant ($p>0.05$).

4.4 Characterisation of Established Osteosarcoma Derived Induced Pluripotent Stem Cells (OS-iPSC)

The established osteosarcoma derived induced pluripotent stem cells (OS-iPSC) were characterised to verify the success of reprogramming. A series of standard methods was employed for comprehensive characterisation on OS-iPSC. As iPSC are deemed as embryonic stem cells (ESC)-like, thus, characterisation of generated OS-iPSC was done following standard ESC characterisation to test the pluripotency of the cells *in vitro* and *in vivo*.

4.4.1 Morphological observation from G-292-Derived Induced Pluripotent Stem Cells (iG-292) and Saos-2-Derived Induced Pluripotent Stem Cells (iSaos-2)

Generation of G-292-derived iPSC, termed as iG-292, and Saos-2-derived iPSC, termed as iSaos-2, were achieved with a single transduction of retroviral with OSKM transcription factors. Various iG-292 and iSaos-2 clones were picked for further passaging and maintenance. Figure 4.8 showed representative images of different clones generated from G-292 at various passages, and Figure 4.9 showed representative images of different clones generated from Saos-2 at various passages. Morphologies of all the selected clones resembled ESC with clear defined borders and consisting of cells with high nucleus to cytoplasm ratio. Formation of ESC-like colonies was the first characteristic observed in reprogramming. ESC-like morphology includes high ratio of nucleus to cytoplasm, prominent nucleoli, tightly packed cells and clear

defined borders of each colony (Thomson et al., 1998; Heins et al., 2004). Reprogrammed cells are highly distinctive in morphology from its initial parental cells. Among the selected clones, iG-292 Clone 2 and iSaos-2 Clone 2 were able to be passaged more than Passage 15 and were subsequently used for all characterisation and other down-stream work.

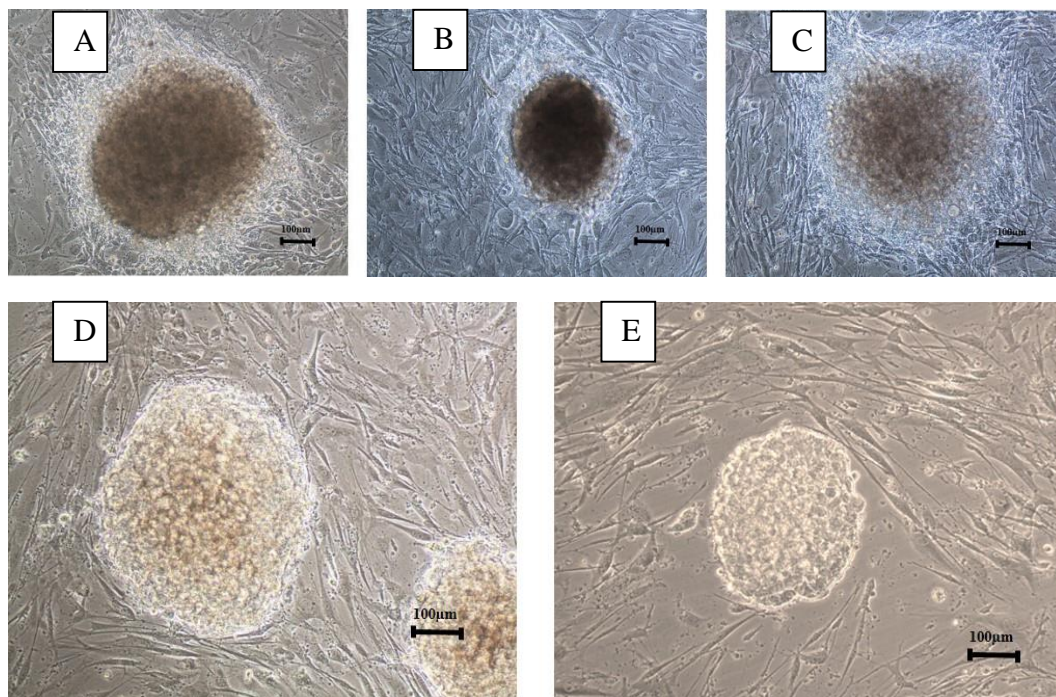


Figure 4.8. Various iG-292 clones at different passages. (A) iG-292 Clone 1 at Passage 1. (B) iG-292 Clone 1 at Passage 4. (C) iG-292 Clone 3 at Passage 4. (D) iG-292 Clone 2 at Passage 15 and (E) iG-292 Clone 2 at Passage 34. Nikon inverted microscope, original magnification: 10x.

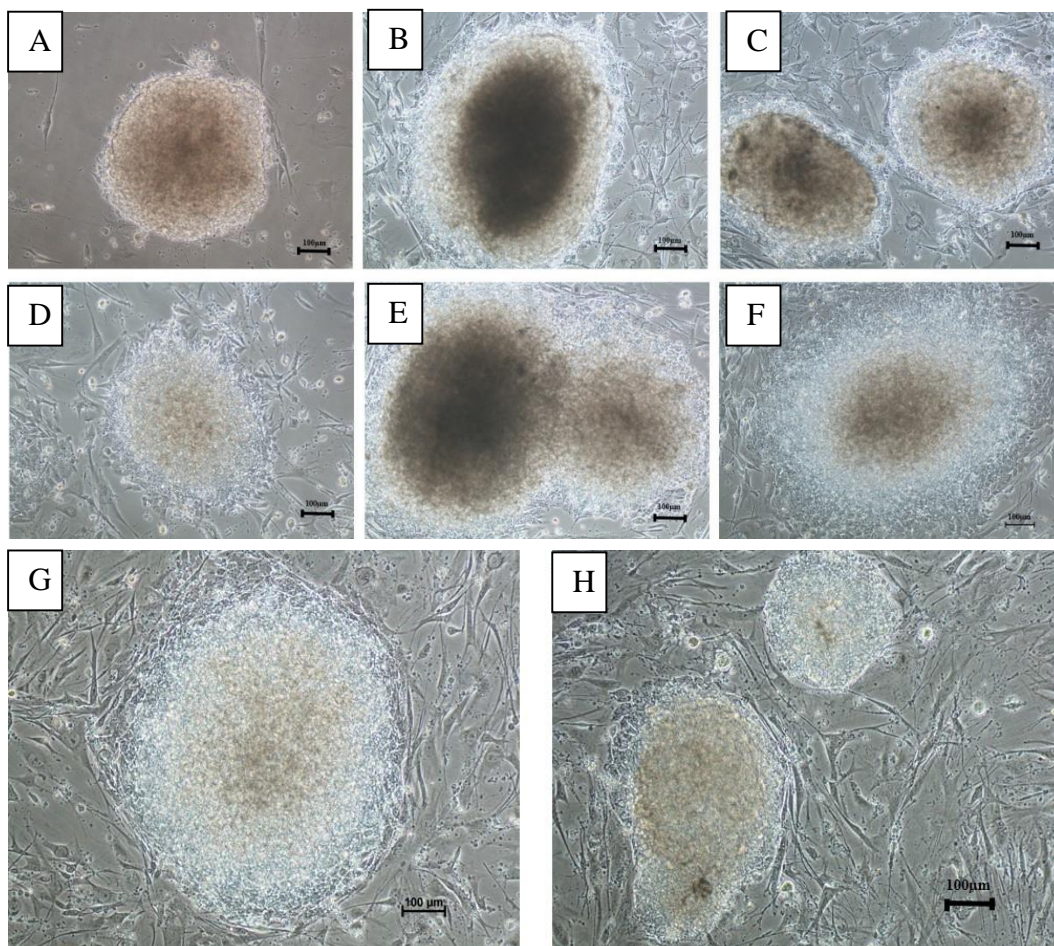


Figure 4.9. Various iSaos-2 clones at different passages. (A) iSaos-2 Clone 2 at Passage 1. (B) iSaos-2 Clone 2 at Passage 3. (C) iSaos-2 Clone 3 at Passage 3. (D) iSaos-2 Clone 6 at Passage 3. (E) iSaos-2 Clone 17 at Passage 3. (F) iSaos-2 Clone 19 at Passage 3. (G) iSaos-2 Clone 19 at Passage 5. (H) iSaos-2 Clone 2 at Passage 14. Nikon inverted microscope, original magnification: 10x.

4.4.2 Alkaline Phosphatase (AP) Live Staining on OS-iPSC

After the morphology observation, alkaline phosphatase (AP) staining was used to stain putative ESC-like colonies. AP is a phenotypic staining that has been widely used to stain ESC-like colonies as part of iPSC characterisation. Though AP was expressed in most cell types, its expression is highly elevated in pluripotent stem cells (PSC). AP live staining allows cells to continue to propagate after removal of the dye. Both iG-292 and iSaos-2 clones expressed alkaline phosphatase (AP) as detected via fluorescence-live staining (Figure 4.10). As showed in Figure 4.10, AP stained iPSC but not the feeder cells. Positive clones were selected for further propagation.

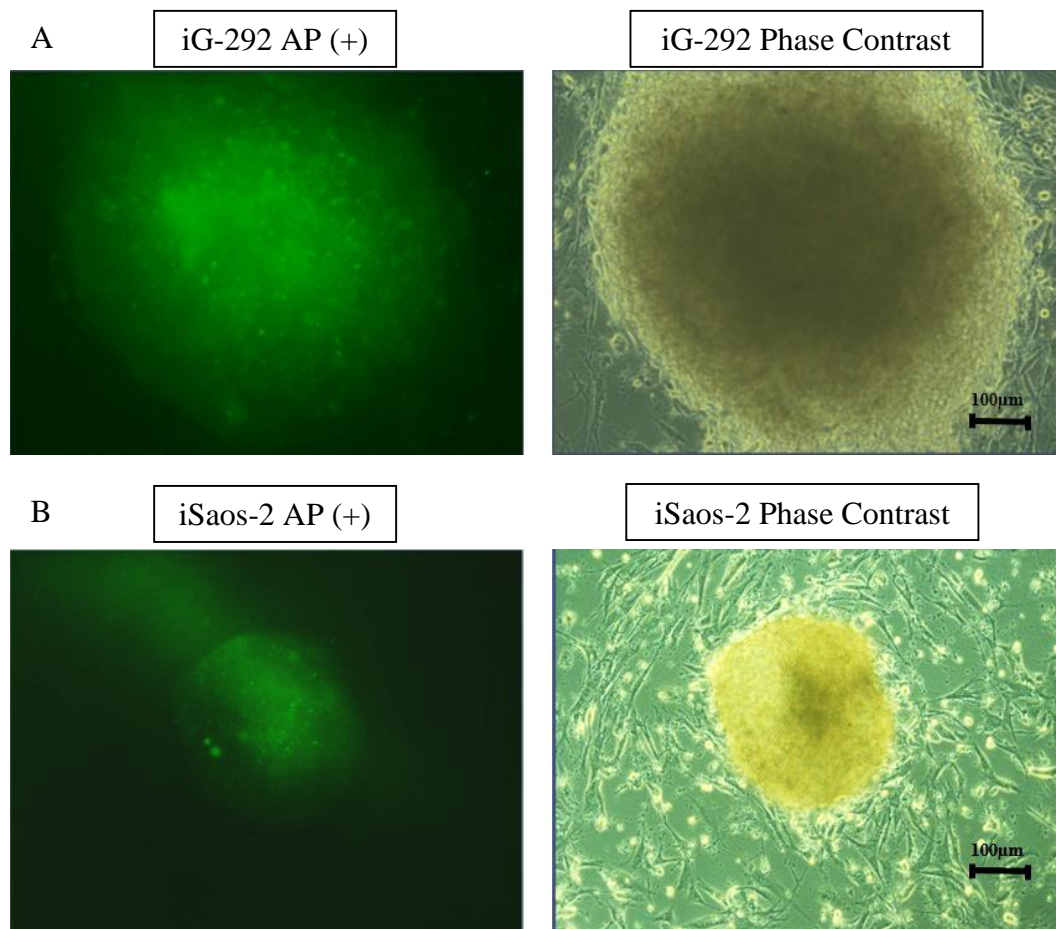


Figure 4.10. Alkaline phosphatase staining. (A) Fluorescent staining on iG-292 Clone 2 at Passage 1, and (B) iSaos-2 Clone 2 at Passage 1. Zeiss Axiovert Inverted Microscope, original magnification: 10x

4.4.3 Expression of Pluripotent Markers via Immunofluorescence (IF) Staining

Pluripotent markers are markers expressed at higher level in pluripotent stem cells than terminally differentiated cells. Detection of these pluripotent markers distinguished between pluripotent cells, such as ESC and iPSC, from somatic cells.

Immunofluorescence for detection of pluripotent markers were performed on both parental and reprogrammed counterpart. Presence of intracellular pluripotent markers (OCT4) and intercellular pluripotent markers (SSEA4, TRA-1-60 and TRA-1-81) were detected in reprogrammed cells, iG-292 and iSaos-2, but not in their parental cells (Figure 4.11 and Figure 4.12). Figure 4.12 showed both reprogrammed iG-292 and iSaos-2 maintained their pluripotent markers expressions at Passage 5 and Passage 15.

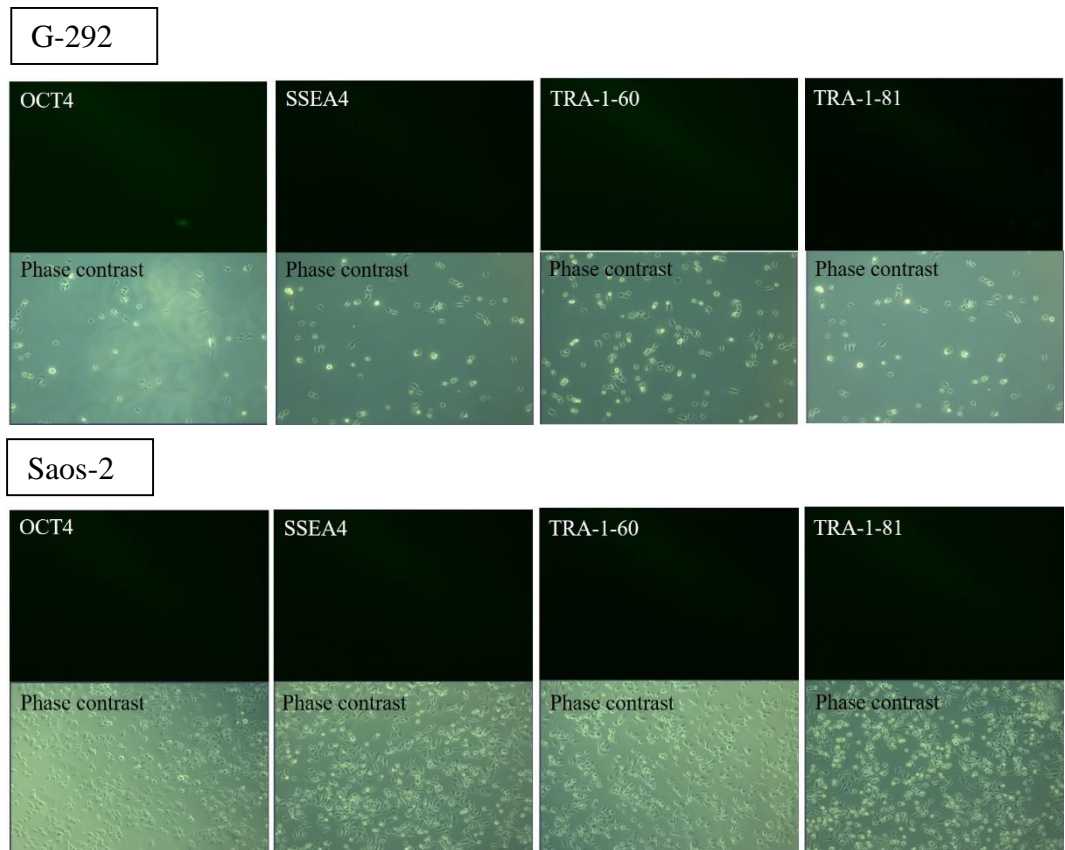


Figure 4.11. Immunofluorescence (IF) staining of parental G-292 and Saos-2 cells. Parental cells were stained for pluripotent markers: Intracellular markers (OCT4) and intercellular markers (SSEA4, TRA-1-60 and TRA-1-81). Pluripotent markers expressions were not detected in both parental cells. Zeiss Axiovert Inverted Microscope, original magnification: 10x

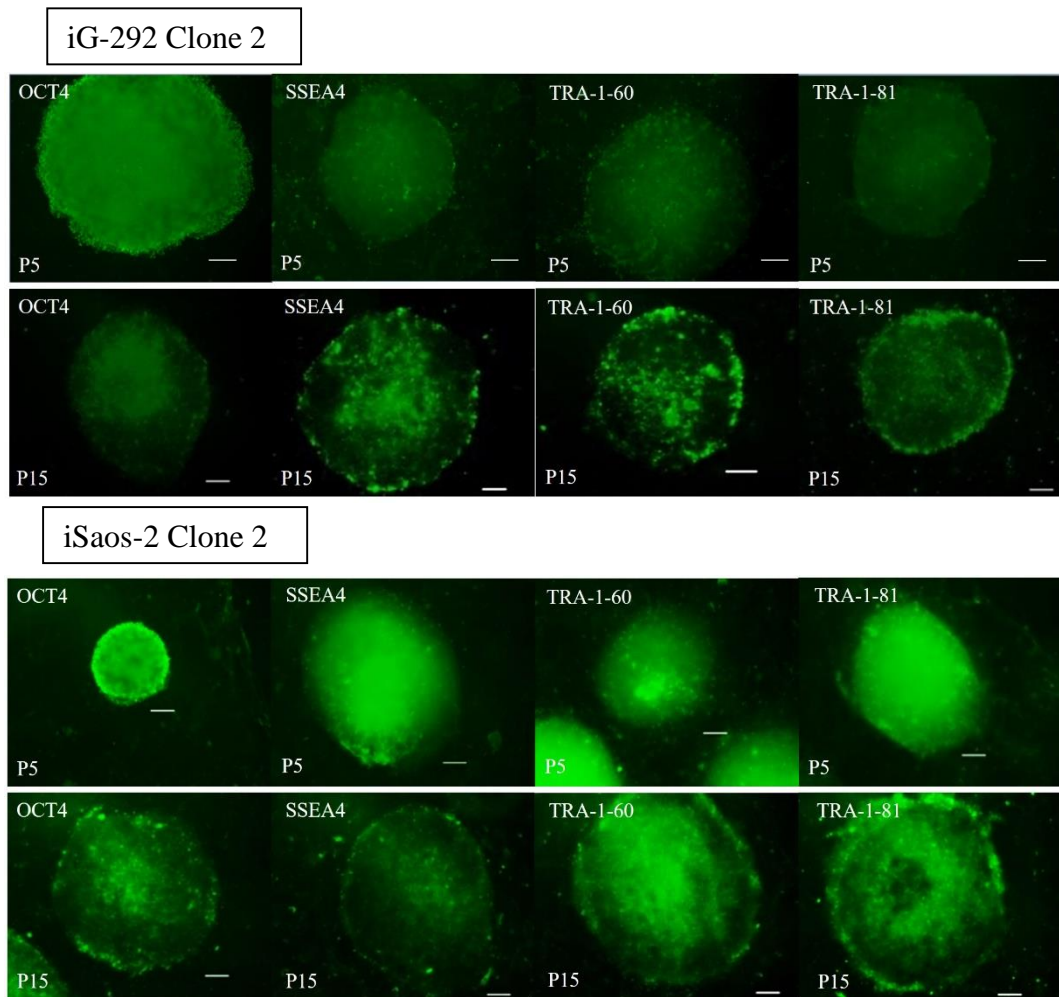


Figure 4.12. Immunofluorescence (IF) staining of iG-292 and iSaos-2 cells at Passage 5 and Passage 15. Reprogrammed cells were stained for pluripotent markers: Intracellular markers (OCT4) and intercellular markers (SSEA4, TRA-1-60 and TRA-1-81). Pluripotent markers expressions were detected in both reprogrammed cells at both passages. Zeiss Axiovert Inverted Microscope, original magnification: 10x. Scale bar: 100 μ m.

4.4.4. mRNA Expression of Pluripotent Markers in Reprogrammed OS cells

Expressions of pluripotent markers were also assessed in mRNA level in both parental and reprogrammed OS cells. Higher level of expressions of *OCT3/4*, *SOX2*, *NANOG* and *REX1* were detected in both reprogrammed OS cells as compared to their parental counterparts. Fold change (FC) was used as the comparison indicator and FC was calculated by $\Delta\Delta C_T$ method between parental and reprogrammed OS cells.

Reprogrammed G-292, iG-292, expressed higher level of *OCT3/4*, *SOX2*, *NANOG* and *REX1* than parental G-292 as shown in Figure 4.13. However, iG-292 showed decreased expression of *c-MYC* than parental cells. iSaos-2 demonstrated similar expression pattern for all 5 pluripotent genes as iG-292 and the expression level for *OCT4*, *SOX2* and *NANOG* were lower in iSaos-2 than iG-292. Expression of pluripotent markers as shown by IF and qPCR suggested iG-292 and iSaos-2 were reprogrammed to ESC-like state.

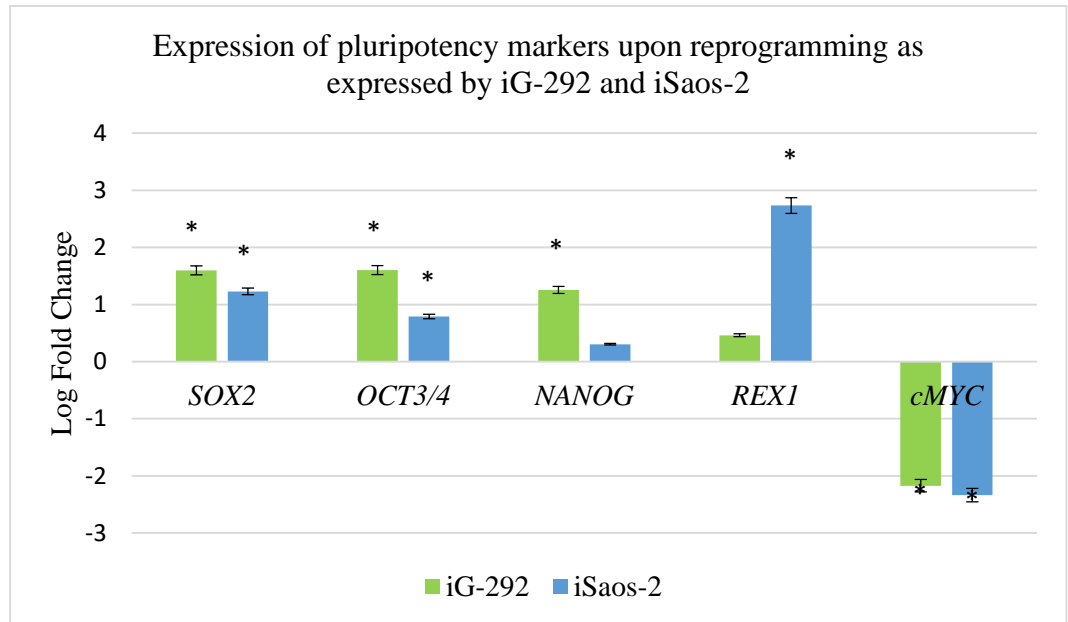


Figure 4.13. Expression of pluripotent genes in reprogrammed OS. Both iG-292 and iSaos-2 expressed *SOX2*, *OCT3/4* and *NANOG*. Expression of pluripotent markers as shown by IF and qPCR suggested iG-292 and iSaos-2 were reprogrammed to ESC-like state. Asterisk (*) indicate significance level at $p < 0.05$.

4.4.5. Embryoid body (EB) formation and spontaneous differentiation

Embryoid body formation is another trademark for ESC and iPSC characteristics. The ability to cluster together and form suspension floating body is often associated with pluripotency (Li and Rana, 2012). Reprogrammed G-292, iG-292, and reprogrammed Saos-2, iSaos-2, were able to form embryoid body when cultured in suspension culture with EB medium. The EB were first cultured as spheres for 10 days (Figure 4.14) in ESC medium without bFGF, before being transferred to standard tissue culture flasks coated with 0.1% gelatin, containing ESC medium without bFGF where the EB attached to the surface. EB spheres formed from both iG-292 and iSaos-2 showed similar morphology to ESC EB with round borders.

Attached EB were cultured for another 8 days for spontaneous differentiation before RNA was extracted for three germ-layer detection via qPCR. EBs from iG-292 expressed mesodermal markers, *MSX1*, *GATA2* and *hBRACHYURY*; endoderm markers, *FOXA2* and *GATA4*; and ectoderm marker, *CDX2*. Meanwhile, iSaos-2 only expressed *MSX1* and *GATA2* (mesoderm); *GATA6* (endoderm) and *TUJ1* (ectoderm).

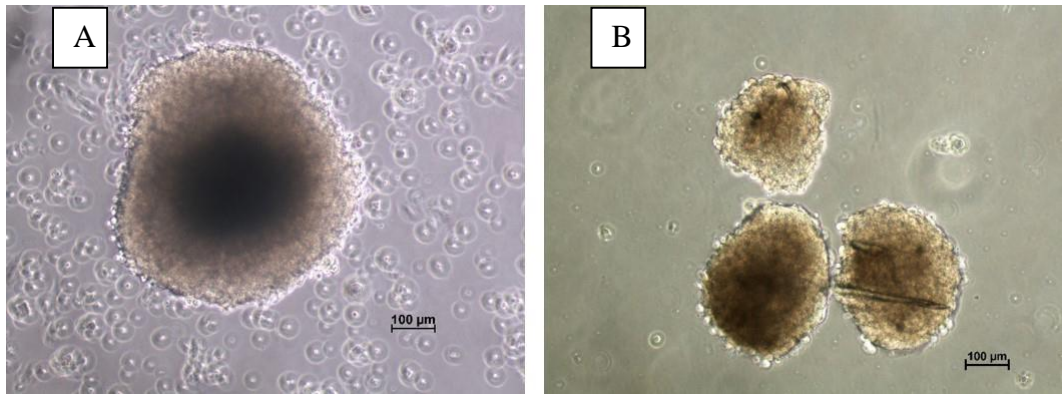


Figure 4.14. Embryoid bodies (EB) formation. Representative images of (A) iSaos-2-EB and (B) iG-292-EB in suspension culture. Nikon inverted microscope, original magnification: 10x.

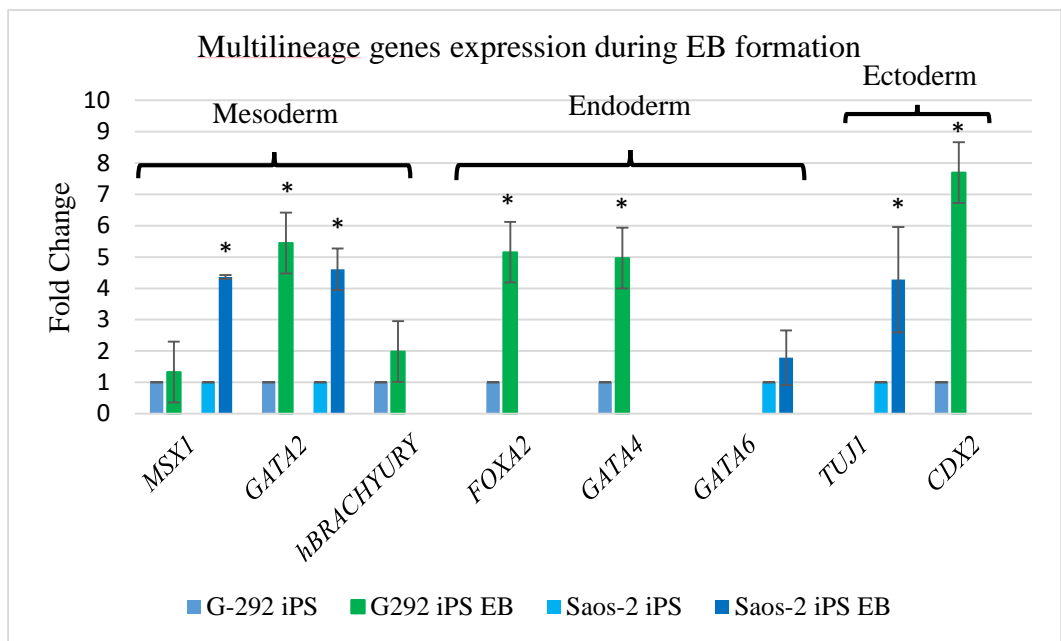


Figure 4.15. Multilineage genes expression during EB formation in iG-292 and iSaos-2. Both reprogrammed OS expressed markers from three germ layers indicating attained pluripotency post reprogramming. Asterisk (*) indicate significance level at $p < 0.05$.

4.4.6. Differentiation into adipocytes and osteoblasts (Mesoderm lineage differentiation)

Adipogenic medium was used for adipocyte differentiation in both parental and reprogrammed OS cells. Representative images were shown in Figure 4.16 and Figure 4.17. Oil Red O staining, as indicated in red staining, was used to stain lipid droplets in the cells. In Figure 4.16 (A) and Figure 4.17 (A), both iG-292 and iSaos-2 cells showed presence of lipid droplets as compared to parental counterparts, G-292 and Saos-2, which failed to form lipid droplets.

Osteogenic medium was used for osteoblast differentiation in both parental and reprogrammed OS cells. Representative images were shown in Figure 4.16 (B) and Figure 4.17 (B). Alizarin Red staining was used to detect the presence of calcium deposition upon osteogenesis. Calcium deposits were stained as red precipitates in both reprogrammed OS cells, iG-292 and iSaos-2. However, iSaos-2 showed brighter red staining as compared to iG-292. Meanwhile, Saos-2 cells also showed bright Alizarin Red staining because Saos-2 are known to be able to mineralise and formed calcium complexes upon mineralisation.

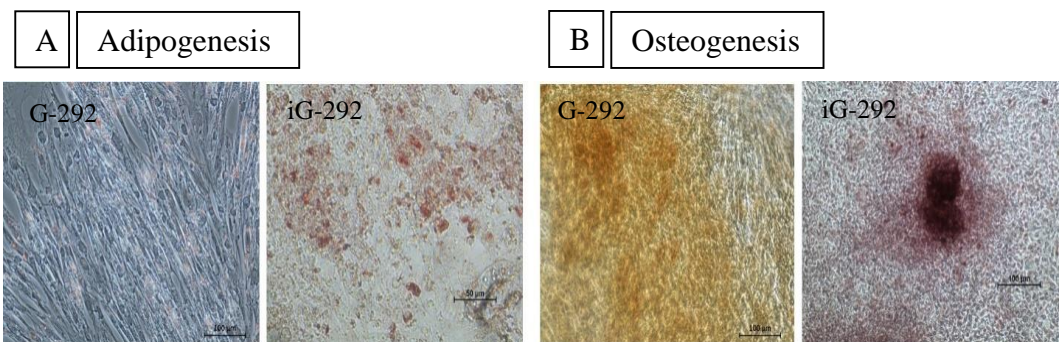


Figure 4.16. Adipogenesis and osteogenesis in G-292 and iG-292. (A) iG-292 showed presence of lipid droplets as stained by Oil Red O. Nikon inverted microscope, original magnification: 10x. (B) iG-292 showed presence of calcium deposits as stained by Alizarin Red. Nikon inverted microscope, original magnification: 20x.

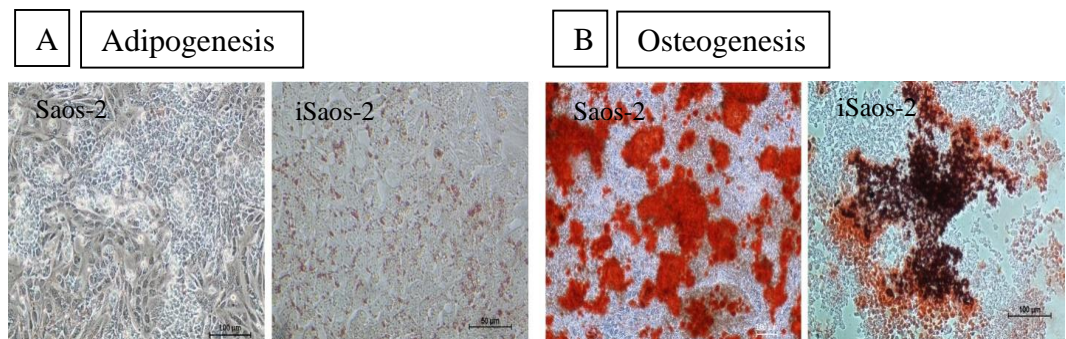


Figure 4.17. Adipogenesis and osteogenesis in Saos-2 and iSaos-2. (A) iSaos-2 showed presence of lipid droplets as stained by Oil Red O. Nikon inverted microscope, original magnification: 10x. (B) Both Saos-2 and iSaos-2 showed presence of calcium deposits as stained by Alizarin Red. Nikon inverted microscope, original magnification: 20x.

4.4.7 Teratoma/ Xenograft Formation

Teratoma/xenograft formation *in vivo* is one of the crucial developmental characteristic of pluripotent stem cells. Pluripotency of reprogrammed OS cells was tested in teratoma formation. Nude mice were used and any tumour formed subcutaneously with an approximate size of 1 cm were excised. Only G-292, iG-292 and Saos-2 were able to form tumour *in vivo*. iSaos-2 failed to form any visible tumour in nude mice. Upon excision, the tumour were processed and stained with H&E for further histological analysis. G-292 and iG-292 tumours took an average of 80.5 days and 65 days post injection respectively to reach 1 cm in size, while Saos-2 tumours took 49 days post injection to reach 1 cm in size. Tumours excised from both parental G-292 and Saos-2 showed only homogeneous population of tumour cells as shown in Figure 4.18.

Histological analysis using H&E staining showed that only iG-292 managed to form teratoma *in vivo*. 4 out of 5 nude mice injected with iG-292 formed teratoma with morphology of cells representing three germ layers; ectoderm, mesoderm and endoderm. Figure 4.19 (B-D) showed representative images of structure formed in iG-292 teratoma that resembles formation of neuronal rosette-like structures (shown by arrow) indicating ectoderm layer; formation of capillary-sized blood vessels (shown by arrow), adipocytes cells, and also fibrous muscle-like cells indicating mesoderm layer and formation of columnar epithelial cells seen as lining glands (shown by arrow), and the papillary structures indicating endoderm layers.

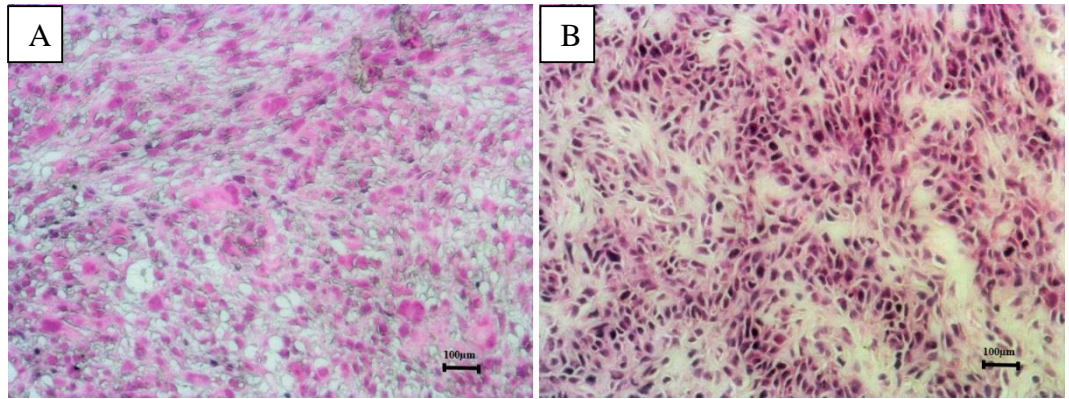


Figure 4.18. Tumour from parental G-292 and Saos-2. Representative image of G-292 (A) and Saos-2 (B) tumours showing homogeneous population of tumour cells.

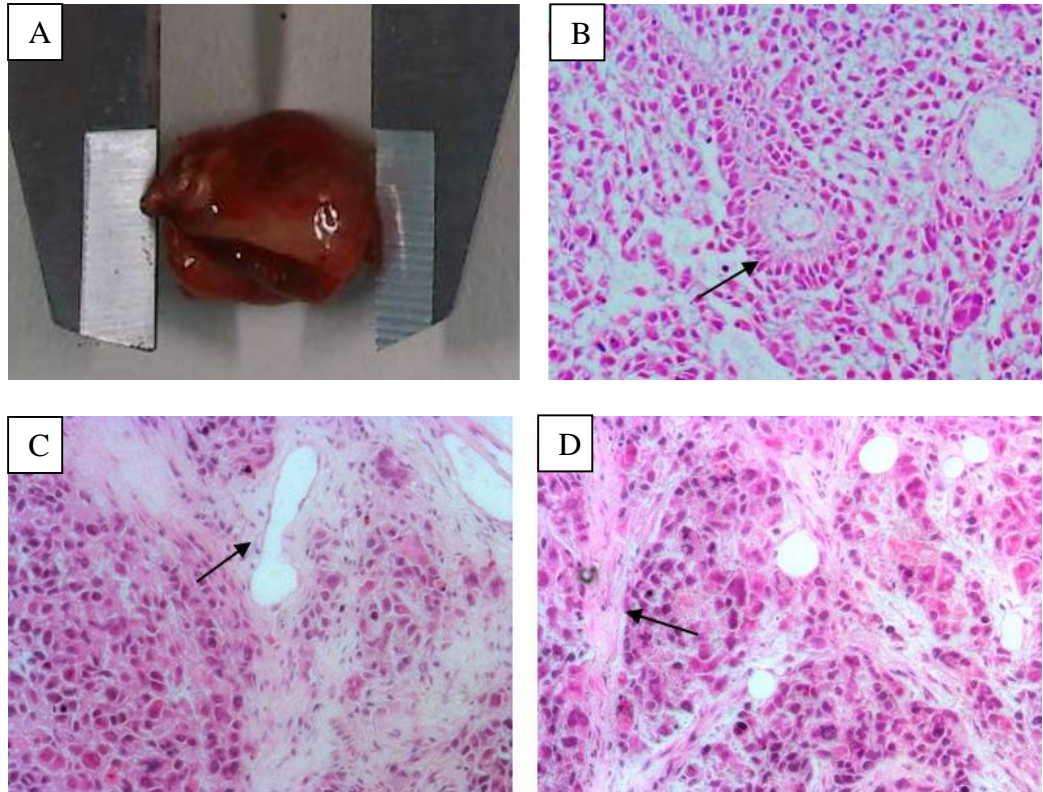


Figure 4.19. Formation of iG-292 teratoma and three germ layers. (A) iG-292 xenograft extracted from nude mice measuring approximately 1 cm. Formation of three germ layers as depicted in B, C and D. (B) Formation of neuronal rosette-like structures indicating ectoderm layer. (C) Formation of capillary-sized blood vessels, adipocytes cells, and also fibrous muscle-like cells indicating mesoderm layer. (D) Formation of columnar epithelial cells seen as lining glands, and the papillary structures indicating endoderm layers.

4.5 Discussion

4.5.1 Reprogramming of osteosarcoma cell lines, G-292 and Saos-2

Reprogramming of osteosarcoma (OS) cell lines offers a new opportunity to study osteosarcoma disease at primitive level. Traditionally, cell lines were generated from primary tumour excised from cancer patients. These primary cell lines carry phenotypes and genotypes known to the disease at the time of onset, which is normally at a terminal stage of neoplastic transformation. Any information of the disease at more primitive or early stage of progression was lost or unknown.

Introduction of reprogramming technology by Prof Shinya Yamanaka in 2006 brought new perspective to both clinical and fundamental studies (Takahashi and Yamanaka, 2006). The ability to change a cell fate from terminally differentiated state to a pluripotent stem cell state has driven cancer researchers to study this technology for cancer diseases. This novel technology unlocks available information of cancer disease at a more primitive state than the original cell lines.

Two osteosarcoma (OS) cell lines, G-292 and Saos-2, were utilised as the target cells in this study. G-292 clone A141B1 cell line was established from a primary osteosarcoma of a 9-year-old Caucasian female. This cell line has fibroblastic phenotype and exhibited mutation in *p53* gene (Chandar et al., 1992; Zhang et al., 1995). While, Saos-2 cell line was derived from the primary

osteogenic sarcoma of an 11-year-old Caucasian female since 1973 (Chandar et al., 1992; Zhang et al., 1995). Both OS cell lines were subjected to single retroviral transduction of four transcription factors, OSKM. Retroviral transduction was employed in our study because this is the most established and most used reprogramming method for both somatic and cancer reprogramming (Takahashi & Yamanaka 2006; Takahashi et al., 2007; Miyoshi et al., 2010; Kumano et al., 2012). Moloney murine leukaemia virus (MMLV)-derived retrovirus such as pMXs was the original delivery system used by Yamanaka in 2006 (Takahashi and Yamanaka, 2006). MMLV-based retroviral system also reported higher efficiency than non-viral methods (González et al., 2011).

Two separate reprogramming attempts were done on both OS cell lines. In both attempts, fresh retroviral supernatants were obtained from 293 FT cells for all four transcription factors. Fresh viral supernatants are one of the crucial determinants on the success of reprogramming (Sugii et al., 2011). To overcome the challenges of retroviral slow diffusion to target cells, spinfection method (centrifugation at 800 x g for 50 minutes) was used. Generation of OS-induced pluripotent stem cells (iPSC) was conducted on a feeder environment as feeder cells are better in supporting the generation and maintenance of iPSC.

Usage of small molecules such as valproic acid (VPA) also helped to increase the reprogramming efficiency. Valproic acid, a histone deacetylase inhibitor, was shown to be able to increase reprogramming efficiency in human fibroblasts and could even replace *KLF4* and *cMYC* in the reprogramming cocktail (Huangfu et al., 2008a; Huangfu et al., 2008b). This effect of VPA on

reprogramming suggested the involvement of chromatin remodelling in reprogramming process (Kretsovali et al., 2012).

Reprogramming efficiency in this study was around 0.17% for G-292 and 0.3% for Saos-2 as shown in Figure 4.7. This efficiency percentage is higher than what was reported in reprogramming of gastrointestinal cancer cell lines by Miyoshi and colleagues using retroviral OSKM which achieved a 0.001% reprogramming efficiency (Miyoshi et al., 2010). Another study on melanocytes reprogramming using doxycycline-inducible lentivirus OSKM demonstrated reprogramming efficiency of 0.05% (Utikal et al., 2009). This same paper also reported successful reprogramming of human melanoma cells. However, the paper did not mention the reprogramming efficiency of human melanoma.

There have been a debate on usage of all four transcription factors, OSKM, in cancer reprogramming. Some studies showed removal of certain transcription factors, such as *cMYC*, was possible for somatic reprogramming (Mikkelsen et al., 2008; Nakagawa et al., 2008). Another study demonstrated the usage of only *OCT4* to obtain pluripotency in neural stem cells (Kim et al., 2009). However, in the case of reprogramming in chronic myeloid leukaemia (CML) cell line, KBM7, all four transcription factors, OSKM, were indispensable. The exclusion of *OCT4*, *SOX2* or *KLF4* led to fewer colony formation while elimination of *cMYC* resulted in cell death (Carette et al., 2010). Thus, we included all four transcription factors in our reprogramming cocktail.

4.5.2 Characterisation of Established Osteosarcoma Derived Induced Pluripotent Stem Cells (OS-iPSC)

Expression of alkaline phosphatase (AP) is regarded as one of the essential phenotypic expression analysis of pluripotent stem cells. AP live staining was used in early passages (Passage 1) of both iG-292 and iSaos-2 to distinguish the putative ESC-like clones from non-ESC-like clones. Usage of live staining enable further culturing of the selected colonies after the removal of dye. However, AP expression alone is insufficient for confirmation of pluripotency. Expression of additional pluripotent markers are needed to authenticate the identity of the pluripotent colonies.

Pluripotency markers expression was analysed at protein level via immunofluorescence staining and at mRNA level via qPCR. Among the commonly used markers for immunofluorescence include intracellular marker, OCT4, and intercellular markers, SSEA4, TRA-1-60 and TRA-1-81 (Pera et al., 2000; Zhao et al., 2012; Martí et al., 2013). iG-292 and iSaos-2 clones were stained positive for these markers at Passage 5 and Passage 15 indicating prolonged maintenance of pluripotency in both reprogrammed OS. These protein markers were also reported in both somatic and cancer reprogramming studies (Aasen et al., 2008; Oka et al., 2010; Hu et al., 2011; Kumano et al., 2012; Stricker et al., 2013).

Gene expression of pluripotent markers for *OCT4*, *SOX2*, *NANOG* and *c-MYC* was conducted using qPCR approach to calculate the fold change (FC)

expression of the markers as compared to their parental counterparts. Both iG-292 and iSaos-2 expressed *OCT4*, *SOX2* and *NANOG*. *OCT4*, *SOX2* and *NANOG* are proteins associated in the self-renewal of undifferentiated ESC (Chambers and Tomlinson, 2009; Johansson and Simonsson, 2010). *OCT4* also known as *POU5F1*, a mammalian POU family transcription factor, has been observed to be expressed by early embryo cells and germ cells but not differentiated cells (Nichols et al., 1998; Tai et al., 2005). Thus, the expression of *OCT4* is regarded as essential for the identity of pluripotency in reprogramming study. *SOX* proteins [sex-determining region Y (*SRY*)-related box proteins] has been linked to embryogenesis development (Kiefer, 2007). *SOX2*, from the *SoxB1* transcription factor family, is a key transcriptional regulator in pluripotent stem cells (PSCs) (Zhang and Cui, 2014). Together with *OCT4* and *NANOG*, *SOX2* has been identified as the core intrinsic factors for regulating pluripotency in mammalian.

As one of the core factors for pluripotency, *NANOG* expression in reprogrammed OS but not the parental counterparts demonstrated that reprogrammed OS achieved higher level of pluripotency. *NANOG*, a homeodomain factor, is an essential regulator of early embryogenesis (Chambers et al., 2003). Study by Boyer et al. (2005) showed that *OCT4*, *SOX2* and *NANOG* co-occupied their target genes and collaborated to form regulatory enclosure that contributed to pluripotency and self-renewal (Boyer et al., 2005). The expression of these three important transcription factors showed that the reprogrammed OS attained pluripotency comparable to that of ESC.

REX1 is a zinc finger protein expressed mainly in undifferentiated stem cells (Scotland et al., 2009). REX1 is also linked to cancer formation. Two studies collectively showed decreased expression of REX1 in renal cell carcinoma (Raman et al., 2006; Scotland et al., 2009). Another study by Lee et al. (2010) also demonstrated lack of REX1 expression in prostate cancer cell line, PC-3 (Lee et al., 2010). Expression of REX1 was detected in breast cancer cell line, MDA-MB-468 and oral cavity squamous carcinoma cells, SCC15. However the expression of REX1 was not detected in several other carcinomas, including oral cavity squamous cell carcinoma cells (SCC-4, SCC-9, SCC-25), breast carcinoma cell lines (MCF7, MDA-MB-231, MDA-MB-453, HS578T, SK-BR-3), acute promyelocytic leukemia cell lines (HL60 and NB-4), prostate carcinoma cell line (LnCAP) and renal carcinoma cell line (SK-39) (Mongan et al., 2006). Both reprogrammed OS showed up-regulation of REX1 further supported the distinct differences from parental OS.

Expression of c-MYC is often debated in reprogramming of both somatic and cancer cells. c-MYC is a known oncogene, playing great role in cellular growth regulation and metabolism (Miller et al., 2012). Overexpression of c-MYC has been linked to increased cellular proliferation and malignant transformation in affected cells (Miller et al., 2012). Down-regulation of c-MYC expression was reported in previous sarcoma reprogramming (Zhang et al., 2013) similar to our observation in both reprogrammed OS. Though expression of c-MYC has always been reported to be up-regulated in somatic reprogramming (Aasen et al., 2008; Hester et al., 2009; Zhao et al., 2010; Park et al., 2012), this down-regulation of c-MYC in our reprogrammed OS was

expected due to the involvement of c-MYC in OS progression (Broadhead et al., 2011; Han et al., 2012). Overexpression of c-MYC has been associated to increased OS invasion ability through the activation of MEK-ERK pathway (Han et al., 2012). Previous studies have revealed that reprogramming could reduce the tumorigenic property of parental cancer cells (Mahalingam et al., 2012; Zhang et al., 2014; Bernhardt et al., 2017). This down-regulation of c-MYC expanded the ability of reprogramming to reverse oncogenic effects in cancer cells and this observation could be important for discovery of novel therapeutic strategies for OS.

To provide a comprehensive evaluation on the functional pluripotency of reprogrammed OS, spontaneous differentiation via embryoid bodies (EB) formation was used. EB are non-adherent spheroids formed from aggregation of cells. Mature EB have shown to contain cells from three germ lineages; endoderm, ectoderm and mesoderm (Schuldiner et al., 2000; Kopper et al., 2010). Removal of beta-fibroblast growth factor (bFGF) from EB medium for 7-8 days may initiate spontaneous differentiation (Schuldiner et al., 2000). The differentiation of human ESC into EB is spontaneous, thus making it hard to determine which cell types will form *in vitro* (Thomson et al., 1998; Itskovitz-Eldor et al., 2000). Both reprogrammed OS, iG-292 and iSaos-2, expressed markers from three germ layers, denoting the pluripotency of iG-292 and iSaos-2.

Loss of differentiation ability is known in OS and this defect is associated with prognostic significance in OS, with well-differentiated tumours

classified as low-grade and poorly differentiated tumours falling into high-grade category (Thomas et al., 2004). It was reported that osteocalcin, a late marker of osteogenic differentiation, was untraceable in more than 75% of osteosarcomas (Thomas et al., 2004). As OS is derived from mesodermal lineage, differentiation into adipocytes and osteoblasts were used to test the possibility of reprogramming in changing this differentiation ability in reprogrammed OS. As expected G-292 and Saos-2 did not form adipocytes when cultured in adipogenesis induction medium, while both iG-292 and iSaos-2 form lipid droplets indicating formation of adipocytes. When cultured in osteogenic induction medium, iG-292 showed formation of calcium deposit but not parental counterpart, G-292. Though iSaos-2 demonstrated calcium deposit after osteogenic induction, parental cells, Saos-2, exhibited more intense calcium deposit than iSaos-2. This is because Saos-2 is a known calcifying osteogenic cell line and has shown matrix deposition ability in previous study (Prideaux et al., 2014). Mesodermal directed differentiation study presented mediocre expression by less intensity of lipid droplets formation and calcium deposition in both reprogrammed OS. This suggested that differentiation of terminal cells from ESC-like stage needed more stimulation to become mesenchymal stem cell (MSC)-like cells prior to adipogenesis and osteogenesis. Thus, implying that our reprogrammed OS might be more primitive than MSC.

Formation of teratoma by pluripotent stem cells is regarded as the hallmark of pluripotency. Recently, there have been debates on using this method as the 'gold standard' for determining pluripotency in iPSC work. Teratoma formation is often associated with high cost, needs skilled personnel

to handle the procedure and lacks reliability across methodologies (Muller et al., 2010). Reprogrammed cancer cells were also known as induced pluripotent cancer (iPC) cells instead of iPSC attributed to the nature of the parental cells. The term iPC was first introduced by Miyoshi et al. during reprogramming of gastrointestinal cancer cells (Miyoshi et al., 2010). In their study, they demonstrated the success of inducing gastrointestinal cancer cells to pluripotency stage. However, they did not perform teratoma study to test the *in vivo* pluripotency of the induced cells.

Subsequent study by Zhang et al. showed reduced tumourigenicity of sarcoma cell lines upon reprogramming (Zhang et al., 2013). Their study clearly demonstrated that there were no teratoma formation from the reprogrammed cancer cells. However, the tumour formed from the reprogrammed cell lines showed decreased tumour size and were associated with necrosis leading to interpretation as reduced tumourigenicity in reprogrammed sarcoma. In both aforementioned studies, the authors avoided naming their reprogrammed cancer cells as iPSC. This could be due to the failure to form teratoma when injected into immune-compromise mice in *in vivo* study. In contrast, Carette et al. generated cancer-derived iPSC from CML cell line, KBM7 and KBM7-iPSC formed teratoma when injected subcutaneously into NOD SCID mice (Carette et al., 2010). Similarly, Hu et al. managed to reprogramme bone marrow mononuclear cells from a chronic phase CML patient and showed that the iPSC formed teratoma in subcutaneous of NOD mice (Hu et al., 2011).

Based on the *in vivo* results from our study, reprogramming changed primary cancerous property of parental G-292 to a teratoma-forming ability in iG-292. Following on the characterisation done, iG-292 proved to pass all the iPSC characteristic tests. Therefore, iG-292 is believed to be fully reprogrammed in contrast to iSaos-2, which did not form teratoma *in vivo*.

Reprogramming roadblock or resistance have been reported in a few studies using both somatic cells and diseased cells. There are many reasons that attributed to this reprogramming roadblock. One of the major hindrance in reprogramming is the expression of p53. It have been reported in a few studies that p53 deficiency improves reprogramming efficiency of somatic cells (Kawamura et al., 2009; Hong et al., 2009; Brosh et al., 2013; Ebrahimi, 2015). In a study to improve reprogramming efficiency in somatic cells conducted by Zhao and colleagues, the team found that knockout p53 and UTF1 overexpression greatly enhances iPSC generation efficiency in human adult fibroblasts (Zhao et al., 2008).

In a study conducted by Hanna et al. to study the stochastic process of reprogramming, they found that additional p53 knockdown increased cell cycle division rate and accelerated iPSC formation via a cell division-dependent mechanism (Hanna et al., 2009). Besides that, p53 was reported to restrict reprogramming by using apoptosis mechanism to remove DNA-damaged cells at the early stages of reprogramming process (Marión et al., 2009). All these studies provided valuable information on how p53 deficiency could benefit reprogramming.

Further study conducted by Sarig et al. (2010) on the role of mutated p53 (mut-p53) in somatic cell reprogramming demonstrated that the presence of mutated p53 rather than the absence of the p53 expression (p53 knockout) were able to enhance reprogramming efficiency. Similar results were also reported by Verusingam et al. in studying oral squamous cell carcinoma (OSCC) reprogramming (Verusingam et al., 2017). This could explain the different reprogramming aptitude displayed by both G-292 and Saos-2. Though both cell lines are p53 deficient, G-292 carries mutated p53 (Chandar et al., 1992) while Saos-2 is p53-null (Chen et al., 1996; Sun et al., 2015). Based on the aforementioned studies, the difference of p53 expression in G-292 and Saos-2 could explain the fully reprogrammed status of G-292 and incomplete reprogramming of Saos-2.

4.6 Conclusion

Reprogramming using retroviral OSKM method on OS cell lines, G-292 and Saos-2, was successful in generating OS-iPSC cells, iG-292 and iSaos-2. Both reprogrammed OS demonstrated characteristics similar to ESC in *in vitro* characterisation experiments conducted. However, only iG-292 formed teratoma when injected into nude mice.

CHAPTER 5

RESULTS & DISCUSSION: PART 2

Evaluation of DNA repair, cell cycle and apoptosis processes from global gene expression of the reprogrammed OS cells using microarray technology

5.1 Introduction

Microarray technology had been widely used to study the whole genome expression at the molecular level. By using microarray technology, it allows comparison of gene expression patterns between two or more study groups by interrogating thousands of expressed genes simultaneously. Beside that, microarray is a highly efficient technology for further characterisation of iPSC properties.

Affymetrix Human PrimeView Gene Chip microarray technology employs oligonucleotide approach that uses shorter and uniformed length probes (25 bases) that were synthesised directly onto a matrix using photolithographic technology (Loi et al., 2007).

5.2 RNA preparation and integrity

Purity and integrity of extracted RNA samples are very essential for global gene expression study. All RNA samples were extracted using Qiagen RNeasy® Mini Kit prior to quality check using A_{260}/A_{280} ratio and A_{260}/A_{230} ratio. The A_{260}/A_{280} ratios of all extracted RNA samples were 1.8 or higher indicating high RNA purity and A_{260}/A_{230} ratios were 1.7 or higher indicating RNA samples were free from impurities during extraction (Table 5.1).

Table 5.1. Purity, integrity and concentration of RNA samples extracted from parental OS and reprogrammed OS cells

Cell Lines	A₂₆₀/A₂₈₀	A₂₆₀/A₂₃₀	RIN	Concentration (ng/uL)
G-292	1.983	1.790	8.7	562
G-292	2.019	1.717	8.7	848
iG-292 Clone 2 P30	2.074	2.154	8.6	224
iG-292 Clone 2 P42	2.000	2.185	8.6	660
iG-292 Clone 2 P28	2.012	1.968	7.7	652
Saos-2	1.967	2.143	8.3	2490
Saos-2	1.830	1.982	8.3	1102
iSaos-2 Clone 2 P22	1.976	2.200	8.9	1162
iSaos-2 Clone 2 P38	1.957	2.074	8.8	736
iSaos-2 Clone 2 P30	1.950	2.050	8.7	524

RIN = RNA integrity number, is an algorithm assigning integrity values to RNA measurements. The closer the value to 10, the higher the integrity of the RNA.

5.3 Global gene expression profile in parental and reprogrammed OS

Global gene expression profile was conducted on both parental and reprogrammed OS cells using Affymetrix platform and the raw data from microarray were imported into GeneSpring GX 13.0 software for analysis. RNA from three iG-292 sub-clones and three iSaos-2 sub-clones together with RNA from both parental cells were extracted and subjected to microarray experiments. Raw data generated from Affymetrix platform was deposited to NCBI GEO Omnibus with accession number GSE107855.

In GeneSpring GX 13.0 analysis, the data were filtered based on their expression to remove probe sets with signal intensities for all the groups that were in the lowest 20 percentile of overall intensity value. Moderated T-Test combining the Benjamini- Hochberg test correction was utilised to detect differentially expressed genes between parental and reprogrammed groups. The level of significance was set at $p < 0.05$.

Upon using unsupervised hierarchical clustering analysis, global gene expression profile of both parental and reprogrammed OS was performed to depict the differential gene expression upon reprogramming (Figure 5.1). The clustering demonstrated distinctive separation of two clustered populations, in which cluster 1 grouped the parental samples together and cluster 2 grouped the reprogrammed samples together. Three biological samples from each of the reprogrammed OS, iG-292 and iSaos-2, showed similarity when clustered, demonstrating that parental OS have acquired similar genomic expression

upon induction of pluripotency. The highly differential expression of genes between the parental and reprogrammed cells indicated that the reprogramming process managed to change cell fate of OS parental cells.

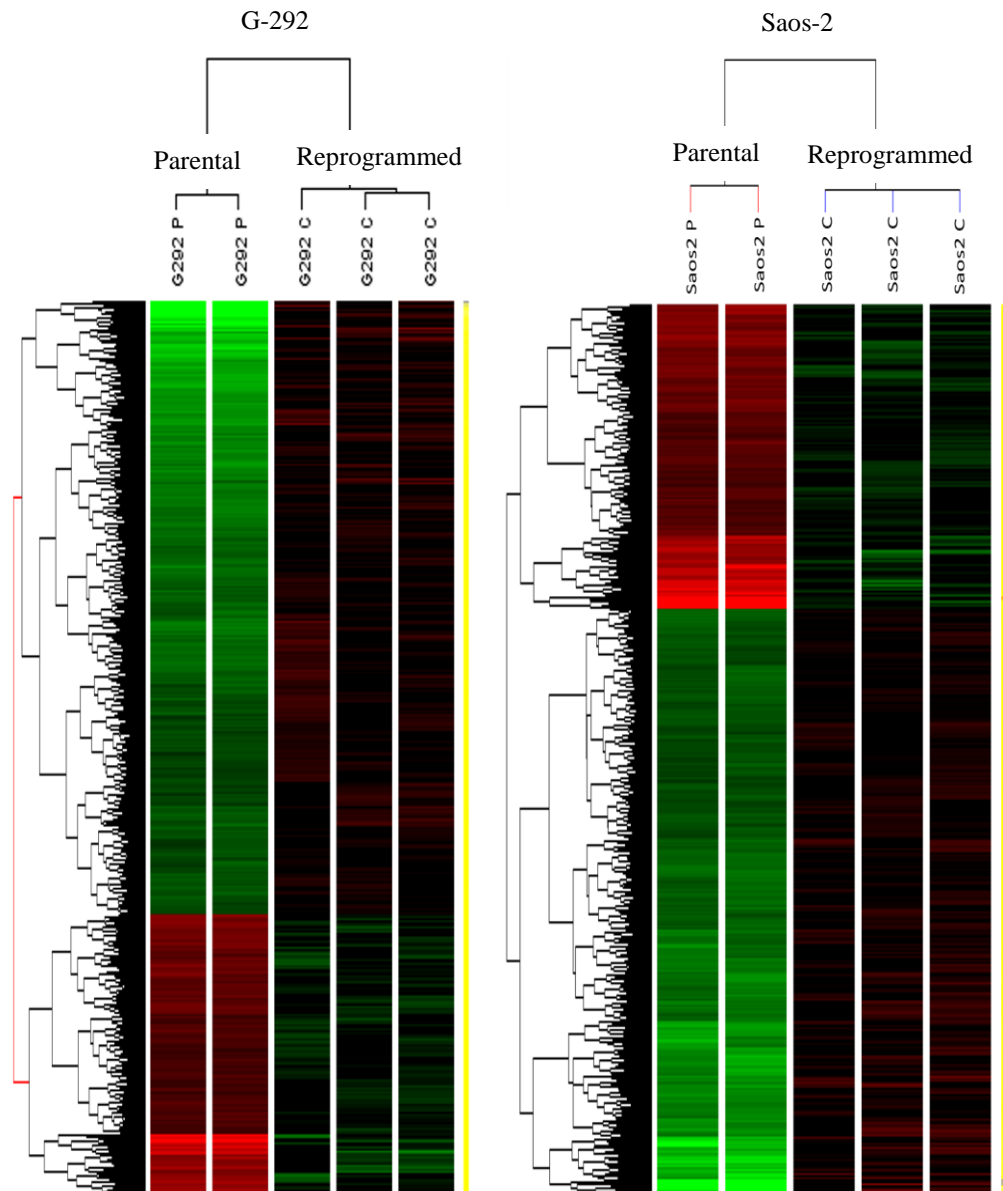


Figure 5.1. Hierarchical clustering analysis of parental and reprogrammed OS. The analysis was performed using GeneSpring GX 13.0 showing distinctive clustering between parental and reprogrammed OS cells. Clustering were done based on differential expression more than 2-fold and significance level $p < 0.05$. Red and green colour codes represent relative mRNA expression levels below and above the reference channel respectively.

Among 48,658 entities (covering ~25k genes) analysed, 4,654 entities representing 2,867 genes showed differential expression of more than 2-fold between parental G-292 and reprogrammed iG-292 (Table 5.1), whereas 1,666 entities representing 1,140 genes showed differential expression of more than 2-fold between parental Saos-2 and reprogrammed iSaos-2 (Table 5.1). Number of genes are not reflected as entities because certain genes have more than 1 entity to detect the expression in Affymetrix Human PrimeView Gene Chip. Both reprogrammed OS showed more down-regulated differentially expressed genes (DEGs) than up-regulated DEGs (Table 5.1). These highly DEGs were further categorised based on their functional annotation into three categories in Gene ontology, namely cellular component, molecular function and biological processes (Fig. 5.2-5.5).

Table 5.2. Differentially expressed entities and genes between parental and reprogrammed OS with fold change ≥ 2 and significance level, $p < 0.05$.

	Up-Regulated		Down-Regulated		Total Differentially expressed	
	Entities	Genes	Entities	Genes	Entities	Genes
iG-292 vs G-292	1,454	992	3,200	1,875	4,654	2,867
iSaos-2 vs Saos-2	571	410	1,095	730	1,666	1,140

5.4 Gene ontology enrichment analysis of the highly differentially expressed genes

Gene ontology (GO) is a useful tool to group genes and gene products according to the function of each gene and their products into three major categories: cellular component, molecular function and biological processes. GO analysis was used to indicate functional genes that were up-regulated or down-regulated in a statistically significant manner between reprogrammed OS and parental cells (Consortium, 2000).

GO enrichment analysis revealed that a total 685 GO satisfying a fold change of ≥ 2 and statistical p value cut-off at 0.05 were generated when comparing differentially expressed genes in iG-292 against parental G-292. These GO were evenly grouped into molecular function (32.05%), biological processes (32.70%) and cellular component (35.24%) (Figure 5.2), while a total of 122 GO satisfying a fold change of ≥ 2 and p value cut-off at 0.05 were generated from differentially expressed genes in iSaos-2 against parental Saos-2. These GO were classified higher into biological processes (40.79%), followed by cellular component (33.76%) and molecular function (25.45%) (Figure 5.3).

iG-292 DEGs in molecular function category were further broken down into 8 sub-categories. Among the 8 sub-categories, 2 most prominent GO were identified as binding (60.92%) and catalytic activity (28.87%) (Figure 5.2). Cellular component GO for iG-292 were further grouped into 10

sub-domains: with cell (23.17%), cell part (23.17%) and organelle (17.37%) listed as the top three categories. As for biological processes, the top three categories were cellular processes (16.12%), single organism processes (14.22%) and biological regulation (12.81%) among top ten sub-categories.

iSaos-2 DEGs in molecular function could only be divided into two components with binding domain taking 98.9% and catalytic activity only taking 1.1%. Among 9 sub-categories in cellular processes, membrane (26.69%), membrane part (21.37%) and cell/cell part (16.87%) were the top three categories. As for biological processes, it was divided into 9 sub-categories with single organism processes (25.54%) taking the top place followed by cellular processes (19.12%) and multicellular organism processes (14.23%) (Figure 5.3).

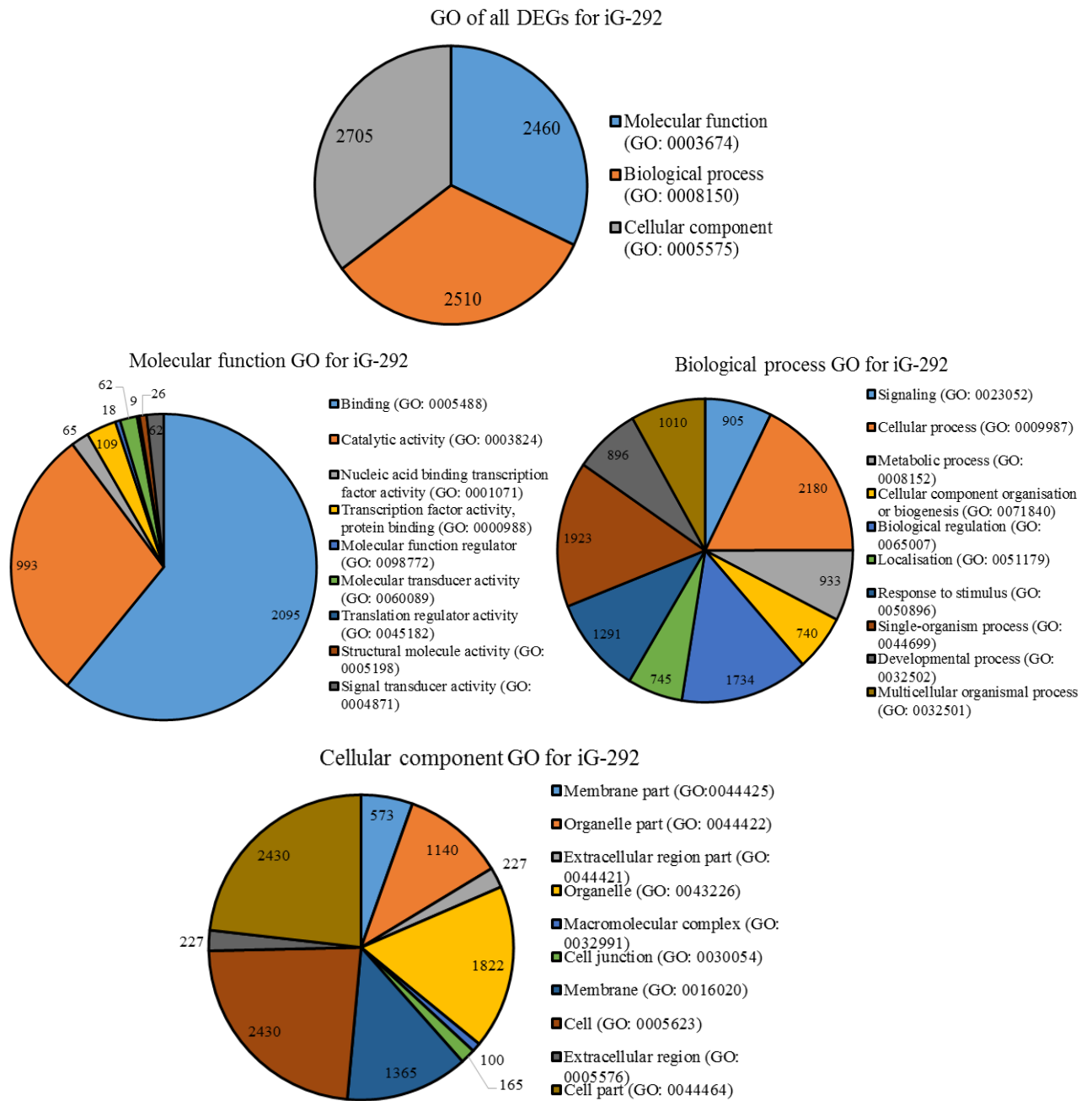


Figure 5.2. Distribution of gene ontology enriched categories for reprogrammed OS, iG-292. GO analysis was generated based on iG-292 DEGs against parental G-292 as the control. Total DEGs were further distributed into 3 main GO domains, molecular function, biological processes and cellular component. Each GO domain was further classified accordingly.

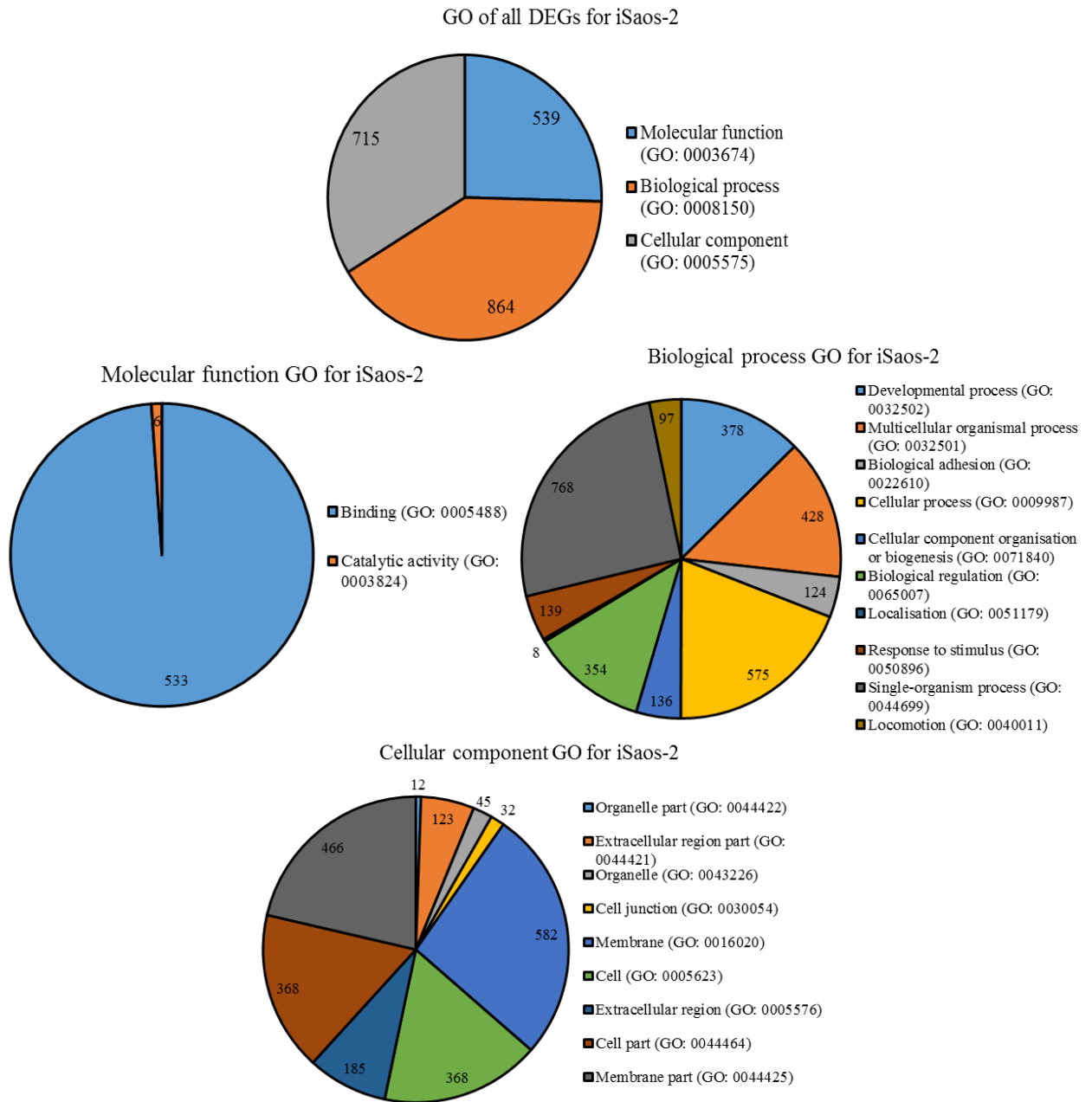


Figure 5.3. Distribution of gene ontology enriched categories for reprogrammed OS, iSaos-2. GO analysis was generated based on iSaos-2 DEGs against parental Saos-2 as the control. Total DEGs were further distributed into 3 main GO domains, molecular function, biological processes and cellular component. Each GO domain was further classified accordingly.

Further analysis on GO based on up-regulated and down-regulated DEGs were shown in Figure 5.4 and Figure 5.5. In up-regulated DEGs, molecular function domain in both reprogrammed OS showed similar up-regulation in binding; iG-292 (60.51%) and iSaos-2 (100%). In biological processes, single organism process was listed as top two contributors in both reprogrammed iG-292 and iSaos-2. Meanwhile, only up-regulated DEGs from iG-292 produced GO enrichment for cellular component, with the majority on cell (49.67%) and cell part (49.67%); while up-regulated DEGs from iSaos-2 did not generate any GO enrichment for cellular component.

For down-regulated DEGs, GO enriched category “binding” was the top in both iG-292 (77.7%) and iSaos-2 (100%) in molecular function domain. In biological processes, the top three categories for iG-292 were cell processes (16.6%) followed by single organism processes (14.57%) and biological regulation (13.28%). While in iSaos-2, the top three categories in biological processes were single organism processes (17.92%), multicellular organism processes (16.35%) and developmental processes (15.94%). For cellular component domain, cell and cell part were listed top in iG-292 (21.91% for both), but were listed as third in iSaos-2 (16.63% respectively). Membrane was listed top in cellular component domain for iSaos-2 (25.02%) (Figure 5.5).

Up- and down-regulated GO enrichment in molecular function and cellular component showed more changes in iG-292 than iSaos-2, supporting the earlier observation that iG-292 was reprogrammed to a different level than iSaos-2.

GO of up-regulated DEGs

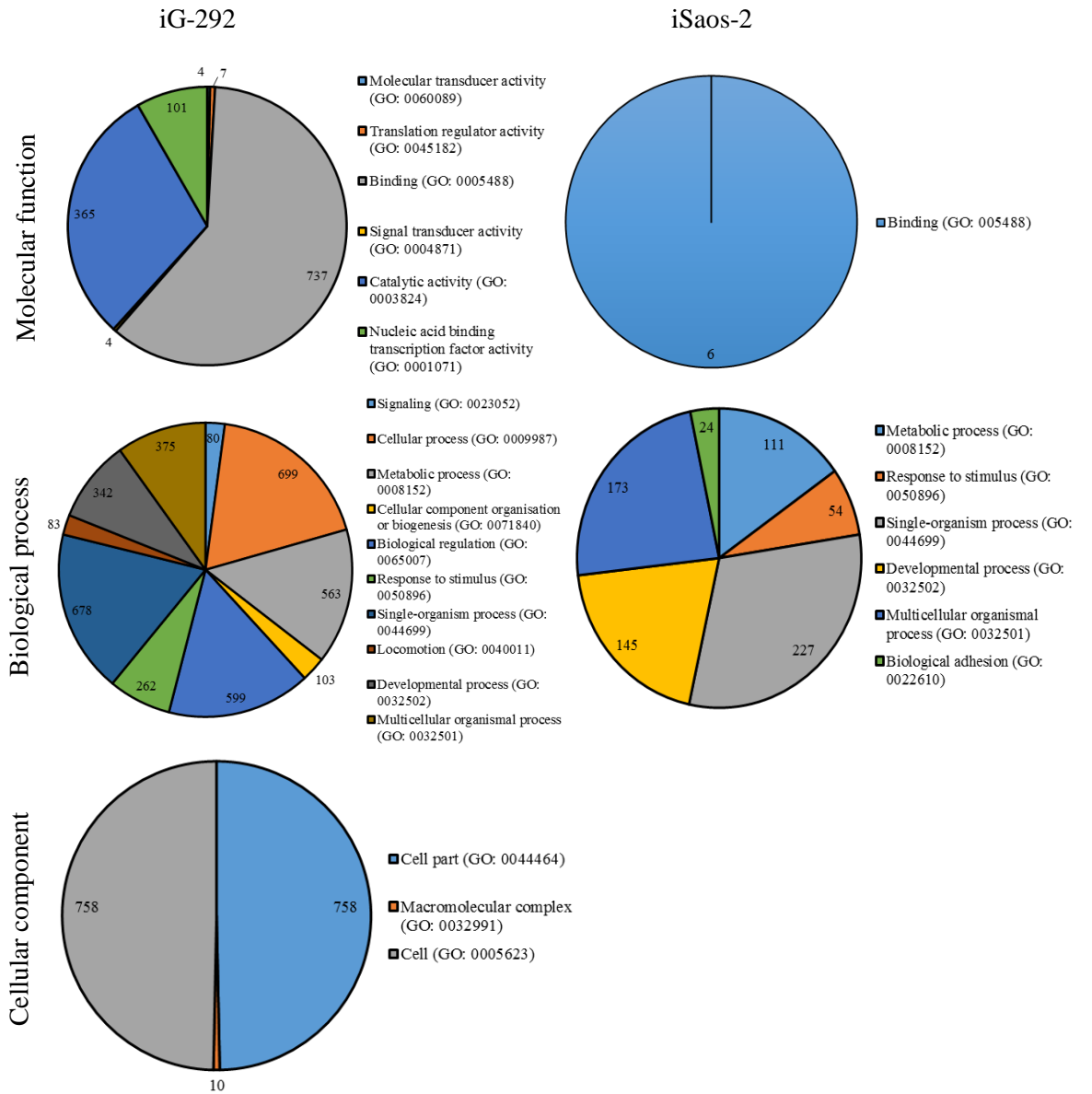


Figure 5.4. Distribution of gene ontology enrichment categories based on up-regulated DEGs in both iG-292 and iSaos-2 respectively. Each GO domain was generated from up-regulated DEGs in a statistically significant manner between reprogrammed OS and parental cells.

GO of down-regulated DEGs

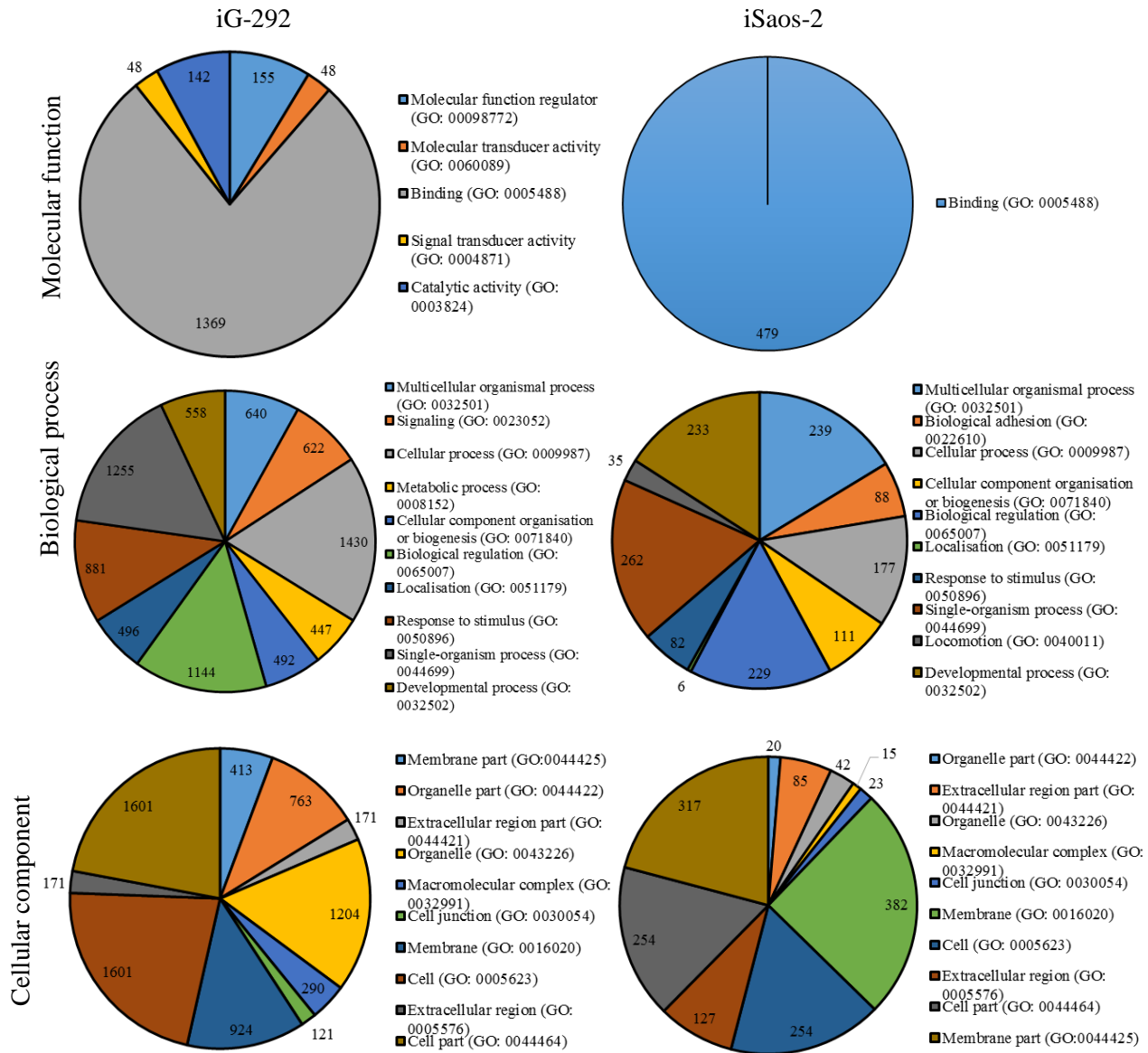


Figure 5.5. Distribution of gene ontology enrichment categories based on down-regulated DEGs in both iG-292 and iSaos-2 respectively. Each GO domain was generated from down-regulated DEGs in a statistically significant manner between reprogrammed OS and parental cells.

5.5 Elucidation of DNA Damage Response (DDR) pathways upon OS reprogramming via global gene expression profiling

As DNA Damage Response (DDR) comprise DNA repair mechanism, cell cycle checkpoint and apoptosis processes, differentially expressed genes (DEGs) were grouped in accordance to the pathway in which they participate in DDR system; DNA repair (Figure 5.6), cell cycle (Figure 5.7) and apoptosis (Figure 5.8). All data were generated using GeneSpring GX 13.0 with fold change more than 1.5 and significance level, $p < 0.05$. Fold change reported in each figure was generated by GeneSpring GX 13.0 with each parental counterpart acting as the normaliser.

iG-292 displayed more DEGs in each pathway as compared to iSaos-2 (Fig. 5.6). iG-292 showed up-regulation of 8 DNA repair genes while iSaos-2 only showed up-regulation of 4 genes. Besides, iG-292 also showed down-regulation of 17 genes and iSaos-2 only showed down-regulation of 4 genes. There were contradictory expression between iG-292 and iSaos-2 in 3 genes, *CASP8*, *PARP3* and *MLH1*, where iG-292 showed down-regulation while iSaos-2 showed up-regulation of these genes. Only *PARP1* was up-regulated in both iG-292 and iSaos-2.

Based on Figure 5.7, 8 cell cycle genes were up-regulated in iG-292 and 2 genes were up-regulated in iSaos-2. Meanwhile, 15 genes were down-regulated in iG-292 and 3 genes were down-regulated in iSaos-2. Only 1 gene, *MCM9*, showed conflicting expression with up-regulation in iG-292 but down-

regulated in iSaos-2. While, only *CCNA1* showed up-regulation in both iG-292 and iSaos-2.

As for apoptosis gene list analysis as showed in Figure 5.8, 11 apoptotic genes were up-regulated in iG-292 and 5 genes were up-regulated in iSaos-2. Whereas, 26 genes were down-regulated in iG-292 and 5 genes were down-regulated in iSaos-2. There were 2 genes, *DAPK1* and *CASP8*, which demonstrated differing expression in iG-292 and iSaos-2. In iG-292, *DAPK1* was up-regulated and *CASP8* was down-regulated, but iSaos-2 showed the opposed expression. Only *IGF2* was up-regulated in both iG-292 and iSaos-2 while *CASP4*, *TNFRSF1A* and *MYC* were down-regulated in both iG-292 and iSaos-2.

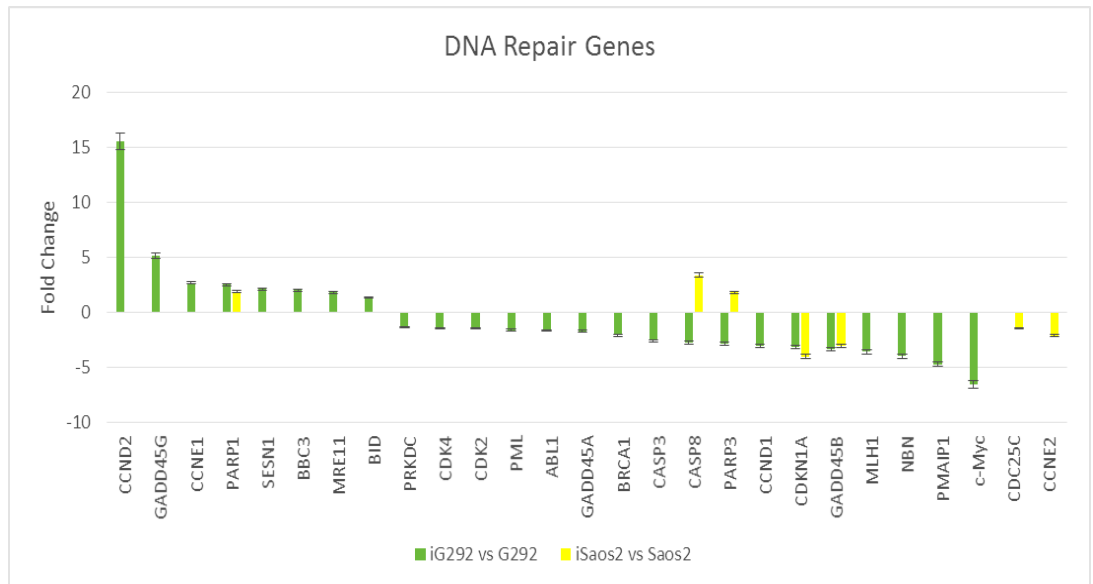


Figure 5.6. Analysis of DNA repair gene expression in both reprogrammed OS. Differentially expressed genes were obtained from reprogrammed OS against parental cells using GeneSpring GX 13.0 with fold change more than 1.5 and significance level $p < 0.05$.

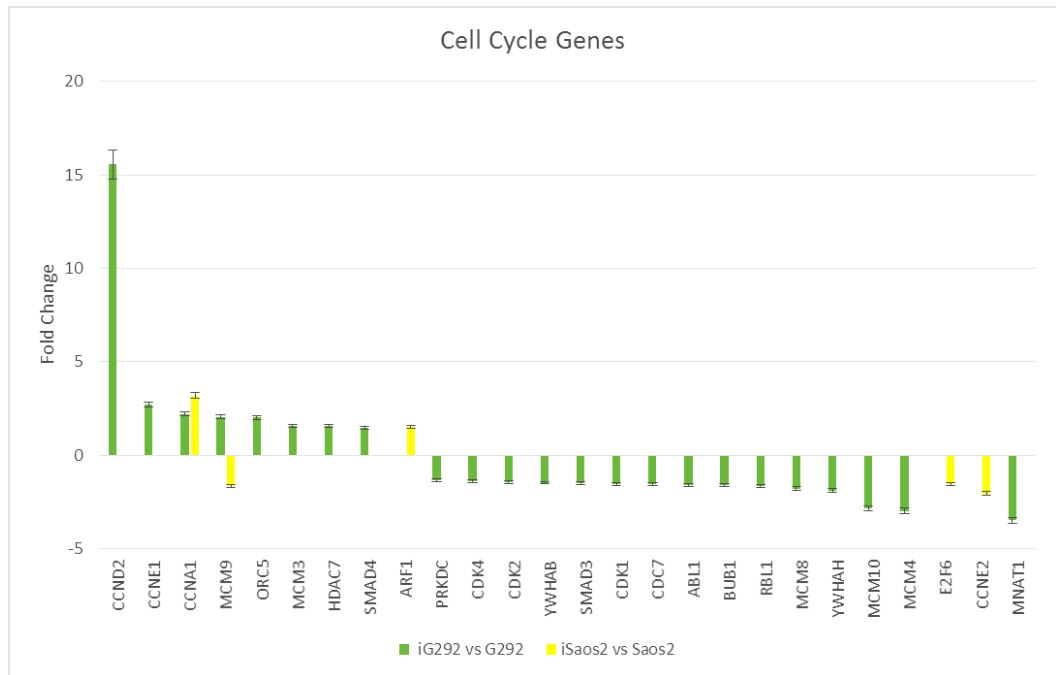


Figure 5.7. Analysis of cell cycle gene expression in both reprogrammed OS. Differentially expressed genes were obtained from reprogrammed OS against parental cells using GeneSpring GX 13.0 with fold change more than 1.5 and significance level $p < 0.05$.

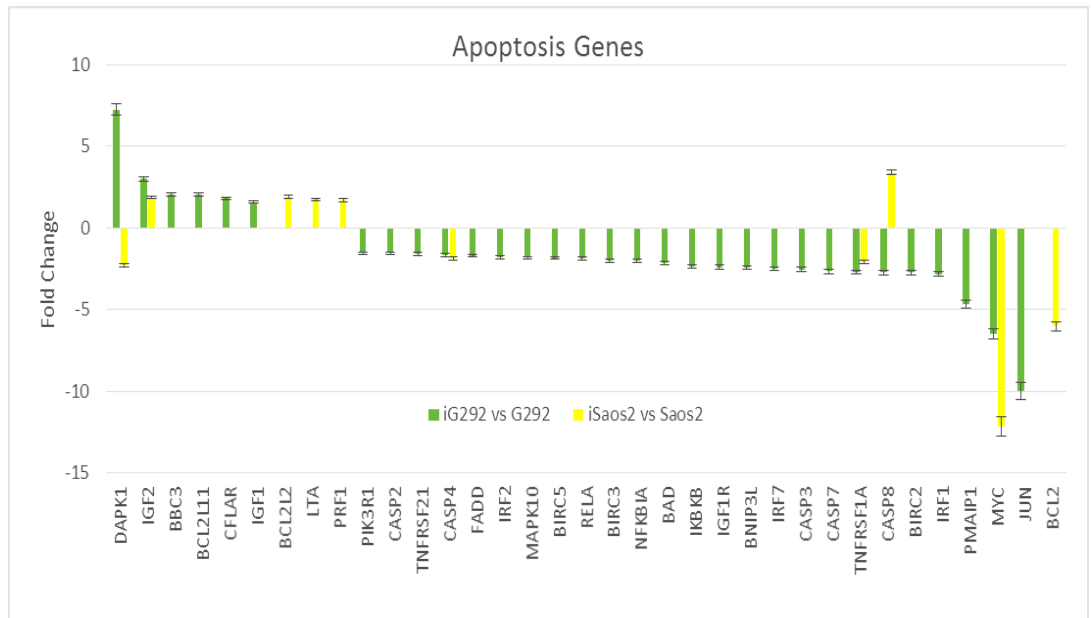


Figure 5.8. Analysis of apoptosis gene expression in both reprogrammed OS. Differentially expressed genes were obtained from reprogrammed OS against parental cells using GeneSpring GX 13.0 with fold change more than 1.5 and significance level $p < 0.05$.

5.6 Validation of differentially expressed genes associate in DNA repair, cell cycle and apoptosis processes

A few differentially expressed genes in each DNA repair, cell cycle and apoptosis processes were selected for validation using qPCR. The DEGs were selected based on their function in each processes and level of expression as reported in the microarray results. Table 5.3 list the selected DEGs for DNA repair, cell cycle and apoptosis processes.

In the validation study, only iG-292 was used because iG-292 was fully reprogrammed and showed more DEGs associated with DNA repair than iSaos-2. Figure 5.9, Figure 5.10 and Figure 5.11 showed similar expression pattern of the analysed genes in qPCR results with microarray data. DEGs associated with DNA repair, cell cycle and apoptosis generated from microarray have been verified by qPCR.

Table 5.3. Differentially expressed genes (DEGs) from each DNA repair, cell cycle and apoptosis processes were selected for validation with the microarray results reported in fold change (FC).

Processes		Microarray results (FC)	
		iG-292	iSaos-2
DNA repair	Pathway		
1. <i>PARP1</i>	BER	2.55	1.92
2. <i>PARP3</i>	BER	- 2.81	1.86
3. <i>MLH1</i>	MMR	- 3.55	-
4. <i>MRE11A</i>	DSB	1.85	-
Cell cycle			
1. <i>CCND2</i>	G1 phase & G1/S transition	15.56	-
2. <i>CCNE1</i>	G1 phase & G1/S transition	2.72	-
3. <i>MNAT1</i>	G2 phase & G2/M transition	-3.5	-
Apoptosis			
1. <i>BCL2L11</i>	Positive regulator	2.05	-
2. <i>BNIP3L</i>	Negative regulator	-2.43	-
3. <i>CASP8</i>	Positive regulator	-2.72	3.8
4. <i>DAPK1</i>	Positive regulator	7.25	-2.34

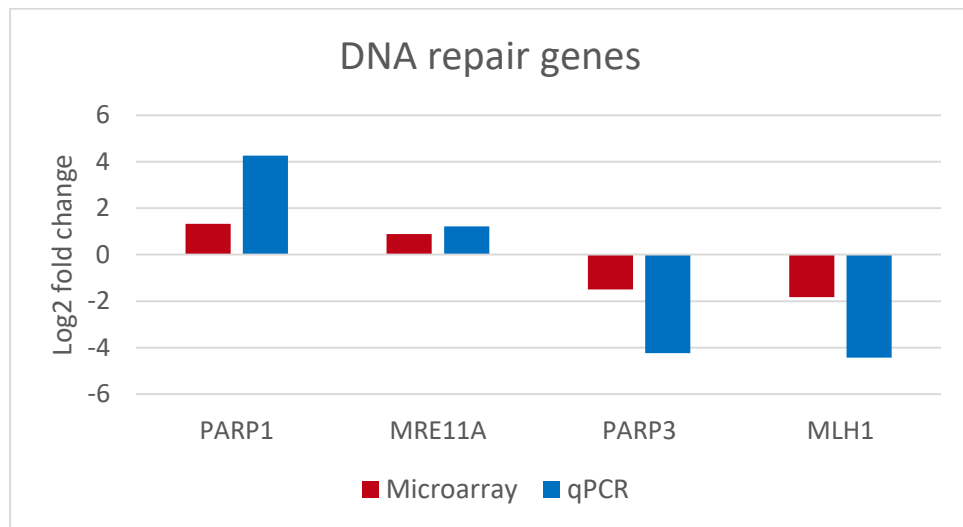


Figure 5.9. Comparison between microarray data and qPCR validation data for DNA repair genes. Expression of DNA repair genes was analysed in log₂ fold change of iG-292 against parental counterpart, G-292.

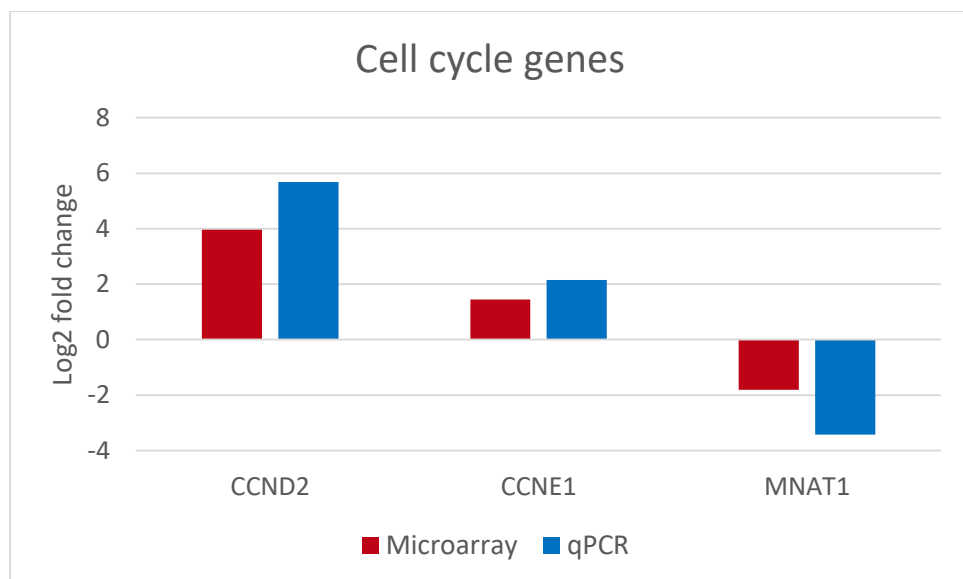


Figure 5.10. Comparison between microarray data and qPCR validation data for cell cycle genes. Expression of cell cycle genes was analysed in log₂ fold change of iG-292 against parental counterpart, G-292.

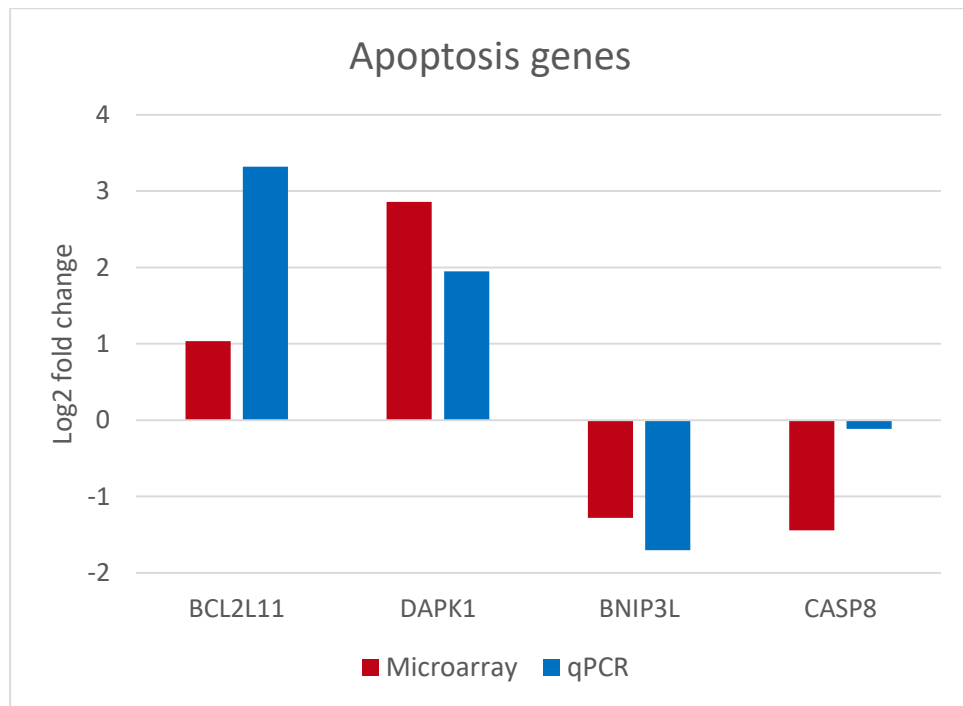


Figure 5.11. Comparison between microarray data and qPCR validation data for apoptosis genes. Expression of apoptosis genes was analysed in log₂ fold change of iG-292 against parental counterpart, G-292.

5.7 Discussion

5.7.1 Reprogrammed OS are genotypically different from parental via global gene expression profiling

Microarray technology with global gene transcription pattern was used to measure similarity or disparity between two populations, such as reprogrammed cells against their parental counterpart. Beside that, global gene expression profiling is one of the best used methods to characterise reprogrammed population and to identify the degree of reprogramming on target cells as it offers unbiased, whole genome approach to examine both populations (Park et al., 2011; Liu et al., 2012; Medvedev et al., 2013).

Global gene expression profiling as shown in unsupervised hierarchical clustering of differentially expressed genes (DEGs) (Figure 5.1) was able to distinguish reprogrammed OS, iG-292 and iSaos-2, from their parental counterparts. Reprogrammed cells, iG-292 and iSaos-2, are genotypically different from their parental counterparts, G-292 and Saos-2, respectively. Whole genome transcriptome profile showed iG-292 expressed more DEGs than iSaos-2.

Expression of more DEGs by iG-292 further enhanced the perception that iG-292 was reprogrammed at a different level than that of iSaos-2. As this study did not incorporate microarray study from ESC and iPSC from somatic cell lines, the similarity of the reprogrammed OS and ESC or iPSC was not

assessed. However, based on characterisation studies in the previous part, only iG-292 exhibited the ability to form teratoma *in vivo* demonstrating that iG-292 had reached a fully reprogrammed state.

Microarray analysis was also used in miR-302 reprogramming study by Lin et al. (Lin et al., 2008) to monitor variations in genome-wide gene expression patterns in skin cancer cell line, Colo, before and after the transfection of miR-302s for reprogramming. Their results also revealed that the gene expression patterns of reprogrammed cells showed only 53% similarity between miRPS-Colo and parental, Colo.

In another study conducted by Kumano et al. (Keiki Kumano et al., 2012), the microarray results from reprogrammed chronic myelogenous leukaemia samples, CML-iPSC, showed distinct clustering of CML-iPSC from CML CD34+ cells used as control in the study. Both mentioned researches, demonstrated the ability of reprogramming to genotypically change the gene expression of the reprogrammed targets from their parental counterparts.

5.7.2 Diverse Gene Ontology enrichment analysis on reprogrammed OS

The overall gene ontology (GO) enrichment analysis showed diverse enrichment of GO categories between iG-292 and iSaos-2. The variability of GO enriched categories between the two populations implying the different reprogramming responses from both parental cell lines, G-292 and Saos-2.

There are a few GO terms that were enriched in the same pattern, up- or down-regulated, in both iG-292 and iSaos-2. One of the GO is developmental process. Developmental process is a biological process that include the developmental progression of an integrated living organism over time from an initial condition to a later condition (source: AmiGO). This is indicative that genes and gene products involved in developmental process were differentially regulated during reprogramming of OS cells. This is consistent with a study by Liu et al. (Liu et al., 2011) which demonstrated that iPSC generated from endoderm, ectoderm or mesoderm showed enrichment of genes associated with developmental process.

Nevertheless, there were two key biological process that were up-regulated only in iG-292 dataset, which were signaling (GO: 0023052) and cellular process (GO: 0009987). Signaling (GO: 0023052) is a major GO term in biological process that triggers cellular response. Thus, the activation of both signaling and cellular process during reprogramming of G-292 into iG-292 play a significant role in the success of reprogramming in G-292.

5.7.3 Elucidation of DNA damage response (DDR) pathways of reprogrammed OS, iG-292 and iSaos-2

DNA damage response (DDR) is a major process to protect genome integrity. DNA is the storehouse of genetic materials in each cell, its integrity and stability are essential to life.

Reprogrammed OS demonstrated down-regulation of DNA repair, cell cycle and apoptosis genes, all of which are associated with DDR. The microarray data was validated with qPCR to authenticate the microarray results. These observations corresponded with increased DNA repair and combined cell cycle alterations and apoptosis resistance in OS, which can be held responsible for treatment failure and recurrence after a disease-free duration (PosthumaDeBoer et al., 2013). Down-regulation of DDR genes profile in our data suggested reprogrammed OS showing more of the normal cell DDR profile rather than a cancerous DDR profile.

Furthermore, current chemotherapy used for OS treatment involved combination of high-dosage of methotrexate, doxorubicin and cisplatin (MAP) (Carrle and Bielack, 2006). This regimen is limited by tumour resistance to platinum-based cisplatin (Lourda et al., 2007). The mode of action on platinum agents is to adduct to DNA, thus leading to cell death (Siddik, 2003). Resistance to cisplatin may result from increased DNA repair capacity in OS (Siddik, 2003; PosthumaDeBoer et al., 2013). The observation of decreased expression of DDR genes in our study suggested that down-regulation of DDR genes and gene

products could be the reason reprogrammed cells are more sensitive to drugs. Therefore, it is essential in developing new therapeutic intervention to specifically target resistance mechanisms in effort to improve treatment sensitivity in OS.

However, there are a few genes which showed up-regulation in reprogrammed OS. One of them is poly (ADP-ribose) polymerase-1 (*PARP1*), one of the DNA repair genes depicted in the microarray data, showing up-regulation in iG-292 and iSaos-2. *PARP1* is a nuclear enzyme that catalyses the production of poly (ADP-ribose) from nicotinamide adenine dinucleotide (NAD⁺) (Sato and Lindahl, 1992). *PARP1* is well known for its role in sensing and initiating DNA repair, including base excision repair, BER and double strand break (homologous recombination, HR and non-homologous end joining, NHEJ) (De Vos et al., 2012). A study conducted by Masutani et al. (Masutani et al., 2004) aimed to examine *PARP1* expression in various human cancer cell lines showed that OS cell line, Saos-2, expressed low level of *PARP1* gene, which is consistent with our result. A low expression of *PARP1* in human cancer could possibly impact growth of cancer cell, differentiation and development by afflicting genomic instability. This could also affect the response of cancer cells to chemo- and radiotherapy (Masutani et al., 2004).

The second PARP family member reported in the microarray data is *PARP3*. Conflicting *PARP3* expression was observed in both iG-292 and iSaos-2, where it was down-regulated in iG-292 but up-regulated in iSaos-2. Unlike *PARP1*, *PARP3* is not well studied. Recent study by Beck et al. (Beck et al.,

2014) supported the role of *PARP3* in double-strand break (DSB). Their work provided good guide that *PARP3* limits end resection, thus aiding the decision of repair between HR and NHEJ pathways. Apart from *PARP3* role in DSB, another study showed that *PARP3* is involved in telomerase activity (Fernández-marcelo et al., 2014). The study indicated that in some cancer cells, suppression of *PARP3* could be accountable for an increased telomerase activity, thus contributing to telomere maintenance and subsequently governing genome stability. Therefore, suggesting down-regulation of *PARP3* in iG-292 could play an important part in governing genome stability in reprogrammed cells.

Aberrant activities and increased expressions of cell cycle associated kinases, such as cyclin-dependent kinases (CDKs) have been linked with neoplastic development and progression of several human cancers, including OS (Vella et al., 2016). CDKs being the key regulator of cell cycle must be tightly regulated to ensure proper coordination of cell cycle mechanism (Morgan, 1995). It was revealed in a review by Johnson and Shapiro (Johnson and Shapiro, 2010) that the inhibition of CDKs increases sensitivity of cancer cells to DNA damaging agents. This effect was due to CDKs inhibition role in revoking DNA-damage-induced checkpoint and repair pathways, thus increasing cancer cells sensitivity to DNA damaging agents. Our microarray data showed down-regulation of a few CDKs genes, *CDK1*, *CDK2* and *CDK4* in iG-292 samples. Gene expression profiling analyses from twenty-one cases of high-grade OS showed that *CDK2* expression was significantly higher in OS samples as compared to normal tissues (Vella et al., 2016). Vella et al. also detected high level of *CDK2* expression in Saos-2 cell line.

Apoptosis is an important regulation system of various physiological and pathological conditions. Caspase-8, which is encoded by *CASP8* gene, is a member of the cysteine proteases, playing roles in apoptosis and cytokine processing (Kruidering and Evan, 2000). Our microarray and qPCR validation results showed increased *CASP8* expression in iSaos-2 but decreased expression in iG-292. Expression of *CASP8* was observed to be unmethylated in Saos-2 in a study by Harada et al. conducted to examine methylation status of 181 paediatric tumours (Harada et al., 2002). In another study conducted by Xu et al. to evaluate the effect of miR-21 suppression in Saos-2 cell lines, demonstrated that overexpression of miR-21 suppressed Saos-2 cell apoptosis by direct targeting of *CASP8* (Xu et al., 2017). Thus, the increased expression of *CASP8* in iSaos-2 after reprogramming could assist in better apoptotic response from iSaos-2. However, further functional apoptotic study need to be conducted to investigate this observation.

Apart from *CASP8*, death-associated protein kinase-1 (*DAPK1*) is a pro-apoptotic gene that cause cellular apoptosis after provocation by internal and external apoptotic stimulating agents (Celik et al., 2015). iG-292 showed up-regulation of *DAPK1*, while iSaos-2 showed down-regulation of *DAPK1*. The silencing of *DAPK1* may cause uncontrolled tumour cell growth, suggesting that its expression is needed for tumour suppression (Gozuacik and Kimchi, 2006). Li and colleague demonstrated that demethylation with demethylating agent 5-Aza-2'-deoxycytidine increases OS cells radiosensitivity by arresting cells at G2/M phase and enhancing apoptosis, which is mediated by up-regulation of *14-3-3 σ* , *CHK2* and *DAPK1* genes (Li et al., 2014).

Therefore it is likely that the expression of *DAPK1* may justify for cell cycle arrest and induction of apoptosis to sensitise cancer cells toward radiotherapy.

The up- and down-regulated genes in iG-292 and iSaos-2 discussed above, suggested that reprogramming process changed cancerous genotype of OS to less cancerous and reverting back to normal cell genotype.

5.8 Conclusions

Global gene expression analysis revealed distinct clustering between reprogrammed OS and parental implying generation of a different entity in comparison to parental counterpart. Reprogramming was able to phenotypically and genotypically affect the target cells. Expression of more DEGs by iG-292 further enhanced the perception that iG-292 was reprogrammed at a different level than that of iSaos-2. The overall GO enrichment analysis showed different enrichment of GO categories between iG-292 and iSaos-2, with activation of signaling and cellular process in iG-292 play a significant role in the success of reprogramming in G-292. Down-regulation of DDR genes after reprogramming was observed in both iG-292 and iSaos-2. Down-regulation of DDR genes is consistent with improved genomic stability in reprogrammed OS and reverting back to primitive normal phenotype which is not cancerous.

CHAPTER 6

RESULTS & DISCUSSION: PART 3

Functional assay to explicate genes related to DNA repair mechanism in reprogrammed OS

6.1 Introduction

Genetic polymorphism in nucleotide excision repair (NER) was significantly related with lower chemotherapy response and unfavourable survival of osteosarcoma (Sun et al., 2015). Another study showed that polymorphisms in NER and homologous recombination repair (HRR) pathways modulate the risk of developing osteosarcoma (Jin et al., 2015). Both studies suggested NER role in OS. It has also been shown that a DNA repair deficiency of NER genes is related to the presence of single nucleotide polymorphisms (SNPs) (Goode et al., 2002; Biason et al., 2012). Thus, in our functional study we aim to figure out the effect of reprogramming on cancer cells, focusing on OS, and their NER response upon UV irradiation as well as the functionality of genes related to NER in reprogrammed OS. Treatment of cells with priming dose of UV light appears to stimulate both global genomic repair (GGR) and transcription coupled repair (TCR), suggesting that these processes are inducible (McKay et al., 1999).

Functional test such as physical stress (UV irradiation) was used to generate damage to DNA of both reprogrammed and parental OS. Upon UV irradiation, single-strand break dimers, cyclobutane pyrimidine dimers (CPD), which is the most cytotoxic lesions, are the most abundantly produce. UV irradiation induces activation of NER pathway. NER is a leading DNA repair pathway that safeguard the genome to remain functionally intact for transmission to next generation. NER was discovered in the 1960s through studies on the effects of UV irradiation on DNA synthesis and repair replication in bacteria. Since then it has been characterised extensively in mammals and has been described as the principal repair pathway for the removal of bulky adducts induced by UV irradiation or other environmental carcinogens.

6.2 Morphological observation on reprogrammed and parental OS after UV irradiation

Morphological changes at different time-point were first evaluated after UV irradiation on reprogrammed OS, iG-292 and iSaos-2, and their parental counterparts. Most of the parental and reprogrammed cells survived the irradiation (Figure 6.1, Figure 6.2, Figure 6.3 and Figure 6.4). Both parental and reprogrammed cells gradually showed morphological changes, such as more rounded and flatten shape, with the nucleus became bigger and more obvious after UV irradiation.

The cells showed necrotic effect such as swelling of the nucleus and cell body, as well as disruption of the plasma membrane. Mild condensation of chromatin and nuclear membrane disruption were also observed. However, no apoptotic changes such as nuclear membrane shrinkage, fragmentation into apoptotic bodies and cells detaching from plastic surface, were found. These morphological changes on both parental and reprogrammed cells indicating UV irradiation at 40 J/m^2 (UVC) was enough to caused damage to the cells but not enough to cause cell death.

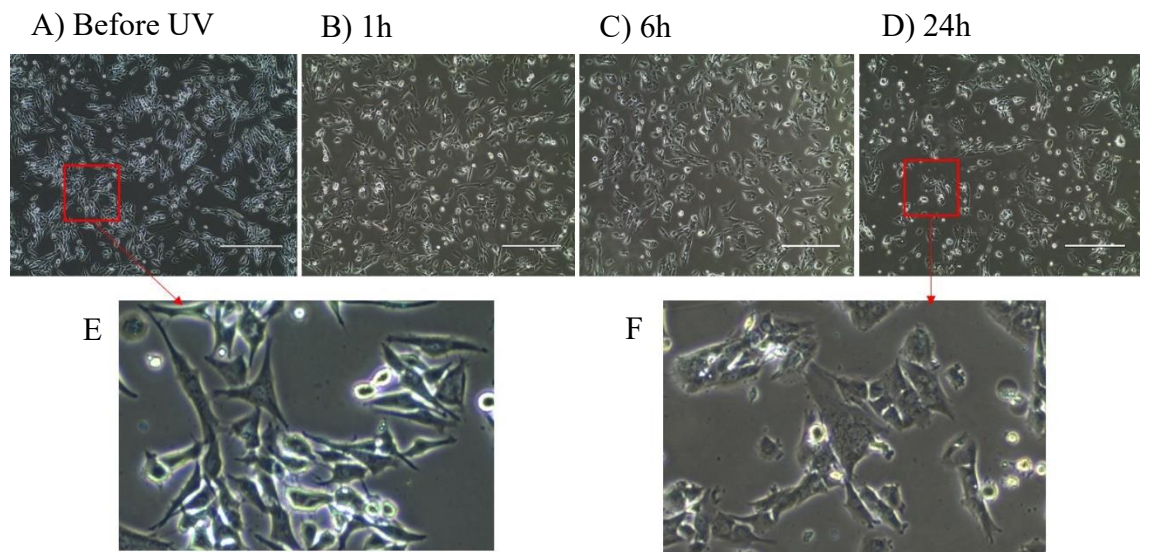


Figure 6.1. Representative images on parental G-292 after 40 J/m² UV irradiation. (A) G-292 cells before UV irradiation. (B-D) G-292 after UV irradiation and cultured for 1h, 6h and 24h, respectively, for recovery. (E-F) Enlarged images of selected area from cells before UV irradiation and 24 hour post UV irradiation for comparison. EVOS XL cell imaging system, original magnification: 10x. Scale bar: 100 μ m.

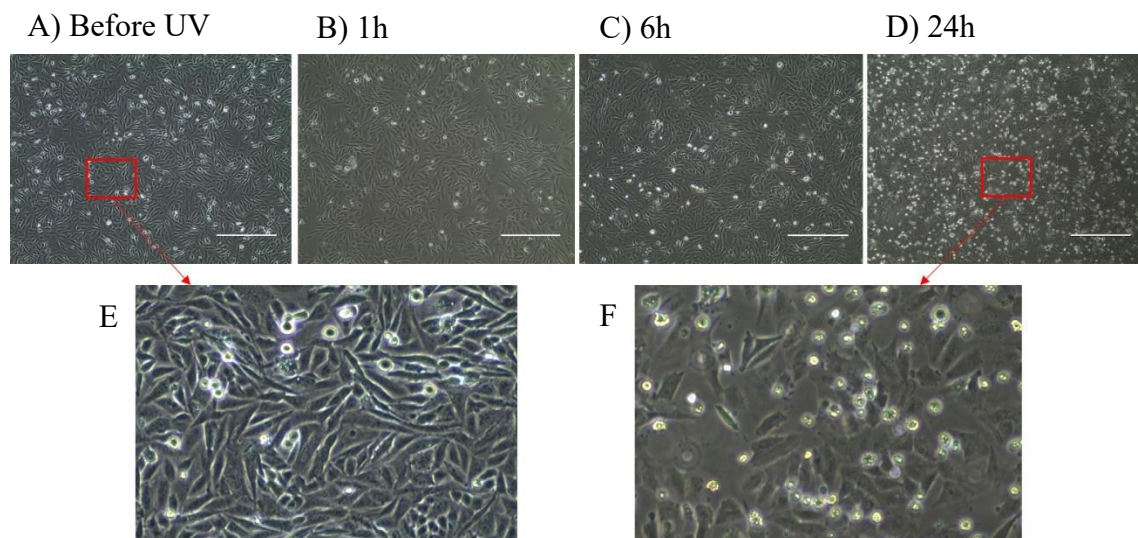


Figure 6.2. Representative images on parental Saos-2 after 40 J/m² UV irradiation. (A) Saos-2 cells before UV irradiation. (B-D) Saos-2 after UV irradiation and cultured for 1h, 6h and 24h, respectively, for recovery. (E-F) Enlarged images of selected area from cells before UV irradiation and 24 hour post UV irradiation for comparison. EVOS XL cell imaging system, original magnification: 10x. Scale bar: 100 μ m.

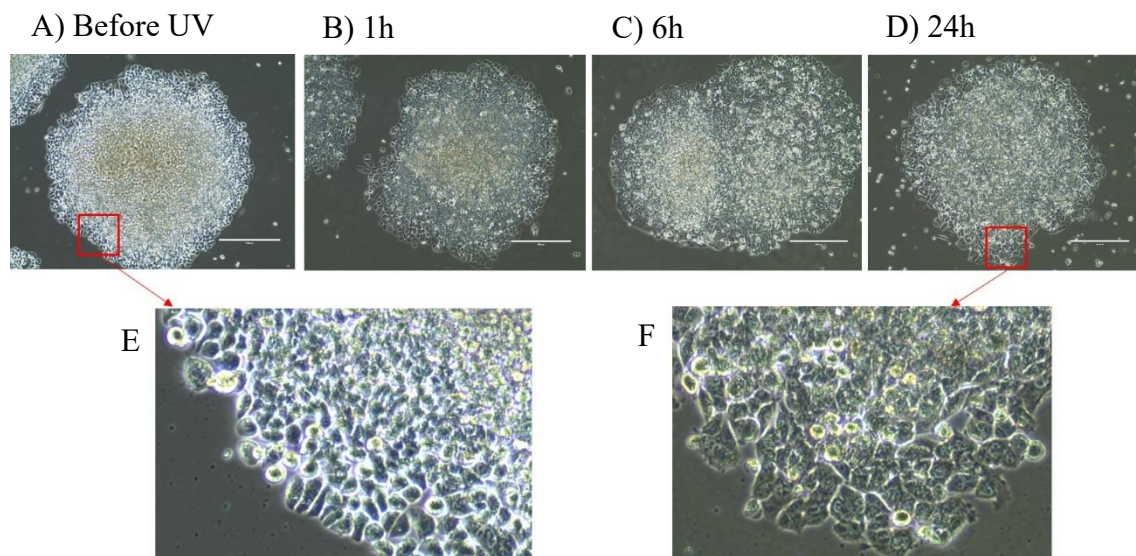


Figure 6.3. Representative images on reprogrammed iG-292 after 40 J/m² UV irradiation. (A) iG-292 cells before UV irradiation. (B-D) iG-292 after UV irradiation and cultured for 1h, 6h and 24h, respectively, for recovery. (E-F) Enlarged images of selected area from cells before UV irradiation and 24 hour post UV irradiation for comparison. EVOS XL cell imaging system, original magnification: 10x. Scale bar: 100 μ m.

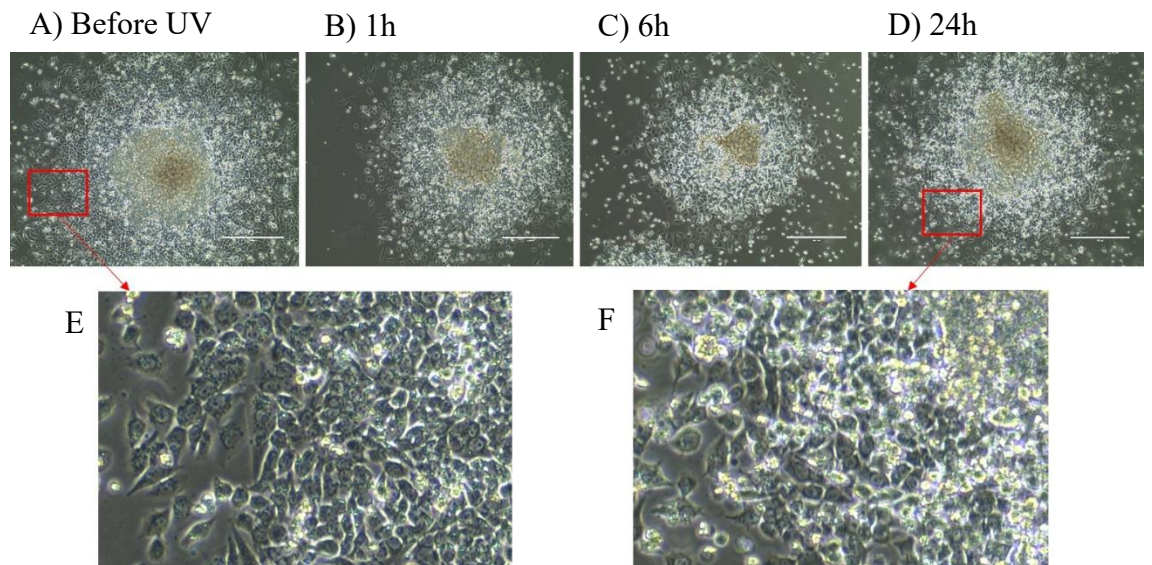


Figure 6.4. Representative images on reprogrammed iSaos-2 after 40 J/m² UV irradiation. (A) iSaos-2 cells before UV irradiation. (B-D) iSaos-2 after UV irradiation and cultured for 1h, 6h and 24h, respectively, for recovery. (E-F) Enlarged images of selected area from cells before UV irradiation and 24 hour post UV irradiation for comparison. EVOS XL cell imaging system, original magnification: 10x. Scale bar: 100 μ m.

6.3 Detection of cyclobutane pyrimidine dimers (CPDs) in reprogrammed and parental OS upon UV irradiation

Cyclobutane pyrimidine dimers (CPDs) are produced on the DNA of cells after UV damage. Concentration of CPDs corresponds to the level of UV damage on the DNA of affected cells. CPDs are repaired by the NER pathways. Reprogrammed and parental OS were subjected to single UV irradiation (UVC) at 40 J/m² and investigated for the formation of CPDs.

Quantification of CPDs were done using ELISA kit. Data showed significantly lower level of CPDs in iG-292 than G-292 at three different time-points suggesting iG-292 may have more effective CPDs removal mechanism as compared to G-292 (Figure 6.5). However, similar CPDs removal pattern was observed on iSaos-2 and Saos-2 (Figure 6.5), which is consistent with the hypothesis that iSaos-2 was incompletely reprogrammed and observation of differential DDR gene expression as compared to iG-292. Our initial findings showed that reprogrammed OS, iG-292 demonstrated more effective DNA repair response compared to parental counterpart, G-292.

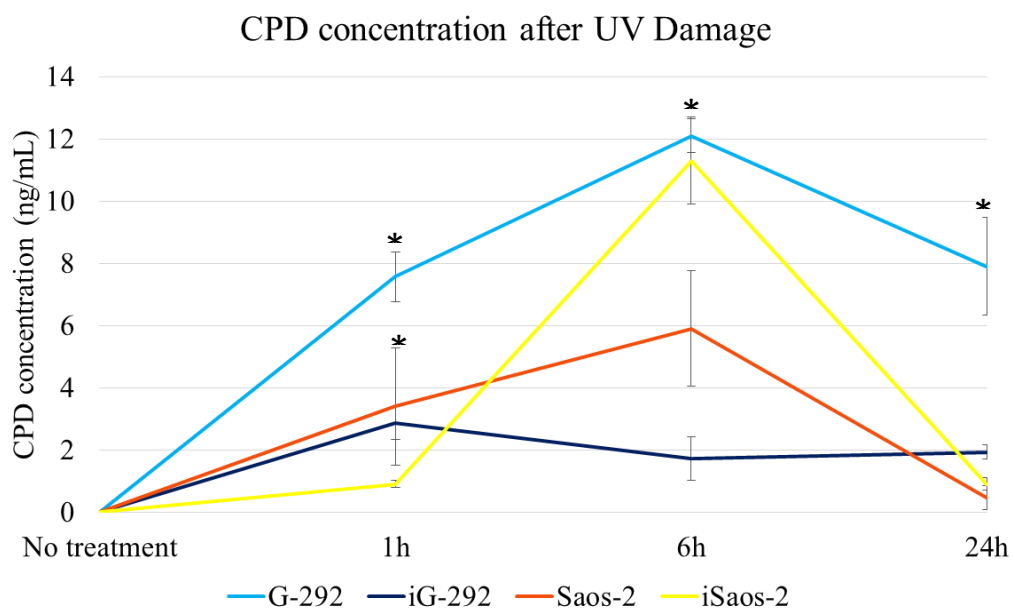


Figure 6.5. Cyclobutane pyrimidine dimers (CPDs) concentration in parental and reprogrammed OS after UV irradiation. Line bar showed CPDs concentration in parental and reprogrammed OS at 1h, 6h and 24h post UV irradiation. Asterick (*) denote significant level, $p < 0.05$, calculated from reprogrammed OS against parental OS at each time-point.

6.4 Analyses of Nucleotide Excision Repair (NER) genes expression in reprogrammed and parental OS upon UV irradiation

After the detection of CPDs, analyses of NER genes expression in reprogrammed and parental OS were performed to correlate the NER genes expression with CPDs removal. In the previous microarray dataset (Part 2 Results and Discussion), GADD45G was shown to be up-regulated in iG-292 but not iSaos-2 even before UV irradiation (Figure 5.6).

Upon UV irradiation on reprogrammed OS, iG-292 and parental, G-292, GADD45G was significantly up-regulated in all irradiated cells (Figure 6.6) indicating UV stress activated this gene. Most NER genes are up-regulated in iG-292 6h and 24h post-irradiation while down-regulated in G-292 6h and 24h post-irradiation, against iG-292 and G-292 before irradiation as control. XPA, involved in the early step of NER and responsible for DNA unwinding after initiation of repair, was significantly up-regulated in iG-292 6h post irradiation. This observation correspond with the ability to remove CPDs adduct in iG-292 (subtitle 6.3).

On the other hand, most NER genes were down-regulated in iSaos-2 and Saos-2 (Figure 6.7) implying that UV irradiation did not activate the relevant genes. Both reprogrammed iSaos-2 and parental Saos-2 exhibited similar pattern of NER genes expression and this arrangement correspond with the CPDs removal pattern in subtitle 6.3. This result could be due to incomplete

reprogramming of Saos-2. The overall outcome from this experiment suggested that NER pathway was more efficient in fully reprogrammed cells.

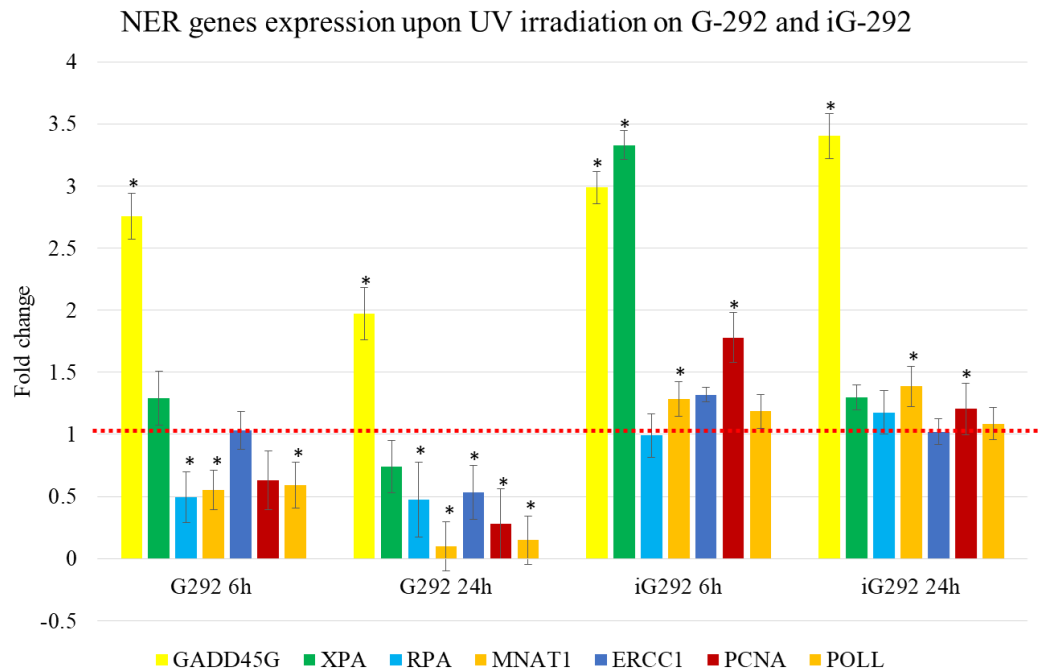


Figure 6.6. Nucleotide excision repair (NER) genes expression after UV irradiation on G-292 and iG-292. G-292 and iG-292 before UV irradiation were used as control respectively to obtain expression fold change for each gene. Asterick (*) denote significant level, $p < 0.05$.

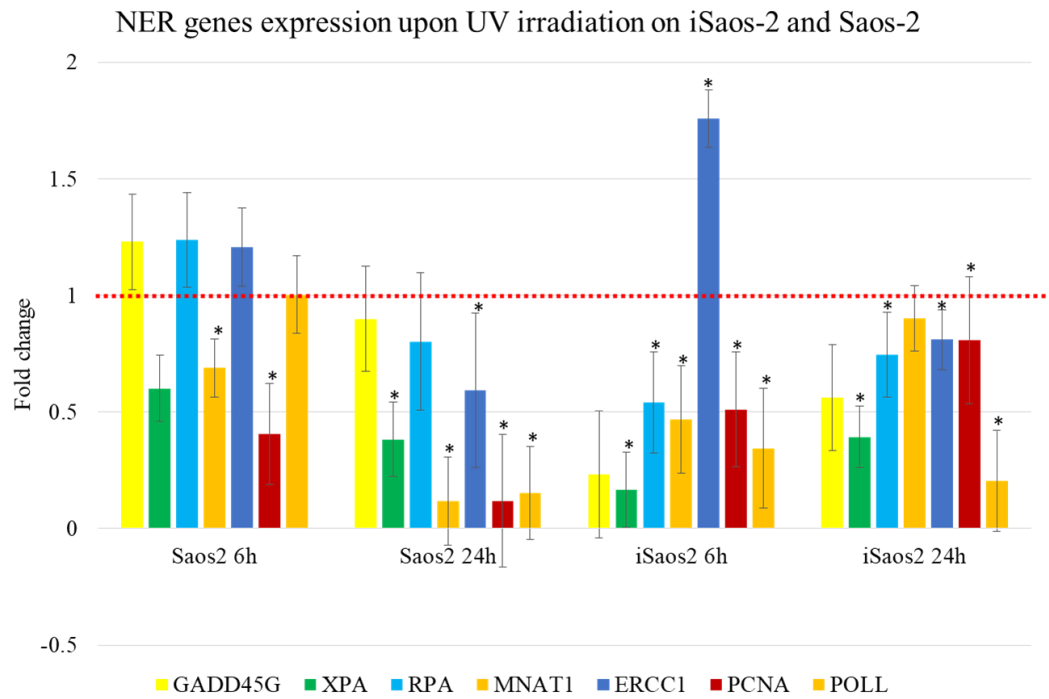


Figure 6.7. Nucleotide excision repair (NER) genes expression after UV irradiation on Saos-2 and iSaos-2. Saos-2 and iSaos-2 before UV irradiation were used as control respectively to obtain expression fold change for each gene. Asterick (*) denote significant level, $p < 0.05$.

6.5 Discussion

Reprogrammed cells derived from G292 was different from that of Saos-2 in terms of characterisation and microarray results (discussed in Part 1 and Part 2). Functional studies were conducted on both reprogrammed OS cells to assess the DNA repair capability of these two different pluripotent cells and to answer whether cancer cells need to be fully reprogrammed to be more efficient in DNA repair mechanism.

Efficiency of DNA repair system is regarded as one of the most crucial mechanisms affecting patients' outcome in chemotherapy. Previous studies have linked single nucleotide polymorphisms (SNPs) of NER genes to the response of chemotherapy in osteosarcoma (Caronia et al., 2009; Biazon et al., 2012; Bai et al., 2013; Jin et al., 2015). Caronia et al. showed that mutation in NER related genes are associated with resistance to cisplatin (Caronia et al., 2009). Meanwhile, Biazon et al. and Bai et al. showed that certain polymorphisms in NER genes correlated well with response to chemotherapy and prognosis of OS (Biazon et al., 2012; Bai et al., 2013). Together, these studies suggested the importance of NER pathway in OS resistance to chemotherapy and subsequent progression.

Ultraviolet (UV) irradiation commonly generates two major DNA lesions: cyclobutane pyrimidine dimers (CPDs) and pyrimidine-(6,4)-pyrimidone-photoproducts (6,4-PP) (Lima-Bessa et al., 2008). NER pathway is the main repair pathway in the DNA repair mechanisms that repairs bulky

lesions, including CDPs and 6,4-PP (Van Sloun et al., 1999; Conconi et al., 2002). NER has been associated with several tumour progression including OS and response to platinum-based chemotherapy (Reed, 1998; Stoehlmacher et al., 2004; Marteiijn et al., 2014). The NER pathway consists of complex network of proteins involved in recognition of lesion, lesion excision, DNA resynthesise and ligation to repair the damaged site (Sancar, 1996; Smith and Seo, 2002; Costa et al., 2003; Petruseva et al., 2014).

6.5.1 Reprogrammed OS, iG-292, demonstrated more effective DNA repair response in rapid removal of CPDs and up-regulation of NER genes

Detection of CPDs using direct ELISA kit was useful in determining the level of UV damage on the DNA of affected cells. Concentration of CPDs is correlated to the degree of damage on the DNA (Matsunaga, 2007). UVC, with a wavelength of 256 nm, was used as irradiation source as the active spectrum for induction of CPDs, the most frequent lesion formed following UV irradiation, was shown to be most efficient around 260 nm (Clingen et al., 1995).

Based on the concentration of CPDs in a time-dependent manner in iG-292 and G-292, data indicated rapid removal of CPDs in iG-292 as compared to the parental counterpart. However, iSaos-2 showed similar CPDs concentration pattern as the parental counterpart, Saos-2, and this could be due to failure to obtain the full reprogramming status. A recent study conducted by

Luo et al. (Luo et al., 2012) showed that pluripotent cells exhibit lower CPD levels than fibroblasts exposed to equal UVC fluxes, demonstrating that pluripotent cells possess higher DNA repair capacities for NER.

Up-regulation of *GADD45G*, *XPA* and *PCNA* at 6 hours post UV irradiation in iG-292 are consistent with the role of each genes in NER pathway (Figure 6.6). Potential role of *GADD45G* and *PCNA* shall be discussed later in this discussion topic under 6.5.2. Xeroderma pigmentosum complementation group A (*XPA*) play a role in binding to damaged DNA and facilitates assembly of repair complex at the damage site with replication protein A (*RPA*) (de Laat et al., 1999; Shen et al., 2014; Sugitani et al., 2017). It has been showed in previous reports that absence of *XPA* caused no stable pre-incision complex to form (Mu et al., 1997; Evans et al., 1997), thus no NER occurs. Therefore, cells deficient in *XPA* protein are not capable for NER and are hypersensitive to damage caused by UV irradiation (Satokata et al., 1993; Köberle et al., 2006).

Genomic instability is believed to be the compelling inducement behind cancer development (Malkin, 1993; Thoms et al., 2007; Cassidy and Venkitaraman, 2012). p53, the famous tumour suppressor is regarded as the guardian of the genome (Spike and Wahl, 2011) as well as DNA damage sensor (Hanahan and Weinberg, 2011), is often mutated or deleted in OS (Sampson et al., 2015). Mutation of p53 significantly correlates with DNA instability and is viewed as a major genetic contributing factor to high levels of genome instability in OS (Overholtzer et al., 2003).

Both our and Luo et al. (Luo et al., 2012) results showed pluripotent stem cells possess higher efficiency in DNA repair network, which is no surprise as pluripotent stem cells need to maintain genome stability as they self-renewal to form new daughter cells. This ability is needed to make sure no DNA lesions is pass on to the next generation for preserving genome integrity (Rocha et al., 2013).

Multiple genes and important enzymes of the DNA repair system, have been discovered as OS biomarkers that could potentially predict patient susceptibility and prognosis (Liu et al., 2017). Nucleotide excision repair (NER) is the main repair system in DDR responsible for recognising and excising DNA lesions (Sertic et al., 2012). Two rate-limiting enzymes in NER process, excision repair cross-complementation group 1 (ERCC1) and 2 (ERCC2), have been associated with OS prognosis (Hao et al., 2012; Gómez-Díaz et al., 2015; Zhang et al., 2015; Ma et al., 2016). These studies linked OS to NER process and any changes in NER pathway is fundamental for better management of the disease.

6.5.2 GADD45G roles in tumour suppression and enhancing NER

It was interesting to observe the up-regulation of Growth Arrest and DNA Damage-inducible 45 (GADD45)- γ in our microarray data even before functional assay was utilised. GADD45 proteins has several roles in the regulation of many cellular functions including DNA repair, cell cycle control,

senescence and genotoxic stress (Carrier et al., 1994; Liebermann and Hoffman, 2002). GADD45 gene family encodes for GADD45 α , β , and γ (Fornace et al., 1988). GADD45 γ or also known as GADD45G is also known as a stress sensor and tumour suppressor gene (TSG) (Takekawa and Saito, 1998; Ying et al., 2005). Furthermore, GADD45G has been reported to be able to negatively regulates cell cycle progression mediated by inhibition of cyclinB1- CDK1 activity (Vairapandi et al., 2002).

Expression of GADD45G is often suppressed in tumours and re-expression of this gene and gene product could results in apoptosis (Zhang et al., 2002; Chung et al., 2003; Campanero et al., 2008). A study done by Zhang et al. demonstrated the transfection of a human GADD45G into human pituitary tumour results in a considerable inhibition of tumour cell growth. These results suggested that GADD45G may play essential role in regulating cell proliferation in the pituitary. The study showed that loss of GADD45G expression and function may possibly cause uncontrolled cell growth and tumour progression in the human pituitary (Zhang et al., 2002).

Another similar study by Chung et al. showed that GADD45G expression was significantly lower in anaplastic cancer cell lines as compared to normal thyrocytes. The study also demonstrated that re-expression of GADD45G in anaplastic cancer cells inhibited proliferation via activation of apoptosis pathway. This study suggested the use of GADD45G gene as a potential candidate gene for gene therapy against anaplastic thyroid cancer (Chung et al., 2003).

As a stress inducer, UV irradiation was shown to be able to cause up-regulation of GADD45G. However, this stress response could be obliterated when its promoter becomes hypermethylated as shown by Ying et al. in several tumours including non-Hodgkin's lymphoma, Hodgkin's lymphoma, nasopharyngeal carcinoma, cervical carcinoma, esophageal carcinoma, and lung carcinoma (Ying et al., 2005). This could be the reason why UV irradiation did not activate GADD45G gene in both iSaos-2 and Saos-2 cells (Figure 6.7).

Apart from the role in tumorigenesis, GADD45 family of genes participate in the DNA repair machinery, NER through the interaction with Proliferating Cell Nuclear Antigen (PCNA) (Tamura et al., 2012). Interaction of GADD45G and PCNA is also linked to inhibition of GADD45G as a negative regulator of cellular growth (Vairapandi et al., 2000; Azam et al., 2001). However, as both studies were conducted on non-damaged or non-irradiated cells, the role of GADD45G and PCNA in UV irradiated cells could be linked, but remains to be defined.

PCNA has a multiple function in lifecycle of cells. When cells are not engaged in DNA replication, PCNA often assigns cells to cell cycle arrest and DNA repair, but if repair is not possible, PCNA may drive cells into apoptosis (Paunesku et al., 2001). PCNA is needed for efficient DNA synthesis, as PCNA plays a role as a processivity factor of DNA polymerases (Costa et al., 2003).

As GADD45G was significantly up-regulated in iG-292 before and after UV irradiation, we postulated that up-regulation of GADD45G helps to speed up the excision mechanism together with PCNA (Figure 6.8).

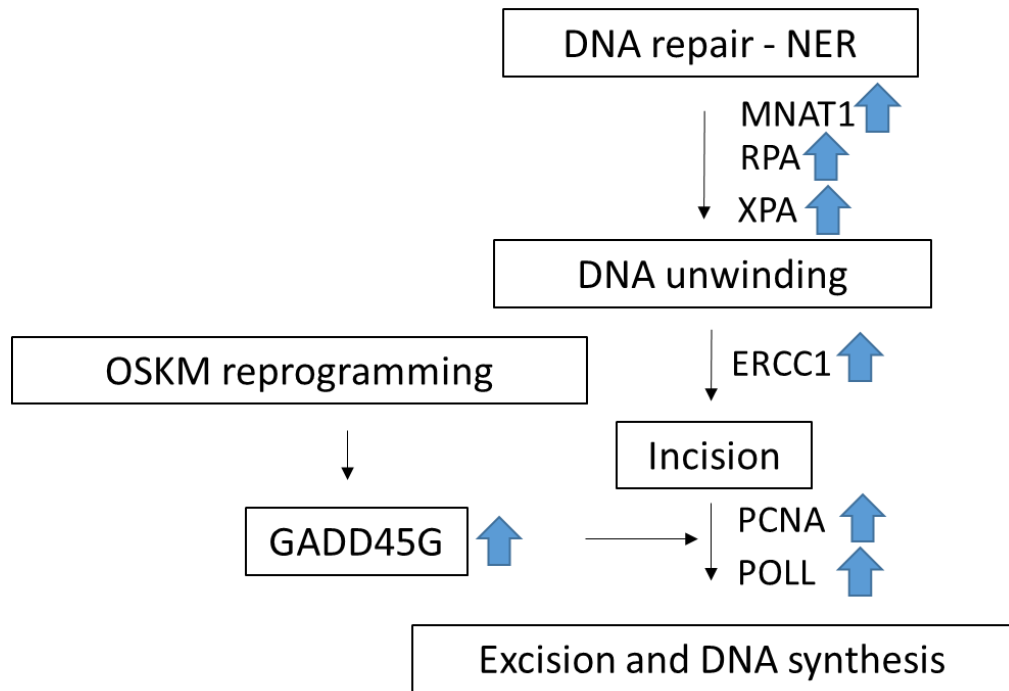


Figure 6.8. A schematic diagram showing potential effect of GADD45G on NER upon reprogramming. Up-regulation of GADD45G in iG-292 after reprogramming and UV irradiation interacted with PCNA to pace up excision and DNA synthesis process.

6.6 Conclusions

Reprogrammed iG-292 showed more effective CPDs removal and DNA repair response compared to parental, G-292. Up-regulation of NER genes in iG-292 after UV irradiation is consistent with CPDs removal capability of iG-292. Combination of immunoassays such as ELISA using CPD-specific monoclonal antibody and NER genes expression study are great tools for the detection and removal of DNA adducts in human cells as well as to understand the mechanism of cellular NER response.

CHAPTER 7

CONCLUSIONS AND FUTURE STUDIES

7.1 Conclusions

Reprogramming of osteosarcoma cell line, G-292, was successful with generation of reprogrammed G-292, named as iG-292 that displayed all the hallmark characteristics of iPSC, especially teratoma formation. Further microarray analysis on fully reprogrammed OS, iG-292, against incomplete reprogrammed OS, iSaos-2, showed more differentially expressed genes were found in iG-292 than iSaos-2.

Analysis from GO enrichment showed activation of signaling and cellular process in iG-292, which may play a role in the success of G-292 reprogramming. The expression of down-regulation of DDR genes is consistent with improved genomic stability in reprogrammed OS, thus suggested the ability of reprogramming in reverting back OS to primitive normal phenotype which is not cancerous.

In functional assay, reprogrammed iG-292 showed better CPDs removal and DNA repair response compared to parental, G-292. Up-regulation of NER genes in iG-292 after UV irradiation is consistent with CPDs removal capability of iG-292. The expression of GADD45G was significantly up-regulated in iG-

292 before and after UV irradiation, leading to improved excision mechanism. Since the expression of GADD45G was never reported in OS development and disease progression, reprogramming of OS enable the discovery of the role of this gene in OS. The alteration of GADD45G may play an important role in the development of OS and could serve as a target for prevention or arrest of OS development.

In conclusion, all results presented in this project elucidated the DNA damage response pathways and functional efficiency of DNA repair genes associated with reprogrammed osteosarcoma cell lines, iG-292 and iSaos-2.

7.2 Future Studies

The advancement of reprogramming of cancer cells open an enormous opportunity to study tumour development and progression as well as drug therapy development. The DDR genes expression analysis predicted possible increased sensitivity of reprogrammed OS towards chemotherapeutic agents. Therefore, we proposed to study drug sensitivity in reprogrammed OS in our future study.

Apart from drug sensitivity, gene expression and functional data suggested the involvement of GADD45G in OS development and progression that remain to be elucidated. Future study involving overexpression of GADD45G in OS and other cancer cells may provide more important information on the role of GADD45G as a tumour suppressor and stress inducer.

Lastly, as a model of OS disease, it is worthy to study the progression of OS from OS-iPSC to differentiation into terminal osteoblast and to elucidate the aberrations in oncogenes expression during OS development. These progression and differential expression analysis could be conducted using next gene sequencing to establish gene expression profiles between OS-iPSC and different stages of OS development. Therefore, cancer progression model of OS can be developed to understand the complex process of tumourigenicity in OS.

LIST OF REFERENCES

- Aasen, T. et al., 2008. Efficient and rapid generation of induced pluripotent stem cells from human keratinocytes. *Nature Biotechnology*, 26(11), pp.1276–1284.
- Allegrucci, C. et al., 2011. Epigenetic reprogramming of breast cancer cells with oocyte extracts. *Molecular Cancer*, 10(1), p.7.
- Ando, K. et al., 2013. Current therapeutic strategies and novel approaches in osteosarcoma. *Cancers*, 5(2), pp.591–616.
- Armstrong, L. et al., 2010. Human induced pluripotent stem cell lines show stress defense mechanisms and mitochondrial regulation similar to those of human embryonic stem cells. *Stem Cells*, 28(4), pp.661–673.
- Azam, N., Vairapandi, M., Zhang, W., Hoffman, B. and Liebermann, D.A., 2001. Interaction of CR6 (GADD45 γ) with Proliferating Cell Nuclear Antigen impedes negative growth control. *Journal of Biological Chemistry*, 276(4), pp.2766–2774.
- Bai, S.B., Chen, H.X., Bao, Y.X., Luo, X.G. and Zhong, J.J., 2013. Predictive impact of common variations in DNA repair genes on clinical outcome of osteosarcoma. *Asian Pacific Journal of Cancer Prevention*, 14(6), pp.3677–3680.
- Beck, C. et al., 2014. PARP3 affects the relative contribution of homologous recombination and nonhomologous end-joining pathways. *Nucleic Acids Research*, 42(9), pp.5616–5632.
- Bernhardt, M. et al., 2017. Melanoma-derived iPCCs show differential tumorigenicity and therapy response. *Stem Cell Reports*, 8(5), pp.1379–1391.
- Biason, P. et al., 2012. Nucleotide excision repair gene variants and association with survival in osteosarcoma patients treated with neoadjuvant chemotherapy. *The Pharmacogenomics Journal*, 12(6), pp.476–483.
- Boyer, L.A. et al., 2005. Core transcriptional regulatory circuitry in human embryonic stem cells. *Cell*, 122(6), pp.947–956.
- Broadhead, M.L., Clark, J.C.M., Myers, D.E., Dass, C.R. and Choong, P.F.M., 2011. The molecular pathogenesis of osteosarcoma: a review. *Sarcoma*, 2011, p.959248.
- Brosh, R. et al., 2013. p53 counteracts reprogramming by inhibiting mesenchymal-to-epithelial transition. *Cell Death and Differentiation*, 20(2), pp.312–320.

Campanero, M.R., Herrero, A. and Calvo, V., 2008. The histone deacetylase inhibitor trichostatin A induces GADD45 gamma expression via Oct and NF-Y binding sites. *Oncogene*, 27(9), pp.1263–1272.

Carette, J.E. et al., 2010. Generation of iPSCs from cultured human malignant cells. *Blood*, 115(20), pp.4039–4042.

Caronia, D. et al., 2009. Common variations in *ERCC2* are associated with response to cisplatin chemotherapy and clinical outcome in osteosarcoma patients. *The Pharmacogenomics Journal*, 9(5), pp.347–353.

Carrier, F. et al., 1994. Characterization of human GADD45, a p53-regulated protein. *Journal of Biological Chemistry*, 269(51), pp.32672–32677.

Carrle, D. and Bielack, S.S., 2006. Current strategies of chemotherapy in osteosarcoma. *International Orthopaedics*, 30(6), pp.445–451.

Cassidy, L.D. and Venkitaraman, A.R., 2012. Genome instability mechanisms and the structure of cancer genomes. *Current Opinion in Genetics and Development*, 22(1), pp.10–13.

Celik, S. et al., 2015. Methylation analysis of the DAPK1 gene in imatinib-resistant chronic myeloid leukemia patients. *Oncology Letters*, 9(1), pp.399–404.

Chambers, I. et al., 2003. Functional expression cloning of Nanog , a pluripotency sustaining factor in embryonic stem cells. *Cell*, 113, pp.643–655.

Chambers, I. and Tomlinson, S.R., 2009. The transcriptional foundation of pluripotency. *Development*, 136(14), pp.2311–2322.

Chandar, N., Billig, B., McMaster, J. and Novak, J., 1992. Inactivation of p53 gene in human and murine osteosarcoma cells. *British Journal of Cancer*, 65, pp.208–214.

Chen, X., Ko, L.J., Jayaraman, L. and Prives, C., 1996. p53 levels, functional domains, and DNA damage determine the extent of the apoptotic response of tumor cells. *Genes & Development*, 10, pp.2438–2451.

Chen, X. et al., 2014. Recurrent somatic structural variations contribute to tumorigenesis in pediatric osteosarcoma. *Cell Reports*, 7(1), pp.104–112.

Chung, H.K. et al., 2003. GADD45 γ expression is reduced in anaplastic thyroid cancer and its reexpression results in apoptosis. *Journal of Clinical Endocrinology and Metabolism*, 88(8), pp.3913–3920.

Clingen, P.H. et al., 1995. Induction of cyclobutane pyrimidine dimers, pyrimidine(6-4)pyrimidone photoproducts, and Dewar valence isomers by natural sunlight in normal human mononuclear cells. *Cancer Research*, 55(11), pp.2245–2248.

- Conconi, A., Bepalov, V.A. and Smerdon, M.J., 2002. Transcription-coupled repair in RNA polymerase I-transcribed genes of yeast. *Proceedings of the National Academy of Sciences of the United States of America*, 99(2), pp.649–654.
- Consortium, T.G.O., 2000. Gene ontologie: Tool for the unification of biology. *Nature Genetics*, 25(1), pp.25–29.
- Costa, R.M.A., Chiganças, V., Galhardo, R.S., Carvalho, H. and Menck, C.F.M., 2003. The eukaryotic nucleotide excision repair pathway. *Biochimie*, 85(11), pp.1083–1099.
- Dimos, J.T. et al., 2008. Induced pluripotent stem cells generated from patients with ALS can be differentiated into motor neurons. *Science*, 321(5893), pp.1218–21.
- Ebrahimi, B., 2015. Reprogramming barriers and enhancers: strategies to enhance the efficiency and kinetics of induced pluripotency. *Cell Regeneration*, 4(1), p.4:10.
- Evans, E., Moggs, J.G., Hwang, J.R., Egly, J.M. and Wood, R.D., 1997. Mechanism of open complex and dual incision formation by human nucleotide excision repair factors. *European Molecular Biology Organization Journal*, 16(21), pp.6559–6573.
- Fan, J. et al., 2011. Human induced pluripotent cells resemble embryonic stem cells demonstrating enhanced levels of DNA repair and efficacy of nonhomologous end-joining. *Mutation Research*, 713(1–2), pp.8–17.
- Fernández-marcelo, T. et al., 2014. Poly (ADP-ribose) polymerase 3 (PARP3), a potential repressor of telomerase activity. *Journal of Experimental & Clinical Cancer Research*, 33, p.19.
- Fornace, A.J., Alamo, I. and Hollander, M.C., 1988. DNA damage-inducible transcripts in mammalian cells. *Proceedings of the National Academy of Sciences of the United States of America*, 85(23), pp.8800–8804.
- Fuchs, B. and Pritchard, D.J., 2002. Etiology of osteosarcoma. *Clinical Orthopaedics and Related Research*, (397), pp.40–52.
- Gatta, G. et al., 2014. Childhood cancer survival in Europe 1999-2007: results of EURO CARE-5-a population-based study. *The Lancet Oncology*, 15, pp.35–47.
- Gokgoz, N. et al., 2001. Comparison of *p53* mutations in patients with localized osteosarcoma and metastatic osteosarcoma. *Cancer*, 92(8), pp.2181–2189.
- Gómez-Díaz, B. et al., 2015. Analysis of *ERCC1* and *ERCC2* gene variants in osteosarcoma, colorectal and breast cancer. *Oncology Letters*, 9(4), pp.1657–1661.

González, F., Boué, S. and Izpisua Belmonte, J.C., 2011. Methods for making induced pluripotent stem cells: reprogramming à la carte. *Nature Reviews: Genetics*, 12(4), pp.231–242.

Goode, E.L., Ulrich, C.M. and Potter, J.D., 2002. Polymorphisms in DNA repair genes and associations with cancer risk. *Cancer Epidemiology Biomarkers & Prevention*, 11, pp.1513–1530.

Goričar, K. et al., 2015. Genetic variability of DNA repair mechanisms and glutathione-S-transferase genes influences treatment outcome in osteosarcoma. *Cancer Epidemiology*, 39(2), pp.182–188.

Gottesman, M.M., 2002. Mechanisms of cancer drug resistance. *Annual Review of Medicine*, 53, pp.615–627.

Gozuacik, D. and Kimchi, A., 2006. DAPk protein family and cancer. *Autophagy*, 2(2), pp.74–79.

Han, G., Wang, Y. and Bi, W., 2012. C-Myc overexpression promotes osteosarcoma cell invasion via activation of MEK-ERK pathway. *Oncology Research*, 20(4), pp.149–56.

Hanahan, D. and Weinberg, R.A., 2011. Hallmarks of cancer: the next generation. *Cell*, 144(5), pp.646–674.

Hanna, J. et al., 2007. Treatment of sickle cell anemia mouse model with iPS cells generated from autologous skin. *Science*, 318(5858), pp.1920–1923.

Hanna, J. et al., 2009. Direct cell reprogramming is a stochastic process amenable to acceleration. *Nature*, 462(7273), pp.595–601.

Hansen, M.F. et al., 1985. Osteosarcoma and retinoblastoma: a shared chromosomal mechanism revealing recessive predisposition. *Proceedings of the National Academy of Sciences of the United States of America*, 82(18), pp.6216–6220.

Hansen, M.F., 2002. Genetic and molecular aspects of osteosarcoma. *Journal of Musculoskeletal & Neuronal Interactions*, 2(6), pp.554–560.

Hao, T., Feng, W., Zhang, J., Sun, Y.J. and Wang, G., 2012. Association of four ERCC1 and ERCC2 SNPs with survival of bone tumour patients. *Asian Pacific Journal of Cancer Prevention*, 13(8), pp.3821–3824.

Harada, K. et al., 2002. Deregulation of caspase 8 and 10 expression in pediatric tumors and cell lines. *Cancer Research*, 62(20), pp.5897–5901.

Hawkins, R.D. et al., 2010. Distinct epigenomic landscapes of pluripotent and lineage-committed human cells. *Cell Stem Cell*, 6(5), pp.479–491.

Heins, N. et al., 2004. Derivation, characterization and differentiation of human embryonic stem cells. *Stem Cells*, 22, pp.367–376.

Henderson, J. et al., 2002. Preimplantation human embryos and embryonic stem cells show comparable expression of stage-specific embryonic antigens. *Stem Cells*, 20, pp.329–337.

Hester, M.E. et al., 2009. Two factor reprogramming of human neural stem cells into pluripotency. *PloS One*, 4(9), p.e7044.

Hong, H. et al., 2009. Suppression of induced pluripotent stem cell generation by the p53-p21 pathway. *Nature*, 460(7259), pp.1132–1135.

Hu, K. et al., 2011. Efficient generation of transgene-free induced pluripotent stem cells from normal and neoplastic bone marrow and cord blood mononuclear cells. *Blood*, 117(14), pp.e109-e119.

Huangfu, D., et al., 2008a. Induction of pluripotent stem cells by defined factors is greatly improved by small-molecule compounds. *Nature Biotechnology*, 26(7), pp.795–797.

Huangfu, D., et al., 2008b. Induction of pluripotent stem cells from primary human fibroblasts with only OCT4 and SOX2. *Nature Biotechnology*, 26(11), pp.1269–1275.

Itskovitz-Eldor, J. et al., 2000. Differentiation of human embryonic stem cells into embryoid bodies comprising the three embryonic germ layers. *Molecular medicine*, 6(2), pp.88–95.

Jin, G. et al., 2015. Single nucleotide polymorphisms of nucleotide excision repair and homologous recombination repair pathways and their role in the risk of osteosarcoma. *Pakistan Journal of Medical Sciences*, 31(2), pp.269–273.

Johansson, H. and Simonsson, S., 2010. Core transcription factors, Oct4, Sox2 and Nanog, individually form complexes with nucleophosmin (Npm1) to control embryonic stem (ES) cell fate determination. *Aging*, 2(11), pp.815–822.

Johnson, N. and Shapiro, G.I., 2010. Cyclin-dependent kinases (CDKs) and the DNA damage response: rationale for CDK inhibitor - chemotherapy combinations as an anticancer strategy for solid tumors. *Expert Opinion on Therapeutic Targets*, 14(11), pp.1199–1212.

Johnson, S.F. and Telesnitsky, A., 2010. Retroviral RNA dimerization and packaging: The what, how, when, where, and why. *PLoS Pathogens*, 6(10), pp.10–13.

Kansara, M., Teng, M.W., Smyth, M.J. and Thomas, D.M., 2014. Translational biology of osteosarcoma. *Nature Reviews Cancer*, 14(11), pp.722–735.

- Kasemeier-Kulesa, J.C. et al., 2008. Reprogramming multipotent tumor cells with the embryonic neural crest microenvironment. *Developmental Dynamics*, 237(10), pp.2657–2666.
- Kawamura, T. et al., 2009. Linking the p53 tumor suppressor pathway to somatic cell reprogramming. *Nature*, 460(7259), pp.1140–1144.
- Kenyon, J. and Gerson, S.L., 2007. The role of DNA damage repair in aging of adult stem cells. *Nucleic Acids Research*, 35(22), pp.7557–7565.
- Kiefer, J.C., 2007. Back to basics: Sox genes. *Developmental Dynamics*, 236, pp.2356–2366.
- Kim, J. et al., 2013. An iPSC line from human pancreatic ductal adenocarcinoma undergoes early to invasive stages of pancreatic cancer progression. *Cell Reports*, 3(6), pp.2088–2099.
- Kim, J.B. et al., 2009. Oct4-induced pluripotency in adult neural stem cells. *Cell*, 136(3), pp.411–419.
- Kim, K. et al., 2010. Epigenetic memory in induced pluripotent stem cells. *Nature*, 467(7313), pp.285–290.
- Ko, H.C. and Gelb, B.D., 2014. Concise review: drug discovery in the age of the induced pluripotent stem cell. *Stem Cells Translational Medicine*, 3(4), pp.500–509.
- Köberle, B., Roginskaya, V. and Wood, R.D., 2006. XPA protein as a limiting factor for nucleotide excision repair and UV sensitivity in human cells. *DNA Repair*, 5(5), pp.641–648.
- Kopper, O., Giladi, O., Golan-Lev, T. and Benvenisty, N., 2010. Characterization of gastrulation-stage progenitor cells and their inhibitory crosstalk in human embryoid bodies. *Stem Cells*, 28(1), pp.75–83.
- Kretsovali, A., Hadjimichael, C. and Charmpilas, N., 2012. Histone deacetylase inhibitors in cell pluripotency, differentiation, and reprogramming. *Stem Cells International*, 2012, p.184154.
- Kruidering, M. and Evan, G., 2000. Caspase-8 in apoptosis: The beginning of “The End”? *International Union of Biochemistry and Molecular Biology Life*, 50(2), pp.85–90.
- Kumano, K., Arai, S. and Hosoi, M., 2012. Generation of induced pluripotent stem cells from primary chronic myelogenous leukemia patient samples. *Blood*, 119(26), pp.6234-6242.
- Ladanyi, M. et al., 1993. MDM2 gene amplification in metastatic osteosarcoma. *Cancer Research*, 53, pp. 16-18.

- de Laat, W., Jaspers, N. and Hoeijmakers, J., 1999. Molecular mechanism of nucleotide excision repair. *Genes & Development*, 13(7), pp.768–785.
- Lee, D.F. et al., 2015. Modeling familial cancer with induced pluripotent stem cells. *Cell*, 161(2), pp.240–254.
- Lee, M.Y., Lu, A. and Gudas, L.J., 2010. Transcriptional regulation of Rex1 (zfp42) in normal prostate epithelial cells and prostate cancer cells. *Journal of Cell Physiology*, 224(1), pp.17–27.
- Li, Y. et al., 2014. Enhancement of radiosensitivity by 5-Aza-CdR through activation of G2/M checkpoint response and apoptosis in osteosarcoma cells. *Tumor Biology*, 35(5), pp.4831–4839.
- Li, Z. and Rana, T.M., 2012. A kinase inhibitor screen identifies small-molecule enhancers of reprogramming and iPS cell generation. *Nature Communications*, 3, p.1085.
- Liebermann, D.A. and Hoffman, B., 2002. Myeloid differentiation (MyD) primary response genes in hematopoiesis. *Oncogene*, 21, pp.3391–3402.
- Lima-Bessa, K.M. de et al., 2008. CPDs and 6-4PPs play different roles in UV-induced cell death in normal and NER-deficient human cells. *DNA Repair*, 7(2), pp.303–312.
- Lin, S.L. et al., 2008. Mir-302 reprograms human skin cancer cells into a pluripotent ES-cell-like state. *RNA*, 14(10), pp.2115–2124.
- Lin, Y.H. et al., 2017. Osteosarcoma: molecular pathogenesis and iPSC modeling. *Trends in Molecular Medicine*, 23(8), pp.737–755.
- Linn, D.E. et al., 2010. A role for OCT4 in tumor initiation of drug-resistant prostate cancer cells. *Genes & Cancer*, 1(9), pp.908–916.
- Liu, H., Kim, Y., Sharkis, S., Marchionni, L. and Jang, Y.Y., 2011. *In vivo* liver regeneration potential of human induced pluripotent stem cells from diverse origins. *Science Translational Medicine*, 3(82), p.1-10.
- Liu, X., Zhang, Z., Deng, C., Tian, Y. and Ma, X., 2017. Meta-analysis showing that ERCC1 polymorphism is predictive of osteosarcoma prognosis. *Oncotarget*, 8(37), pp.62769–62779.
- Liu, Y., Cheng, D., Li, Z., Gao, X. and Wang, H., 2012. The gene expression profiles of induced pluripotent stem cells (iPSCs) generated by a non-integrating method are more similar to embryonic stem cells than those of iPSCs generated by an integrating method. *Genetics and Molecular Biology*, 35(3), pp.693–700.

- Loi, S., Piccart, M. and Sotiriou, C., 2007. The use of gene-expression profiling to better understand the clinical heterogeneity of estrogen receptor positive breast cancers and tamoxifen response. *Critical Reviews in Oncology/Hematology*, 61(3), pp.187–194.
- Lonardo, F., Ueda, T., Huvos, A.G., Healey, J. and Ladanyi, M., 1997. Correlation p53 and MDM2 alterations in osteosarcomas with clinicopathologic features and proliferative rate. *Cancer*, 79(8), pp. 1541-1547.
- Lorenz, S. et al., 2016. Unscrambling the genomic chaos of osteosarcoma reveals extensive transcript fusion, recurrent rearrangements and frequent novel TP53 aberrations. *Oncotarget*, 7(5), pp.5273–5288.
- Lourda, M., Trougakos, I.P. and Gonos, E.S., 2007. Development of resistance to chemotherapeutic drugs in human osteosarcoma cell lines largely depends on up-regulation of Clusterin/Apolipoprotein J. *International Journal of Cancer*, 120(3), pp.611–622.
- Luetke, A., Meyers, P.A., Lewis, I. and Juergens, H., 2014. Osteosarcoma treatment – Where do we stand? A state of the art review. *Cancer Treatment Reviews*, 40(4), pp.523–532.
- Luo, L.Z. et al., 2012. DNA repair in human pluripotent stem cells is distinct from that in non-pluripotent human cells. *PloS One*, 7(3), p.e30541.
- Ma, X., Zhang, Y., Sun, T.S. and Yao, J.H., 2016. Role of ERCC2 and ERCC3 gene polymorphisms in the development of osteosarcoma. *Genetics and Molecular Research*, 15(1), pp.1–6.
- Mahalingam, D. et al., 2012. Reversal of aberrant cancer methylome and transcriptome upon direct reprogramming of lung cancer cells. *Scientific Reports*, 2, p.592.
- Maherali, N. et al., 2007. Directly reprogrammed fibroblasts show global epigenetic remodeling and widespread tissue contribution. *Cell Stem Cell*, 1(1), pp.55–70.
- Malkin, D., 1993. p53 and the Li-Fraumeni syndrome. *Cancer Genetics and Cytogenetics*, 66(2), pp.83–92.
- Mankin, H.J, Hornicek, F.J., Rosenberg, A.E., Harmon, D.C. and Gebhardt, M.C., 2004. Survival data for 648 patients with osteosarcoma treated at one institution. *Clinical Orthopaedics and Related Research*, (429), pp.286–291.
- Marión, R.M. et al., 2009. A p53-mediated DNA damage response limits reprogramming to ensure iPS cell genomic integrity. *Nature*, 460(7259), pp.1149–1153.

- Marteijn, J.A., Lans, H., Vermeulen, W. and Hoeijmakers, J.H.J., 2014. Understanding nucleotide excision repair and its roles in cancer and ageing. *Nature Reviews: Molecular Cell Biology*, 15(7), pp.465–481.
- Martí, M. et al., 2013. Characterization of pluripotent stem cells. *Nature Protocols*, 8(2), pp.223–253.
- Martin, J.W., Squire, J.A. and Zielenska, M., 2012. The genetics of osteosarcoma. *Sarcoma*, 2012, doi:10.1155/2012/627254.
- Masutani, M. et al., 2004. Poly (ADP-ribose) polymerase-1 gene in human tumor cell lines : Its expression and structural alteration. *Proceeding of the Japan Academy, Series B*, 80, pp.114–118.
- Matsunaga, T., 2007. *In vitro* assays for evaluating the cellular responses to DNA damage induced by solar UV. *Japanese Society for Alternatives to Animal Experiments*, 14, pp.637–640.
- McKay, B.C., Ljungman, M. and Rainbow, A.J., 1999. Potential roles for p53 in nucleotide excision repair. *Carcinogenesis*, 20(8), pp.1389–1396.
- Medvedev, S.P. et al., 2013. Characteristics of induced human pluripotent stem cells using DNA microarray technology. *Bulletin of Experimental Biology and Medicine*, 155(1), pp.122–128.
- Merimsky, O. et al., 2004. Palliative treatment for advanced or metastatic osteosarcoma. *Israel Medicine Association Journal*, 6, pp.34–38.
- Meyers, P.A. and Gorlick, R., 1997. Osteosarcoma. *Pediatric Clinics of North America*, 44(4), pp.973–989.
- Mikkelsen, T.S. et al., 2008. Dissecting direct reprogramming through integrative genomic analysis. *Nature*, 454(7200), pp.49–55.
- Miller, D.M. et al., 2012. c-Myc and cancer metabolism. *Clinical Cancer Research*, 18(20), pp.5546–5553.
- Miyoshi, N. et al., 2010. Defined factors induce reprogramming of gastrointestinal cancer cells. *Proceedings of the National Academy of Sciences of the United States of America*, 107(1), pp.40–45.
- Mongan, N.P., Martin, K.M. and Gudas, L.J., 2006. The putative human stem cell marker, Rex-1 (Zfp42): Structural classification and expression in normal human epithelial and carcinoma cell cultures. *Molecular Carcinogenesis*, 45, pp.887–900.
- Morgan, D.O., 1995. Principles of CDK regulation. *Nature*, 374, pp.131–134.

- Mu, D., Wakasugi, M., Hsu, D.S. and Sancar, A., 1997. Characterization of reaction intermediates of human excision repair nuclease. *Journal of Biological Chemistry*, 272(46), pp.28971–28979.
- Muller, F.J., Goldmann, J., Loser, P. and Loring, J.F., 2010. A call to standardize teratoma assays used to define human pluripotent cell lines. *Cell Stem Cell*, 6(5), pp.412–414.
- Nakagawa, M. et al., 2008. Generation of induced pluripotent stem cells without Myc from mouse and human fibroblasts. *Nature Biotechnology*, 26, pp.101–106.
- Nichols, J. et al., 1998. Formation of pluripotent stem cells in the mammalian embryo depends on the POU Transcription Factor Oct4. *Cell*, 95, pp.379–391.
- Niforou, K.N. et al., 2006. The proteome profile of the human osteosarcoma Saos2 cell line. *Cancer Genomics & Proteomics*, 3, pp.325–346.
- Odes, E.J. et al., 2016. Earliest hominin cancer: 1.7-million-year-old osteosarcoma from Swartkrans Cave, South Africa. *South African Journal of Science*, 112112(5), pp.1-5.
- Oka, Y. et al., 2010. 293FT cells transduced with four transcription factors (OCT4, SOX2, NANOG, and LIN28) generate aberrant ES-like cells. *Journal of Stem Cells & Regenerative Medicine*, 6(3), pp.149–156.
- Okita, K. et al., 2008. Generation of mouse induced pluripotent stem cells without viral vectors. *Science*, 322, pp.949–953.
- Overholtzer, M. et al., 2003. The presence of p53 mutations in human osteosarcomas correlates with high levels of genomic instability. *Proceedings of the National Academy of Sciences of the United States of America*, 100(20), pp.11547–11552.
- Papp, B. and Plath, K., 2011. Reprogramming to pluripotency: stepwise resetting of the epigenetic landscape. *Cell Research*, 21, pp.486–501.
- Park, H.Y. et al., 2012. Efficient generation of virus-free iPS cells using liposomal magnetofection. *PloS One*, 7(9), p.e45812.
- Park, J. et al., 2011. Reprogramming of mouse fibroblasts to an intermediate state of differentiation by chemical induction. *Cellular Reprogramming*, 13(2), pp.121–131.
- Paunesku, T. et al., 2001. Proliferating cell nuclear antigen (PCNA): Ringmaster of the genome. *International Journal of Radiation Biology*, 77(10), pp.1007–1021.
- Pera, M.F., Reubinoff, B. and Trounson, A., 2000. Human embryonic stem cells. *Journal of Cell Science*, 113(1), pp.5–10.

- Petruseva, I.O., Evdokimov, A.N. and Lavrik, O.I., 2014. Molecular mechanism of global genome nucleotide excision repair. *Acta Naturae*, 6(1), pp.23–34.
- PosthumaDeBoer, J., van Royen, B. and Helder, M., 2013. Mechanisms of therapy resistance in osteosarcoma: a review. *Oncology Discovery*, 1(1), p.8.
- Prideaux, M. et al., 2014. SaOS2 osteosarcoma cells as an in vitro model for studying the transition of human osteoblasts to osteocytes. *Calcified Tissue International*, 95(2), pp.183–193.
- Raman, J.D. et al., 2006. Decreased expression of the human stem cell marker, Rex-1 (zfp-42), in renal cell carcinoma. *Carcinogenesis*, 27(3), pp.499–507.
- Reed, E., 1998. Nucleotide excision repair and anti-cancer chemotherapy. *Cytotechnology*, 27(1–3), pp.187–201.
- Rocha, C.R.R. et al., 2013. The role of DNA repair in the pluripotency and differentiation of human stem cells. *Mutation Research*, 752(1), pp.25–35.
- Samardzija, C., Quinn, M., Findlay, J.K. and Ahmed, N., 2012. Attributes of Oct4 in stem cell biology: perspectives on cancer stem cells of the ovary. *Journal of Ovarian Research*, 5(1), p.37.
- Sampson, V.B., Gorlick, R., Kamara, D. and Anders Kolb, E., 2013. A review of targeted therapies evaluated by the pediatric preclinical testing program for osteosarcoma. *Frontiers in Oncology*, 3(May), p.132.
- Sampson, V.B. et al., 2015. MicroRNAs and potential targets in osteosarcoma: Review. *Frontiers in Pediatrics*, 3, p.69.
- Sancar, A., 1996. DNA Excision Repair. *Annual Review of Biochemistry*, 65(1), pp.43–81.
- Satoh, M.S. and Lindahl, T., 1992. Role of poly(ADP-ribose) formation in DNA repair. *Nature*, 356(6367), pp.356–358.
- Satokata, I. et al., 1993. Genomic characterization of the human DNA excision repair-controlling gene XPAC. *Gene*, 136(1–2), pp.345–348.
- Schopperle, W.M. and DeWolf, W.C., 2007. The TRA-1-60 and TRA-1-81 human pluripotent stem cell markers are expressed on podocalyxin in embryonal carcinoma. *Stem Cells*, 25(3), pp.723–730.
- Schuldiner, M. et al., 2000. Effects of eight growth factors on the differentiation of cells derived from human embryonic stem cells. *Proceedings of the National Academy of Sciences of the United States of America*, 97(21), pp.11307–11312.
- Scotland, K.B., Chen, S., Sylvester, R. and Gudas, L.J., 2009. Analysis of REX1 (ZFP42) function in embryonic stem cell differentiation. *Developmental Dynamics*, 238(8), pp.1863–1877.

Selvarajah, S. et al., 2007. Identification of cryptic microaberrations in osteosarcoma by high-definition oligonucleotide array comparative genomic hybridization. *Cancer Genetics and Cytogenetics*, 179(1), pp.52–61.

Sertic, S. et al., 2012. NER and DDR: Classical music with new instruments. *Cell Cycle*, 11(4), pp.668–674.

Shen, J.-C., Fox, E.J., Ahn, E.H. and Loeb, L.A., 2014. A rapid assay for measuring nucleotide excision repair by oligonucleotide retrieval. *Scientific Reports*, 4, p.4894.

Siddik, Z.H., 2003. Cisplatin: mode of cytotoxic action and molecular basis of resistance. *Oncogene*, 22(47), pp.7265–7279.

Sigal, A. and Rotter, V., 2000. Oncogenic mutations of the p53 tumor suppressor: the demons of the guardian of the genome. *Cancer Research*, 60, pp. 6788-6793.

Sinha, R.P. and Häder, D.-P., 2002. UV-induced DNA damage and repair: a review. *Photochemical & Photobiological Sciences*, 1(4), pp.225–236.

Van Sloun, P.P.H. et al., 1999. The role of nucleotide excision repair in protecting embryonic stem cells from genotoxic effects of UV-induced DNA damage. *Nucleic Acids Research*, 27(16), pp.3276–3282.

Smith, M.L. and Seo, Y.R., 2002. p53 regulation of DNA excision repair pathways. *Mutagenesis*, 17(2), pp.149–156.

Spike, B.T. and Wahl, G.M., 2011. p53, stem cells, and reprogramming: Tumor suppression beyond guarding the genome. *Genes & Cancer*, 2(4), pp.404–419.

Stadtfeld, M., Maherali, N., Breault, D.T. and Hochedlinger, K., 2008. Defining molecular cornerstones during fibroblast to iPS cell reprogramming in mouse. *Cell Stem Cell*, 2(3), pp.230–240.

Stephens, P.J. et al., 2011. Massive genomic rearrangement acquired in a single catastrophic event during cancer development. *Cell*, 144(1), pp.27–40.

Stoehlmacher, J. et al., 2004. A multivariate analysis of genomic polymorphisms: prediction of clinical outcome to 5-FU/oxaliplatin combination chemotherapy in refractory colorectal cancer. *British Journal of Cancer*, 91(2), pp.344–354.

Stricker, S.H. et al., 2013. Widespread resetting of DNA methylation in glioblastoma-initiating cells suppresses malignant cellular behavior in a lineage-dependent manner. *Genes & Development*, 27, pp.654–669.

Sugii, S., Kida, Y., Berggren, W.T. and Evans, R.M., 2011. Feeder-dependent and feeder-independent iPS cell derivation from human and mouse adipose stem cells. *Nature Protocols*, 6(3), pp.346–358.

- Sugitani, N. et al., 2017. Analysis of DNA binding by human factor xeroderma pigmentosum complementation group A (XPA) provides insight into its interactions with nucleotide excision repair substrates. *Journal of Biological Chemistry*, 292(41) 16847–16857.
- Sun, M. et al., 2015. Hiporfin-mediated photodynamic therapy in preclinical treatment of osteosarcoma. *Photochemistry and Photobiology*, 91(3), pp.533–544.
- Sun, Y. et al., 2015. Genetic polymorphisms in nucleotide excision repair pathway influences response to chemotherapy and overall survival in osteosarcoma. *International Journal of Clinical Experimental Pathology*, 8(7), pp.7905–7912.
- Tafani, M., 2012. Reprogramming Cancer Stem Cells. *Journal of Cancer Science & Therapy*, 04(12), pp.xxv–xxvi.
- Tai, M.-H. et al., 2005. Oct4 expression in adult human stem cells: evidence in support of the stem cell theory of carcinogenesis. *Carcinogenesis*, 26(2), pp.495–502.
- Takahashi, K. et al., 2007. Induction of pluripotent stem cells from adult human fibroblasts by defined factors. *Cell*, 131(5), pp.861–872.
- Takahashi, K. and Yamanaka, S., 2006. Induction of pluripotent stem cells from mouse embryonic and adult fibroblast cultures by defined factors. *Cell*, 126(4), pp.663–676.
- Takekawa, M. and Saito, H., 1998. A family of stress-inducible GADD45-like proteins mediate activation of the stress-responsive MTK1/MEKK4 MAPKKK. *Cell*, 95(4), pp.521–530.
- Tamura, R.E. et al., 2012. GADD45 proteins: central players in tumorigenesis. *Current Molecular Medicine*, 12(5), pp.634–651.
- Teng, J.W., Yang, Z., Li, J. and Xu, B., 2013. Predictive role of glutathione S-transferases (GSTs) on the prognosis of osteosarcoma patients treated with chemotherapy. *Pakistan Journal of Medical Sciences*, 29(5), pp.1182–1186.
- Thomas, D.M. et al., 2004. Terminal osteoblast differentiation, mediated by Runx2 and p27 KIP1, is disrupted in osteosarcoma. *Journal of Cell Biology*, 167(5), pp.925–934.
- Thoms, K., Kuschal, C. and Emmert, S., 2007. Lessons learned from DNA repair defective syndromes. *Experimental Dermatology*, 16, pp.532–544.
- Thomson, J.A. et al., 1998. Embryonic stem cell lines derived from human blastocysts. *Science*, 282, pp.1145–1148.

- Utikal, J., Maherali, N., Kulalert, W. and Hochedlinger, K., 2009. Sox2 is dispensable for the reprogramming of melanocytes and melanoma cells into induced pluripotent stem cells. *Journal of Cell Science*, 122(19), pp.3502–3510.
- Vairapandi, M. et al., 2000. Characterization of MyD118, Gadd45, and proliferating cell nuclear antigen (PCNA) interacting domains. *Journal of Biological Chemistry*, 275(22), pp.16810–16819.
- Vairapandi, M., Balliet, A.G., Hoffman, B. and Liebermann, D.A., 2002. GADD45b and GADD45g are cdc2/cyclinB1 kinase inhibitors with a role in S and G2/M cell cycle checkpoints induced by genotoxic stress. *Journal of Cellular Physiology*, 192(3), pp.327–338.
- Varshney, J., Scott, M., Largaespada, D. and Subramanian, S., 2016. Understanding the osteosarcoma pathobiology: A comparative oncology approach. *Veterinary Sciences*, 3(1), p.3.
- Vella, S. et al., 2016. Targeting CDKs with Roscovitine increases sensitivity to DNA damaging drugs of human osteosarcoma cells. *PLoS One*, 11(11), p.e0166233.
- Verusingam, N.D. et al., 2017. Susceptibility of human oral squamous cell carcinoma (OSCC) H103 and H376 cell lines to retroviral OSKM mediated reprogramming. *PeerJ*, 5, p.e3174.
- Vos, H., 2016. *Pharmacogenetics of osteosarcoma treatment*.
- De Vos, M., Schreiber, V. and Dantzer, F., 2012. The diverse roles and clinical relevance of PARPs in DNA damage repair: Current state of the art. *Biochemical Pharmacology*, 84(2), pp.137–146.
- Wang, D., Luo, M. and Kelley, M.R., 2004. Human apurinic endonuclease 1 (APE1) expression and prognostic significance in osteosarcoma: enhanced sensitivity of osteosarcoma to DNA damaging agents using silencing RNA APE1 expression inhibition. *Molecular Cancer Therapeutics*, 3(6), pp.679–686.
- Wang, M.J., Zhu, Y., Guo, X.J. and Tian, Z.Z., 2015. Genetic variability of genes involved in DNA repair influence treatment outcome in osteosarcoma. *Genetics and Molecular Research*, 14(3), pp.11652–11657.
- Wernig, M. et al., 2007. *In vitro* reprogramming of fibroblasts into a pluripotent ES-cell-like state. *Nature*, 448(7151), pp.318–324.
- Wood, R.D., Mitchell, M., Sgouros, J. and Lindahl, T., 2001. Human DNA repair genes. *Science*, 291(5507), pp.1284–1289.
- Xu, B. et al., 2017. MicroRNA-21 inhibits the apoptosis of osteosarcoma cell line SAOS-2 via targeting Caspase 8. *Oncology Research*, 25, pp.1161–1168.

Ying, J. et al., 2005. The stress-responsive gene GADD45G is a functional tumor suppressor, with its response to environmental stresses frequently disrupted epigenetically in multiple tumors. *Clinical Cancer Research*, 11(18), pp.6442–6449.

Yusa, K. et al., 2011. Targeted gene correction of α 1-antitrypsin deficiency in induced pluripotent stem cells. *Nature*, 478(7369), pp.391–394.

Zaehres, H. et al., 2005. High-efficiency RNA interference in human embryonic stem cells. *Stem Cells*, 23(3), pp.299–305.

Zainal, A. and Nor, S., 2007. *National Cancer Registry Report*.

Zeng, S. et al., 2016. Generation of induced pluripotent stem cells (iPSCs) from a retinoblastoma patient carrying A.C. 2663G > A mutation in RB1 gene. *Stem Cell Research*, 17(2), pp.208–211.

Zhang, N., An, M.C., Montoro, D. and Ellerby, L.M., 2010. Characterization of human Huntington's disease cell model from induced pluripotent stem cells. *PLoS Currents*, 2, pp.1–11.

Zhang, Q. et al., 2015. Investigation of ERCC1 and ERCC2 gene polymorphisms and response to chemotherapy and overall survival in osteosarcoma. *Genetics and Molecular Research*, 14(3), pp.11235–11241.

Zhang, S.L. et al., 2012. Predictive potential of glutathione S-transferase polymorphisms for prognosis of osteosarcoma patients on chemotherapy. *Asian Pacific Journal of Cancer Prevention*, 13(6), pp.2705–2709.

Zhang, S. and Cui, W., 2014. Sox2 , a key factor in the regulation of pluripotency and neural differentiation. *World Journal of Stem Cells*, 6(3), pp.305–311.

Zhang, S., Zhong, B. and Chen, M., 2014. Epigenetic reprogramming reverses the malignant epigenotype of the MMP/TIMP axis genes in tumor cells. *International Journal of Cancer*, 134(7), pp.1583–1594.

Zhang, W., Dziak, R.M. and Aletta, J.M., 1995. EGF-mediated phosphorylation of extracellular signal-regulated kinases in osteoblastic cells. *Journal of Cellular Physiology*, 162(3), pp.348–358.

Zhang, X. et al., 2002. Loss of expression of GADD45 gamma, a growth inhibitory gene, in human pituitary adenomas: Implications for tumorigenesis. *Journal of Clinical Endocrinology and Metabolism*, 87(3), pp.1262–1267.

Zhang, X. et al., 2013. Terminal differentiation and loss of tumorigenicity of human cancers via pluripotency-based reprogramming. *Oncogene*, 32(18), pp.2249–2260.

Zhao, W. et al., 2012. Embryonic stem cell markers. *Molecules*, 17(6), pp.6196–6236.

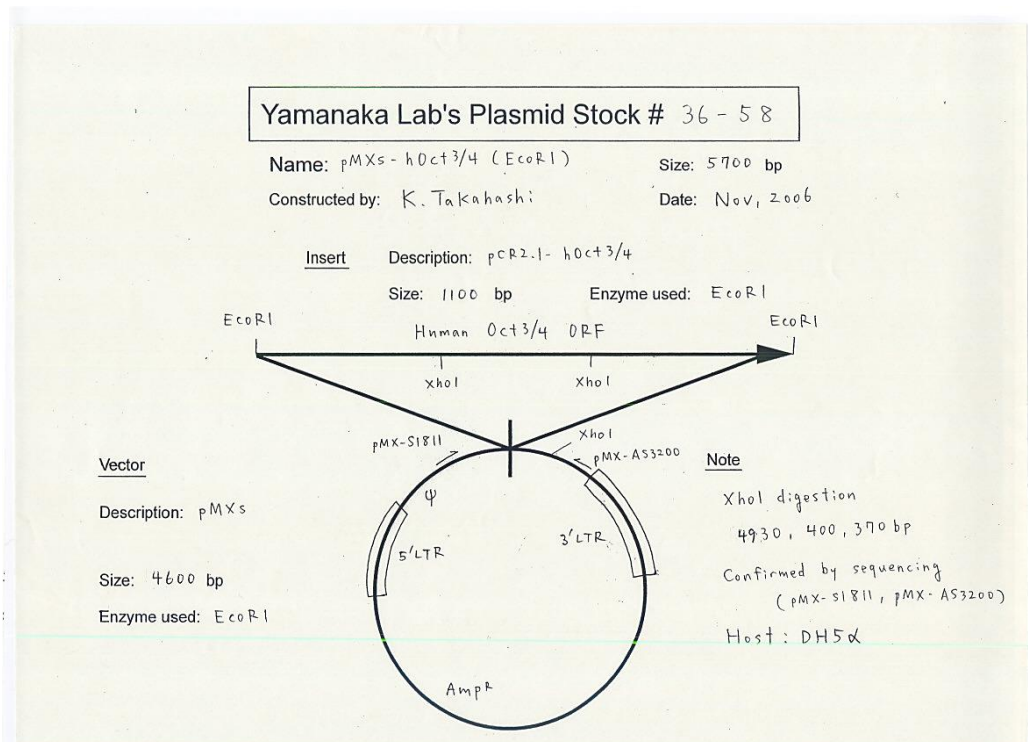
Zhao, X.Y. et al., 2010. Efficient and rapid generation of induced pluripotent stem cells using an alternative culture medium. *Cell Research*, 20(3), pp.383–386.

Zhao, Y. et al., 2008. Two supporting factors greatly improve the efficiency of human iPSC generation. *Cell Stem Cell*, 3(5), pp.475–479.

APPENDICES

APPENDIX A

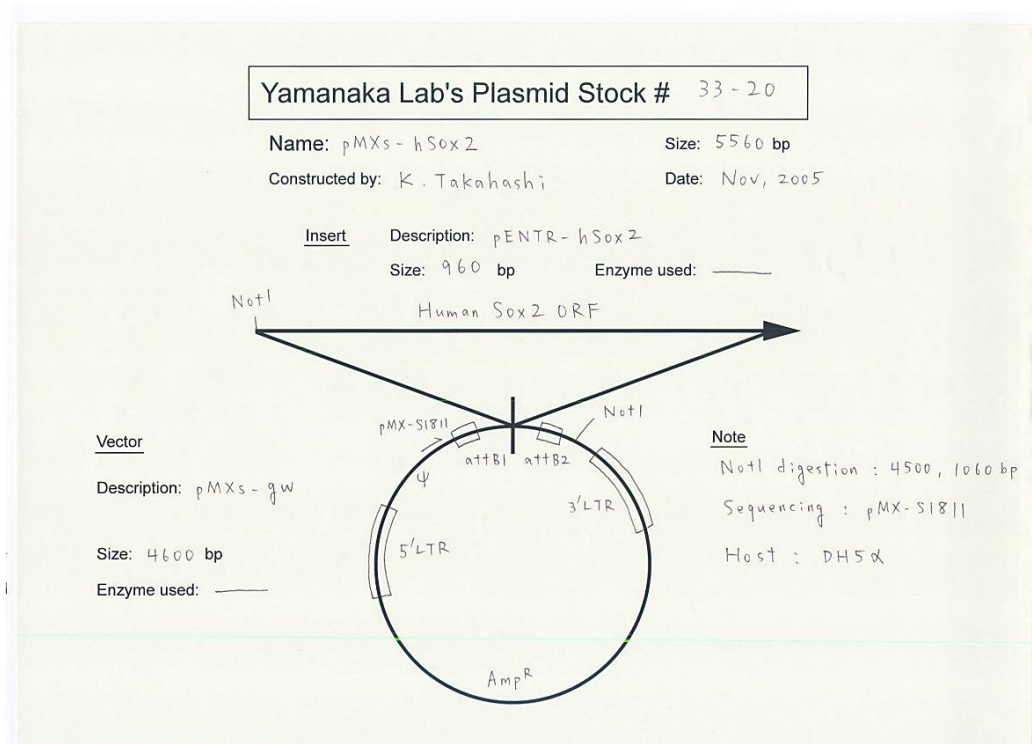
Full sequence map for pMXs-hOCT3/4



(Source: Addgene website)

APPENDIX B

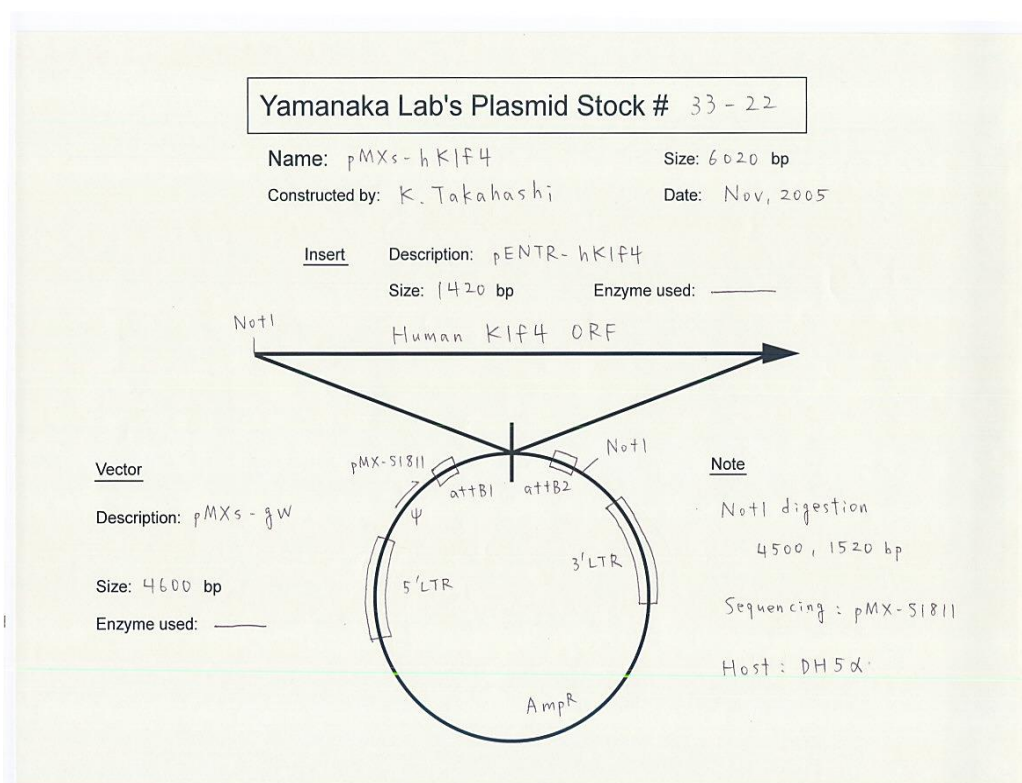
Full sequence map for pMXs-hSOX2



(Source: Addgene website)

APPENDIX C

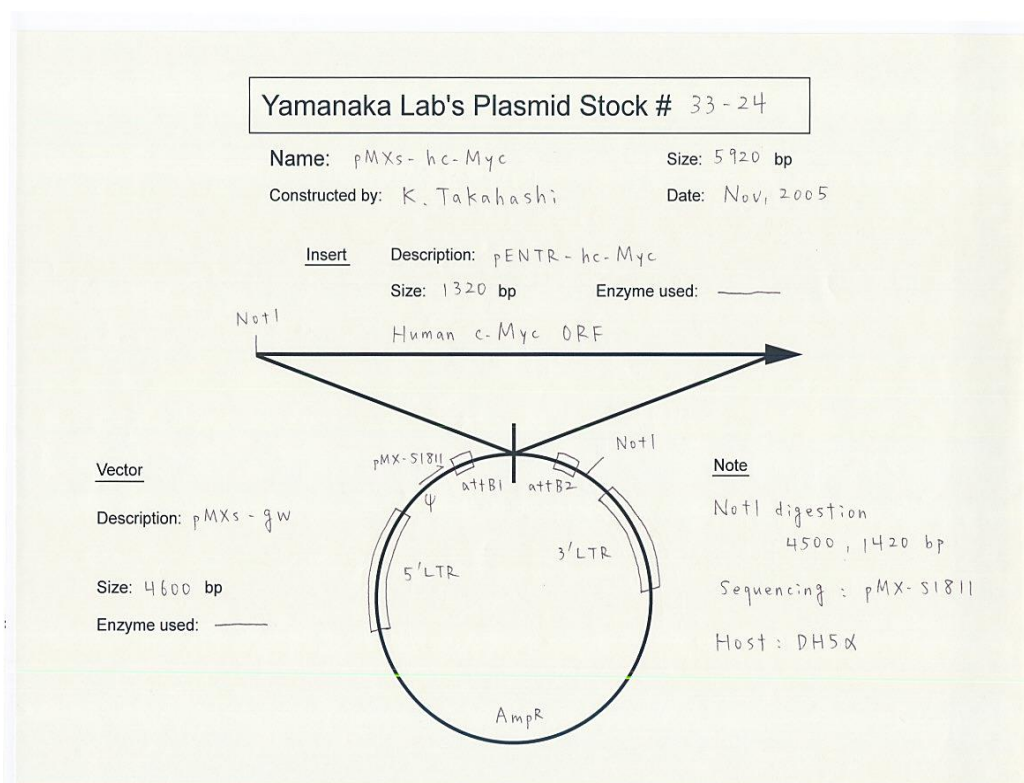
Full sequence map for pMXs-hKLF4



(Source: Addgene website)

APPENDIX D

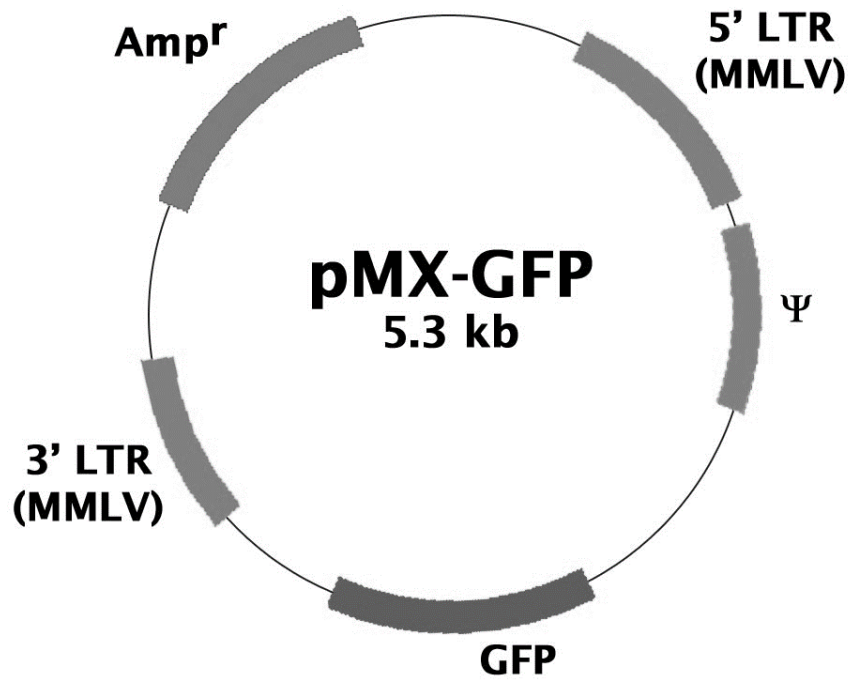
Full sequence map for pMXs-hc-MYC



(Source: Addgene website)

APPENDIX E

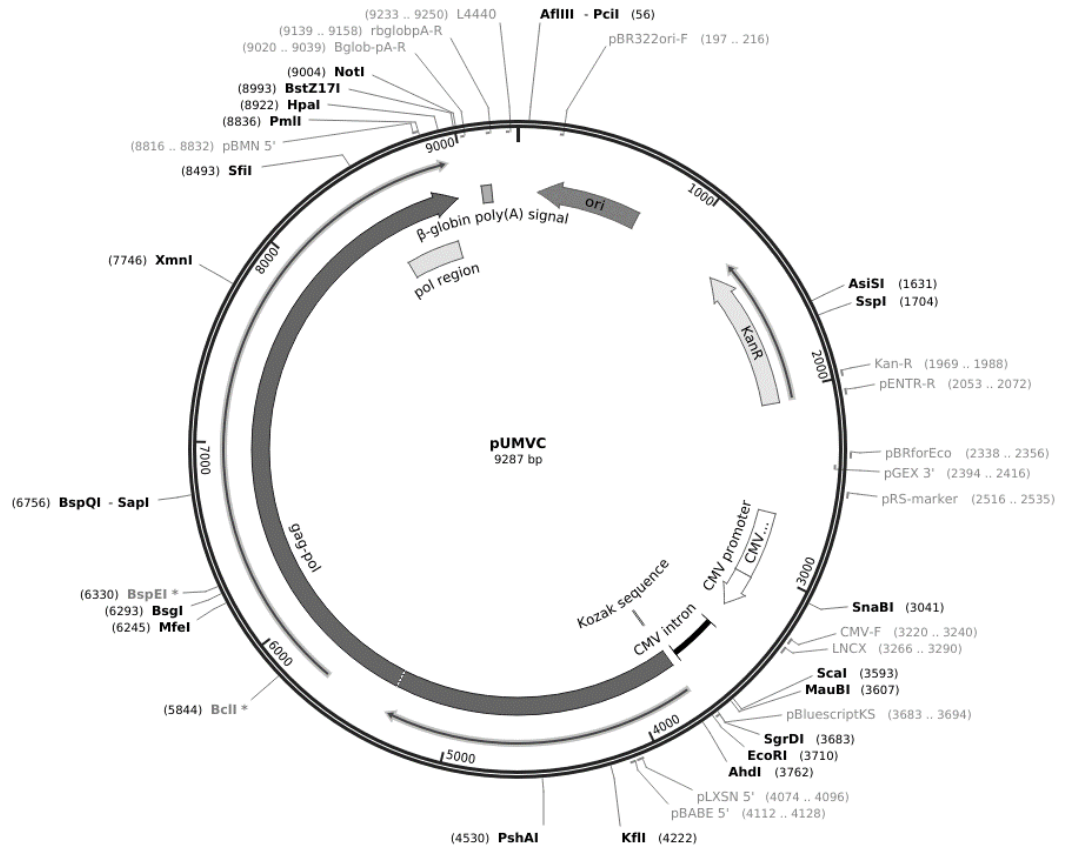
Full sequence map for pMX-GFP



(Source: Addgene website)

APPENDIX F

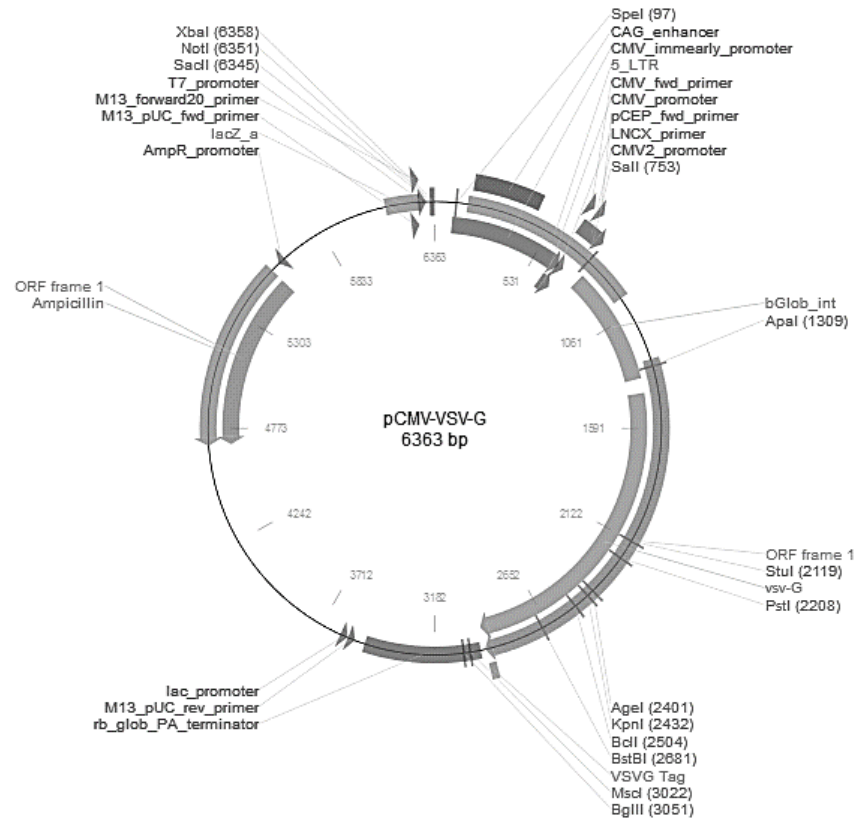
Full sequence map for packaging plasmid Gag-Pol



(Source: Addgene website)

APPENDIX G

Full sequence map for packaging plasmid VSV-G



APPENDIX H

Plasmid concentration and purity

PLASMID	CONC (ng/uL)	A260/280	A260/230
pMX-hOCT3/4	2810	1.83	2.27
pMX-hSOX2	7540	1.85	2.37
pMX-hKLF4	7025	1.79	2.21
pMX-hc-MYC	6190	1.84	2.38
pMX-GFP	7225	1.82	2.40
GAG-POL	2880	1.82	2.47
VSV-G	3150	1.83	2.33

APPENDIX I

Types of restriction enzymes (RE) and plasmid DNA (OSKM) sizes

PLASMID	SIZE (RE)
pMX-hOCT3/4	4600bp, 1100bp (ECOR1)
pMX-hSOX2	4500bp, 1060bp (NOT1)
pMX-hKLF4	4500bp, 1520bp (NOT1)
pMX-hc-MYC	4500bp, 1420bp (NOT1)

APPENDIX J

List of primers used for expression of pluripotent markers

No	Primer name	Primer sequence (5' => 3')
1	OCT4 ENDO (F)	GAC AGG GGG AGG GGA GGA GCT AGG
2	OCT4 ENDO (R)	CTT CCC TCC AAC CAG TTG CCC CAA AC
3	SOX2 ENDO (F)	GGG AAA TGG GAG GGG TGC AAA AGA GG
4	SOX2 ENDO (R)	TTG CGT GAG TGT GGA TGG GAT TGG TG
5	NANOG (F)	TTT GGA AGC TGC TGG GGA AG
6	NANOG (R)	GAT GGG AGG AGG GGA GAG GA
7	c-MYC ENDO (F)	GCG TCC TGG GAA GGG AGA TCC GGA GC
8	c-MYC ENDO (R)	TTG AGG GGC ATC GTC GCG GGA GGC TG
9	REX1 (F)	GTG GAT GCG CAC GTG CGT ACG C
10	REX1 (R)	CTG GAG GAA TAC CTG GCA TTG
11	GAPDH (F)	GAA ATC CCA TCA CCA TCT TCC AGG
12	GAPDH (R)	GAG CCC CAG CCT TCT CCA TG

APPENDIX K

List of primers used for expression of three germ layers

No	Primer name	Primer sequence (5' => 3')
1	MSX1 (F)	GAG TTC TCC AGC TCG CTC AG
2	MSX1 (R)	TCT CCA GCT CTG CCT CTT GT
3	GATA2 (F)	GCT GCA CAA TGT TAA CAG GC
4	GATA2 (R)	TCT CCT GCA TGC ACT TTG AC
5	hBRACHYURY (F)	CCA CCT TCC AAG TGA AGC TC
6	hBRACHYURY (R)	CGA AGT CCA TGA GCA GCA TA
7	FOXA2 (F)	CCA TGC ACT CGG CTT CCA G
8	FOXA2 (R)	TGT TGC TCA CGG AGG AGT AG
9	GATA4 (F)	CCA AGC AGG ACT CTT GGA AC
10	GATA4 (R)	GGG AAG AGG GAA GAT TAC GC
11	GATA6 (F)	TCT ACA GCA AGA TGA ACG GCC TCA
12	GATA6 (R)	TCT GCG CCA TAA GGT GGT AGT TGT
13	TUJ1 (F)	AGT GAT GAG CAT GGC ATC GAC CC
14	TUJ1 (R)	GGC ACG TAC TTG TGA GAA GAG GC
15	CDX2 (F)	AAA GGC TTG GCT GGT GTA TG
16	CDX2 (R)	GTC AGG CCT GGA GTC CAA TA

APPENDIX L

List of TaqMan® probe used for validation

No	TaqMan® probe	Assay ID
1	PARP1	Hs00242302_m1
2	PARP3	Hs00193946_m1
3	MLH1	Hs00979919_m1
4	MRE11A	Hs00967437_m1
5	CCND2	Hs00153380_m1
6	CCNE1	Hs01026536_m1
7	MNAT1	Hs01041571_m1
8	BCL2L11	Hs00708019_s1
9	BNIP3L	Hs00188949_m1
10	CASP8	Hs01018151_m1
11	DAPK1	Hs00234480_m1

APPENDIX M

List of TaqMan® probe used for NER study

No	TaqMan® probe	Assay ID
1	GADD45G	Hs02566147_s1
2	XPA	Hs00902270_m1
3	RPA	At02217444_g1
4	MNAT1	Hs01041571_m1
5	ERCC1	Hs01012158_m1
6	PCNA	Hs00427214_g1
7	POLL	Hs00203191_m1

APPENDIX N

List of up-regulated genes in iG-292

No	Gene	No	Gene	No	Gene	No	Gene	No	Gene
1	ABCA3	61	ATP10D	121	C9orf41	181	CNN2	241	DMD
2	ABCA5	62	ATP11C	122	C9orf72	182	CNNM3	242	DNAH10
3	ABCC1	63	ATP6V0A2	123	C9orf91	183	CNR1	243	DNAJA4
4	ABLIM1	64	ATP8A1	124	CA11	184	CNTN3	244	DNAJC11
5	ACAT2	65	ATRNL1	125	CA4	185	CNTNAP2	245	DNAJC12
6	ACP1	66	B3GALNT1	126	CACHD1	186	CNTNAP4	246	DNAJC2
7	ACP6	67	B3GNT5	127	CACNA1C	187	COA5	247	DNMT3A
8	ACTA1	68	B4GALT3	128	CACNA2D2	188	COCH	248	DOK6
9	ACTG2	69	BACE2	129	CACNA2D4	189	COL11A1	249	DPH3P1
10	ADAMTS3	70	BAIAP2L1	130	CACNB2	190	COL21A1	250	DPM3
11	ADAMTSL3	71	BAMBI	131	CACNB4	191	COL2A1	251	DPPA4
12	ADC	72	BARX1	132	CADM1	192	COMTD1	252	DPYSL5
13	ADCY2	73	BBC3	133	CALML4	193	CORO7-PAM	253	DSEL
14	ADCY3	74	BCHE	134	CASZ1	194	COX10	254	DSG2
15	ADD2	75	BCL11A	135	CBX2	195	COX5B	255	DSP
16	ADI1	76	BCL11B	136	CCDC121	196	COX6A1	256	DUS1L
17	ADIPOR2	77	BCL2L11	137	CCDC28B	197	CPT1A	257	DUSP2
18	AGA	78	BCL7A	138	CCDC3	198	CPT2	258	DUSP9
19	AGBL5	79	BCOR	139	CCDC74B	199	CPVL	259	DYNC111
20	AGPAT2	80	BCR	140	CCDC77	200	CRABP1	260	DYNC2LI1
21	AGPAT3	81	BDH1	141	CCDC8	201	CREBZF	261	DYRK1A
22	AGTR1	82	BEND7	142	CCDC88C	202	CREG1	262	DYRK2
23	AIF1L	83	BGN	143	CCNA1	203	CRIP1	263	DYRK4
24	AKAP1	84	BHLHE22	144	CCND2	204	CRIP3	264	EBF1
25	AKAP7	85	BHMT2	145	CCNE1	205	CSMD3	265	EBP
26	AKNA	86	BLMH	146	CD247	206	CTSC	266	ECE2
27	ALDH2	87	BMP1	147	CD55	207	CTSH	267	ECRP
28	ALDH5A1	88	BMP3	148	CD9	208	CTSL2	268	EDNRA
29	ALDOC	89	BMP7	149	CDC42	209	CTSZ	269	EFEMP1
30	ALX1	90	BMPR1B	150	CDCA7L	210	CUX1	270	EFHC2
31	ANGEL1	91	BOLA1	151	CDH12	211	CXorf57	271	EFNA1
32	ANK3	92	BRI3BP	152	CDH19	212	CYP51A1	272	EFNA5
33	ANKHD1	93	BTG2	153	CDH22	213	CYTL1	273	EFR3B
34	ANKRA2	94	BTNL9	154	CDH23	214	D4S234E	274	EGF
35	ANKRD20A5P	95	C10orf2	155	CDH6	215	DAB1	275	EGFL8
36	ANKRD6	96	C10orf35	156	CDK18	216	DACH1	276	EGLN3
37	ANKS6	97	C11orf71	157	CDS1	217	DAPK1	277	EHF
38	ANO2	98	C11orf75	158	CEBPG	218	DAPK2	278	EIF4A2
39	ANOS	99	C12orf4	159	CELF1	219	DARS2	279	EIF4B
40	ANP32E	100	C12orf45	160	CELF2	220	DCAF7	280	EIF4EBP2
41	APBA2	101	C12orf5	161	CELSR2	221	DCLK1	281	EIF5A
42	APOA1BP	102	C12orf56	162	CENPV	222	DCP1B	282	ELF2
43	APOOL	103	C14orf1	163	CEP350	223	DCP2	283	ELL2
44	APP	104	C15orf59	164	CGREF1	224	DDIT4	284	ELMOD1
45	ARAP2	105	C15orf61	165	CHD7	225	DDR1	285	ELOVL7
46	ARHGEF16	106	C17orf108	166	CHL1	226	DDX3X	286	ENC1
47	ARHGEF26	107	C18orf1	167	CHN2	227	DESI1	287	ENSA
48	ARHGEF9	108	C1orf31	168	CHPT1	228	DGKZ	288	EP400
49	ARL2BP	109	C1orf56	169	CHRFAM7A	229	DHCR24	289	EPB41L3
50	ARNT2	110	C1orf61	170	CHRNA5	230	DHCR7	290	EPHA3
51	ARPC5	111	C1orf9	171	CHST11	231	DHODH	291	EPHA4
52	ARTN	112	C2orf15	172	CIAO1	232	DHRS12	292	EPHA5
53	ASNS	113	C2orf16	173	CLCN5	233	DIAPH2	293	EPHA7
54	ASRGL1	114	C2orf44	174	CLDN7	234	DLGAP1	294	EPHB3
55	ASXL1	115	C2orf68	175	CLEC2B	235	DLL1	295	ERMP1
56	ASXL3	116	C4orf32	176	CLEC7A	236	DLL3	296	ERO1LB
57	ATAD2B	117	C4orf46	177	CLMN	237	DLX1	297	ESRRG
58	ATF5	118	C7orf26	178	CMBL	238	DLX2	298	EWSR1
59	ATL2	119	C9orf123	179	CNDP2	239	DLX5	299	EXPH5
60	ATOH7	120	C9orf142	180	CNKSR2	240	DLX6	300	EYA4
								301	F11R
								302	FAHD2A
								303	FAM104B
								304	FAM110B
								305	FAM117A
								306	FAM125B
								307	FAM134B
								308	FAM136A
								309	FAM169A
								310	FAM184A
								311	FAM195A
								312	FAM206A
								313	FAM213A
								314	FAM222A
								315	FAM5C
								316	FAM65B
								317	FAM69B
								318	FAM84B
								319	FASN
								320	FASTKD1
								321	FBXL16
								322	FDPS
								323	FGD6
								324	FGF11
								325	FGF12
								326	FGF9
								327	FGFR4
								328	FILIP1L
								329	FKBP11
								330	FKBP4
								331	FKBP5
								332	FLAD1
								333	FLRT3
								334	FLVCR1
								335	FLVCR1-AS1
								336	FNDC1
								337	FOLH1
								338	FOXA1
								339	FOXO1
								340	FOXO4
								341	FRAS1
								342	FRS2
								343	FRY
								344	FXN
								345	FZD4
								346	FZD5
								347	GAB1
								348	GABRB2
								349	GABRB3
								350	GABRG1
								351	GADD45G
								352	GAL
								353	GALK2
								354	GALNT12
								355	GALNT14
								356	GATM
								357	GCA
								358	GCHFR

APPENDIX N (CONTINUE)

No	Gene	No	Gene	No	Gene	No	Gene	No	Gene	No	Gene
361	GCLC	421	IGK	481	LDOC1L	541	MECP2	601	NFIB	661	PDRG1
362	GGCT	422	IGSF3	482	LEF1	542	MED12	602	NFIX	662	PEX5L
363	GIT2	423	IGSF8	483	LETM1	543	MEOX2	603	NFS1	663	PFN1
364	GKAP1	424	IGSF9	484	LGI2	544	MEST	604	NFXL1	664	PFN2
365	GLS	425	IL17RB	485	LHX8	545	METTL7A	605	NHLH2	665	PGBD5
366	GLUL	426	IL28RA	486	LIFR	546	MEX3A	606	NHLRC1	666	PGP
367	GNAZ	427	IMPA1	487	LIG3	547	MEX3B	607	NKAIN1	667	PHF16
368	GNG4	428	IMPA2	488	LIMCH1	548	MFSO6	608	NKAIN2	668	PHF17
369	GOLM1	429	INADL	489	LIPG	549	MGAT4A	609	NKAIN3	669	PHLPP1
370	GOT1	430	INHBE	490	LIPT1	550	MGAT4C	610	NLGN4X	670	PIAS2
371	GOT2	431	INPP4A	491	LIX1	551	MGP	611	NMB	671	PID1
372	GPD1L	432	INPP5J	492	LMAN1	552	MGST1	612	NMU	672	PIK3AP1
373	GPM6B	433	INSIG1	493	LMCD1	553	MGST2	613	NOM1	673	PIK3C2B
374	GPR98	434	IQGAP2	494	LMO3	554	MIF4GD	614	NPL	674	PIP5K1B
375	GPRC5B	435	IRAK3	495	LOC100128644	555	SNORA84	615	NPW	675	PIR
376	GPT2	436	IRF8	496	MAFIP	556	UCK2	616	NPY1R	676	PIRT
377	GPX7	437	IRS2	497	SPARC	557	MKLN1	617	NR3C2	677	PLA2G3
378	GRB14	438	ISL1	498	TTC21B	558	MKX	618	NR5A2	678	PLAGL1
379	GREM1	439	ISL2	499	NELL2	559	MLKL	619	NRCAM	679	PLD6
380	GRIA1	440	ISYNA1	500	LOC150568	560	MLLT3	620	NSD1	680	PLEKHA5
381	GRINA	441	ITFG2	501	WDR5	561	MLYCD	621	NSDHL	681	PLEKHA8
382	GRIP1	442	ITPR1	502	LONRF2	562	MMAB	622	NSUN5	682	PLEKHG1
383	GSC	443	JAKMIP2	503	LOX	563	MOSPD2	623	NTF3	683	PLEKHH2
384	GSTM1	444	JHDM1D	504	LOXL4	564	MPHOSPH9	624	NTPCR	684	PLS1
385	GSTM2P1	445	JMY	505	LPHN1	565	MPPED2	625	NUFIP2	685	PM20D2
386	HAGHL	446	JPH1	506	LPIN1	566	MPZL3	626	NUP210	686	PMS2
387	HBB	447	JTB	507	LPL	567	MRP63	627	NUPR1	687	PNMA3
388	HCK	448	KAL1	508	LPPR5	568	MRPS15	628	OC90	688	PNMA6A
389	HDDC2	449	KANK4	509	LRMP	569	MRS2	629	ODC1	689	PNPLA3
390	HES6	450	KAZALD1	510	LRP8	570	MSI1	630	OGDHL	690	POLR3E
391	HEY2	451	KAZN	511	LRPPRC	571	MSI2	631	ONECUT2	691	POP1
392	HEX	452	KCNG3	512	LRRC16A	572	MSMO1	632	ORC5	692	POU3F2
393	HIC1	453	KCNH2	513	LRRC4C	573	MST4	633	OSBPL10	693	POU3F3
394	HIST1H4A	454	KCNH3	514	LRRTM3	574	MSX1	634	P2RX5	694	POU5F1
395	HMGCR	455	KCNJ2	515	LSAMP	575	MTHFD2	635	PABPC4L	695	POU5F1P3
396	HMGCS1	456	KCNK1	516	LSM11	576	MTHFD2L	636	PAFAH1B1	696	PPAP2C
397	HMHA1	457	KCNK5	517	LUZP2	577	MTL5	637	PAG1	697	PPDPF
398	HMX2	458	KCNT2	518	LYPD6	578	MTUS1	638	PAIP2	698	PPIA
399	HOXA5	459	KDM5A	519	LYZ	579	MXRA5	639	PAK3	699	PPIC
400	HOXB13	460	KIAA0182	520	MAB21L1	580	MYADM	640	PAK6	700	PPM1B
401	HOXB9	461	KIAA0922	521	MAF	581	MYBBP1A	641	PALMD	701	PPM1E
402	HOXC11	462	KIAA1549	522	MAFB	582	MYBL2	642	PANK3	702	PPP1R14C
403	HOXC4	463	KIAA1598	523	MAFG	583	MYEF2	643	PARD6B	703	PPP1R15B
404	HOXD13	464	KIAA1958	524	MAGI2	584	MYLIP	644	PARP1	704	PPP1R26
405	HOXD3	465	KIAA1984	525	MAP2	585	N4BP2L1	645	PAWR	705	PRAME
406	HPDL	466	KIF1A	526	MAP2K5	586	N4BP2L2	646	PBX1	706	PRCC
407	HS6ST2	467	KIF21A	527	MAP3K4	587	NANOS1	647	PCBD1	707	PRDM13
408	HSBP1L1	468	KIF26A	528	MAP4K3	588	NAP1L2	648	PCBD2	708	PRDM6
409	HSD17B14	469	KIT	529	MAP7	589	NARG2	649	PCDH15	709	PREPL
410	HSD17B7	470	KLHL13	530	MAPKAP1	590	NCLN	650	PCDH17	710	PRICKLE1
411	HTATIP2	471	KLHL24	531	MAR1	591	NDFIP1	651	PCDH20	711	PRKAA2
412	IBSP	472	KRAS	532	MAR2	592	NDRG2	652	PCK2	712	PRL
413	ICA1	473	KRT18	533	MARF1	593	NDST3	653	PCLO	713	PROM1
414	IDI1	474	L3MBTL4	534	MARS2	594	NDUFA9	654	PCSK9	714	PRSS12
415	IDI1	475	LAMA1	535	MAZ	595	NDUFAF4	655	PDE3B	715	PRUNE
416	IER5L	476	LAMC1	536	MBNL2	596	NEDD4L	656	PDE6B	716	PSAT1
417	IFI30	477	LARP1B	537	MBTD1	597	NELF	657	PDGFR	717	PSEN2
418	IGF2	478	LCE2B	538	MCM9	598	NELL1	658	PDIA3	718	PSMA2
419	IGFBP2	479	LCP1	539	MDK	599	NFE2L3	659	PDIK1L	719	PSMC4
420	IGFBPL1	480	LDLRAP1	540	MECOM	600	NFIA	660	PDK4	720	PSPH

APPENDIX N (CONTINUE)

No	Gene	No	Gene	No	Gene	No	Gene	No	Gene	No	Gene
721	PTGER3	771	RPS6KA1	821	SLC25A13	871	STRA6	921	TRAF4	971	ZBTB39
722	PTGFRN	772	RRAGD	822	SLC25A15	872	STRBP	922	TRAF7	972	ZC3H8
723	PTPN3	773	RUNDC3B	823	SLC25A19	873	STX17	923	TRAM1L1	973	ZCCHC2
724	PTPRD	774	RUNX1T1	824	SLC25A20	874	SULF2	924	TRAP1	974	ZCCHC7
725	PTPRF	775	RUNX3	825	SLC25A44	875	SUV39H1	925	TRAPPC12	975	ZDBF2
726	PURB	776	SALL1	826	SLC25A45	876	SYBU	926	TRIB3	976	ZDHHC23
727	PUS1	777	SAMD11	827	SLC27A5	877	SYNGR2	927	TRIL	977	ZFAND3
728	PUS7	778	SAMD5	828	SLC29A3	878	TAF5	928	TRIO	978	ZHX2
729	PYCARD	779	SAT1	829	SLC2A8	879	TBC1D30	929	TRMT61B	979	ZIC3
730	PYCR1	780	SBNO1	830	SLC30A1	880	TBKBP1	930	TROVE2	980	ZNF140
731	QPRT	781	SC5DL	831	SLC31A2	881	TBX5	931	TSC22D3	981	ZNF213
732	RAB26	782	SCARB1	832	SLC35F2	882	TCOF1	932	TSHZ2	982	ZNF238
733	RAB38	783	SCARNA14	833	SLC35G1	883	TDRKH	933	TSPAN12	983	ZNF318
734	RAB6A	784	SCARNA20	834	SLC37A4	884	TEAD4	934	TSPAN13	984	ZNF331
735	RAD51C	785	SCD	835	SLC38A4	885	TEC	935	TSPAN9	985	ZNF385A
736	RAET1L	786	SCIN	836	SLC39A8	886	TET1	936	TSSC1	986	ZNF423
737	RALGDS	787	SCN1A	837	SLC5A7	887	TET3	937	TTC32	987	ZNF480
738	RAPGEF5	788	SCN1B	838	SLC7A11	888	TFAP2B	938	TUB	988	ZNF593
739	RASGRP1	789	SCN9A	839	SLC7A2	889	TFAP2E	939	TUBA4A	989	ZNF641
740	RAVER2	790	SDK2	840	SLC7A5	890	TFDP2	940	TUBB6	990	ZNF761
741	RBM38	791	SEC11C	841	SLC8A2	891	TGIF2	941	TUBE1	991	ZNF84
742	RBP1	792	SEL1L3	842	SLC04A1	892	THADA	942	TUFM	992	ZXDC
743	RBPMS2	793	SELENBP1	843	SLC05A1	893	THNSL2	943	TULP3		
744	RCOR2	794	SEMA4D	844	SLITRK5	894	THRA	944	TYSND1		
745	RDH10	795	SEMA6D	845	SLMO1	895	THRB	945	UBE2O		
746	RELN	796	SEP6	846	SMG7	896	THSD7A	946	UCHL5		
747	REERG	797	SESN1	847	SNHG7	897	THUMP2	947	UCP2		
748	RERGL	798	SETD5	848	SNHG8	898	TLL2	948	UFM1		
749	REV1	799	SETD6	849	SNORA12	899	TMEM144	949	UGGT1		
750	RGNEF	800	SFXN4	850	SNX10	900	TMEM151B	950	UGT8		
751	RGS19	801	SGCZ	851	SOBP	901	TMEM163	951	UHRF1BP1		
752	RGS5	802	SH3BGR2	852	SOCS1	902	TMEM170B	952	ULK2		
753	RHOB	803	SH3BP5L	853	SORBS1	903	TMEM178A	953	UNC119		
754	RHPN1	804	SH3GL3	854	SORD	904	TMEM18	954	USP27X		
755	RMND5A	805	SH3PXD2A	855	SOX2	905	TMEM216	955	USP44		
756	RNASE2	806	SHMT2	856	SOX4	906	TMEM220	956	VANGL2		
757	RNASEH1	807	SIGMAR1	857	SP3	907	TMEM48	957	VASH2		
758	RNASEL	808	SIM2	858	SP8	908	TMEM97	958	VAV3		
759	RNASET2	809	SKIL	859	SPARCL1	909	TMTC1	959	VCAM1		
760	RNF11	810	SLAIN1	860	SPP1	910	TMTC4	960	VLDLR		
761	RNF125	811	SLC10A4	861	SPR	911	TNFSF12	961	VWCE		
762	RNF135	812	SLC12A7	862	SREBF2	912	TOB1	962	WBSCR17		
763	RNF175	813	SLC12A8	863	SRSF10	913	TOM1L1	963	WNK1		
764	ROBO1	814	SLC16A10	864	SRSF12	914	TOR3A	964	WNK2		
765	ROBO2	815	SLC16A14	865	SSBP3	915	TOR4A	965	XK		
766	ROR2	816	SLC16A9	866	ST20	916	TP63	966	XPR1		
767	RORB	817	SLC18B1	867	ST6GAL1	917	TP73-AS1	967	YDJC		
768	RPP25	818	SLC19A2	868	STAC	918	TPD52	968	YPEL2		
769	RPRM	819	SLC1A2	869	STAG3L4	919	TPD52L1	969	ZAR1		
770	RPS15	820	SLC1A4	870	STOX1	920	TPM1	970	ZBED3		

APPENDIX O

List of down-regulated genes in iG-292

No	Gene	No	Gene	No	Gene	No	Gene	No	Gene	No	Gene	No	Gene
1	ABC84	61	ANKRD26	121	AR5J	181	BIRC2	241	C7orf10	301	CD74	361	CNRIP1
2	ABCC9	62	ANKRD28	122	ASAH1	182	BIRC5	242	C8orf44-SGK3	302	CD81	362	COL12A1
3	ABHD2	63	ANKRD29	123	ASAP1	183	BIVM	243	C8orf58	303	CD97	363	COL13A1
4	ABI1	64	ANLN	124	ASAP3	184	BMP2K	244	C9orf89	304	CD99	364	COL14A1
5	ABI3BP	65	ANO1	125	ASF1B	185	BMP4	245	CA12	305	CDC123	365	COL18A1
6	ABLIM3	66	ANPEP	126	ASH2L	186	BMPR2	246	CACNA2D3	306	CDC16	366	COL1A1
7	ACAN	67	ANTXR2	127	ASL	187	BNC1	247	CADP5	307	CDC42EP3	367	COL1A2
8	ACBD5	68	ANXA1	128	ASPH	188	BNIP3L	248	CALCOCO2	308	CDCA2	368	COL22A1
9	ACO1	69	ANXA11	129	ASTN1	189	BPGM	249	CALD1	309	CDH11	369	COL5A1
10	ACP2	70	ANXA2	130	ATAD2	190	BRCA1	250	CALHM2	310	CDH13	370	COL5A2
11	ACSS3	71	ANXA2R	131	ATG14	191	BRF2	251	CALM1	311	CDK17	371	COL6A1
12	ACTG2	72	ANXA4	132	ATG4C	192	BRK1	252	CALU	312	CDKN1A	372	COL6A2
13	ACTN1	73	ANXA5	133	ATL1	193	BRMS1L	253	CAMK2D	313	CDKN2B	373	COL6A3
14	ACTR10	74	AP3S2	134	ATL3	194	BTBD11	254	CAMK2N2	314	CDKN2C	374	COL7A1
15	ACTR8	75	AP5S1	135	ATP11B	195	BTBD6	255	CAMSAP2	315	CDKN2D	375	COL12A2
16	ACVR1	76	APBB2	136	ATP13A3	196	BTFL4	256	CAP1	316	CDKN3	376	COMMD4
17	ACVR1C	77	APCDD1	137	ATP1B3	197	BTG3	257	CAPG	317	CDO1	377	COMMD7
18	ADAM10	78	APCDD1L	138	ATP2B1	198	BTN3A2	258	CAPN2	318	CEBPD	378	COMT
19	ADAM12	79	APH1B	139	ATP2B4	199	BTN3A3	259	CARD10	319	CELSR1	379	COPG2
20	ADAM19	80	APOBEC3A	140	ATP5S	200	BZRAP1	260	CARD8	320	CENPN	380	COPZ2
21	ADAM9	81	APOBEC3B	141	ATPGAP2	201	C10orf10	261	CARHSP1	321	CEP128	381	CORO1C
22	ADAMTS12	82	APOBEC3C	142	ATP6V0D1	202	C10orf90	262	CASP1	322	CEP41	382	COTL1
23	ADAMTS1L	83	APOBEC3G	143	ATP6V1B2	203	C11orf41	263	CASP3	323	CEP57	383	CPE
24	ADM	84	APOLD1	144	ATP6V1C1	204	C11orf70	264	CASP4	324	CEP57L1	384	CPEB1
25	ADORA2B	85	APBP2	145	ATP6V1D	205	C11orf74	265	CASP7	325	CEPT1	385	CPED1
26	ADRA1D	86	ARF4	146	ATP6V1G2	206	C11orf87	266	CASP8	326	CFH	386	CPM
27	ADRB2	87	ARF6	147	ATP6V1H	207	C12orf23	267	CAST	327	CFL1	387	CPNE3
28	ADSS1L	88	ARFGAP3	148	ATP8B1	208	C12orf75	268	CAV1	328	CFL2	388	CPOX
29	AGAP1	89	ARG2	149	ATP9A	209	C13orf33	269	CAV2	329	CGRFR1	389	CPQ
30	AGFG1	90	ARHGAP1	150	ATRN	210	C14orf135	270	CBLB	330	CH25H	390	CPS1
31	AGPAT5	91	ARHGAP12	151	ATXN3	211	C14orf149	271	CBR1	331	CHCHD7	391	CPT1C
32	AHCYL1	92	ARHGAP21	152	ATXN7	212	C14orf166	272	CBR3	332	CHRAC1	392	CPZ
33	AHNAK	93	ARHGAP22	153	AXIN2	213	C14orf28	273	CC2D2A	333	CHST1	393	CRBN
34	AHNAK2	94	ARHGAP23	154	AXL	214	C14orf37	274	CCBE1	334	CHST15	394	CREB3L2
35	AHR	95	ARHGAP24	155	B2M	215	C15orf52	275	CCBL2	335	CHST3	395	CREM
36	AHRR	96	ARHGAP28	156	B3GNT1	216	C16orf45	276	CCDC102B	336	CHSY1	396	CRNKL1
37	AIDA	97	ARHGAP29	157	B4GALNT1	217	C16orf62	277	CCDC109B	337	CHURC1	397	CRTPA
38	AIDA	98	ARHGAP35	158	BALC	218	C17orf79	278	CCDC112	338	CIRBP	398	CRYAB
39	AIM1	99	ARHGEF10	159	BACE1	219	C19orf66	279	CCDC15	339	CLCF1	399	CRYZL1
40	AJAP1	100	ARHGEF18	160	BAD	220	C1D	280	CCDC18	340	CLDN11	400	CSDE1
41	AJUBA	101	ARHGEF40	161	BAG3	221	C1GALT1	281	CCDC23	341	CUC2	401	CSGALNACT1
42	AK1	102	ARHGEF9	162	BAG4	222	C1R	282	CCDC25	342	CLIP3	402	CSNK1A1
43	AK5	103	ARID4A	163	BATF3	223	C1S	283	CCDC50	343	CLMP	403	CSPG4
44	AKAP12	104	ARID5B	164	BAZ1A	224	C1orf173	284	CCDC53	344	CLN8	404	CSR2
45	AKAP2	105	ARL13B	165	BBS12	225	C1orf198	285	CCDC80	345	CLSTN1	405	CST3
46	AKR1B1	106	ARL2	166	BBS5	226	C1orf21	286	CCDC82	346	CLTC	406	CSTB
47	AKR1C1	107	ARL2-SNX15	167	BBS7	227	C1orf54	287	CCDC85B	347	CLU	407	CSTF3
48	AKR1C3	108	ARL4C	168	BCAP29	228	C1orf63	288	CCDC88A	348	CLVS1	408	CTBS
49	ALCAM	109	ARL4D	169	BCAP31	229	C1orf86	289	CCL20	349	CMAHP	409	CTDSPL
50	ALDH3B1	110	ARL6IP5	170	BCAR3	230	C20orf194	290	CCND1	350	CMPK1	410	CTGF
51	ALK	111	ARL8B	171	BCL10	231	C20orf3	291	CCNJL	351	CMPK2	411	CTHRC1
52	ALPK2	112	ARMC1	172	BCL2L13	232	C20orf72	292	CCNY	352	CMTM3	412	CTNBP1
53	AMIGO2	113	ARMC8	173	BCL6	233	C21orf91	293	CD109	353	CMTM6	413	CTNND1
54	AMOTL1	114	ARMCX1	174	BDH2	234	C2CD2	294	CD44	354	CMTM8	414	CTR9
55	AMPD3	115	ARMCX2	175	BDKRB1	235	C3orf18	295	CD46	355	CNIH	415	CTSB
56	ANGPT2	116	ARMCX5-GPRASP2	176	BDNF	236	C3orf52	296	CD47	356	CNIH3	416	CTSL1
57	ANGPTL2	117	ARMCX6	177	BECN1	237	C4orf22	297	CD58	357	CNIH4	417	CTTN
58	ANKH	118	ARNTL2	178	BEGAIN	238	C4orf46	298	CD59	358	CNN2	418	CTTNBP2NL
59	ANKMY2	119	ARPC3	179	BEX1	239	C5orf62	299	CD63	359	CNOT10	419	CUL2
60	ANKRD12	120	ARRDC3	180	BICC1	240	C6orf225	300	CD68	360	CNOT7	420	CUL4A

APPENDIX O (CONTINUE)

No	Gene	No	Gene	No	Gene	No	Gene	No	Gene	No	Gene		
421	CXADR	481	DR1	541	ETS1	601	FBXO34	661	GDI2	721	HAS2	781	HTRA1
422	CXCL12	482	DRAM1	542	ETS2	602	FBXO8	662	GEM	722	HAS3	782	IDS
423	CXXCS	483	DRAP1	543	ETV1	603	FCHSD2	663	GIN51	723	HBEGF	783	IFI16
424	CYB561D1	484	DSCR3	544	EXOC5	604	FEM1C	664	GIN54	724	HCFC2	784	IFI27
425	CYB5R3	485	DST	545	EXOG	605	FGF2	665	GJA1	725	HCP5	785	IFI35
426	CYBRD1	486	DSTN	546	EXT1	606	FGF5	666	GLB1	726	HDHD1	786	IFI44
427	CYLD	487	DSTNP2	547	EYA2	607	FGFR1	667	GLI3	727	HDLBP	787	IFI44L
428	CYP27C1	488	DTX3L	548	EZH2	608	FGGY	668	GLIPR1	728	HDX	788	IFI6
429	CYP2J2	489	DUSP10	549	F2RL1	609	FHIT	669	GLIPR2	729	HEATR5A	789	IFIH1
430	CYP2U1	490	DUSP11	550	F2RL2	610	FHL2	670	GLIS3	730	HEBP1	790	IFIT1
431	CYR61	491	DUSP27	551	F3	611	FHOD3	671	GLRX	731	HECW2	791	IFIT2
432	CYS1	492	DUSP3	552	F8	612	FIBIN	672	GLT8D1	732	HEG1	792	IFIT3
433	CYSTM1	493	DUSP4	553	FABP3	613	FIBP	673	GLT8D2	733	HENMT1	793	IFIT5
434	DAB2	494	DUSP5	554	FAM101B	614	FILIP1L	674	GLTP	734	HEPH	794	IFITM1
435	DAD1	495	DYNC11L1	555	FAM102B	615	FIP1L1	675	GMFB	735	HERC3	795	IFITM2
436	DAG1	496	DZIP3	556	FAM114A1	616	FJX1	676	GMPR	736	HERC6	796	IFITM3
437	DCBLD2	497	EAPP	557	FAM127A	617	FKBP1A	677	GMPR2	737	HEXA	797	IFNAR1
438	DCLRE1B	498	EBF3	558	FAM129A	618	FKBP3	678	GNA14	738	HEY1	798	IFNGR2
439	DCLRE1C	499	EBNA1BP2	559	FAM129B	619	FKBP7	679	GNAI3	739	HGF	799	IFT46
440	DCN	500	ECE1	560	FAM134A	620	FKBP9	680	GNAQ	740	HIF1A	800	IFT57
441	DDHD1	501	ECM1	561	FAM13C	621	FLNC	681	GNB4	741	HIPK2	801	IGF1R
442	DDHD2	502	EDARADD	562	FAM155A	622	FLRT2	682	GNG11	742	HK1	802	IGFBP3
443	DDX42	503	EEA1	563	FAM168A	623	FMN2	683	GNG2	743	HLA-A	803	IGFBP4
444	DDX5	504	EEF1A1	564	FAM171A1	624	FN1	684	GNG5	744	HLA-B	804	IGFBP5
445	DDX58	505	EFEMP2	565	FAM171B	625	FNBP1L	685	GNPNAT1	745	HLA-C	805	IGFBP6
446	DDX60	506	EFHD2	566	FAM176A	626	FNDC3B	686	GOLGA4	746	HLA-DMA	806	IGFBP7
447	DDX60L	507	EFNB3	567	FAM176C	627	FNIP1	687	GOLGB1	747	HLA-DMB	807	IKBIP
448	DECR1	508	EHBP1L1	568	FAM177A1	628	FOSL1	688	GOLT1B	748	HLA-DOA	808	IKBKB
449	DENND5A	509	EHD1	569	FAM178A	629	FOSL2	689	GPATCH2	749	HLA-DPA1	809	IKZF2
450	DEPDC1	510	EHD2	570	FAM179B	630	FOXF2	690	GPC4	750	HLA-DPB1	810	IL10RB
451	DEPDC7	511	EHD4	571	FAM180A	631	FOXL1	691	GPD2	751	HLA-DQA1	811	IL11
452	DFNA5	512	EID3	572	FAM188A	632	FOXP1	692	GPHN	752	HLA-DRA	812	IL11RA
453	DGAT2	513	EIF4EBP1	573	FAM189A1	633	FOXQ1	693	GNPMB	753	HLA-DRB1	813	IL1R1
454	DHRS1	514	EIF5A2	574	FAM195B	634	FRMD4A	694	GPR112	754	HLA-DRB5	814	IL4R
455	DHRS3	515	ELAVL2	575	FAM208A	635	FRMD5	695	GPR124	755	HLA-E	815	IL7
456	DHRS7	516	ELK3	576	FAM20C	636	FRMD6	696	GPR137C	756	HLA-F	816	IL8
457	DHTKD1	517	ELOVL1	577	FAM3C	637	FSTL1	697	GPR37	757	HLTF	817	IMPAD1
458	DIAPH3	518	ELP3	578	FAM43A	638	FUT8	698	GPR39	758	HMCN1	818	INA
459	DIRAS3	519	EMILIN1	579	FAM46A	639	FXYD5	699	GPR56	759	HMG2A	819	ING2
460	DIXDC1	520	EMILIN2	580	FAM46C	640	FYCO1	700	GPR68	760	HMGCL	820	INPP4B
461	DKK1	521	EMP1	581	FAM73A	641	FZD1	701	GPRASP1	761	HMMR	821	INPP5A
462	DKK2	522	EMP2	582	FAM76A	642	FZD6	702	GPSM2	762	HMOX1	822	INSIG2
463	DKK3	523	EMP3	583	FAM82B	643	FZD7	703	GPX8	763	HNRNPU	823	INTS10
464	DLC1	524	ENG	584	FAM84A	644	GAA	704	GRAMD1C	764	HOMER2	824	IP6K2
465	DLGAP5	525	ENPP1	585	FAM89B	645	GADD45B	705	GRAMD3	765	HOMER3	825	IQGAP1
466	DNAAF2	526	ENPP2	586	FAM91A1	646	GADL1	706	GREM1	766	HOOK3	826	IRAK1
467	DNAJB1	527	EOGT	587	FAM92A1	647	GALC	707	GRIK2	767	HPCAL1	827	IRAK2
468	DNAJC4	528	EOMES	588	FANCM	648	GALNT1	708	GRIN2A	768	HPGD	828	IRF1
469	DNAJC6	529	EPAS1	589	FAP	649	GALNT10	709	GRN	769	HPS5	829	IRF7
470	DNASE1L1	530	EPM2AIP1	590	FAR1	650	GALNT4	710	GSN	770	HRH1	830	IRF9
471	DNMBP	531	EPS15	591	FAT1	651	GALNT5	711	GSPT1	771	HS2ST1	831	IRS1
472	DNTTIP2	532	EPS8	592	FBLN2	652	GALNTL1	712	GTF2H1	772	HS3ST1	832	IRX5
473	DOCK10	533	ERAP2	593	FBLN5	653	GAS1	713	GUCY1B3	773	HS6ST1	833	ISG15
474	DOCK4	534	ERG	594	FBN1	654	GAS6	714	GXYLT2	774	HSPA12A	834	ISG20
475	DOCK5	535	ERI1	595	FBXL2	655	GBP1	715	GYG2	775	HSPA13	835	ISM1
476	DONSON	536	ERLIN2	596	FBXL3	656	GBP2	716	GYPC	776	HSPA14	836	ISY1-RAB43
477	DOPEY2	537	ERMAP	597	FBXO17	657	GBP3	717	H2AFV	777	HSPB11	837	ITGA10
478	DPH3	538	ERO1L	598	FBXO27	658	GCLM	718	H3F3A	778	HSPB7	838	ITGA3
479	DPP4	539	ERRF1	599	FBXO32	659	GCNT1	719	H6PD	779	HTR2A	839	ITGA7
480	DPYSL2	540	ESYT2	600	FBXO33	660	GDAP2	720	HABP4	780	HTR7	840	ITGB1

APPENDIX O (CONTINUE)

No	Gene	No	Gene	No	Gene	No	Gene	No	Gene	No	Gene		
841	ITGB5	901	LAMTOR1	961	LRRN3	1021	MIER1	1081	NAV1	1141	NUDT22	1201	PDCD10
842	ITGBL1	902	LAMTOR3	962	LRRN4CL	1022	MIOS	1082	NAV2	1142	NUDT5	1202	PDCD1LG2
843	ITSN1	903	LAP3	963	LSM1	1023	MIR21	1083	NAV3	1143	NUDT6	1203	PDE4B
844	JAK1	904	LARGE	964	LSM14A	1024	MIR22	1084	NBN	1144	NUMB	1204	PDE7A
845	JAM2	905	LARP6	965	LSM5	1025	MIS18BP1	1085	NCAPG	1145	NUP62	1205	PDE7B
846	JKAMP	906	LASP1	966	LTBP1	1026	MKI67	1086	NCEH1	1146	NUP98	1206	PDGFA
847	JRKL	907	LATS2	967	LTBP2	1027	MKLN1	1087	NDC80	1147	NXPE3	1207	PDGFRA
848	JUN	908	LAYN	968	LUM	1028	MLH1	1088	NDP	1148	OAS1	1208	PDGFRB
849	KAT6A	909	LBH	969	LY6K	1029	MLL5	1089	NDRG1	1149	OAS2	1209	PKD1
850	KATNAL1	910	LCORL	970	LY96	1030	MMD	1090	NDUFV3	1150	OAS3	1210	PDLIM2
851	KBTBD11	911	LCTL	971	LYPD1	1031	MME	1091	NEDD1	1151	OASL	1211	PDLIM3
852	KBTBD2	912	LDB2	972	LZTFL1	1032	MMP1	1092	NEDD4	1152	OBSL1	1212	PDLIM4
853	KCNA1	913	LDHA	973	LZTS1	1033	MMP13	1093	NEDD8	1153	OCA2	1213	PDLIM5
854	KCNK2	914	LDOC1	974	MACF1	1034	MMP14	1094	NEGR1	1154	ODF2L	1214	PDP1
855	KCNK3	915	LEPR	975	MAD1L1	1035	MMP2	1095	NEIL2	1155	OLFML2A	1215	PDZRN3
856	KCNMA1	916	LEPREL1	976	MAFF	1036	MNAT1	1096	NEK6	1156	OLFML2B	1216	PFN1
857	KCNMB2	917	LEPROTL1	977	MAMDC2	1037	MNS1	1097	NEMF	1157	OLFML3	1217	PFKFB3
858	KCNN4	918	LGALS1	978	MAML2	1038	MOB3A	1098	NETO2	1158	OPTN	1218	PGBD1
859	KCTD7	919	LGALS3	979	MAMLD1	1039	MOK	1099	NEXN	1159	OS9	1219	PGM2L1
860	KCTD9	920	LHFP	980	MAN1A1	1040	MORC4	1100	NFASC	1160	OSBPL8	1220	PGM3
861	KDELRL2	921	LHFPL2	981	MANEAL	1041	MPP5	1101	NFATC4	1161	OSGIN2	1221	PGM5
862	KDELRL3	922	LIMA1	982	MAP3K5	1042	MRAP2	1102	NFIL3	1162	OSMR	1222	PHACTR2
863	KHNYN	923	LINC00341	983	MAP3K6	1043	MRPL52	1103	NFKBIZ	1163	OSR2	1223	PHC1
864	KIAA0040	924	LITAF	984	MAP4	1044	MRPS6	1104	NID1	1164	OSTF1	1224	PHF11
865	KIAA0101	925	LMNA	985	MAP4K4	1045	MRV11	1105	NID2	1165	OTUD1	1225	PHF15
866	KIAA0196	926	LMNB2	986	MAP4K5	1046	MSN	1106	NIN	1166	OTUD6B	1226	PHF19
867	KIAA0368	927	LMO2	987	MAP7D1	1047	MSRA	1107	NIPAL2	1167	OXCT1	1227	PHF20L1
868	KIAA0391	928	LNX1	988	MAPK1	1048	MSRB3	1108	NKD2	1168	P2RX5	1228	PHLDA1
869	KIAA0586	929	NEDD8	989	MAPK1IP1L	1049	MT1E	1109	NLRCS	1169	P2RY6	1229	PHLDB2
870	KIAA1143	930	LOC100134259	990	MAPKAPK2	1050	MT1JP	1110	NLRP11	1170	P4HA2	1230	PHTF1
871	KIAA1217	931	PTN	991	MAPKAPK3	1051	MT1M	1111	NMI	1171	PAFAH1B3	1231	PHYH
872	KIAA1671	932	LOC100287896	992	MAR7	1052	MT2A	1112	NMT2	1172	PALLD	1232	PIEZO2
873	KIF1B	933	SPARC	993	MAST4	1053	MTAP	1113	NNMT	1173	PAM	1233	PIGF
874	KIF20B	934	RUNX1	994	MASTL	1054	MTMR6	1114	NOL9	1174	PAMR1	1234	PIGK
875	KIF2C	935	MATN2	995	MAVS	1055	MTMR9	1115	NOTCH2	1175	PANK2	1235	PIH1D1
876	KIF5A	936	LOC100506748	996	MAX	1056	MTPAP	1116	NOV	1176	PANX1	1236	PIK3C3
877	KIF5B	937	PGK1	997	MBIP	1057	MTSS1	1117	NOX4	1177	PAOX	1237	PIK3CD
878	KIF5C	938	TGFBI	998	MCC	1058	MUM1L1	1118	NPAS2	1178	PAPOLA	1238	PIP4K2A
879	KIFC3	939	NTM	999	MCFD2	1059	MVP	1119	NPC1	1179	PAPPA	1239	PKIA
880	KIN	940	NRBP2	1000	MCM10	1060	MX1	1120	NPR3	1180	PAQR8	1240	PKIB
881	KLC1	941	PI4K2B	1001	MCM4	1061	MX2	1121	NPTN	1181	PARD3	1241	PKIG
882	KLF2	942	LOC642852	1002	MCPH1	1062	MXRA7	1122	NPTX1	1182	PARD6G	1242	PKN2
883	KLF3	943	SVIL	1003	MDFIC	1063	MXRA8	1123	NPTX2	1183	PARP14	1243	PKNOX1
884	KLF4	944	LOXL2	1004	MED19	1064	MYC	1124	NR2F2	1184	PARP2	1244	PLA2G4A
885	KLF6	945	LPAR1	1005	MED6	1065	MYH9	1125	NR4A3	1185	PARP3	1245	PLAT
886	KLHDC1	946	LPCAT2	1006	MED8	1066	MYL12A	1126	NRAS	1186	PARP9	1246	PLAU
887	KLHL28	947	LPHN2	1007	MEF2A	1067	MYLK	1127	NRIP1	1187	PARPBP	1247	PLAUR
888	KLRC1	948	LPP	1008	MEF2C	1068	MYO10	1128	NRIP3	1188	PBK	1248	PLEC
889	KLRC2	949	LPXN	1009	MELK	1069	MYO1B	1129	NRN1	1189	PBLD	1249	PLEKHA2
890	KLRC4	950	LRFN5	1010	MERTK	1070	MYO5B	1130	NRP1	1190	PBRM1	1250	PLEKHA3
891	KLRC4-KLRK1	951	LRIF1	1011	MET	1071	MYOF	1131	NSFL1C	1191	PCDH18	1251	PLEKHA4
892	KPNA1	952	LRIG1	1012	METRNL	1072	MYO22	1132	NSMAF	1192	PCDH7	1252	PLIN3
893	KRCC1	953	LRP10	1013	METTL10	1073	NAA20	1133	NSMCE2	1193	PCDHB14	1253	PLP2
894	KRTAP1-5	954	LRP12	1014	MEX3D	1074	NABP1	1134	NT5E	1194	PCDHB3	1254	PLS3
895	KTN1	955	LRRC15	1015	MFAP5	1075	NAGA	1135	NTAN1	1195	PCGF2	1255	PLSCR1
896	LACC1	956	LRRC27	1016	MFHAS1	1076	NAP1L1	1136	NTN4	1196	PCGF5	1256	PLSCR4
897	LAMA2	957	LRRC32	1017	MFSD1	1077	NAPB	1137	NTNG1	1197	PCM1	1257	PLXDC1
898	LAMA3	958	LRRC42	1018	MGAT2	1078	NAPG	1138	NTRK2	1198	PCMTD1	1258	PMAIP1
899	LAMP1	959	LRRFIP2	1019	MGLL	1079	NASP	1139	NTSR1	1199	PCNX	1259	PMEPA1
900	LAMP2	960	LRRIQ1	1020	MIB1	1080	NAT1	1140	NUDT16	1200	PCSK5	1260	PML

APPENDIX O (CONTINUE)

No	Gene	No	Gene	No	Gene	No	Gene	No	Gene	No	Gene	No	Gene
1261	PMM1	1321	PTGR1	1381	REEP2	1441	SACS	1501	SH3KBP1	1561	SNX7	1621	STXBP5
1262	PNISR	1322	PTGS2	1382	REXO2	1442	SAE1	1502	SH3RF3	1562	SNX9	1622	STYX
1263	PNPO	1323	PTHLH	1383	RFTN1	1443	SAMD4A	1503	SHB	1563	SOC3	1623	STYXL1
1264	PODXL	1324	PTP4A2	1384	RFX2	1444	SAMD9	1504	SHC4	1564	SOC5	1624	SULF1
1265	POLD3	1325	PTPN13	1385	RFX8	1445	SAMD9L	1505	SHISA5	1565	SOC56	1625	SUMF1
1266	POLD4	1326	PTPN21	1386	RGMB	1446	SAMHD1	1506	SHOC2	1566	SORBS2	1626	SUMO3
1267	POLE2	1327	PTPRA	1387	RGS17	1447	SAP30	1507	SHROOM2	1567	SORBS3	1627	SUSD5
1268	POLR3A	1328	PTPRG	1388	RGS20	1448	SATB2	1508	SHROOM3	1568	SORT1	1628	SUV420H1
1269	POLR3GL	1329	PTRF	1389	RGS3	1449	SAV1	1509	SIK2	1569	SOS2	1629	SVIL
1270	POSTN	1330	PTTG1IP	1390	RHOA	1450	SBF2	1510	SIPA1	1570	SOX6	1630	SWAP70
1271	PPAP2B	1331	PTX3	1391	RHOC	1451	SCARA3	1511	SIPA1L1	1571	SP100	1631	SYDE1
1272	PPAPDC1A	1332	PVRL2	1392	RICTOR	1452	SCCPDH	1512	SIRPA	1572	SP140L	1632	SYNC
1273	PPAPDC1B	1333	PXDN	1393	RIMKLB	1453	SCD5	1513	SLC12A6	1573	SPAG9	1633	SYNJ2
1274	PPARG	1334	PXK	1394	RIMS2	1454	SCFD2	1514	SLC14A1	1574	SPATA2	1634	SYPL2
1275	PPF1A1	1335	PXN	1395	RIN1	1455	SCUBE3	1515	SLC16A3	1575	SPATA6	1635	SYT11
1276	PPF1BP1	1336	PYGB	1396	RIN2	1456	SDC1	1516	SLC17A5	1576	SPATA7	1636	SYTL2
1277	PIIP5K2	1337	QARS	1397	RIPK2	1457	SDC4	1517	SLC1A1	1577	SPATS2L	1637	SYTL5
1278	PPM1A	1338	QKI	1398	RIPK4	1458	SDCBP	1518	SLC1A3	1578	SPCS2	1638	TACC1
1279	PPP1R12A	1339	RAB11FIP5	1399	RND3	1459	SEC22C	1519	SLC20A2	1579	SPEG	1639	TACC2
1280	PPP1R18	1340	RAB13	1400	RNF11	1460	SEC23A	1520	SLC22A4	1580	SPOCD1	1640	TADA3
1281	PPP1R3B	1341	RAB18	1401	RNF114	1461	SEC24D	1521	SLC25A21	1581	SPRED1	1641	TAF9B
1282	PPP1R3C	1342	RAB20	1402	RNF121	1462	SEC62	1522	SLC25A24	1582	SPRY2	1642	TAGLN
1283	PPP2CB	1343	RAB22A	1403	RNF139	1463	SECISBP2L	1523	SLC2A1	1583	SPTBN1	1643	TAGLN2
1284	PPP2R2B	1344	RAB23	1404	RNF141	1464	SELK	1524	SLC2A10	1584	SPTLC3	1644	TAOK3
1285	PPP2R3A	1345	RAB27A	1405	RNF144A	1465	SELM	1525	SLC2A14	1585	SPTSSA	1645	TAP1
1286	PPP2R3C	1346	RAB2A	1406	RNF170	1466	SEMA3A	1526	SLC30A7	1586	SPTSSB	1646	TARSL2
1287	PPP2R5C	1347	RAB31	1407	RNF182	1467	SEMA3E	1527	SLC35E4	1587	SQRDL	1647	TBC1D19
1288	PPP3CA	1348	RAB3IP	1408	RNF213	1468	SEMA4B	1528	SLC35F5	1588	SREK1IP1	1648	TBC1D2
1289	PPP3CC	1349	RAB6A	1409	RNF24	1469	SEMA5A	1529	SLC35G2	1589	SRP54	1649	TBC1D23
1290	PPP6R3	1350	RAB6B	1410	RNF26	1470	SENP7	1530	SLC38A2	1590	SRPX	1650	TBC1D4
1291	PQLC3	1351	RAB8B	1411	RNGTT	1471	SEP10	1531	SLC38A6	1591	SRPX2	1651	TBC1D9
1292	PRDM16	1352	RABL3	1412	RNH1	1472	SEP8	1532	SLC43A3	1592	SRR	1652	TBRG1
1293	PRDM8	1353	RALB	1413	ROCK1	1473	SERINC1	1533	SLC44A5	1593	SSFA2	1653	TBX18
1294	PRELID2	1354	RAP1A	1414	ROCK2	1474	SERPINB3	1534	SLC4A4	1594	SSH1	1654	TBX2
1295	PREX1	1355	RAP2B	1415	ROR1	1475	SERPINB4	1535	SLC4A7	1595	SSPN	1655	TBX3
1296	PRICKLE2	1356	RAPH1	1416	RORA	1476	SERPINB7	1536	SLC7A8	1596	SSX2IP	1656	TBXA2R
1297	PRKAA1	1357	RARB	1417	RPF1	1477	SERPINB8	1537	SLC8A1	1597	ST3GAL1	1657	TCEAL3
1298	PRKACB	1358	RARRES3	1418	RPL31	1478	SERPINE1	1538	SLFN12	1598	ST3GAL3	1658	TCEAL6
1299	PRKCA	1359	RASA1	1419	RPL32	1479	SERPINE2	1539	SLIT2	1599	ST3GAL5	1659	TCEAL8
1300	PRKCDPB	1360	RASA3	1420	RPL36AL	1480	SERPINF1	1540	SLITRK4	1600	ST6GAL2	1660	TCF4
1301	PRMT2	1361	RASA4	1421	RPL37	1481	SERPINI1	1541	SLK	1601	ST6GALNAC3	1661	TCF7
1302	PRNP	1362	RASD1	1422	RPP30	1482	SERTAD2	1542	SMAD7	1602	ST6GALNAC5	1662	TCTN1
1303	PROS1	1363	RASSF1	1423	RPS20	1483	SERTAD4	1543	SMAGP	1603	ST8SIA1	1663	TEAD1
1304	PROSC	1364	RASSF2	1424	RPS6KA2	1484	SETBP1	1544	SMAP2	1604	ST8SIA2	1664	TEK
1305	PRPF18	1365	RASSF8	1425	RRAGB	1485	SETD3	1545	SMARCAL1	1605	ST8SIA5	1665	TFAP2A
1306	PRPF39	1366	RBBP9	1426	RRAGC	1486	SFRP1	1546	SMOX	1606	STAG1	1666	TFAP2C
1307	PRR16	1367	RBFOX2	1427	RRAS	1487	SFT2D3	1547	SMURF2	1607	STAM	1667	TFDP1
1308	PRRX1	1368	RBM17	1428	RRS1	1488	SFXN3	1548	SNAI2	1608	STAT1	1668	TFG
1309	PRSS23	1369	RBM20	1429	RSAD2	1489	SGCB	1549	SNAP25	1609	STAT6	1669	TFPI
1310	PRTFDC1	1370	RBM27	1430	RSPO2	1490	SGCD	1550	SNAP29	1610	STAU2	1670	TG
1311	PSD3	1371	RBM7	1431	RSU1	1491	SGK223	1551	SNAPC1	1611	STC1	1671	TGFB111
1312	PSMB8	1372	RBMS2	1432	RTCA	1492	SGOL2	1552	SNED1	1612	STEAP1	1672	TGFB2
1313	PSMB9	1373	RBPJ	1433	RTKN2	1493	SGTB	1553	SNRPA1	1613	STIM2	1673	THAP1
1314	PSMC6	1374	RBPMS	1434	RTN4	1494	SH2B3	1554	SNTB1	1614	STK17A	1674	THBS1
1315	PSME1	1375	RCAN1	1435	S100A10	1495	SH3BGRL	1555	SNX12	1615	STK17B	1675	THBS2
1316	PSMG1	1376	RCAN2	1436	S100A11	1496	SH3BGRL3	1556	SNX15	1616	STK3	1676	THY1
1317	PSTPIP2	1377	RDH11	1437	S100A13	1497	SH3BP2	1557	SNX16	1617	STX12	1677	TICAM2
1318	PTGER2	1378	REC8	1438	S100A16	1498	SH3BP4	1558	SNX29	1618	STX1A	1678	TIMP1
1319	PTGER4	1379	RECK	1439	S100A6	1499	SH3GL2	1559	SNX5	1619	STX7	1679	TIMP2
1320	PTGIS	1380	RECQL	1440	SACM1L	1500	SH3GLB1	1560	SNX6	1620	STXBP3	1680	TIMP3

APPENDIX O (CONTINUE)

No	Gene	No	Gene	No	Gene	No	Gene	No	Gene
1681	TINF2	1721	TNFAIP8L1	1761	TUBB3	1801	VEGFA	1841	YME1L1
1682	TIPARP	1722	TNFRSF12A	1762	TUBB6	1802	VEGFC	1842	YPEL5
1683	TJP2	1723	TNFRSF19	1763	TUBGCP3	1803	VEPH1	1843	YWHAH
1684	TLR4	1724	TNFRSF1A	1764	TUSC2	1804	VGLL3	1844	ZAK
1685	TM2D2	1725	TNFRSF21	1765	TUSC3	1805	VIM	1845	ZBTB1
1686	TM2D3	1726	TNKS	1766	TWF2	1806	VIMP	1846	ZBTB38
1687	TM4SF1	1727	TNS3	1767	TWIST1	1807	VOPP1	1847	ZC2HC1A
1688	TMBIM1	1728	TOMM70A	1768	TWIST2	1808	VPS13D	1848	ZC3HAV1
1689	TMCO3	1729	TOX	1769	TWSG1	1809	VPS37A	1849	ZEB1
1690	TMED5	1730	TOX4	1770	TXNDC12	1810	VSNL1	1850	ZFP37
1691	TMEFF2	1731	TPBG	1771	TYMS	1811	VSTM4	1851	ZFPM2
1692	TMEM101	1732	TPM1	1772	UACA	1812	VTI1B	1852	ZMIZ1
1693	TMEM108	1733	TPM3	1773	UBA52	1813	VWA5A	1853	ZMYM6
1694	TMEM109	1734	TPM4	1774	UBASH3B	1814	WBP1L	1854	ZNF175
1695	TMEM119	1735	TPRG1L	1775	UBE2A	1815	WBP5	1855	ZNF187
1696	TMEM158	1736	TRAF3IP2	1776	UBE2D2	1816	WDFY1	1856	ZNF20
1697	TMEM165	1737	TRAK1	1777	UBE2E2	1817	WDHD1	1857	ZNF226
1698	TMEM167B	1738	TRAM2	1778	UBE2L6	1818	WDR1	1858	ZNF287
1699	TMEM182	1739	TRAPP10	1779	UBE2Q2	1819	WDR26	1859	ZNF365
1700	TMEM19	1740	TRAPP6B	1780	UBLCP1	1820	WDR44	1860	ZNF385B
1701	TMEM200A	1741	TRDMT1	1781	UBR7	1821	WDR47	1861	ZNF395
1702	TMEM244	1742	TRIM22	1782	UFSP2	1822	WDR48	1862	ZNF404
1703	TMEM246	1743	TRIM34	1783	UHRF2	1823	WDR54	1863	ZNF436
1704	TMEM35	1744	TRIM5	1784	UPF2	1824	WDR76	1864	ZNF469
1705	TMEM44	1745	TRIOBP	1785	UPRT	1825	WHAMM	1865	ZNF503
1706	TMEM45A	1746	TRPC1	1786	UROD	1826	WHSC1L1	1866	ZNF506
1707	TMEM47	1747	TRPT1	1787	USP25	1827	WIF1	1867	ZNF559
1708	TMEM5	1748	TSC22D1	1788	USP33	1828	WIPF1	1868	ZNF654
1709	TMEM50A	1749	TSHZ3	1789	USP53	1829	WISP1	1869	ZNF703
1710	TMEM50B	1750	TSN	1790	USP6NL	1830	WLS	1870	ZNF77
1711	TMEM55A	1751	TSPAN19	1791	VAMP3	1831	WNT5A	1871	ZNF790
1712	TMEM64	1752	TSPAN31	1792	VAMP4	1832	WNT7B	1872	ZNF792
1713	TMEM65	1753	TSPAN4	1793	VAMP5	1833	WRN	1873	ZNFX1
1714	TMF1	1754	TSPAN5	1794	VANGL1	1834	WWTR1	1874	ZNHIT6
1715	TMOD2	1755	TSTA3	1795	VASN	1835	XAF1	1875	ZYG11B
1716	TMSB15A	1756	TTC23	1796	VAT1	1836	XKR5		
1717	TMX1	1757	TTC28	1797	VAV2	1837	XRN1		
1718	TNC	1758	TTC3	1798	VCL	1838	XRN2		
1719	TNFAIP3	1759	TTPAL	1799	VCPIP1	1839	XYLT1		
1720	TNFAIP8	1760	TUBA1A	1800	VDR	1840	YAP1		

APPENDIX P

List of up-regulated genes in iSaos-2

No	Gene	No	Gene	No	Gene	No	Gene	No	Gene
1	ABCC4	51	CCDC88C	101	EMB	151	GUK1	201	LYAR
2	ACOT4	52	CCNA1	102	ENC1	152	HBQ1	202	MAB21L1
3	ACSS1	53	CD97	103	EPHA7	153	HCK	203	MAGEA10
4	ACTG1P4	54	CDK2AP1	104	EPHX2	154	HDAC9	204	MAGEA11
5	ACTG2	55	CDKN1C	105	ERVMER34-1	155	HENMT1	205	MAGEA4
6	ADAMTS3	56	CELF1	106	ETFA	156	HLA-DPA1	206	MAGEA9
7	ADD2	57	CELF2	107	ETFB	157	HLA-DPB1	207	MAGEB1
8	ADPRHL1	58	CEP41	108	ETV1	158	HOOK1	208	MAGEB2
9	ADRB1	59	CH25H	109	F12	159	HORMAD1	209	MAML3
10	AEBP1	60	CHCHD10	110	FABP6	160	HOXB4	210	MAP3K5
11	AGMAT	61	CHCHD4	111	FAM122B	161	HOXC8	211	MAP3K9
12	ALDH1L1	62	CHSY3	112	FAM149A	162	HOXD13	212	MAP7
13	ALDH2	63	CKMT1A	113	FAM162A	163	HPDL	213	MAR1
14	AMDHD1	64	CLEC2B	114	FAM174B	164	HPGD	214	MCCC2
15	AMY1A	65	CMBL	115	FAM198B	165	HTATIP2	215	MCOLN2
16	ANGPTL4	66	COL6A3	116	FAM213A	166	ICAM2	216	MECOM
17	ANK2	67	COL7A1	117	FAM9C	167	IL13RA2	217	MEOX2
18	ANKLE1	68	COMTD1	118	FAR2	168	IL18	218	METTL7A
19	ANP32E	69	COX6A1	119	FBL	169	IL28RA	219	METTL8
20	APOE	70	CPT1A	120	FBLN1	170	IL32	220	MFAP2
21	ARMCX2	71	CPT1C	121	FBXO28	171	IMPDH2	221	MFHAS1
22	ARTN	72	CRABP1	122	FERMT1	172	IRAK3	222	MGST1
23	ASS1	73	CRABP2	123	FES	173	ISYNA1	223	MLKL
24	ATF5	74	CRYAB	124	FEZ1	174	ITPR1	224	MPP6
25	ATP8A1	75	CSDA	125	FGF13	175	JAK3	225	MRPL55
26	BAI3	76	CSGALNACT1	126	FGFR4	176	KBTBD6	226	MRPS25
27	BCHE	77	CTAG2	127	FJX1	177	KCND2	227	MSI2
28	BEND4	78	CTCFL	128	FTL	178	KCNG3	228	MT1F
29	BEX1	79	CXCL14	129	FTO	179	KCNH2	229	MTL5
30	BEX2	80	CXorf48	130	GAGE1	180	KCNJ8	230	MUC15
31	BEX4	81	CYB5R2	131	GAGE10	181	KCNK10	231	MXRA5
32	BMP2	82	CYP1B1	132	GAGE12B	182	KCNK5	232	NAA15
33	BMP5	83	CYP24A1	133	GAL	183	KCNMB4	233	NDP
34	BMPR1B	84	CYR1	134	GALK2	184	KCNT2	234	NDRG4
35	C11orf1	85	DACH1	135	GATM	185	KIAA0040	235	NDUFS3
36	C16orf54	86	DCAF12L2	136	GCK	186	KIAA0564	236	NEFH
37	C16orf73	87	DCTD	137	GDF6	187	KIAA1598	237	NES
38	C1orf106	88	DGKH	138	GEM	188	KIT	238	NEURL
39	C5orf58	89	DIMT1	139	GJA3	189	KLHL14	239	NFATC4
40	C6orf108	90	DLG3	140	GPM6A	190	KLRC1	240	NFE2L3
41	C8orf46	91	DNAH14	141	GPR158	191	KLRC2	241	NHLRC1
42	C9orf135	92	DNAJC12	142	GPR37	192	LCP1	242	NMNAT3
43	CACHD1	93	DSC2	143	GPX7	193	SNAP2	243	NMRAL1
44	CACNA2D3	94	DSG2	144	GRB10	194	LOC100287497	244	NOLC1
45	CADPS2	95	DUSP2	145	GRB14	195	PLIN2	245	NOP16
46	CADPS2	96	DUSP23	146	GRHL3	196	LOC151760	246	NPAS3
47	CAPG	97	ECE2	147	GRIA3	197	LOX	247	NPFFR2
48	CASP8	98	EDNRB	148	GRIN2D	198	LPL	248	NPSR1-AS1
49	CBR4	99	EFCAB4B	149	GRPEL2	199	LRRC6	249	NR2F1
50	CCDC169	100	EFEMP1	150	GSTM1	200	LRRC7	250	NR3C2

APPENDIX P (CONTINUE)

No	Gene	No	Gene	No	Gene	No	Gene	No	Gene
251	NXT2	283	PRDM13	315	RTP3	347	SNORA76	379	TMEM246
252	OGDHL	284	PRDX2	316	RUVBL1	348	SOX2	380	TMEM48
253	OPLAH	285	PRKCZ	317	S100A16	349	SP5	381	TMEM52
254	OXNAD1	286	PRKD1	318	SAMD13	350	SPANXC	382	TMPRSS15
255	PAFAH1B1	287	PROCR	319	SAT1	351	SPANXD	383	TOX3
256	PAFAH1B3	288	PRPS1	320	SCG2	352	SPATA22	384	TP53RK
257	PAGE1	289	PSAT1	321	SCN1B	353	SSX2	385	TPD52
258	PAQR8	290	PTEN	322	SDE2	354	SSX2IP	386	TPD52L1
259	PASD1	291	PTPMT1	323	SEC13	355	SSX3	387	TPM2
260	PCBD1	292	PUS7	324	SELENBP1	356	SSX4	388	TRHDE
261	PCDH19	293	QKI	325	SEMA3E	357	ST7	389	TRIM14
262	PCDH8	294	RAB3IP	326	SERP2	358	STAG3	390	TRIM9
263	PCDHA1	295	RAB6A	327	SEZ6L2	359	STC1	391	TUBB2B
264	PDE3B	296	RASGEF1A	328	SFRP2	360	STEAP1	392	TUBB6
265	PEX26	297	RASIP1	329	SH2D2A	361	STEAP1	393	UAP1
266	PFDN2	298	RBMXL1	330	SKIL	362	STEAP2	394	UGT8
267	PHF15	299	RBP1	331	SLAIN1	363	SUPT3H	395	VCAM1
268	PHLDA2	300	RDM1	332	SLC10A4	364	SWAP70	396	WDR66
269	PLA2G16	301	REG1A	333	SLC16A9	365	SYK	397	WDR88
270	PLAT	302	RGMA	334	SLC17A9	366	SYNGR3	398	WNT10A
271	PLCB1	303	RGNEF	335	SLC18B1	367	T1560	399	WNT5A
272	PLCH1	304	RGS14	336	SLC25A19	368	TAF7L	400	XAGE1A
273	PLCXD2	305	RGS16	337	SLC25A20	369	TBX4	401	ZDHHC20
274	PNMA5	306	RHOA	338	SLC27A5	370	TCEA3	402	ZDHHC4
275	PNPLA4	307	RNASET2	339	SLC29A2	371	TEAD2	403	ZFAND3
276	POLE2	308	RND2	340	SLC6A15	372	TES	404	ZNF239
277	POLR1C	309	RNF125	341	SLC6A6	373	TEX19	405	ZNF330
278	POU5F1	310	RNF150	342	SLITRK4	374	TFAP2A	406	ZNF334
279	POU5F1P3	311	RNF175	343	SLMO2	375	TFAP2C	407	ZNF365
280	PPIA	312	RNF207	344	SMPDL3B	376	TFIP11	408	ZNF662
281	PRAME	313	RNF212	345	SNAP91	377	THEM4	409	ZNF804A
282	PRAMEF1	314	RPS15	346	SNCA	378	TMEM144	410	ZNF883

APPENDIX Q

List of down-regulated genes in iSaos-2

No	Gene	No	Gene	No	Gene	No	Gene	No	Gene	No	Gene
1	A2M	61	BCL2	121	CNTRL	181	ESYT2	241	GLT8D2	301	ITGA10
2	AAK1	62	BDNF	122	COL10A1	182	ETNK1	242	GNAZ	302	ITGB1
3	ABHD12	63	BEAN1	123	COL12A1	183	ETS1	243	GNG4	303	ITGB5
4	ABHD13	64	BEND6	124	COL13A1	184	EXOC2	244	GNPTG	304	ITPR2
5	ACP1	65	BEX5	125	COL14A1	185	EXT2	245	GNS	305	ITSN1
6	ACPL2	66	BICC1	126	COL3A1	186	F3	246	GPC1	306	JAK2
7	ACYP2	67	BMP1	127	COL5A1	187	FAM101B	247	GPC4	307	JPH3
8	ADAMT55	68	BMP6	128	COL5A2	188	FAM111B	248	GPC6	308	KAL1
9	ADAMT59	69	BMP8A	129	COL6A1	189	FAM120C	249	GPR107	309	KALRN
10	ADCY9	70	C11orf92	130	COLEC12	190	FAM126A	250	GPR137C	310	KANK1
11	ADNP2	71	C12orf57	131	COPS7A	191	FAM129B	251	GPR18	311	KCNB1
12	AFF3	72	C14orf37	132	CORO2B	192	FAM13B	252	GPR98	312	KCNJ2
13	AFTPH	73	C17orf103	133	COTL1	193	FAM176A	253	GPX8	313	KCNMA1
14	AGFG1	74	C18orf32	134	CPQ	194	FAM188A	254	GRHL1	314	KCNN3
15	AGPAT3	75	C19orf10	135	CREB3L1	195	FAM189A1	255	GRIA4	315	KCNN4
16	AGT	76	C1GALT1C1	136	CRIM1	196	FAM189A2	256	GSN	316	KCNS3
17	AHNAK2	77	C1QTNF2	137	CRIPT	197	FAM24B	257	GSPT2	317	KCTD10
18	AHRR	78	C1R	138	CRISPLD1	198	FAM43A	258	GSTT1	318	KCTD15
19	AIG1	79	C1orf198	139	CSRP1	199	FAM46A	259	GTPBP6	319	KDSR
20	AJAP1	80	C2orf18	140	CTDP1	200	FAM49A	260	GUCY1B3	320	KIAA0408
21	AJUBA	81	C2orf68	141	CTNNB1	201	FAM82A1	261	GULP1	321	KIAA0930
22	AK5	82	C6orf47	142	CTSB	202	FARP1	262	GYG2	322	KIAA1217
23	AKAP17A	83	C6orf48	143	DAB2	203	FAT4	263	GYP A	323	KIAA1432
24	AKAP5	84	CA2	144	DAPK1	204	FAXC	264	H2AFV	324	KIAA1468
25	AKAP6	85	CA3	145	DCX	205	FBLIM1	265	HAPLN1	325	KIAA1522
26	ALDH4A1	86	CACNA1C	146	DDOST	206	FBN1	266	HCFC2	326	KIAA1644
27	ALPL	87	CADM1	147	DDX58	207	FBXW2	267	HDAC11	327	KIF11
28	AMIGO2	88	CALU	148	DENND5B	208	FGFBP2	268	HEATR7A	328	KIF1B
29	AMOT	89	CAMTA1	149	DHRX	209	FGFR1	269	HECW2	329	KITLG
30	AMOTL2	90	CARS2	150	DISP2	210	FGFR2	270	HEY2	330	KLF12
31	ANKRD13C	91	CAST	151	DLC1	211	FHOD3	271	HGSNAT	331	KLF2
32	ANTXR1	92	CAV3	152	DLEU2	212	FKBP7	272	HHIP	332	KLF3
33	ANTXR2	93	CCBE1	153	DNAJC1	213	FKBP9	273	HIST1H1C	333	KRCC1
34	APBB2	94	CCDC150	154	DNAJC22	214	FKTN	274	HKR1	334	LAMA4
35	APLP2	95	CCDC68	155	DNAJC3	215	FLI1	275	HLX	335	LAMP1
36	APOL6	96	CCDC80	156	DNMBP	216	FLNC	276	HNRNPR	336	LAPTM4A
37	ARHGAP23	97	CCNE2	157	DOCK10	217	FLOT1	277	HNRPLL	337	LATS2
38	ARHGAP26	98	CD24	158	DSCR3	218	FLRT2	278	HS3ST3B1	338	LBH
39	ARHGAP31	99	CD59	159	DSCR6	219	FOLH1	279	HS6ST1	339	LCLAT1
40	ARHGAP5	100	CD63	160	DSTN	220	FOXF1	280	HSD17B11	340	LGMN
41	ARHGEF18	101	CD70	161	DTX4	221	FOXF2	281	HSPB3	341	LGR4
42	ARHGEF6	102	CD99	162	DYSF	222	FOXQ1	282	HYAL4	342	LHFPL2
43	ASAH1	103	CDC42EP3	163	ECM1	223	FRAS1	283	IBSP	343	LHX2
44	ASAP1	104	CDCA3	164	EFEMP1	224	FRMD3	284	ICA1L	344	LHX6
45	ASAP2	105	CDH11	165	EFHA2	225	FST	285	ID4	345	LIFR
46	ASPH	106	CDH2	166	EFHD1	226	FSTL1	286	IER5L	346	LIMA1
47	ASPSCR1	107	CDK5R1	167	EFNA5	227	FUCA1	287	IFFO1	347	LIMCH1
48	ATAD2B	108	CDKN1A	168	EGFR	228	FUCA2	288	IFI6	348	LINC00312
49	ATL1	109	CDON	169	EIF2AK3	229	GADD45B	289	IFIT1	349	LIPC
50	ATP11A	110	CELSR1	170	ELL2	230	GALNS	290	IFIT2	350	LMAN2L
51	ATP2B1	111	CFD	171	EML4	231	GALNT11	291	IFITM2	351	LN X1
52	ATP6V1C1	112	CFI	172	EMP2	232	GALNT14	292	IFITM5	352	SPARC
53	ATRN	113	CHMP3	173	ENPP1	233	GALNT3	293	IFNAR1	353	LOC100506013
54	B4GALNT1	114	CHN2	174	ENPP2	234	GANAB	294	IFNAR2	354	RUNX1
55	B4GALT1	115	CLIC5	175	ENTPD3	235	GBA	295	IGF2BP2	355	MATN2
56	B4GALT4	116	CLU	176	EPB41L2	236	GDAP1	296	IGFBP6	356	PHF21B
57	BAALC	117	CNDP2	177	EPDR1	237	GEN1	297	IGFBP7	357	LPAR1
58	BACE1	118	CNN2	178	EPHA2	238	GGCX	298	IL10RB	358	LPCAT3
59	BAIAP2	119	CNR1	179	ERLEC1	239	GJA1	299	INADL	359	LRP11
60	BCAR3	120	CNRIP1	180	ERP29	240	GLB1	300	ITGA1	360	LRRC17

APPENDIX Q (CONTINUE)

No	Gene	No	Gene	No	Gene	No	Gene	No	Gene	No	Gene
361	LRRC8A	423	NRGN	485	PSIP1	547	SLC20A1	609	TGOLN2	671	ZBED1
362	LRRN1	424	NRIP3	486	PTCH1	548	SLC22A15	610	THBS1	672	ZBTB46
363	LUZP2	425	NRP1	487	PTH1R	549	SLC25A6	611	TIA1	673	ZC3H12C
364	LYPD6	426	NT5E	488	PTPLA	550	SLC2A6	612	TIMP1	674	ZC3H6
365	LYPD6B	427	NTN4	489	PTPN21	551	SLC35A5	613	TM7SF3	675	ZEB2
366	LZTS1	428	NTRK2	490	PTTG1IP	552	SLC35G2	614	TMCC3	676	ZFP112
367	MAFB	429	NTRK3	491	PVRL2	553	SLC38A9	615	TMCO1	677	ZFP30
368	MAGT1	430	NXN	492	PXDC1	554	SLC40A1	616	TMCO3	678	ZNF107
369	MANEAL	431	ONECUT2	493	QPCT	555	SLC4A4	617	TMED9	679	ZNF117
370	MAP3K3	432	OPTN	494	RAB11FIP5	556	SLC8A1	618	TMEM119	680	ZNF134
371	MAP3K6	433	OS9	495	RAB15	557	SLC8A3	619	TMEM132A	681	ZNF136
372	MAVS	434	PAIP1	496	RANBP17	558	SLIT3	620	TMEM18	682	ZNF184
373	MBD2	435	PAX7	497	RANBP2	559	SMARCA2	621	TMEM182	683	ZNF222
374	MBOAT2	436	PBX3	498	RANBP3L	560	SMARCD3	622	TMEM2	684	ZNF223
375	MCFD2	437	PCDH20	499	RANBP6	561	SMC6	623	TMEM30A	685	ZNF254
376	MDM1	438	PCDH7	500	RAPH1	562	SNN	624	TMEM50A	686	ZNF256
377	MED22	439	PCDHB12	501	RARRES3	563	SOCS1	625	TMEM50B	687	ZNF260
378	MEGF6	440	PCDHB2	502	RASSF8	564	SOCS6	626	TMEM57	688	ZNF273
379	MEPE	441	PCDHB5	503	RBFOX2	565	SORBS2	627	TMIE	689	ZNF320
380	MGAT4A	442	PCDHB7	504	RCAN1	566	SOST	628	TMOD2	690	ZNF322
381	MGLL	443	PCDHGA1	505	RCAN2	567	SOX18	629	TMX3	691	ZNF347
382	MGMT	444	PCF11	506	REEP1	568	SPAG1	630	TNC	692	ZNF362
383	MICAL2	445	PCOLCE	507	RGPD3	569	SPARCL1	631	TNFRSF1A	693	ZNF415
384	MID1IP1	446	PCYOX1	508	RHOQ	570	SPATS2L	632	TNFSF9	694	ZNF423
385	MIR4647	447	PDCL	509	RIMS2	571	SPECC1L	633	TNRC6A	695	ZNF439
386	MLLT10	448	PDE4D	510	ROCK2	572	SPEG	634	TNS3	696	ZNF44
387	MLLT4	449	PDE5A	511	RRBP1	573	SPNS2	635	TOM1L2	697	ZNF442
388	MME	450	PDE8B	512	RRM2	574	SPP1	636	TOR1A	698	ZNF443
389	MMP2	451	PDGFD	513	RTN4	575	SPTAN1	637	TOR1B	699	ZNF527
390	MPDZ	452	PDGFRA	514	RTN4RL1	576	SPTB	638	TPM1	700	ZNF529
391	MPPED2	453	PDGFRL	515	RTTN	577	SPTBN1	639	TPST1	701	ZNF540
392	MRO	454	PDI4A	516	RUNX3	578	SRPX2	640	TRAPPC10	702	ZNF543
393	MSRB3	455	PGF	517	S1PR1	579	SRSF1	641	TRAPPC12	703	ZNF549
394	MTMR6	456	PHF20L1	518	SALL3	580	ST6GAL2	642	TRPC3	704	ZNF567
395	MYC	457	PI15	519	SAMD4A	581	STAM	643	TSC22D2	705	ZNF573
396	MYH10	458	PID1	520	SAMD9	582	STAM2	644	TSPAN11	706	ZNF577
397	MYL1	459	PIGF	521	SASH1	583	STARD13	645	TSPAN6	707	ZNF585A
398	MYLIP	460	PIGK	522	SCAI	584	STAT3	646	TSPAN9	708	ZNF585A
399	MYLK	461	PIGN	523	SCD5	585	STAU2	647	TSSC1	709	ZNF606
400	MYO6	462	PLCE1	524	SCIN	586	STC2	648	TUSC3	710	ZNF607
401	MYOF	463	PLCG2	525	SCPEP1	587	STEAP3	649	TXNDC15	711	ZNF608
402	NAALAD2	464	PLEKHF2	526	SCUBE1	588	STIM1	650	UACA	712	ZNF610
403	NAGK	465	PLEKHG3	527	SDC2	589	STK17B	651	UBASH3B	713	ZNF613
404	NAV1	466	PLXND1	528	SEC14L1	590	STS	652	UGGT2	714	ZNF615
405	NAV2	467	PNMA2	529	SEC24D	591	STXBP6	653	ULBP2	715	ZNF638
406	NAV3	468	PPAPDC1B	530	SEMA3B	592	SUN2	654	ULK2	716	ZNF649
407	NCALD	469	PPAPDC2	531	SEMA4F	593	SURF4	655	USP46	717	ZNF671
408	NCAM1	470	PPM1H	532	SEMA6D	594	SUSD4	656	VANGL1	718	ZNF680
409	NCAPD3	471	PPP1CB	533	SEP10	595	SUSD5	657	VASN	719	ZNF682
410	NCEH1	472	PPP1R26	534	SEP11	596	SYNPO	658	VAV2	720	ZNF708
411	NCOA3	473	PPP3R1	535	SEP4	597	SYNPO2	659	VCL	721	ZNF709
412	NDNF	474	PPP6C	536	SERPINE2	598	TAF1B	660	VPS4B	722	ZNF772
413	NEBL	475	PQLC3	537	SGCB	599	TAPBPL	661	VVA1	723	ZNF776
414	NEDD4	476	PRKAG1	538	SGCD	600	TAPT1	662	WDPCP	724	ZNF781
415	NEDD4L	477	PRKAG2	539	SH3BGR13	601	TBC1D2B	663	WDR7	725	ZNF793
416	NEU1	478	PRNP	540	SH3RF3	602	TBRG1	664	WISP1	726	ZNF83
417	NEXN	479	PROS1	541	SH3YL1	603	TBX18	665	WNT11	727	ZNF836
418	NFIA	480	PRR3	542	SHROOM2	604	TCF19	666	WWC3	728	ZNF880
419	NLGN4X	481	PRR4	543	SIPA1L1	605	TENC1	667	WWP1	729	ZNF91
420	NOTUM	482	PRR5L	544	SIRPA	606	TFCP2	668	XIST	730	ZZZ3
421	NOV	483	PRUNE2	545	SLC1A3	607	TGFB111	669	YPEL5		
422	NRBP1	484	PSD3	546	SLC1A4	608	TGFB2	670	ZAK		